Synthesis, crosslinking and characterization of disulfonated poly(arylene ether sulfone)s for application in reverse osmosis and proton exchange membranes

Mou Paul

Dissertation submitted to the faculty of the Virginia Polytechnic Institute and State University in partial fulfillment of the requirements for the degree of

Doctor of Philosophy
In
Macromolecular Science and Engineering

Dr. Judy S. Riffle

Dr. James E. McGrath
Dr. Donald G. Baird
Dr. Larry Taylor
Dr. Richey M. Davis

(July 7, 2008)
(Blacksburg, VA)

Keywords: Reverse Osmossis Membrane, Proton Exchange Membrane, Crosslinking, Poly(Arylene Ether Sulfone), Ionomer

ABSTRACT

Synthesis, crosslinking and characterization of disulfonated poly(arylene ether sulfone)s for application in reverse osmosis and proton exchange membranes

Mou Paul

Novel proton exchange (PEM) and reverse osmosis (RO) membranes for application in fuel cell and water purification respectively were developed by synthesis and crosslinking of disulfonated biphenol-based poly (arylene ether sulfone)s (BPS). Crosslinking is a prospective option to reduce the water swelling and improve the dimensional stability of hydrophilic BPS copolymers. Several series of controlled molecular weight, phenoxide-endcapped BPS copolymers were synthesized via direct copolymerization of disulfonated activated aromatic halide monomers. The degree of disulfonation was controlled by varying the molar ratio of sulfonated to non-sulfonated dihalide monomers. The molecular weights of the copolymers were controlled by offsetting the stoichiometry between biphenol and the dihalides. Biphenol was utilized in excess to endcap the copolymers with phenoxide groups, so that the phenoxide groups could be further reacted with a suitable crosslinker. Several crosslinking reagents such as methacrylate, multifunctional epoxy, phthalonitrile and phenylethynyls were investigated. A wide range of crosslinking chemistries i.e. free radical (methacrylate), step growth (epoxy), heterocyclic (phthalonitrile) and acetylenic (phenylethynyl) was explored. The effects of crosslinking on network properties as functions of molecular weight and degree of disulfonation of copolymers, crosslinking time and concentration of crosslinker were studied. The crosslinked membranes were characterized in terms of gel fraction, water uptake, swelling, self-diffusion coefficients of water, proton conductivity, methanol permeability, water permeability and salt rejection. In general, all of the crosslinked membranes had lower water uptake and swelling relative to their uncrosslinked

counterparts, and less water uptake and volume swelling were correlated with increasing gel fractions. It was possible to shift the percolation threshold for water absorption of BPS copolymers to a higher ion exchange capacity (IEC) value compared to that of the uncrosslinked copolymers by means of crosslinking. This reduced water uptake increased the dimensional stability of higher IEC materials and extended their application for potential PEM or RO membranes. The reduction in water uptake and swelling also increased the effective proton concentration, resulting in no significant change in proton conductivity of the membranes after crosslinking. The self-diffusion coefficients of water and methanol permeability decreased with crosslinking, indicating restricted water and methanol transport. Therefore an improvement in the selectivity (ratio of proton conductivity to water swelling or methanol permeability) of PEMs for application in either H_2/air or direct methanol fuel cells was achieved by crosslinking. The epoxy crosslinked BPS copolymers also had significantly enhanced salt rejection with high water permeability when tested in for RO applications. Reductions in salt permeability with increasing crosslinking density suggested that crosslinking inhibited salt transport through the membrane.

In addition to the random copolymers, two series of multiblocks endcapped with either a phenoxide-terminated hydrophilic unit or a hydrophobic unit were synthesized and crosslinked with a multifunctional epoxy. Besides the crosslinking study, the effect of sequence distributions of the hydrophilic and hydrophobic blocks in the multiblock copolymers was also investigated. Similar to randoms, crosslinked multiblocks had lower water uptake and swelling but comparable proton conductivities relative to their uncrosslinked analogues.

Dedicated to my loving parents, Mrs. Sabita Paul and Mr. Amal Paul

--Ma & Baba,

This was not my dream only; this was “our” dream.

Acknowledgements

This is a great opportunity to thank all the people who have motivated and supported me during these five years of my doctoral study. First of all I would like to thank my committee members Prof. James E. McGrath, Prof. Larry Taylor, Prof. Richey Davis, Prof. Donald Baird and Prof. Judy S. Riffle for their valuable suggestions toward my research. I would especially like to express my gratitude to my advisors Prof. Judy S. Riffle and Prof. James E. McGrath. I am deeply grateful to their guidance and support without which I may not have reached to this point. I was inspired by their breadth of knowledge in polymer science, motivated by their dedication to students and research. I believe that these things were and will remain instrumental to shape my life and career.

Many thanks go to all of my lab mates and colleagues from both Prof. Riffle's and Prof. McGrath's groups. Thank you Harry for those long discussions; thanks to Dr. Yanxiang Li and Dr. Xiang Yu for help in the lab. Many thanks go to Rachael, Natalie Ozma, Juan, Dr. Fan and Dr. Zhang. I would also like to thank my colleagues in Riffle group; Dr. Michael Vadala who helped me during my initial days in the graduate school, John Goff, John Boyd, Nikorn, Phil, Tim and Dr. Lin.

I would like to acknowledge our collaborators at University of Texas at Austin, Prof. Benny D. Freeman, Prof. Ho Bum Park and Wei Xie for their excellent support.

My earnest thanks go to Laurie Good, Millie Ryan and Angie Flynn for their constant assistance and help. They were always there to solve any official problem.

Finally, I would like to thank my parents, Mrs. Sabita Paul and Mr. Amal Paul for their love, support and guidance. They have shaped my life, instilled the values and will always be my ideals. Thank you ma and baba, for your life-long sacrifice, endless patience, encouragement and unconditional love. I want to specially thank my big uncle, Mr. Anil Paul and my aunt Mrs Uma Paul for their support and love. I would also like to

thank my parent-in-laws Mr. Arunabha Roy and Mrs. Manju Roy for their love and support. Thanks to my sweet sister-in-law, Miss Abhinanda Roy for always bringing joy to life. I am thankful that I have become a part of such a loving family.

At last, I want to thank my husband, best friend and soulmate, Dr. Abhishek Roy for his selfless love and constant support. He has encouraged me, guided me and was always besides me during difficult times. I may not have reached to this point without him.

Finally, I thank Dear God, my Lord ShriKrishna for always being with me.

Table of Contents

List of Figures

List of Tables

1. CHAPTER 1 – LITERATURE REVIEW

1.1. Introduction to ion-exchange membranes

Ion-exchange membranes are comprised of ion containing polymers where interactions among the ion-aggregates determine the bulk properties of the polymers.[1] Ion-exchange membranes have major applications in electro-membrane devices and processes including fuel cells, electrodialysis, electrolysis and also in various separation processes such reverse osmosis and pervaporation. Hydrophilic ionomer membranes allow water to transport through the membranes preferentially and thus can be utilized for dehydrating water-containing solvent mixtures. The ion-exchange groups of ionomer membranes can reject charged solutes or charged molecules such as ammonium ions and carboxylates and thus can be utilized for desalination or water purification. Ion-exchange membranes also can transport charged ions and have applications as transport membranes in fuel cells or electrolysis.

Ionomer membranes with hydrophilic ionic groups are susceptible to high water uptake. This may lead to loss in dimensional stability. The structural integrity of the membranes can be improved by reducing water uptake and swelling and in that respect, crosslinking is a prospective option. Specific interactions between macromolecules can serve as potential crosslinking strategies. Physical crosslinks can be achieved through van der Waals interactions, dipole-dipole interactions, hydrogen bonds, or electrostatic interactions. Chemical crosslinks are achieved through covalent bonds.[2, 3]

This review will address crosslinking of various types of ionomers. The focus will be on the type/nature, procedure of crosslinking of the ionomers and effects of crosslinking on membrane properties. As the research described in this dissertation focuses on synthesis and crosslinking of poly(arylene ether sulfone)s, a detailed description of the synthesis and the crosslinking of poly(arylene ether sulfone)s is included.

1.1.1. Crosslinking of polystyrene based ionomers

Styrenic monomers are readily available, versatile modification methods have been developed and their polymers can be synthesized through conventional free radical and other polymerization techniques. Polystyrenic polymers and their networks synthesized via styrene/divinylbenzene copolymerization, can be sulfonated to produce cation-exchange resins. In 1960, the Gemini Space Program was a pioneer in utilization of polymer electrolyte fuel cells. The membranes were comprised of polystyrene that were crosslinked with 1.25 % divinylbenzene. These membranes had very short lifetimes due to oxidative degradation of the sulfonated polystyrene.

One strategy for improving the stability of the sulfonated polystyrenes was to crosslink the materials with fluoropolymers. One interesting method was to utilize radiation to graft styrene onto fluoropolymers, and this simultaneously crosslinked the materials. The networks were then sulfonated. Graft polymers, in which the ion containing polymer grafts are attached to activated centers on the base polymer backbone, potentially have a broad spectrum of applications in membrane separation processes such as electrodialysis, reverse osmosis, filtration, pervaporation etc.[4] The structure-property relationships of grafted membranes can be somewhat controlled by varying the number density and length of the grafted chains.[5] In the radiation grafting process, first a preformed base polymer is synthesized and then activated centers are generated on the base polymer backbone by irradiation with an electron beam or γ rays. Polymer chains of the second component are then grafted onto those activated centers through radical polymerization.

The well-known susceptibility of polystyrene towards oxidative degradation in the fuel cell environment has led to searches for more stable substituted styrenic monomers for potential use in radiation grafting processes. The monomers are shown in Figure 1.1.[4]

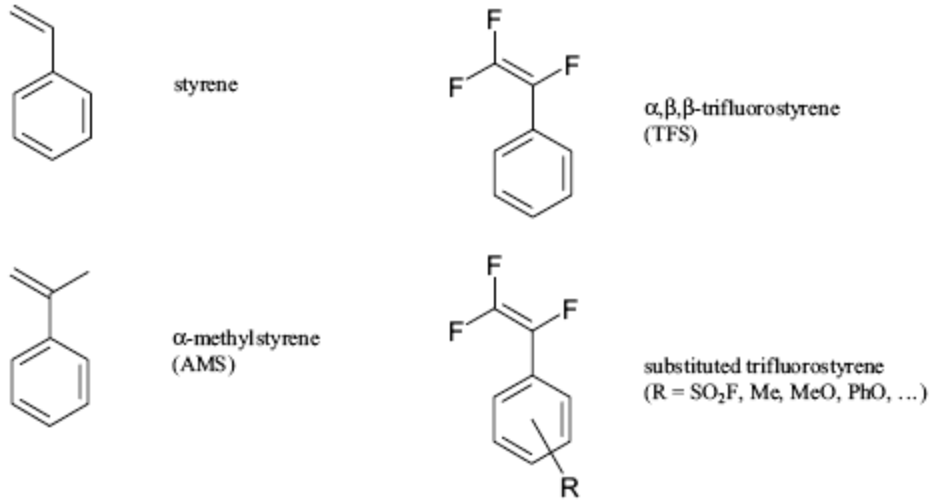

Figure 1.1 Substituted styrenic monomers for radiation grafted membranes; Reprinted with permission [4], from John Wiley & Sons, Inc

α,β,β-Trifluorostyrene (TFS) has better chemical stability than styrene due to the absence of vinyl protons, but it suffers from poor polymerization kinetics and longer grafting times.[6-8] It is also more difficult to sulfonate. Ballard power systems have utilized substituted TFS monomers including para-methoxy, phenoxy or methyl TFS which are activated towards grafting.[9, 10] Also, the use of para-sulfonylfluoride-TFS eliminates the necessity of sulfonation step. Another simpler and cheaper monomer is α-methylstyrene (AMS). AMS is also chemically more stable than styrene due to its protected α position,[11] but its polymerization rate is low and the resulting polymer has a very low decomposition temperature (60 °C). This problem can be somewhat mediated through copolymerization with, for example, acrylontrile.[12]

Crosslinking reagents can also be utilized as co-monomers (Figure 1.2) in radiation grafting processes. They contain two or more vinyl groups so that a bridge can be formed between the grafted polymer chains.

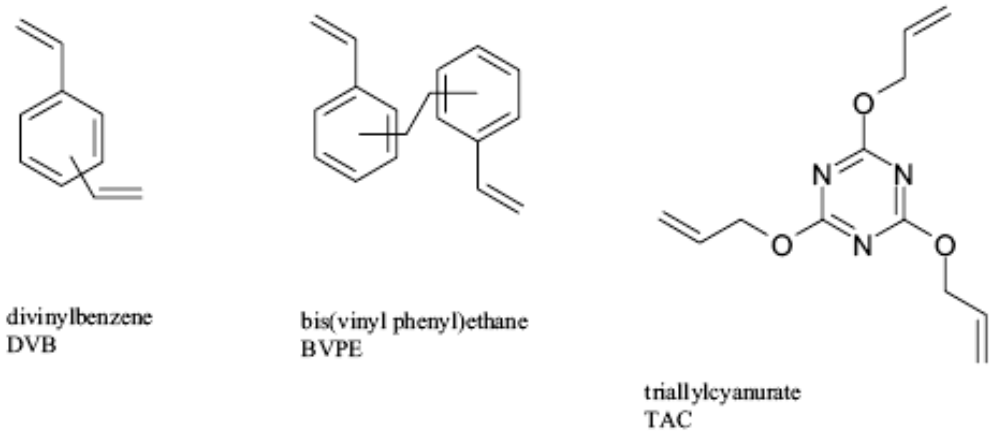

Figure 1.2 Multifunctional co-monomers for radiation-grafted membranes; Reprinted with permission from John Wiley & Sons, Inc[4]

Divinylbenzene (DVB) is one of the most frequently used crosslinkable monomers in radiation grafting process. Membranes crosslinked with DVB exhibit lower water uptake and lower proton conductivities.[13, 14,15]

A range of base polymers have been radiation-grafted. The requirements for the base polymers are that they possess a high melting temperature, stability against radiation and that they are amenable to radiation induced grafting. Poly(ethylene-alt-tetrafluoroethylene) (ETFE), poly(vinylidene fluoride) (PVDF) and poly(tetrafluoroethylene-*co*-hexafluoropropylene) (FEP) are among the promising candidates.

Gupta et al.[16, 17] and Buchi et al.[14] have reported radiation grafting of tetrafluoroethylene-*co*-hexafluoropropylene (FEP). Membranes were prepared by pre-irradiation grafting of styrene/divinylbenzene mixtures into FEP films and subsequent sulfonation with chlorosulfonic acid.[17] The structure of the grafted membrane is provided in Figure 1.3[14] (crosslinks not shown).

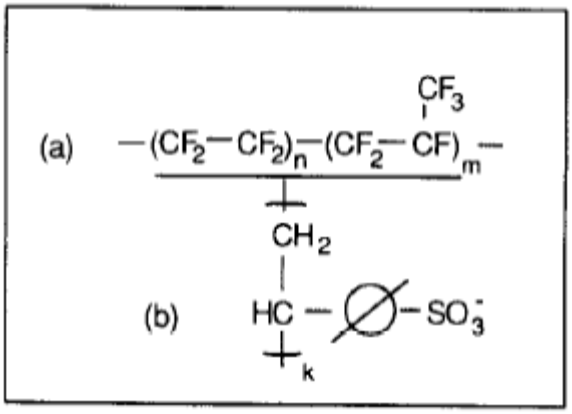

Figure 1.3 Structure of radiation grafted membrane (a) FEP main chain, (b) Sulfonated Polystyrene grafted chain; Reprinted from [14] with permission from Elsevier

The degree of crosslinking of the grafted membranes had prominent influence on their potential for applications in fuel cells. Crosslinking enhanced the gas separation properties of thin membranes (based on 50 μm FEP films) and improved long term stability of the membranes.[14, 18] These phenomena can be explained by a lower reactant crossover rate as a result of higher structural density with increasing crosslinking. The optimum DVB concentration in polystyrene-divinylbenzene networks was found to be 10 % to achieve the combination of reasonable conductivity and membrane stability.[19] However, in spite of superior physical and electrochemical properties relative to Nafion, these membranes exhibited inferior fuel cell performance. The authors assumed that oxygen diffused at the anode and formed $HO_2^{\cdot}$ radicals which attacked the tertiary hydrogens at α carbons of the polystyrene graft chains, and that this resulted in loss of ion exchange capacity (IEC) after operation in a fuel cell environment. It was also suggested that the improved stability of the highly-crosslinked films was not only caused by crosslinking of the polystyrene, but was also due to lower gas crossover and subsequently less $HO_2^{\cdot}$ attack on the polystyrene chains. The concept of "double crosslinking" using triallylcyanurate (TAC) in addition to DVB was also applied.[14, 17, 18] Membranes

crosslinked with only TAC exhibited higher water uptake and consequently higher proton conductivity compared to membranes crosslinked with DVB. This was attributed to the more flexible structure of the membranes crosslinked with TAC which has longer side chains and ether functional groups. Membranes crosslinked with both DVB and TAC showed higher power density than Nafion 117 under identical conditions, but long term stabilities of these membranes in the fuel cell environment still were not reported.

ETFE as the base polymer was also explored.[20] ETFE is less prone to irradiation related damage than FEP and also exhibits superior mechanical properties.[21] ETFE based membranes showed lower water uptake and subsequently lower conductivity than FEP based films.[22, 23] This may be due to more effective crosslinks in ETFE based membranes generated from the difference in grafting kinetics of FEP and ETFE base polymers. In a similar study, polystyrene was grafted onto ETFE and FEP films using N,N-methylene-*bis*-acrylamide (MBAA).[24] It was proposed that MBAA would have better oxidative stability than DVB in the fuel cell environment due to its acrylate structure. Though MBAA crosslinked membranes showed better retention of IEC than membranes crosslinked with DVB, yet 10% of the grafts were lost after 100 hour fuel cell operation.

Poly(vinylidene fluoride) (PVDF) membranes, radiation-grafted with styrene and post-sulfonated, were also studied as candidates for proton exchange membranes. The effect of crosslinking was investigated using DVB and bis(vinylphenyl)ethane (BVPE).[13] In comparison to DVB, membranes crosslinked with BVPE did not show any pronounced effect on water uptake, proton conductivity or fuel permeability.[13, 25]

Dais Analytic's proton exchange membranes are based on sulfonated triblock polystyrene ionomers comprised of styrene-ethylene/butylene-styrene (PSEBS) as shown in Figure 1.4.[26]

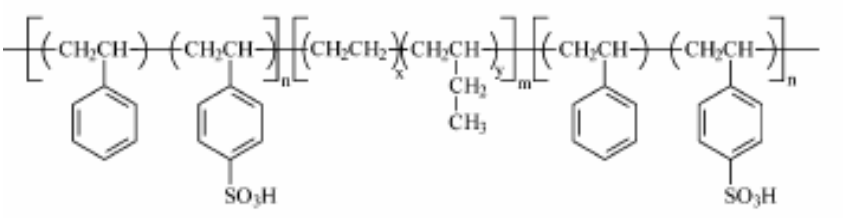

Figure 1.4 Dais polymer electrolyte: sulfonated PSEBS[26] Reprinted with permission. Copyright 2002 American Chemical Society

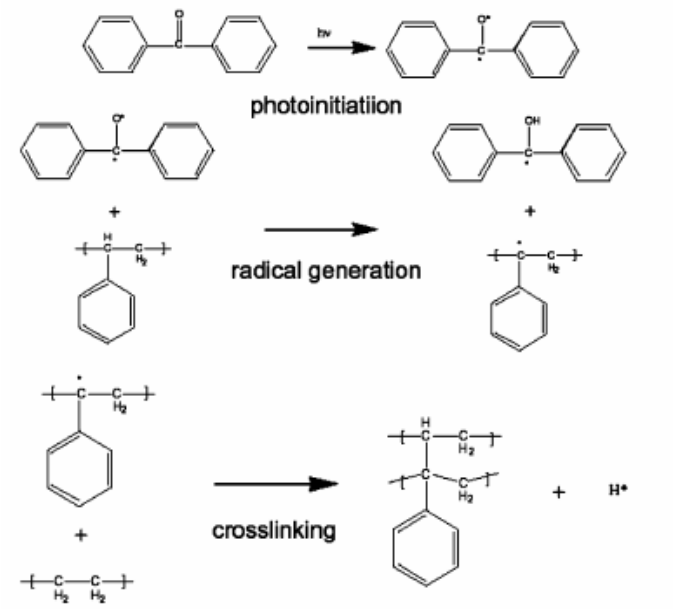

Figure 1.5 Photocrosslinking of PSEBS[27]; Reprinted with permission. Copyright 2005 American Chemical Society

Dais membranes are much less expensive than Nafion, but the main drawback of these hydrocarbon type membranes is their poor oxidative stability due to their partially aliphatic character. Therefore, the main application of this type of membranes is in portable fuel cells of low power source which have low operating temperatures like 60 °C. In a recent study, PSEBS was crosslinked through a photoreaction using benzophenone as the photoinitiator as shown in Figure 1.5.[27]

This formed crosslink's between CH_2 and CH groups in PSEBS so that the oxidation at the benzylic position of the polystyrene moiety was reduced. After crosslinking, the conductivity of PSEBS membranes was reduced due to lower water uptake. As expected, the crosslinked membranes were more stable than uncrosslinked membranes during fuel cell operation. However, with the crosslinked membranes also, the cell voltage decayed (at constant current 600 mA/cm^2) by 10 % after 300 hours of fuel cell operation. This indicated that the polyethylene-butylene block was prone to oxidative degradation and the sensitivity to oxidants and free radicals of the polystyrene blocks remained to some extent even after crosslinking.

1.1.2. Crosslinking of Poly(vinyl alcohol) (PVA) based ionomers

Commercial poly(vinyl alcohol) (PVA) has applications in desalination and pervaporation membranes and oxygen resistant films. PVA membranes are much better methanol barriers than Nafion membranes.[28] Therefore, PVA membranes may be promising for direct methanol fuel cell (DMFC) applications. However, PVA membranes are poor proton conductors as they do not carry any charged ions like carboxylic and sulfonic acid groups. Rhim et al. have reported making conductive PVA membranes by incorporating negatively charged ions by using a crosslinking agent like sulfosuccinic acid (SSA) or poly(acrylic acid-co-maleic acid) (PAM) containing carboxylic acid groups.[29, 30] Crosslinking was achieved through esterification between the hydroxyl groups in PVA and acid groups in SSA or PAM. For the PVA/SSA membranes, the crosslink densities and ion exchange capacities of the membranes

increased with increasing content of sulfosuccinic acid. However, the proton conductivity of the membranes did not increase and the methanol permeability did not decrease proportionately with the amount of SSA. This was attributed to the premise that increasing crosslink density led to reduction of free space for the water molecules around sulfonic acid groups which was necessary for proton conduction. Methanol permeability decreased with increasing crosslink density to a certain level due to a reduction in free volume needed for methanol transport. But above a certain concentration of SSA, the effect of sulfonic acid groups exceeded that of crosslinking and methanol permeability increased. For the PVA/PAM membranes, both the proton conductivity and methanol permeability decreased with increasing concentration of PAM as the carboxylic acid groups in the PAM served both as the crosslinking agent and proton donor. The hydrolytic stability tests showed that the membranes lost weight, an this was attributed to decomposition of ester bonds and release of unreacted polymers.[31] Research on PVA/SiO_2 hybrid membranes was also reported by the same authors. The hybrid membranes showed lower methanol permeability compared to the PVA membranes that did not contain SiO_2 as free water content of the membranes was reduced by the presence of SiO_2 in the organic polymer matrix.[32, 33] These crosslinked PVA membranes functioned as water-selective materials and thus may also be useful for separation of water-alcohol mixtures by pervaporation.[34-37]

1.1.3. Crosslinking of Polyphosphazene based Ionomers

Polyphosphazenes are highly developed inorganic backbone polymer systems. They can be readily functionalized from the basic poly(dichlorophosphazene) and various speciality polymers can be obtained as shown in Figure 1.6.[38] They are particularly suitable for surface modification and side chain attachment due to the stability of the phosphorus-nitrogen backbone. The substituent sites on the polyphosphazenes are amenable to functionalization, for example with sulfonic acid groups, for subsequent crosslinking.

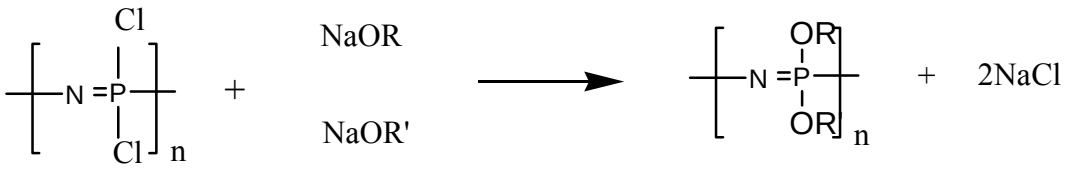

Figure 1.6 Functionalization of Polyphosphazene; Reprinted with permission[38], from John Wiley & Sons, Inc

Sulfonated polyphosphazenes can be used as ion exchange resins, proton exchange membranes, reverse osmosis membranes and non-thrombogenic biomedical materials. Allcock et al.[39] and Pintauro et al.[40, 41] reported successful sulfonation of polyphosphazenes. Pintauro and co-workers have shown that methylphenoxy and ethylphenoxy polyphosphazene polymers can be sulfonated in solution with SO_3.[40] The ethylphenoxy polymers severely degraded during sulfonation. However, the methylphenoxy phosphazenes did not show any detectable degradation and their degree of sulfonation could be controlled. One such sulfonation scheme for poly [bis(3-methylphenoxy)phosphazene] is shown in Figure 1.7.[41]

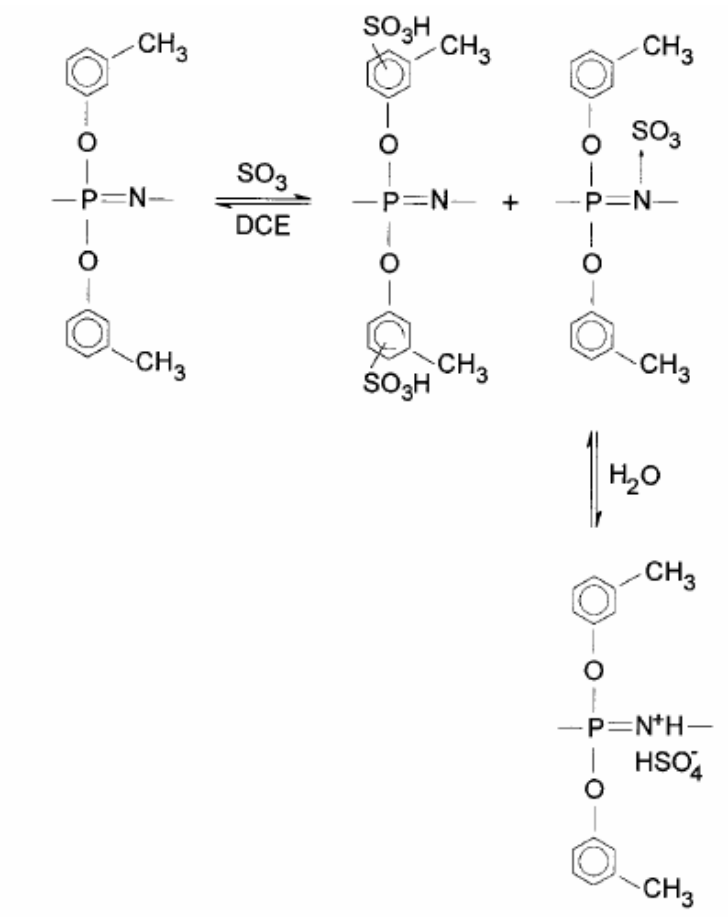

Figure 1.7 Sulfonation of poly [bis(3-methylphenoxy)phosphazene]; Reprinted with permission[41], from John Wiley & Sons, Inc

The reported glass transition temperatures of the unsulfonated and sulfonated poly[bis (3-methylphenoxy) phosphazene] ranged from – 28 to -10 ° C respectively. Due to this low glass transition temperature, polyphosphazene films had poor mechanical properties, particularly in hydrated conditions, and this may lead to membrane failure in fuel cell conditions. Hence reinforcements that can be derived from crosslinking and polymer blends are necessary to improve the mechanical stability of the polyphosphazene films. Pintauro et al. reported photocrosslinking of the non–sulfonated[38, 42] and sulfonated[43] polyphosphazenes. The crosslinking scheme is shown in Figure 1.8.[42]

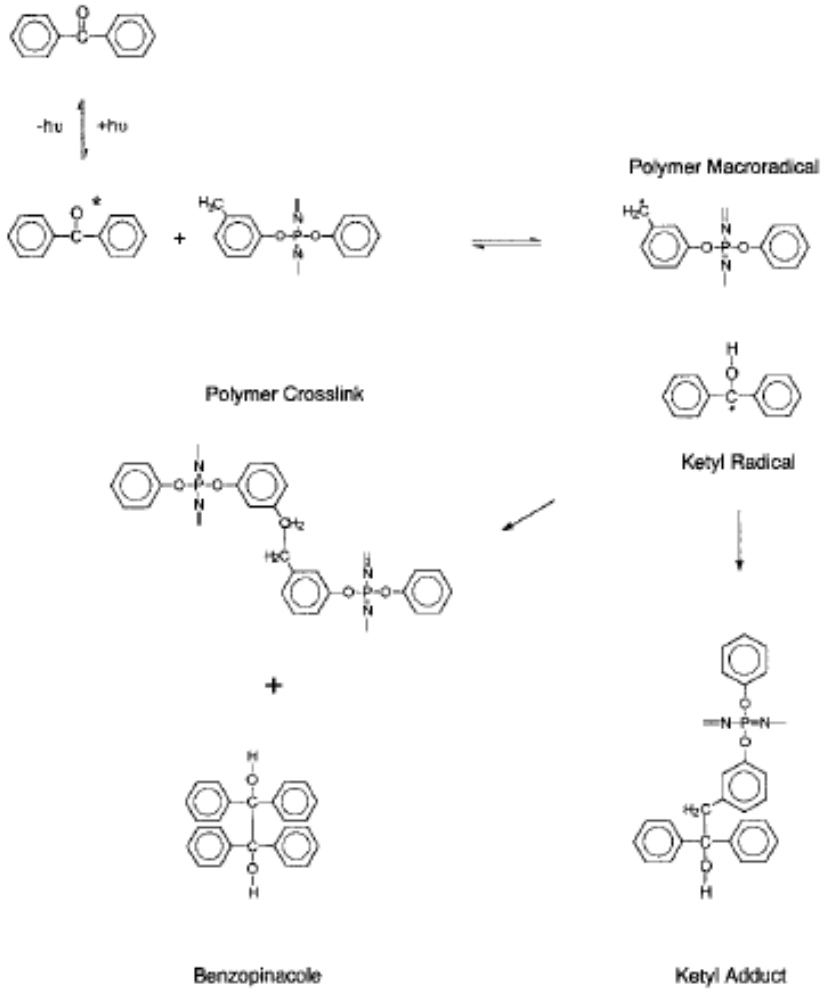

Figure 1.8 Photocrosslinking of alkylphenoxy/phenoxy polyphosphazenes; Reprinted with permission[42], from John Wiley & Sons, Inc

Poly [bis(3-methylphenoxy)phosphazene] was crosslinked after sulfonating with SO_3. Photocuring was enhanced by the low Tg of these polymers. Crosslinking was carried out by dissolving the photo-initiator benzophenone at 15 mol % concentration in the casting solution and then exposing the membranes to UV light after solvent evaporation. The crosslinked films showed reduced swelling in water compared to the uncrosslinked

films. The water and methanol diffusion coefficients of the crosslinked membranes were measured using the weight loss method and the McBain sorption balance apparatus. The methanol diffusivities in the crosslinked polyphosphazene films were significantly lower compared to Nafion, and this is promising in terms of lower methanol crossover in DMFC fuel cells. The lower water diffusion coefficients in the crosslinked membranes compared to the uncrosslinked membranes was attributed to reduced water swelling in the crosslinked networks. However, the proton conductivities of the crosslinked and uncrosslinked films were similar in spite of lower water content of the crosslinked materials. This may be due to the close proximity of sulfonic acid groups on the polyphosphazene's methylphenoxy side chains and the consequent formation of ion clusters in the sulfonated polyphosphazenes. Another possibility is that above a certain hydration level, further increase in water content does not have any effect on conductivity, because of the counterbalancing effect of high water content (i.e. increasing distance between the acidic sites as a result of membrane swelling).[44] The membranes had good thermomechanical stability up to 173 °C. However these polymers suffer from moderate glass transition temperatures and further tests will be necessary to evaluate the stability of the aliphatic (-CH_2-CH_2-) crosslinking unit in the fuel cell environment.

More recently Allcock and coworkers have conducted the crosslinking by ^{60}Co γ-radiation[45] and sol-gel techniques.[46] In the sol-gel process, they synthesized modified sol-gel precursors of poly[bis(methoxyethoxyethoxy)phosphazene] (MEEP) and its hybrid network. The precursor polymer was synthesized by combining MEEP with triethoxysilane which was covalently linked with polymer side chain. After hydrolysis and condensation, a covalently linked organic-inorganic hybrid structure with controlled morphology and physical properties was formed. This combination of silicate network and polyphosphazene has potential for applications requiring solid polymer electrolytes and biomedical hydrogels.

Pintauro et al. have also reported acid-base membranes from sulfonated polyphosphazene and polybenzimidazole (PBI) where PBI acted as the base and crosslinking reagent. However, the hydrogen bonds and electrostatic interactions in the

blend membranes from polysulfonates and polybases were labile in aqueous environments at temperatures above 70 °C, and this resulted in high swelling in water and consequent mechanical instability. This problem limits its application in devices like fuel cells and hence the long term stability of these membranes still needs to be tested.[47]

1.1.4. Crosslinking of Poly(2,6-dimethyl-1,4-phenylene oxide) (PPO) based ionomers

Poly(2,6-dimethyl-1,4-phenylene oxide) (PPO) is a promising material for fuel cell membranes due to its excellent membrane forming ability and high chemical and thermal stability. In a study by Kosmala et al., acid base membranes of polybenzimidazole (PBI) and sulfonated poly(2,6-dimethyl-1,4-phenylene oxide) (PPO) were prepared. These membranes showed good short-term thermo–oxidative stability (~ 300 °C). The crosslink density increased with higher content of PBI. However, the membranes were only conductive above a certain percolated threshold level of SPPO. Below that level, the majority of the sulfonic acid groups of SPPO were likely ionically bound to the PBI basic groups. Membranes with high concentrations of SPPO swelled excessively in water and did not yield reproducible results in fuel cell experiments.[48, 49]

1.2. Poly(arylene ether)s

Poly(arylene ether)s are a class of high performance engineering materials. They are promising candidates for fuel cell and reverse osmosis membranes because of their well-known thermal, mechanical, oxidative and hydrolytic stability. Ionic groups can be introduced in the poly(arylene ether)s by sulfonation. Among the many variations of poly(arylene ethers)s, the main categories are poly(arylene ether sulfone)s and poly(arylene ether ketone)s.

1.2.1. Synthesis Routes of Poly(arylene ether)s

Poly(arylene ether)s can be synthesized in several ways. The major ones will be discussed with greater emphasis on the most commonly used nucleophilic aromatic substitution route.

1.2.1.1.Nucleophilic Aromatic Substitution

Currently, this is the most important route for synthesizing poly(arylene ether)s.[50-54 55, 56 57, 58] It was first developed by Johnson and coworkers in 1967.[59] The reaction involves the condensation of a dialkali metal salt of a dihydric phenol with an activated aromatic dihalide in an anhydrous, aprotic, dipolar solvent at elevated temperatures.

The reaction occurs via a two-step addition-elimination (S_NAr) mechanism as shown in Figure 1.9.

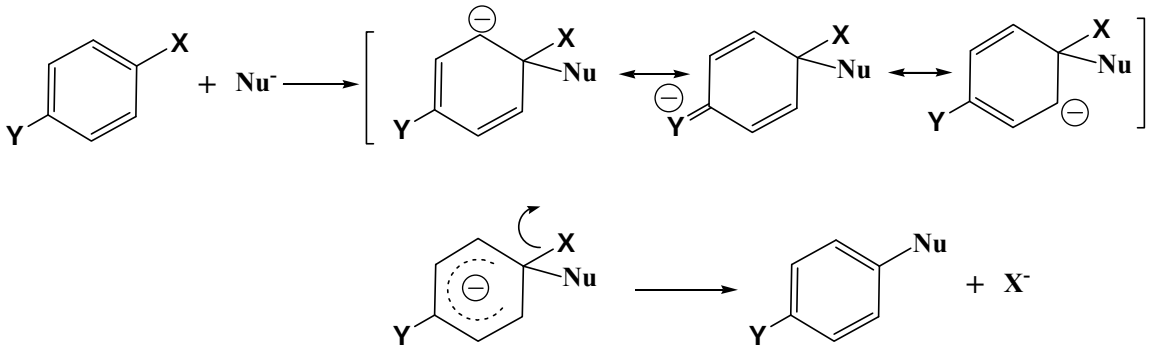

Figure 1.9 Mechanism of Nucleophilic Aromatic Substitution[60]

The first step is the addition of the nucleophile (Nu) to the electron deficient aromatic halide forming a Meisenheimer complex. This step is the slowest and rate determining step for the nucleophilic aromatic substitution. The electron withdrawing activating groups (Y) of the aromatic halides play an important role for nucleophilic aromatic substitution because aromatic halides without any activating group require very high temperature due to their low reactivity.[61, 62] Electron-withdrawing groups, especially in positions ortho and para to the leaving group accelerate aromatic nucleophilic substitutions due to their strong –I effects.[60] Formation of a Meisenheimer complex was supported by low temperature NMR and crystallography data.[63, 64] The activating power of the electron withdrawing groups in increasing order is[65] NO > NO_2 >

SO_2Me > CF_3 > CN > CHO > COR > COOH > F > Cl > Br > I > H > Me > CMe_3 > OMe > NMe_2 > OH > NH_2. The most common activating groups utilized in poly(arylene ether) synthesis are strong electron withdrawing groups like sulfones, ketones and phosphine oxides.[66]

The second step of the reaction is the decomposition of the Meisenhimer intermediate complex with subsequent release of the leaving group. An approximate order of leaving group ability is[67] F > NO_2 > OTs > SOPh > Cl, Br, I > N_3 > NR_3^+ > OAr, OR, SR, SO_2R, NH_2. The leaving group order is quite different than that for the S_N^1 or S_N^2 mechanisms. In those cases, the reactivity order is I>Br>Cl>F because breaking of the carbon-halide bond is the limiting factor. In nucleophilic aromatic substitution, the rate determining step is the formation of the Meisenheimer complex, not the expulsion of the leaving group so that the ease of carbon-halide bond breaking has little effect on the reaction rate. In this case, the reverse order i.e. F>Cl>Br>I is observed since F has the most powerful electron withdrawing effect, and can best activate the aromatic halide towards nucleophilic substitution.

The range of nucleophiles participating in nucleophilic aromatic substitutions includes alkoxides, phenoxides, sulfides, fluoride ions and amines. The reaction rate increases with increasing nucleophilicity of the nucleophiles. The order of nucleophilicity is ArS^- > RO^- > R_2NH > ArO^- > OH^- > $ArNH_2$ > NH_3 > I^- > Br^- > Cl^- > H_2O >ROH.[60, 61] In general, nucleophilicity increases with increasing base strength.

Apart from the abovementioned factors, many other factors like reaction temperature, solvent and the type of base influence the overall reaction.

Role of Solvent

Aprotic dipolar high boiling solvents like N-methylpyrrolidone (NMP), N,N-dimethylacetamide (DMAc), N,N-dimethylformamide (DMF), dimethylsulfoxide (DMSO), and cyclohexylpyrrolidone (CHP) can be used for this reaction. Solubility of

the monomers and the product polymer in the solvent is critical to maintain the proper stoichiometry.

Role of Base

There are two approaches (utilizing a strong or a weaker base) for poly(arylene ether sulfone) syntheses.

Poly(arylene ether sulfone) synthesis using a strong base

The first successful synthesis of high molecular weight poly(arylene ether sulfone)s via the aromatic nucleophilic substitution route was discovered by Johnson et al.[59] in 1960 utilizing a relatively strong base. The bases used were potassium hydroxide or sodium hydroxide. The insolubility of lithium, calcium and magnesium salts of bisphenol A in dimethylsulfoxide inhibits them from taking part in this reaction.[68] The main advantage of this reaction is that high molecular weight copolymers can be formed within a very short time, e.g. 5-6 hours. However, the major disadvantage of this reaction is that strict control of the stoichiometric amount of the base is required. Excess strong base can hydrolyze the activated aromatic dihalide and produce non-reactive phenolates, thus upsetting the stoichiometry of the reaction and decreasing the resultant degree of polymerization. Also, excess base can cleave the activated aromatic-ether linkage of the product polymer and compromise the final molecular weight of the polymer. If the amount of base added is less than the stoichiometric amount, then two effects can result.[68] The stoichiometry of the reaction can be offset and secondly, the phenolates can hydrogen bond with the free phenols, thus decreasing the overall nucleophilicity of the phenolates as shown in Figure 1.10.[69]

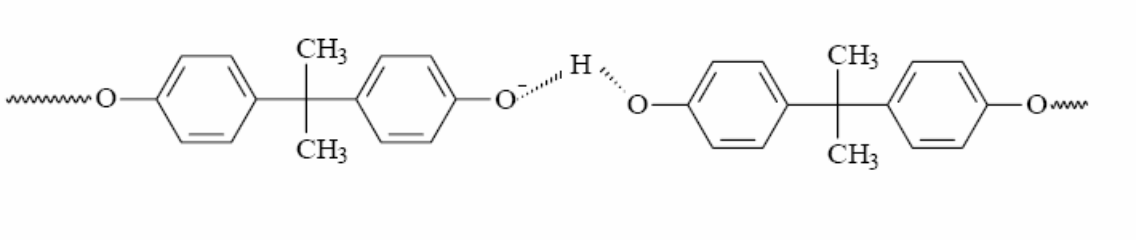

Figure 1.10. Hydrogen bonding between free bisphenol and bisphenolate[68,69]

Careful dehydration of the system is also needed for obtaining high molecular weight polymer as water can also compete as a nucleophile and hydrolyze the activated halide monomers, resulting in an imbalance in stoichiometry.

Poly(arylene ether sulfone) synthesis using a weak base

In this approach, potassium carbonate is utilized as the weak base. The first reported synthesis of poly(arylene ether sulfone)s using potassium carbonate is by Clendinning et al.[70] McGrath and coworkers have also reported synthesis of some novel poly(arylene ether sulfone)s using potassium carbonate.[71-75] The main advantage of this method is that strict control of a stoichiometric amount of the base is not required. Potassium carbonate can be used in excess without any undesirable side reaction[59, 70] or hydrolysis of the activated halides.[71] When potassium carbonate is used in less than the stoichiometric amount, high molecular weight polymers do not form, and this may be due to insufficient phenolate ions. Potassium carbonate is regarded as a better candidate than sodium carbonate due to its higher basicity and relatively better solubility in the reaction medium.[76] In this reaction water can be generated from the decomposition of potassium carbonate as shown in Figure 1.11.[68] This water can act as a competing nucleophile and hydrolyze the activated dihalide with consequent upset in stoichiometry. Hence, an azeotropic reagent such as toluene, xylene or o-dichlorobenzene is generally used to dehydrate the system.

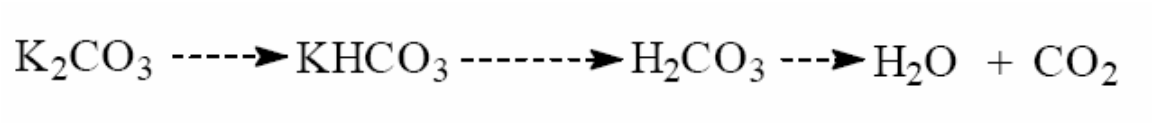

Figure 1.11 Decomposition of potassium carbonate[68]

1.2.1.2.Aromatic Electrophilic Substitution

Another important route for synthesizing poly(arylene ether)s is via Friedel-Crafts electrophilic substitution.[77, 78] The reaction mechanism involves three steps as shown in Figure 1.12.[79]

Step 1 :

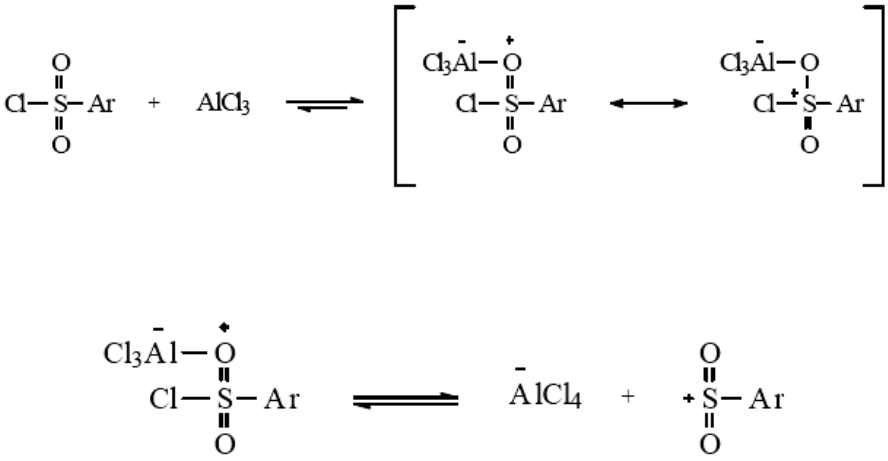

Step 2 :

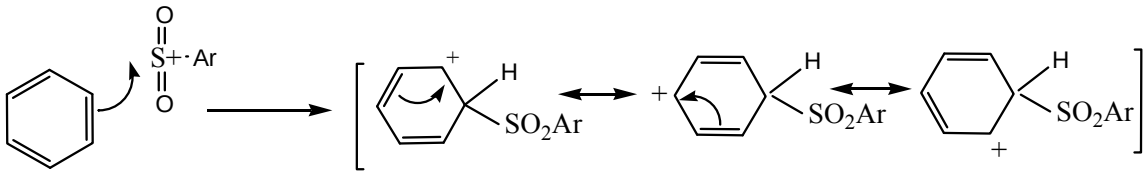

Step 3 :

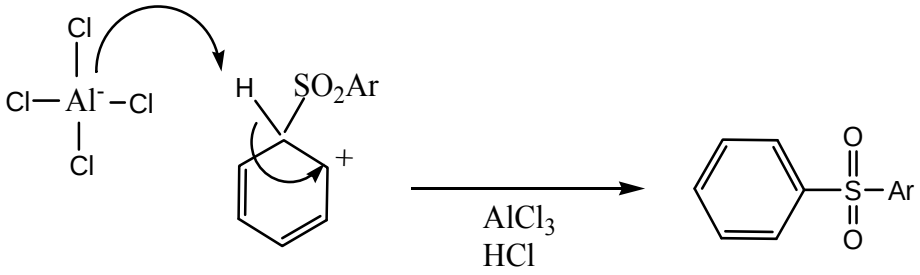

Figure 1.12 Mechanism of aromatic electrophilic substitution[60, 79]

In the first step, a Lewis acid catalyst attacks an aryl sulfonyl chloride to form a sulfonylium cation. In the second step, the electrophilic sulfonylium cation is attacked by

π electrons of the aromatic benzene ring to form a positively charged intermediate arenium complex. This is the slowest step and the rate-limiting step of this reaction. The arenium ion is a highly reactive intermediate. Hence, in the third step, a proton, which is the most common leaving group in aromatic electrophilic substitution, is expelled to restore the aromaticity of the ring resulting in a substituted benzene ring with a sulfone linkage. The third step is always faster than the second step. Since benzene is a poor electron source, Lewis acid catalysts such as $AlCl_3$, $AlBr_3$, $FeCl_3$, $SbCl_5$, BF_3 are needed to activate the electrophile for these reactions.[60, 79]

1.2.1.3.The Ullmann reaction

This synthetic route[80, 81] allows the use of non-activated aromatic halides for synthesis of poly(arylene ether)s, which is not possible by normal activated nucleophilic aromatic substitution. The reaction occurs between a double alkali metal salt of a dihydric phenol and aromatic dihalide in presence of a copper catalyst as shown in Figure 1.13.[80] The copper catalyst can be activated with a complexing agent.

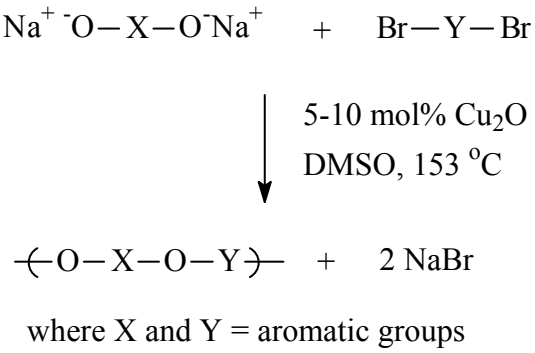

Figure 1.13 Synthesis of poly(arylene ether)s via the Ullmann route[68, 80]

The best leaving group is iodo, but bromides and chlorides are also often utilized. The halide reactivity for this reaction is I > Br > Cl > > F because the rate-determining step is breaking of the aryl halide bond. However, the Ullman reaction has some drawbacks including difficulty in removal of copper salts and the need for speciality brominated monomers.[68, 81, 82]

1.2.1.4.Nickel coupling reaction

This novel synthetic route can utilize both activated and non-activated[83-85] aromatic dihalides for synthesis of poly(arylene ether)s. Another advantage of this reaction is its low polymerization temperature, ranging from 60 – 80 °C.[68] In this reaction, Ni^0 is used to form the carbon-carbon bond.[86] Aromatic phosphine oxide containing polymers were synthesized by Ghassemi et al.[87] via this nickel coupling route.

1.2.2. Post-sulfonation

The first sulfonation of poly(arylene ether sulfone) (PAES) was probably done by electrophilic substitution with chlorosulfonic acid.[88, 89] However, this strong reagent can cause chain scission, branching/crosslinking at the isopropylidene group of bisphenol A based polymers. Hence, a milder sulfonation route utilizing SO_3/ triethylphosphate had

also been utilized.[90-92] In 1993, Nolte et al. described sulfonation of PAES by chlorotrimethylsilane, which was generated in situ by reacting chlorosulfonic acid with trimethylchlorosilane in dichloroethane as the solvent.[93] In another novel sulfonation process, Kerres et al. sulfonated commercial polysulfone (Udel) via metalation of the polymer by lithium, and sulfination by SO_2 gas followed by oxidation of the polymeric sulfinate. [94-96] In principle, all the polymers capable of lithiation can be sulfonated in this manner. Sulfonation of poly(arylene ether ketone)s can be carried out with concentrated sulfuric acid producing one sulfuric acid group per repeat unit. The sulfonation rate can be controlled by reaction time, temperature and acid concentration.[97, 98] However, the post sulfonation process leads to substitution of a sulfonic acid group on the activated position in the aromatic ring and thus the post-sulfonated materials have less stability relative to materials prepared in a direct-sulfonation route. Post-sulfonation also does not lead to precise control of the concentration and location of the acid groups.

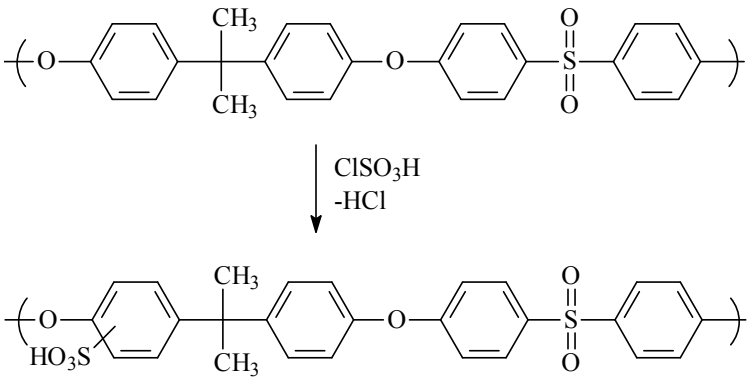

Figure 1.14 Post-sulfonation of poly(arylnene ether sulfone)[89]

1.2.3. Direct Sulfonation

Synthesis of sulfonated monomers for use as a flame retarding materials was first described by Robeson and Matzner.[99] Later, Ueda et al.[100] reported the sulfonation of 4'4''-dichlorodiphenylsulfone. More recently McGrath et al. improved the sulfonation

technique (Fig.1.15).[101-103] Similarly, direct copolymerization of poly(arylene ether ketone)s is also possible by using a sulfonated difluorophenyl ketone monomer. [104] Direct sulfonation can lead to precise control of the concentration and location of the acid groups and thus polymers with well-controlled microstructures can be generated by this method. As the sulfonic acid groups are substituted at a deactivated position in the aromatic ring, the directly sulfonated polymers are more stable compared to post sulfonated materials.

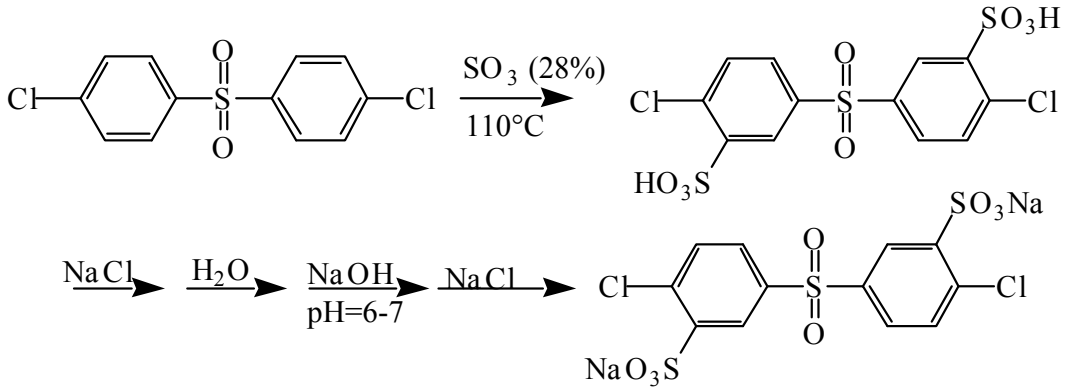

Figure 1.15 Synthesis of disulfonated 4'4''-dichlorodiphenylsulfone

1.3. Crosslinking of Poly(arylene ether sulfone)s

Poly(arylene ether sulfone)s are recognized for their excellent thermal and mechanical properties, particularly resistance to oxidation and acid catalyzed hydrolysis. One of their main advantages is that they can be chemically modified to yield polymers with specific properties. For example, these polymers can be sulfonated to obtain cation-exchange membranes. Sulfonated poly(arylene ether sulfone) membranes combine good electrochemical properties of the perfluorinated materials with low cost and advanced processability. However, such sulfonated membranes must have IECs of a minimum of 1.4 to 1.7 meq/g to have low ionic resistance that is required for applications in electromembrane processes. At such high IECs, the membranes swell strongly and this results in loss in mechanical stability and ion permselectivity. This disqualifies them for

application in electromembrane processes, particularly at high temperatures > 60-80 °C. Therefore, one objective is to reduce the swelling of these membranes and improve their mechanical stability without sacrificing significant proton conductivity. One strategy to achieve these combination of requirements is crosslinking of these membranes.

Nolte et al.[93, 105] functionalized commercially available poly(arylene ether sulfone)s such as Udel (PSU) and Victrex (PES) by sulfonation and covalently crosslinked the polymers. An in-situ crosslinking procedure was developed to crosslink the polymers during membrane processing. Some of the pendant sulfonic acid groups of the polymer were reacted with 1,1'-carbonyldiimidazole. After neutralization of the polymer matrix, the activated groups, N-sulfonylimidazoles were reacted with 4,4'-diaminodiphenylsulfone, forming sulfonamide crosslink bridges as shown in Figure 1.16.

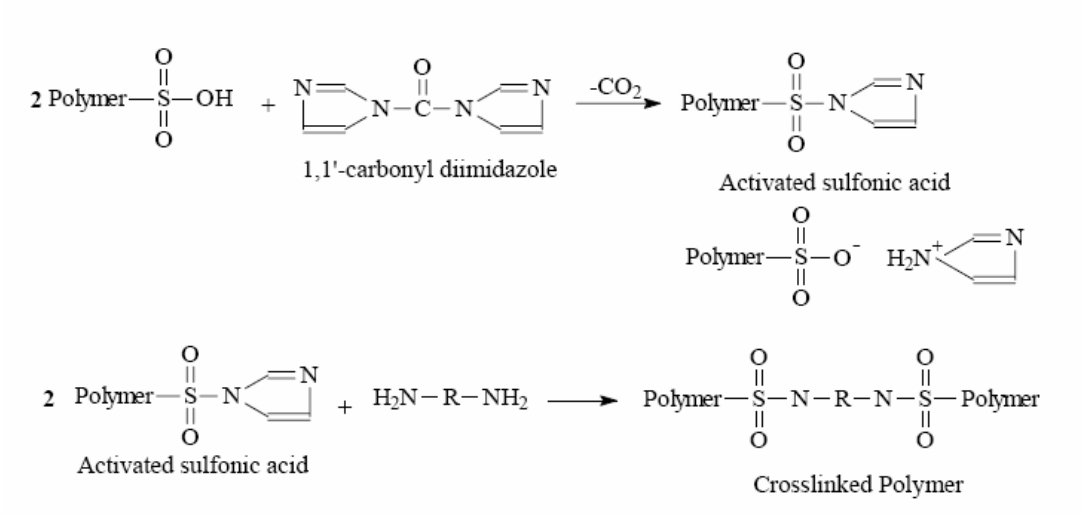

Figure 1.16 Crosslinking of sulfonated poly(arylene ether sulfone) by 1,1'-carbonyldiimidazole; Reprinted from[93] with permission from Elsevier

The crosslinked membranes had remarkable (50 %) reduction in swelling in water compared to the non-crosslinked membranes. However, the stability of the sulfonamide bridges in the strongly acidic environment in fuel cell remains a question.

Hasitosis et al. reported acid-base membranes from sulfonated polysulfones and PBI doped with phosphoric acid. These types of phosphoric acid doped membranes have the potential to be utilized at very high temperatures, e.g. 200 °C, in fuel cells. The blend membranes exhibited higher protonic conductivity and mechanical stability than pure PBI membranes.[106]

Kerres and coworkers have developed different strategies for crosslinking poly(arylene ether sulfone)s including van der Waals interactions, hydrogen bonding, ionic crosslinking, covalent crosslinking, covalent-ionic blends and composite blends.

1.3.1. Blends with Van der Waals and Dipole-Dipole interactions

The concept for this approach was to "reinforce" the sulfonated ionomer membrane with non-sulfonated polymer to improve the mechanical strength. The base polymer was the commercially polysulfone (PSU) Udel. It was discovered that van der Waals and dipole-dipole interactions in the blended membrane[107] between sulfonated and non-sulfonated polysulfone (PSU) Udel suffered from inhomogeneous morphology and consequently high swelling in water and poor mechanical properties. The inhomogeneity likely arose from the hydrophilicity associated with the sulfonic acid groups. Moreover, the very weak nature of the van der Waals and dipole-dipole forces among the two blend components were insufficient to produce a compatible blend.

1.3.2. Blended Membranes with hydrogen-bridge-interactions

Physical crosslinking through hydrogen bonds can be accomplished by blending a sulfonated ionomer with a hydrogen bridge-forming polymer. Such blended membranes from sulfonated poly(etheretherketone), polyamide (PA) and poly(etherimide) (PEI) were synthesized.[108] The membranes showed good proton conductivity. However, this approach also led to membranes with inhomogeneous morphologies, disruption of hydrogen bridges at elevated temperatures (e.g., 90 °C) and consequent high swelling. Moreover, the hydrolytic stabilities of the PA amide bond and PEI imide bond were insufficient to withstand in acidic environment of a fuel cell.

1.3.3. Ionically crosslinked membranes

Ionic crosslinking provides stronger interactions than van der Waals and hydrogen bonding interactions. Ionically crosslinked ionomer networks can be formed by mixing polymeric acids and polymeric bases that form the crosslinks by proton transfer from the polymeric acid onto the polymeric base. The interactions in such an ionically crosslinked network include both electrostatic and hydrogen bridge interactions. A wide variety of acid-base membranes has been reported. Kerres et al. have developed acid-base blended membranes by combining acidic polymers, for example sulfonated poly(ethersulfones) and poly(etherketones), with basic polymers such as polybenzimidazoles, poly(ethylene imine)s and poly(4-vinylpyridine)s. They have also developed novel basic polymers by modifying PSU backbones with NR_2 groups or with side groups including pyridine or tertiary amino groups.[109, 110]

$$P_1\text{-}\ SO_3H + P_2 - NR_2 \longrightarrow [\ P_1\text{-}\ SO_3\ ]^{-}\ [\ HR_2N\text{-}\ P_2\ ]^{+}$$

Figure 1.17 Acid-base blended membranes

These acid-base membranes had reduced brittleness upon drying compared to non-crosslinked or covalently crosslinked ionomer membranes, and this may be attributed to the flexibility of ionic crosslinks. They have also demonstrated good thermal stability, particularly with blended membranes containing PBI.[110]

1.3.4. Covalently crosslinked membranes

In a novel sulfonation process, commercial polysulfone (Udel) was sulfonated via metalation of the polymer with lithium, then sulfination with SO_2 gas followed by oxidation of the polymeric sulfinate as shown in Figure 1.18.[111]

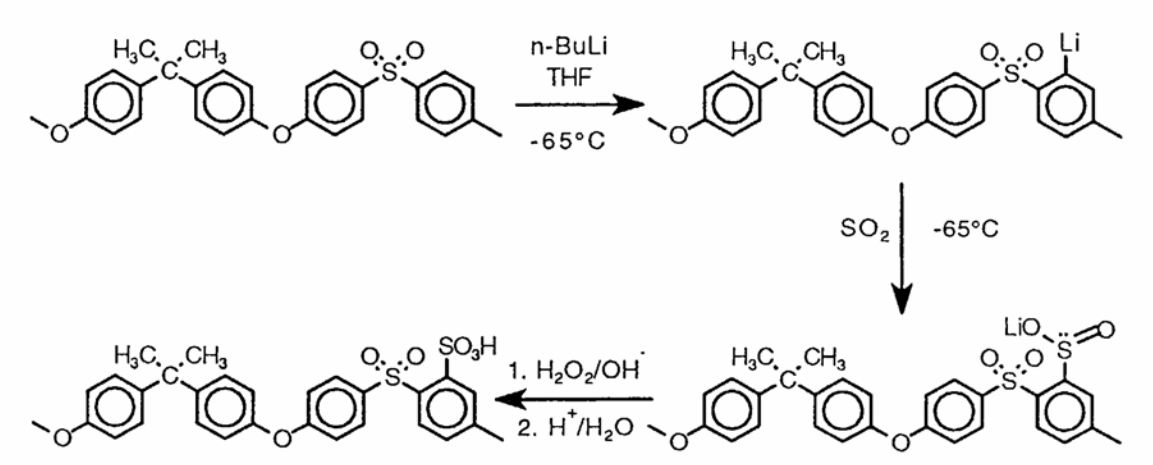

Figure 1.18 Sulfonation of Udel polysulfone via metalation; Reprinted from[111] with permission from Elsevier

In principle, any polymer that can be lithiated can be sulfonated with this approach. By this process, polymers with IECs of 0.5 to 3.2 meq/g were synthesized. However, at IEC's ≥ 2.4 meq/g, the polymers became soluble. Hence there was a need for crosslinking to enhance hydrolytic, thermal and chemical stability. Kerres and coworkers reported crosslinking of polymers containing sulfinate groups by two procedures. First, disproportionation reactions of the sulfinic acid groups led to crosslinked networks.[96] Secondly, S-alkylation of the sulfinate groups with dihalogenoalkanes also led to crosslinked materials.[95]

Crosslinking by disproportionation of the sulfinic acid groups[96]

$$3\ Ar\text{-}SO_2H \longrightarrow Ar\text{-}SO_3H + Ar\text{-}S(O)_2\text{-}S\text{-}Ar \qquad \textbf{Equation 1-1}$$

In this method crosslinked blended membranes of PSU-sulfinate and PSU-sulfonate were obtained where only PSU-sulfinate was crosslinked intra and

intermolecularly. The PSU-sulfonate chains were entangled in that network and a compatible blend was formed due to the mutual affinity of PSU sulfinic acid and PSU sulfonic acid. The crosslinking was conducted via a series of steps. First PSU-sulfinate was mixed with PSU-sulfonate in the salt form in N-methylpyrrolidone (NMP) as the solvent. Then a strongly-acidic cation-exchange resin was added in excess to convert all of the sulfinate and sulfonate groups into their acidic form. This was done in order to generate PSU-SO_2H in-situ because sulfinic acid is thermally unstable. Next the solvent was evaporated and the crosslinking took place through disproportionation of the sulfinic acid groups forming a $S(O)_2$-S- crosslinking bridge during solvent evaporation. The success of the crosslinking was confirmed by the absence of the symmetrical S=O stretching vibration of the sulfinate group in the crosslinked membranes and insolubility of the crosslinked membranes in NMP. However, there was a significant disparity between the theoretical and experimental IECs of the crosslinked blended membranes with low IEC (0, 30 and 50 wt % PSU-SO_3H content). This may be attributed to splitting off of the sulfinic acid groups, which is a competing reaction. Another reason could be that the ionic groups formed an isolated morphology at low IEC's below the percolation threshold limit of ionic conductivity, thus making the groups partially inaccessible for ion exchange. At higher IEC's, i.e. membranes containing ≥65 wt% PSU-SO_3H, the theoretical and experimental IEC's matched well. According to the authors, at 65 wt% of PSU-SO_3H, the membranes crossed the percolation threshold of ionic conductivity connecting the ionic groups and this resulted in their being available for ion exchange. Another possible explanation is that the blended membranes with the PSU-SO_3H and PSU-SO_2H components were only partially microphase separated. At higher PSU-SO_3H concentrations, the PSU-SO_2H became the discontinuous phase and was better protected against splitting off of sulfinic acid groups since the surrounding PSU-SO_3H groups could form hydrogen bonds with the SO_2H groups. These membranes had good thermal stability and they were suitable for electrodialysis, separation of pentene from pentene/pentane mixtures and for proton exchange membranes.

Crosslinking by S-alkylation of the sulfinate groups with dihalogenoalkanes[95]

$2Ar\text{-}SO_2Li + Hal\text{-}(CH_2)_x\text{-} Hal \longrightarrow Ar\text{-}S(O)_2\text{-}(CH_2)_x\text{-}S(O)_2\text{-}Ar$ Equation 1-2

In this process, crosslinked blended membranes of PSU-sulfinate and PSU-sulfonate were formed where only PSU-sulfinate was crosslinked intra and intermolecularly. The PSU-sulfonate chains were entangled in that network. Crosslinking was achieved through a nucleophilic substitution reaction between sulfinates and dihalogenoalkanes leading to S-alkylation of the sulfinate groups. The sulfinate group is an ambident nucleophile, i.e. either S or O can be alkylated. Hence one of the key steps in this process is the choice of counterion of the sulfinate group and the crosslinking halogenoalkane component. It was determined that the counterion should be a "hard" cation such as Na^+ or Li^+ and the halogenoalkane should be a "soft" dibromo or diiodoalkane for successful alkylation at the soft nucleophilic S center of the sulfinate group. First PSU-sulfonate and PSU-sulfinate were dissolved in NMP, then dihalogenoalkane crosslinking reagent was added in solution and crosslinking was completed during evaporation of the solvent. It was observed that 1,4-diiodobutane cured faster than 1,4-dibromobutane, and this was attributed to iodide being a better leaving group than bromide. In fact, polymer blend solutions containing between 40 and 70 wt % PSU-sulfinate gelled when diiodobutane was utilized as the crosslinking reagent, making dibromobutane the necessary reagent for such systems. Here also, a discrepancy in the theoretical and expected IECs of the crosslinked membranes containing high PSU-sulfinate was observed. This may be due to the fact that in those membranes, the crosslinking reaction was incomplete utilizing dibromobutane was incomplete. The crosslinked membranes had good thermal and hydrolysis stability. However, the application temperature of the crosslinked membranes, especially with high PSU-sulfonate content, was limited to below 70 °C due to excessive swelling of the membrane. In each of the above described processes, crosslinked blended membranes were formed easily. A broad property range was obtained by varying the mass ratios of the sulfonated and the sulfinated components, the IEC's of both of the blend components and by varying

the crosslinking reagents. However, the disadvantage of this process is that the sulfonated component can diffuse out of the blend membrane as it is only physically entangled in the network. This problem can be overcome if a crosslinked membrane can be formed which carries both the sulfonated and the sulfinated groups on the same polymer backbone.

A novel crosslinking route was developed in which partial oxidation of the PSU-sulfinate groups was done to generate a polymer containing both sulfinate and sulfonate groups distributed statistically over the macromolecules.[112] The residual sulfinate groups were then alkylated by dihalogenoalkanes to form a completely crosslinked membrane as shown in Figure 1.19.

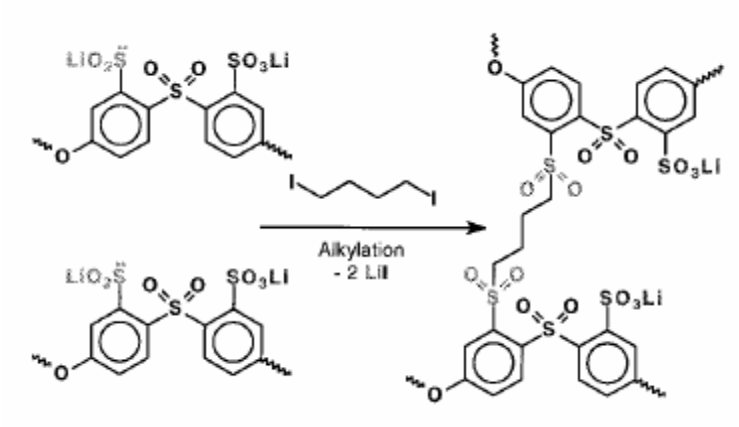

Figure 1.19 Crosslinking of partially oxidized sulfinated PSU Udel via S-alkylation of the sulfinate groups with diiodobutane; Reprinted with permission[112] from John Wiley & Sons, Inc

Crosslinked membranes from PSU-sulfinate with oxidation degrees from 40 to 60 % were of practical interest for their low resistance (100-400 Ω cm) and moderate swelling (15-100 %). The influence of the chain length of the crosslinking component on the membrane properties was also investigated. It was discovered that swelling of the membranes strongly increased with increasing chain length of the crosslinking reagent. The membranes exhibited good thermal stability and low swelling degrees which made

them promising candidates for fuel cell membranes. However, these crosslinked membranes were brittle in their dry state.

1.3.5. Covalent-Ionic Crosslinked Membranes

A procedure was developed in which covalent-ionic croslinked blended membranes were synthesized[113] to reduce brittleness of the covalently crosslinked membranes. This method reduced the disadvantages of the ionic crosslinked membranes (splitting-off of the ionic groups at T = 70-90 °C) and covalently crosslinked membranes (brittleness of dry membranes). Three types of covalent-ionic crosslinked membranes were formed.[2]

(i) A ternary covalent-ionic crosslinked blended membrane was formed comprised of polysulfonates, polysulfinates, polybases and a dihalogenoalkane crosslinking reagent which reacted with both the sulfinate groups and with tertiary amino groups by alkylation. Covalent crosslink's formed between the polysulfinates and the polybases and ionic crosslinks formed between the polysulfonates and the polybases. However, the polysulfinate and the polyamine in this this blended membrane were incompatible and the macrophase separation produced mechanical instability and high swelling at high temperatures.[114]

(ii) The limitation of type (i) was overcome by fabricating a binary blended system in which the sulfinate groups and the tertiary amino groups were distributed statistically on the same polymer backbone. Then a polybase and a dihalogenoalkane crosslinker were added and crosslinking was achieved through alkylation of both the sulfinate and tertiary amino groups.

(iii) A polymer carrying both of sulfinate and sulfonate groups was blended with a polybase to form a binary blend and crosslinking was achieved by alkylation after addition of the dihalogenoalkane crosslinking component. These networks had homogeneous morphologies in contrast to the previous types.[115] Both the ternary and the

binary blend systems showed comparable IECs and proton conductivities,[114, 115] but they differed in swelling behavior. Binary systems showed much reduced water uptake at elevated temperatures (≥ 70 °C) whereas the ternary system experienced extreme swelling at that temperature due to the phase separated morphology and splitting off of the ionic crosslinks.[116]

1.3.6. Composite Blend membranes

At elevated temperatures (≥100 °C), membranes synthesized from pure organic sulfonated ionomers tended to dry out and consequently lose their proton conductivities. An approach to overcome this problem was to introduce inorganic particles to serve as a water reservoir in the ionomer membrane. Kerres and coworkers prepared different types of hybrid membranes of crosslinked ionomers and inorganic particles.

(i) Covalently or ionic crosslinked membranes were filled with μ-sized oxide particles (SiO_2, TiO_2) or layered zirconium phosphate.[114, 115] The problem with these membranes was that the inorganic particles agglomerated in the polymer solution and after solvent evaporation, those large inorganic particles inside the membranes did not effectively adsorb water. Consequently, the proton conductivity of the membranes was reduced significantly.[115]

(ii) The agglomeration problem of type (i) was solved by synthesizing hybrid membranes. Covalent or ionic crosslinked membranes were filled with layered ZrP by a so-called ion-exchange-precipitation method.[97] Transparent membranes with evenly distributed ZrP particles were obtained. However, the proton conductivity of the hybrid membranes was lower than for the organomembranes at room temperature. According to the authors, this was due to preferential growth of the inorganic phase in the vicinity of the SO_3H ion-aggregates and the ion-conducting channels leading to hindered proton transport. At elevated temperature, the hybrid membranes showed better peak power density than the organic membranes, but further work is needed to better understand the influence of the inorganic particles on fuel cell performance.[2]

1.4. Crosslinking of Poly(arylene ether ether ketone)s (PEEK)

PEEK is an aromatic, high performance thermoplastic with high chemical and electrical properties. Its crystallinity makes it extremely thermo-mechanically stable. PEEK has shown promising proton conductivity depending on the degree of sulfonation. However, the mechanical properties of sulfonated PEEK tend to deteriorate with high levels of sulfonation leading to relatively poor long-term stability. The weak mechanical properties of the sulfonated PEEKs has stimulated research on their crosslinking.

The first reported crosslinking of PEEK[117] was achieved through bridging links between sulfonic acid groups and an aromatic or aliphatic amine. The crosslinking molecule was difunctional, having one amine functionality and another crosslinkable constituent. The process first involved sulfonating PEEK, then converting ≥ 5 % sulfonic acid groups into sulfonyl chloride, amination of the latter with amines containing ≥ 1 crosslinkable substituent or another functional group like p-aminocinnamic acid and subsequent hydrolysis of residual unreacted sulfonyl chloride groups. After the modified copolymer was cast into a membrane, the crosslinkable constituents were reacted to form a crosslinked membrane. However, the stability of the sulfonamide bonds in the strongly acidic conditions of a fuel cell was of concern. Later a modification of this process was patented[118] in which PEEK was first modified to have either pendant sulfonyl chloride groups or pendant amide groups. Then a crosslinking reagent with either terminal amide or terminal halide functions was added and an acidic imide group was formed through condensation. The modified membranes were cast into films and the crosslinking reaction was initiated by base. Residual unreacted sulfonyl chloride groups were then hydrolyzed. In this method, the acidity lost by occupation of the acid groups of the polymer in crosslinking can be compensated by the acidic imide groups formed by the crosslinker itself.

In another method,[119] crosslinking of SPEEK was performed through intra/interchain condensation of sulfonic acid functionalities via simple thermal treatment at 120 °C under vacuum. The crosslinking scheme is shown below in Figure 1.20.

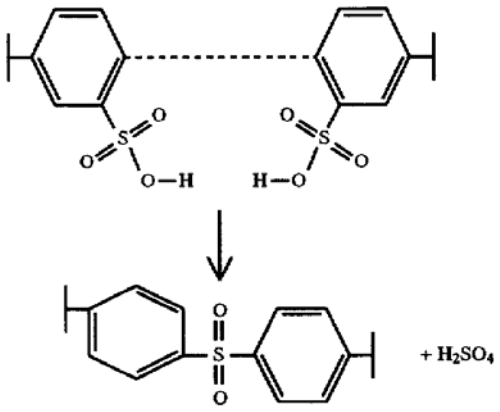

Figure 1.20 Crosslinking of SPEEK by thermal activation[119]

The large number of sulfonic acid groups in these highly sulfonated SPEEK membranes allowed for sacrifice of the sulfonic acid groups for crosslinking. However, according to Guiver et al.,[120] not only thermal treatment, but additional crosslinking reagent is needed for crosslinking of SPEEK via the method described in reference-60. Guiver and coworkers used polyatomic alcohols as the crosslinking reagents and curing was carried out through condensation reactions of the sulfonic acid groups and the alcohols as shown in Figure 1.21.

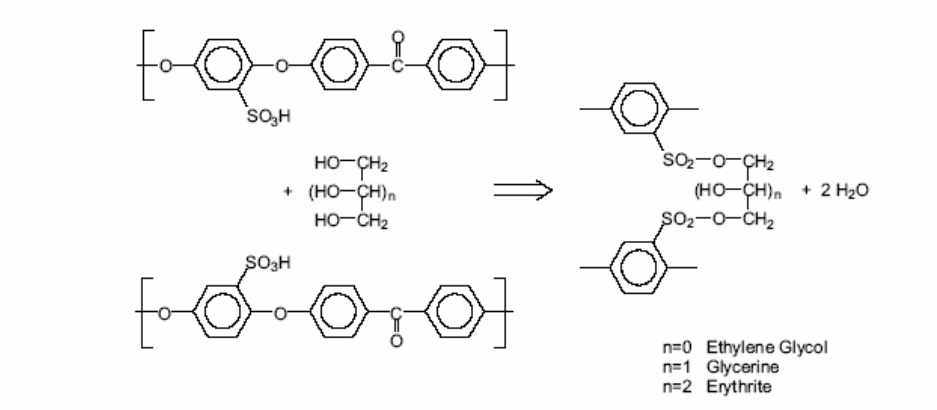

Figure 1.21 Crosslinking of SPEEK; Reprinted from[120] with permission from Elsevier

The best result was obtained from SPEEK with 0.75 < degree of sulfonation < 1.0 using a water-alcohol casting solution and ethylene glycol as the crosslinking reagent at ratios between 1.5 and 3 molecules per SPEEK repeat unit. The curing was conducted at temperatures from 25-150 °C under vacuum. Although crosslinking decreased the number of sulfonic acid groups available for proton conductivity, some of the membranes had moderate conductivity of ~0.02 S/cm at room temperature.

1.5. Reverse osmosis

The osmotic phenomenon was first observed by Abbe` Nollet[121] in 1748. In the following century, osmosis aroused much interest in the biological and medical sciences and this led to experimental research with membranes of animal and plant origin. In 1867 the first inorganic semi-permeable membrane was synthesized by Traube.[122] From then on, several membrane systems were discovered. The first commercial reverse osmosis units were made available to the public in the mid-1960's and since then the growth of the reverse osmosis industry has been enormous.[123]

1.5.1. Description of osmosis and reverse osmosis

If a semipermeable membrane separates a solution and a pure solvent, or two solutions of different concentrations, solvent flows from the less concentrated phase to the other phase to equalize concentrations. This phenomenon is called "osmosis". If pressure is exerted against the solution, the rate of flow will reduce and with increasing pressure it will be totally stopped at one point. This equilibrium pressure is called the "osmotic pressure". Further increase in pressure on the solution side forces solvent to flow to the reverse side i.e. from the solution side to the pure solvent side. This phenomenon is called "reverse osmosis".[124] Reverse osmosis bears some resemblance to filtration, because both of the processes separate liquids from other substances. For this reason, reverse osmosis is sometimes termed "ultrafiltration".

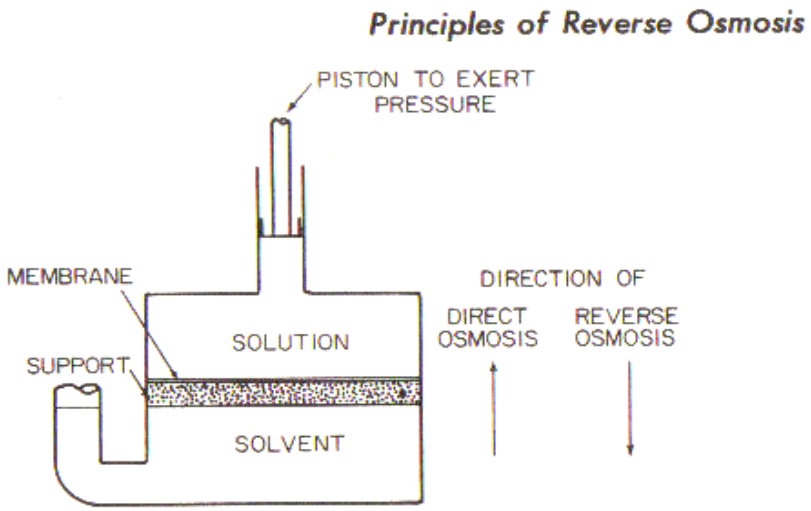

Figure 1.22 Schematic diagram of an osmotic aparatus[124]

The membrane is the key component in reverse osmosis. The membrane needs to be selective in nature i.e. it will allow only certain components of the solution (generally the solvent) to pass through it, but not the other components. Such a selective membrane is called a "semipermeable membrane".

Reverse osmosis has wide application in desalination i.e. purifying water from saline solution. There are some criteria which a membrane must meet for water desalination.[123]

i) The membrane material must be highly permeable to water, but impermeable to solutes.
ii) The membrane must be as thin as possible to maximize water flux, but at the same time should fulfill the strength requirements to withstand the pressure.
iii) The membrane should be chemically inert, mechanically robust, and creep resistant.
iv) Lastly, the membrane should be capable of being fabricated into configurations of high surface-to-volume ratio.

1.5.2. Cellulosic Films

In the mid-1950s, Prof. C. E. Reid at the University of Florida began research on the reverse osmosis process for water desalination and proposed a study entitled *Osmotic Membranes for Demineralization of Saline Water*. They investigated[125] the performance of a variety of commercial polymeric films available in the 1950s. Among those materials, the most promising membrane material was cellulose acetate which exhibited high salt rejection and was chemically inert.[126, 127] However, it suffered from very low water flux. Even very thin films (less than 10 microns) showed flux levels in magnitudes of $\mu L/cm^2h$. Reid and Breton also proposed a theory[126, 122] behind the water transport mechanism in membranes. They proposed that water molecules concentrated in the amorphous region of the membrane, filling the voids of the membrane with bound water and were transported through the membrane by hydrogen bonding with carbonyl oxygens in cellulose acetate. They also proposed that ions and molecules incapable of such hydrogen bonding passed through the membrane by "hole type diffusion" only and that this diffusion process was slow due to the small sizes of the holes. When all the holes became filled with bound water, the ions could not pass through it and the membrane became impermeable to ions.

In 1958, a new approach was attempted for desalination by reverse osmosis by Yuster et al. at UCLA.[122] A solution was pressurized directly against a flat plastic film and small quantities of fresh water resulted from this experiment. Encouraged by this experiment, Loeb, Sourirajan and Yuster developed a membrane with both high water flux and salt rejection. They discovered[128] how to cast very thin asymmetric cellulose acetate membranes. A barrier layer on one side of the asymmetric membrane afforded the salt rejection. These membranes showed some improvement in water flux, but still were not of practical use.

To improve performance, Loeb and Sourirajan hand-cast membranes from cellulose acetate.[122] Casting solutions of cellulose acetate in acetone containing aqueous magnesium perchlorate as a swelling agent or pore-forming agent were prepared and then cast onto glass plates. After briefly air-drying, the membranes were immersed in ice water and this resulted in asymmetric membranes. After several months of effort, the first practical RO membrane was developed by Loeb and Sourirajan.[129, 130] Later a major change in the casting solution was made by Manjikian,[131, 132] who used formamide as a swelling agent instead of magnesium perchlorate. Reproducible membrane synthesis was achieved with this all-organic formulation.

The properties of the asymmetric cellulose acetate membranes can be improved by annealing them in water at temperatures up to about 90 °C.[123] The highly annealed membranes consist of a dense surface skin (~ 0.2 μ) and a porous thicker support ~100 μ thickness.[133] The thin skin served as a barrier to permeation of the ions. Transport within this barrier occurs through a solution-diffusion process.[134] An extremely thin surface and a high selectivity towards water have made these membranes commercially viable.[135]

However, these membranes have some limitations. Salt rejection can be improved by increasing annealing temperature to a certain extent. However, at the same time the water flux reduces at a fixed pressure. With further increases in the annealing temperature above 90 °C, the flux continued to decrease without additional improvement of salt rejection. The other disadvantages of these membranes include poor performance

for single-pass seawater desalination and low rejection of ions such as nitrate and several low molecular weight non-ionic species. Another limitation of this membrane is loss of water flux with time which occurs mainly due to "membrane compaction" and membrane fouling.[123]

Non-Cellulosic Membranes

1.5.3. Polyamide Membranes

The cellulosic membranes had some drawbacks including biodegradability, alkaline degradability, hydrolytic (acid) instability and the tendency to creep under osmotic pressure. Thus, tremendous research was undertaken to develop non-cellulosic membranes for commercial application in reverse osmosis. Among the various polymeric classes, aromatic polyamides and polyamide-hydrazides showed potential due to their high flux and good polymeric properties.

In 1968, Richter and Hoehn[136] of Dupont discovered an aromatic polyamide-hydrazide-based reverse osmosis membrane material. This polymer was synthesized by reacting a mixture of 3-aminobenzhydrazide and 4-aminobenzhydrazide with a mixture of isophthaloyl and terephthaloyl chloride in dimethylacetamide. Membranes from this polymer had high water permeabilities, good salt rejection, good mechanical strength and could withstand high operating pressures for long times. In 1970, hollow fiber devices based on this polymer became commercially available. The fiber devices consisted of approximately a million fibers of about 90 microns in diameter with a dense outer barrier layer (~1 micron) and a moderately porous support wall adjacent to a 40-50 micron central channel.[137] Later polypiperazinamide-based reverse osmosis membranes were developed to further improve flux and salt rejection.[138] This class of polymers could be fabricated into asymmetric membranes.

"Thin film composite" membranes were developed in the 1970s. Cadotte et al. reported[139-141] thermally crosslinked membranes on polysulfone supports for reverse osmosis. A composite consisting of a microporous polysulfone film was coated with

polyethylenimine and crosslinked with toluene diisocyanate. These membranes rejected salt and organic compounds (alcohols, aldehydes, ketones, acids, amines, and acetates) well. Its excellent resistance to biodegradability, no compaction under sustained high pressure, and also good "single-pass" water desalination characteristics compared to cellulosic membranes made this type of membranes strong candidates for reverse osmosis, industrial and wastewater applications.[142]

However, these aromatic polyamide membranes also had some limitations. A major disadvantage was that because of their fiber design, the feed solution resulted in a high potential for plugging and membrane fouling. Aromatic polyamide films also had poor rejection of some materials like phenols, aldehydes, urea, methanol, and methyl acetate compounds that were present in wastewaters.[142] But the most significant shortcoming of the aromatic polyamides was their extremely low chlorine resistance. Aromatic polyamide membranes are strongly susceptible to damage by chlorination. Two possible chlorination pathways are shown in Figure 1.23 where (A) is Orton rearrangement (attack on the amide nitrogen followed by rearrangement involving aromatic ring substitution), and (B) is direct ring chlorination.

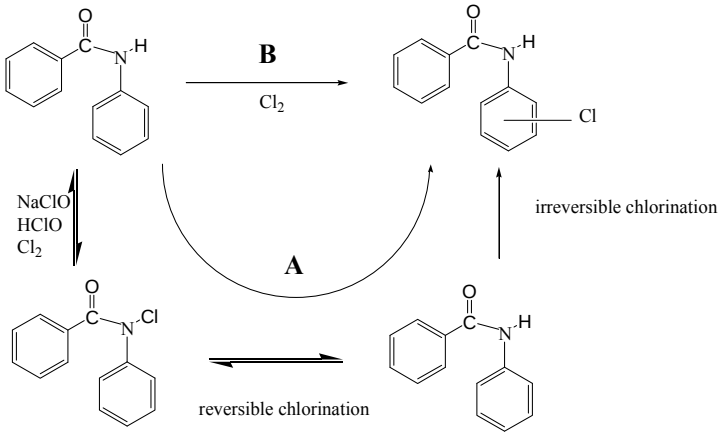

Figure 1.23 Chlorination pathways

Glater and Zachariah[143] studied a model compound benzanilide because it mimicked the repeat unit of poly-m-phenylene isophthalamide, a commercial Du Pont polyamide membrane. IR and NMR spectra suggested that halogen attack occurred on the aromatic ring by electrophilic substitution. The ring substitution comprised a mixture of meta, para and 1,2,4 substitutions because one ring is activated by the –NHCOφ group (ortho-para director), whereas the adjacent ring is deactivated by the –CONHφ group which is a meta director. These substitution patterns for the B-9 polyamide membrane are shown in the Figure 1.24.

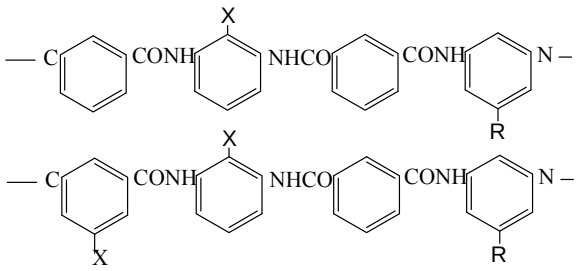

Figure 1.24 Halogen (X) substitution in aromatic polyamides[143]

Kawaguchi and Tamura[144] reported that two chemical processes occur in polyamides including a reversible N-H bond chlorination and another irreversible aromatic ring chlorination. They also demonstrated the importance of amide N-H functionality to aromatic ring chlorination.

As a result of chlorine substituents on the amide nitrogen or aromatic rings, physical deformation or chemical cleavage at amide linkages in the linear polymer chain can occur.[145] Glater et al.[145] suggested that hydrogen bonding shifted from inter to intramolecular hydrogen bonds to halogen substituents within the chain and this shift caused chain deformation followed by failure in membrane properties.[143] Avlonitis et al. proposed that the aromatic chlorination transformed the crystalline polyamides into an amorphous state where chemical attack occurs preferentially.[146] Singh showed that the

viscosity of a polyamide solution decreased after chlorine exposure indicating polymer degradation.[147]

Unlike linear polyamides, there had been fewer reports on performance changes due to chlorine degradation of crosslinked polyamides. Glater et al.[145] proposed that flux decline was due to membrane tightening resulting from chlorine substitution, and flux increase was due to bond cleavage. Soice et al. suggested that a major cause of performance loss was not due to bond cleavage, but physical separation of the polyamide skin layer from the polysulfone support.[148, 149] In a recent report, it was shown that chlorination changed the hydrogen bonding behavior among crosslinked polyamide chains resulting in changes of flexibility of polymer chains followed by deviation from membrane performance.[150]

Chlorine concentrations, pH and exposure time affect chlorination of these aromatic polyamides. Generally polyamide membranes are exposed to 500-2000 ppm.hr of sodium hypochlorite which is used to clean the membrane module or found in residual amounts as a disinfecting reagent. Aqueous chlorine solution contains three species in equilibrium. At pH=1, Cl_2 can be as high as 79%, whereas at pH=7, the solution is approximately 80% HOCl and 20% OCl^- with trace amounts of Cl_2. At pH>7, the major species is OCl^-. The oxidation strength of these species are in the order of Cl_2>HOCl>OCl^-. The dependence of aromatic ring chlorination on pH was demonstrated by Soice in a model study.[149] At pH 4, an intermediate concentration of chlorine was sufficient to cause significant chlorination, whereas the same amount of available chlorine at pH 7 only yielded minor ring chlorination. At pH 10, no ring chlorination was observed.

Sulfonated membranes

1.5.4. Sulfonated 2,6-dimethyl polyphenylene oxide (SPPO)

One of the most promising non-cellulosic membrane systems for reverse osmosis is sulfonated 2,6-dimethyl polyphenylene oxide (SPPO).[137] Ion exchange membranes are

permselective i.e. allow water to pass through but reject salts. SPPO is a negatively charged membrane where the negative sulfonate ions repel the anions of the salts in solution, making the membrane impermeable to salts. The advantage of using SPPO as compared to other polymers is that it can be solvent cast as a very thin (0.1 to 0.2 mil) unsupported membrane with very high water flux and salt rejection characteristics. Water flux and salt rejection can be controlled by controlling the ion exchange capacity of the sulfonated PPO.[151] Synthesis of sulfonated PPO was first described by Plummer et al.[152] PPO was sulfonated in chloroform at ambient conditions using chlorosulfonic acid. Later developments of SPPO systems included the preparation of composite films[153] of SPPO on porous substrates.[154, 155] Composite films having a SPPO membrane thickness of about 0.1 mil showed good performance. The two best substrates were porous polypropylene and polysulfone. The composite SPPO films have also been integrated into tubular and spiral wound RO modules and systems.[154, 156]

1.5.5. Sulfonated polysulfones

Sulfonated polysulfones are interesting candidates for reverse osmosis membrane materials.[153] In 1970 sulfonated polysulfones were prepared from poly(arylene ether sulfone)s containing p-phenylene groups by treating with $ClSO_3H$ or SO_3 in 1,2-dichloroethane.[89] The membranes had good acid, alkali and oxidation resistance against oxidizing agents like chlorine. The excellent chlorine resistance of the sulfonated poly(arylene ether sulfone)s made them attractive candidates compared to aromatic polyamides. Asymmetric semi-permeable membranes were reported from sulfonated poly(arylene ether sulfone)s in 1972.[157] Here also the polymer was sulfonated in 1, 2-dichloroethane by treatment with $ClSO_3H$. The asymmetric membranes were produced by casting the polymer solutions on glass plates, then immersing the support coated with the layer of polymer in a coagulating bath containing a mixture of water, dimethylformamide (DMF) and $NaNO_3$ and then recovering the membrane. However, precise control of the concentration and location of the sulfonic acid groups were lacking in these polymers due to the post-sulfonation technique utilized for their synthesis, and hence their reproducibility was poor.

Recently, McGrath et al. have developed a "direct copolymerization" synthesis of sulfonated biphenol-based poly(arylene ether sulfone)s (BPS) using disulfonated activated aromatic halide monomers.[44, 103, 158-164] These aromatic, film-forming copolymers have well-controlled ion concentrations with excellent oxidative, hydrolytic and mechanical stability. Membranes fabricated from these copolymers have excellent chlorine resistance over a pH range of 4-10. For example, BPS with 40% disulfonation and a commercial polyamide RO membrane were exposed to feed water containing 500 ppm chlorine at a pH of 9.5. The salt rejection of the polyamide membrane decreased by 20% after only 20 hours of exposure and it continued to decrease rapidly. In contrast, the BPS membrane did not show significant change in salt rejection, and this clearly demonstrated its excellent chlorine tolerance relative to conventional desalination membranes.[165-167] These polymers also exhibit low fouling in oily or protein contaminated water, and high water flux with moderate salt rejection.

1.6. References

1. Eisenberg, A.; Rinaudo, M., Polyelectrolytes and ionomers. *Polymer Bulletin (Berlin, Germany)* **1990,** 24, (6), 671.

2. Kerres, J. A., Blended and cross-linked ionomer membranes for application in membrane fuel cells. *Fuel Cells (Weinheim, Germany)* **2005,** 5, (2), 230-247.

3. Xing, D.; Kerres, J.; Schoenberger, F., Improved performance of sulfonated polyarylene ethers for proton exchange membrane fuel cell. *Fudan Xuebao, Ziran Kexueban* **2005,** 44, (5), 752-753.

4. Gubler, L.; Gursel, S. A.; Scherer, G. G., Radiation grafted membranes for polymer electrolyte fuel cells. *Fuel Cells* **2005,** 5, (3), 317-335.

5. Chapiro, A., Radiation-Induced Grafting. *Radiation Physics and Chemistry* **1977,** 9, (1-3), 55-67.

6. Momose, T.; Tomiie, K.; Ishigaki, I.; Okamoto, J., Radiation Grafting of Alpha,Beta,Beta-Trifluorostyrene onto Various Polymer-Films by Preirradiation Method. *Journal of Applied Polymer Science* **1989,** 37, (8), 2165-2168.

7. Momose, T.; Yoshioka, H.; Ishigaki, I.; Okamoto, J., Radiation Grafting of Alpha, Beta, Beta-Trifluorostyrene onto Poly(Ethylene-Tetrafluoroethylene) Film by Preirradiation Method .2. Properties of Cation-Exchange Membrane Obtained by Sulfonation and Hydrolysis of the Grafted Film. *Journal of Applied Polymer Science* **1989,** 38, (11), 2091-2101.

8. Momose, T.; Yoshioka, H.; Ishigaki, I.; Okamoto, J., Radiation Grafting of Alpha,Beta,Beta-Trifluorostyrene onto Poly(Ethylene-Tetrafluoroethylene) Film by Preirradiation Method .1. Effects of Preirradiation Dose, Monomer Concentration,

Reaction Temperature, and Film Thickness. *Journal of Applied Polymer Science* **1989,** 37, (10), 2817-2826.

9. Stone, C.; Steck, A. E.; Choudhury, B. Graft fluoropolymer membranes and ion-exchange membranes formed therefrom. 2001-9341762002137806, 20010821., 2002.

10. Stone, C.; Steck, A. E. Electron beam-grafted trifluorovinyl arom. polymers as ion exchange membranes, especially for fuel cell separators and dialysis membranes. 2000-CA3372001058576, 20000329., 2001.

11. Assink, R. A.; Arnold, C.; Hollandsworth, R. P., Preparation of Oxidatively Stable Cation-Exchange Membranes by the Elimination of Tertiary Hydrogens. *Journal of Membrane Science* **1991,** 56, (2), 143-151.

12. Becker, W.; Schmidt-Naake, G., Properties of polymer exchange membranes from irradiation introduced graft polymerization. *Chemical Engineering & Technology* **2001,** 24, (11), 1128-1132.

13. Lehtinen, T.; Sundholm, G.; Sundholm, F., Effect of crosslinking on the physicochemical properties of proton conducting PVDF-g-PSSA membranes. *Journal of Applied Electrochemistry* **1999,** 29, (6), 677-683.

14. Buchi, F. N.; Gupta, B.; Haas, O.; Scherer, G. G., Study of Radiation-Grafted Fep-G-Polystyrene Membranes as Polymer Electrolytes in Fuel-Cells. *Electrochimica Acta* **1995,** 40, (3), 345-353.

15. Gubler, L.; Kuhn, H.; Schmidt, T. J.; Scherer, G. G.; Brack, H. P.; Simbeck, K., Performance and durability of membrane electrode assemblies based on radiation-grafted FEP-g-polystyrene membranes. *Fuel Cells (Weinheim, Germany)* **2004,** 4, (3), 196-207.

16. Gupta, B.; Scherer, G. G., Proton-Exchange Membranes by Radiation-Induced Graft-Copolymerization of Monomers into Teflon-Fep Films. *Chimia* **1994,** 48, (5), 127-137.

17. Gupta, B.; Buchi, F. N.; Scherer, G. G., Cation-Exchange Membranes by Preirradation Grafting of Styrene into Fep Films .1. Influence of Synthesis Conditions. *Journal of Polymer Science Part a-Polymer Chemistry* **1994,** 32, (10), 1931-1938.

18. Buchi, F. N.; Gupta, B.; Haas, O.; Scherer, G. G., Performance of Differently Cross-Linked, Partially Fluorinated Proton-Exchange Membranes in Polymer Electrolyte Fuel-Cells. *Journal of the Electrochemical Society* **1995,** 142, (9), 3044-3048.

19. Schmidt, T. J.; Simbeck, K.; Scherer, G. G., Influence of cross-linking on performance of radiation-grafted and sulfonated FEP 25 membranes in H-2-O-2 PEFC. *Journal of the Electrochemical Society* **2005,** 152, (1), A93-A97.

20. Brack, H. P.; Buhrer, H. G.; Bonorand, L.; Scherer, G. G., Grafting of pre-irradiated poly(ethylene-alt-tetrafluoroethylene) films with styrene: influence of base polymer film properties and processing parameters. *Journal of Materials Chemistry* **2000,** 10, (8), 1795-1803.

21. Brack, H. P.; Buchi, F. N.; Huslage, J.; Rota, M.; Scherer, G. G., Development of radiation-grafted membranes for fuel cell applications based on poly(ethylene-alt-tetrafluoroethylene). *Membrane Formation and Modification* **2000,** 744, 174-188.

22. Gubler, L.; Prost, N.; Gursel, S. A.; Scherer, G. G., Proton exchange membranes prepared by radiation grafting of styrene/divinylbenzene onto poly(ethylene-alt-tetrafluoroethylene) for low temperature fuel cells. *Solid State Ionics* **2005,** 176, (39-40), 2849-2860.

23. Brack, H. P.; Fischer, D.; Peter, G.; Slaski, M.; Scherer, G. G., Infrared and Raman spectroscopic investigation of crosslinked polystyrenes and radiation-grafted films. *Journal of Polymer Science Part a-Polymer Chemistry* **2004,** 42, (1), 59-75.

24. Becker, W.; Schmidt-Naake, G., Proton exchange membranes by irradiation induced grafting of styrene onto FEP and ETFE: Influences of the crosslinker N,N,-methylene-bis-acrylamide. *Chemical Engineering & Technology* **2002,** 25, (4), 373-377.

25. Hietala, S.; Paronen, M.; Holmberg, S.; Nasman, J.; Juhanoja, J.; Karjalainen, M.; Serimaa, R.; Toivola, M.; Lehtinen, T.; Parovuori, K.; Sundholm, G.; Ericson, H.; Mattsson, B.; Torell, L.; Sundholm, F., Phase separation and crystallinity in proton conducting membranes of styrene grafted and sulfonated poly(vinylidene fluoride). *Journal of Polymer Science Part a-Polymer Chemistry* **1999,** 37, (12), 1741-1753.

26. Serpico, J. M.; Ehrenberg, S. G.; Fontanella, J. J.; Jiao, X.; Perahia, D.; McGrady, K. A.; Sanders, E. H.; Kellogg, G. E.; Wnek, G. E., Transport and structural studies of sulfonated styrene-ethylene copolymer membranes. *Macromolecules* **2002,** 35, (15), 5916-5921.

27. Chen, S. L.; Benziger, J. B.; Bocarsly, A. B.; Zhang, T., Photo-cross-linking of sulfonated styrene-ethylene-butylene copolymer membranes for fuel cells. *Industrial & Engineering Chemistry Research* **2005,** 44, (20), 7701-7705.

28. Pivovar, B. S.; Wang, Y. X.; Cussler, E. L., Pervaporation membranes in direct methanol fuel cells. *Journal of Membrane Science* **1999,** 154, (2), 155-162.

29. Rhim, J. W.; Park, H. B.; Lee, C. S.; Jun, J. H.; Kim, D. S.; Lee, Y. M., Crosslinked poly(vinyl alcohol) membranes containing sulfonic acid group : proton and methanol transport through membranes. *Journal of Membrane Science* **2004,** 238, (1-2), 143-151.

30. Kim, D. S.; Park, H. B.; Lee, C. H.; Lee, Y. M.; Moon, G. Y.; Nam, S. Y.; Hwang, H. S.; Yun, T. I.; Rhim, J. W., Preparation of ion exchange membranes for fuel cell based on crosslinked poly(vinyl alcohol) with poly(acrylic acid-co-maleic acid). *Macromolecular Research* **2005,** 13, (4), 314-320.

31. Rhim, J. W.; Hwang, H. S.; Kim, D. S.; Park, H. B.; Lee, C. H.; Lee, Y. M.; Moon, G. Y.; Nam, S. Y., Aging effect of poly(vifiyl alcohol) membranes crosslinked with poly(acrylic acid-co-maleic acid). *Macromolecular Research* **2005,** 13, (2), 135-140.

32. Einsla, B. R.; Hong, Y. T.; Kim, Y. S.; Wang, F.; Gunduz, N.; Mcgrath, J. E., Sulfonated naphthalene dianhydride based polyimide copolymers for proton-exchange-

membrane fuel cells. I. Monomer and copolymer synthesis. *Journal of Polymer Science Part a-Polymer Chemistry* **2004,** 42, (4), 862-874.

33. Kim, D. S.; Park, H. B.; Rhim, J. W.; Lee, Y. M., Proton conductivity and methanol transport behavior of cross-linked PVA/PAA/silica hybrid membranes. *Solid State Ionics* **2005,** 176, (1-2), 117-126.

34. Rhim, J. W.; Yeom, C. K.; Kim, S. W., Modification of poly(vinyl alcohol) membranes using sulfur-succinic acid and its application to pervaporation separation of water-alcohol mixtures. *Journal of Applied Polymer Science* **1998,** 68, (11), 1717-1723.

35. Rhim, J. W.; Yoon, S. W.; Kim, S. W.; Lee, K. H., Pervaporation separation and swelling measurement of acetic acid-water mixtures using crosslinked PVA membranes. *Journal of Applied Polymer Science* **1997,** 63, (4), 521-527.

36. Rhim, J. W.; Sohn, M. Y.; Lee, K. H., Pervaporation Separation of Binary Organic Aqueous Liquid-Mixtures Using Cross-Linked Pva Membranes .2. Phenol Water Mixtures. *Journal of Applied Polymer Science* **1994,** 52, (9), 1217-1222.

37. Rhim, J. W.; Sohn, M. Y.; Joo, H. J.; Lee, K. H., Pervaporation Separation of Binary Organic-Aqueous Liquid-Mixtures Using Cross-Linked Pva Membranes .1. Characterization of the Reaction between Pva and Paa. *Journal of Applied Polymer Science* **1993,** 50, (4), 679-684.

38. Wycisk, R.; Pintauro, P. N.; Wang, W.; OConnor, S., Polyphosphazene membranes .1. Solid-state photocrosslinking of poly[(4-ethylphenoxy)(phenoxy)phosphazene]. *Journal of Applied Polymer Science* **1996,** 59, (10), 1607-1617.

39. Allcock, H. R.; Fitzpatrick, R. J.; Salvati, L., Sulfonation of (Aryloxy)Phosphazenes and (Arylamino)Phosphazenes - Small-Molecule Compounds, Polymers and Surfaces. *Chemistry of Materials* **1991,** 3, (6), 1120-1132.

40. Wycisk, R.; Pintauro, P. N., Sulfonated polyphosphazene ion-exchange membranes. *Journal of Membrane Science* **1996,** 119, (1), 155-160.

41. Tang, H.; Pintauro, P. N.; Guo, Q. H.; O'Connor, S., Polyphosphazene membranes. III. Solid-state characterization and properties of sulfonated poly[bis(3-methylphenoxy)phosphazene]. *Journal of Applied Polymer Science* **1999,** 71, (3), 387-399.

42. Graves, R.; Pintauro, P. N., Polyphosphazene membranes. II. Solid-state photocrosslinking of poly[(alkylphenoxy)(phenoxy)phosphazene] films. *Journal of Applied Polymer Science* **1998,** 68, (5), 827-836.

43. Guo, Q. H.; Pintauro, P. N.; Tang, H.; O'Connor, S., Sulfonated and crosslinked polyphosphazene-based proton-exchange membranes. *Journal of Membrane Science* **1999,** 154, (2), 175-181.

44. Hickner, M. A.; Ghassemi, H.; Kim, Y. S.; Einsla, B. R.; McGrath, J. E., Alternative polymer systems for proton exchange membranes (PEMs). *Chemical Reviews* **2004,** 104, (10), 4587-4611.

45. Zhou, X. Y.; Weston, J.; Chalkova, E.; Hofmann, M. A.; Ambler, C. M.; Allcock, H. R.; Lvov, S. N., High temperature transport properties of polyphosphazene membranes for direct methanol fuel cells. *Electrochimica Acta* **2003,** 48, (14-16), 2173-2180.

46. Chang, Y. K.; Allcock, H. R., A covalently interconnected phosphazene-silicate hybrid network: Synthesis, characterization, and hydrogel diffusion-related application. *Advanced Materials* **2003,** 15, (6), 537-541.

47. Wycisk, R.; Lee, J. K.; Pintauro, P. N., Sulfonated polyphosphazene-polybenzimidazole membranes for DMFCs. *Journal of the Electrochemical Society* **2005,** 152, (5), A892-A898.

48. Kosmala, B.; Schauer, J., Ion-exchange membranes prepared by blending sulfonated poly(2,6-dimethyl-1,4-phenylene oxide) with polybenzimidazole. *Journal of Applied Polymer Science* **2002,** 85, (5), 1118-1127.

49. Bouzek, K.; Moravcova, S.; Samec, Z.; Schauer, J., H+ and Na+ ion transport properties of sulfonated poly(2,6-dimethyl-1,4-phenyleneoxide) membranes. *Journal of the Electrochemical Society* **2003,** 150, (6), E329-E336.

50. Hedrick, J. L.; Mohanty, D. K.; Johnson, B. C.; Viswanathan, R.; Hinkley, J. A.; McGrath, J. E., Radiation resistant amorphous-all aromatic polyarylene ether sulfones: synthesis, characterization, and mechanical properties. *Journal of Polymer Science, Part A: Polymer Chemistry* **1986,** 24, (2), 287-300.

51. Hedrick, J. L.; Dumais, J. J.; Jelinski, L. W.; Patsiga, R. A.; McGrath, J. E., Synthesis and characterization of deuterated poly(arylene ether sulfones). *Journal of Polymer Science, Part A: Polymer Chemistry* **1987,** 25, (8), 2289-300.

52. Hedrick, J.; Twieg, R.; Matray, T.; Carter, K., Heterocycle-Activated Aromatic Nucleophilic-Substitution - Poly(Aryl Ether Phenylquinoxalines) .2. *Macromolecules* **1993,** 26, (18), 4833-4839.

53. Strukelj, M.; Hedrick, J. C., Synthesis and Characterization of Novel Poly(aryl ether pyridyltriazine)s. *Macromolecules* **1994,** 27, (26), 7511-21.

54. Strukelj, M.; Hedrick, J. C.; Hedrick, J. L.; Twieg, R. J., Solvent Effects on the Preparation of Novel Amorphous Poly(aryl ether benzil)s. *Macromolecules* **1994,** 27, (22), 6277-85.

55. Roovers, J.; Cooney, J. D.; Toporowski, P. M., Synthesis and Characterization of Narrow Molecular-Weight Distribution Fractions of Poly(Aryl Ether Ether Ketone). *Macromolecules* **1990,** 23, (6), 1611-1618.

56. Wang, F.; Roovers, J., Functionalization of Poly(Aryl Ether Ether Ketone) (Peek) - Synthesis and Properties of Aldehyde and Carboxylic-Acid Substituted Peek. *Macromolecules* **1993,** 26, (20), 5295-5302.

57. Singh, R.; Hay, A. S., Synthesis and Physical-Properties of Poly(Aryl Ether Phthalazine)S. *Macromolecules* **1992,** 25, (3), 1025-1032.

58. Singh, R.; Hay, A. S., Synthesis and Physical-Properties of Soluble, Amorphous Poly(Ether Ketone)S Containing the Ortho-Dibenzoylbenzene Moiety. *Macromolecules* **1992,** 25, (3), 1017-1024.

59. Johnson, R. N.; Farnham, A. G.; Clendinning, R. A.; Hale, W. F.; Merriam, C. N., Poly(aryl ethers) by nucleophilic aromatic substitution. I. Synthesis and properties. *Journal of Polymer Science, Polymer Chemistry Edition* **1967,** 5, (9), 2375-98.

60. March, J., *ADVANCED ORGANIC CHEMISTRY Reactions,mechanisms, and structure*. second ed.; McGraw-Hill, Inc.: 1977.

61. Bunnett, J. F.; Zahler, R. E., Aromatic nucleophilic substitution reactions. *Chemical Reviews (Washington, DC, United States)* **1951,** 49, 273-412.

62. Schulze, S. R.; Baron, A. L., Kinetics of solution polycondensation of aromatic polyethers. *Advances in Chemistry Series* **1969,** No. 91, 692-702.

63. Fyfe, C. A.; Koll, A.; Damji, S. W. H.; Malkiewich, C. D.; Forte, P. A., Flow nuclear magnetic resonance detection and characterization of an intermediate on the reaction pathway in a nucleophilic aromatic substitution reaction. *Canadian Journal of Chemistry* **1977,** 55, (9), 1468-72.

64. Messmer, G. G.; Palenik, G. J., Crystal structure of a Meisenheimer complex: the potassium methoxide adduct of 4-methoxy-5,7-dinitrobenzofurazan. *Journal of the Chemical Society [Section] D: Chemical Communications* **1969**, (9), 470.

65. Berliner, E.; Monack, L. C., Nucleophilic displacement in the benzene series. *Journal of the American Chemical Society* **1952,** 74, 1574-9.

66. Carter, K. R., Aryl fluoride monomers in nucleophilic aromatic substitution polymerization: evaluation of monomer reactivity by 19F NMR spectroscopy. *Macromolecules* **1995,** 28, (19), 6462-70.

67. Loudon, J. D.; Shulman, N., Mobility of groups in chloronitrodiphenyl sulfones. *Journal of the Chemical Society* **1941**, 722-7.

68. Harrison, W. L. Synthesis and characterization of sulfonated poly(arylene ether sulfone) copolymers via direct copolymerization: candidates for proton exchange membrane fuel cells, Ph.D. Dissertation, Virginia Polytechnic Institue and State University, Blacksburg, Virginia, 2002.

69. Storozhuk, I. P.; Bakhmutov, V. I.; Mikitaev, A. K.; Valetskii, P. M.; Musaev, Y. I.; Korshak, V. V.; Fedin, E. I., Effect of hydrogen bonding on the formation of poly(arylenesulfone oxides). *Vysokomolekulyarnye Soedineniya, Seriya A* **1977,** 19, (8), 1800-6.

70. Clendinning, R. A.; Farnham, A. G.; Zutty, N. L.; Priest, D. C. 847963, 1970.

71. Viswanathan, R.; Johnson, B. C.; Mcgrath, J. E., Synthesis, Kinetic Observations and Characteristics of Polyarylene Ether Sulfones Prepared Via a Potassium Carbonate Dmac Process. *Polymer* **1984,** 25, (12), 1827-1836.

72. Viswanathan, R.; Mcgrath, J. E., Semi-Crystalline Poly(Arylene Ether Sulfone) Copolymers. *Abstracts of Papers of the American Chemical Society* **1979**, (Sep), 58-58.

73. Mohanty, D. K.; Walstrom, A. M.; Ward, T. C.; Mcgrath, J. E., Synthesis and Characterization of Polyarylene Ether Nitriles. *Abstracts of Papers of the American Chemical Society* **1986,** 192, 93-Poly.

74. Hedrick, J. L.; Mohanty, D. K.; Johnson, B. C.; Viswanathan, R.; Hinkley, J. A.; Mcgrath, J. E., Radiation Resistant Amorphous All Aromatic Polyarylene Ether Sulfones - Synthesis, Characterization, and Mechanical-Properties. *Journal of Polymer Science Part a-Polymer Chemistry* **1986,** 24, (2), 287-300.

75. Hedrick, J. L.; Dumais, J. J.; Jelinski, L. W.; Patsiga, R. A.; Mcgrath, J. E., Synthesis and Characterization of Deuterated Poly(Arylene Ether Sulfones). *Journal of Polymer Science Part a-Polymer Chemistry* **1987,** 25, (8), 2289-2300.

76. Wang, S. PhD Thesis. Ph.D. Thesis, Virginia Polytechnic Institute and State University, Blacksburg, 2000.

77. Ivin, K. J.; Rose, J. B., Polysulfones: organic and physical chemistry. *Advances in Macromolecular Chemistry* **1968,** 1, 335-406.

78. Rose, J. B., Preparation and properties of poly(arylene ether sulfones). *Polymer* **1974,** 15, (7), 456-65.

79. Olah, G. A., Friedel-Crafts Chemistry. *Friedel-Crafts Chemistry Wiley, New York* **1973**, 488.

80. Farnham, A. G.; Johnson, R. N. Polyarylene polyethers. 3332909, 19650715., 1967.

81. Jurek, M. J.; Mcgrath, J. E., Synthesis of Poly(Arylene Ethers) Via the Ullmann Condensation Reaction. *Abstracts of Papers of the American Chemical Society* **1987,** 193, 113-POLY.

82. Burgoyne, W. F., Jr.; Vrtis, R. N.; Robeson, L. M. Nonhalogenated poly(arylene ether) dielectrics. 96-305114758664, 19960711., 1997.

83. Phillips, R. W.; Sheares, V. V.; Samulski, E. T.; DeSimone, J. M., Isomeric Poly(benzophenone)s: synthesis of Highly Crystalline Poly(4,4'-benzophenone) and Amorphous Poly(2,5-benzophenone), a Soluble Poly(p-phenylene) Derivative. *Macromolecules* **1994,** 27, (8), 2354-6.

84. Pei, J.; Yu, W.-L.; Ni, J.; Lai, Y.-H.; Huang, W.; Heeger, A. J., Thiophene-Based Conjugated Polymers for Light-Emitting Diodes: Effect of Aryl Groups on Photoluminescence Efficiency and Redox Behavior. *Macromolecules* **2001,** 34, (21), 7241-7248.

85. Ghassemi, H.; McGrath, J. E., Proton-conducting polymers derived from poly(p-phenylene)s. *Polymer Preprints (American Chemical Society, Division of Polymer Chemistry)* **2002,** 43, (2), 1021-1022.

86. Colon, I.; Kwiatkowski, G. T., High-molecular-weight aromatic polymers by nickel coupling of aryl polychlorides. *Journal of Polymer Science, Part A: Polymer Chemistry* **1990,** 28, (2), 367-83.

87. Ghassemi, H.; McGrath, J. E., Synthesis of poly(arylene phosphine oxide) by nickel-catalyzed coupling polymerization. *Polymer* **1997,** 38, (12), 3139-3143.

88. Brousse, C.; Chapurlat, R.; Quentin, J. P., New membranes for reverse osmosis. I. Characteristics of the base polymer: sulfonated polysulfones. *Desalination* **1976,** 18, (2), 137-53.

89. Quentin, J. P. Polysulfones. DE 70-2021383, 19700430., 1970.

90. Johnson, B. C.; Yilgor, I.; Tran, C.; Iqbal, M.; Wightman, J. P.; Lloyd, D. R.; Mcgrath, J. E., Synthesis and Characterization of Sulfonated Poly(Arylene Ether Sulfones). *Journal of Polymer Science Part a-Polymer Chemistry* **1984,** 22, (3), 721-737.

91. Noshay, A.; Robeson, L. M., Sulfonated polysulfone. *Journal of Applied Polymer Science* **1976,** 20, (7), 1885-903.

92. O'Gara, J. F.; Williams, D. J.; MacKnight, W. J.; Karasz, F. E., Random homogeneous sodium sulfonate polysulfone ionomers: preparation, characterization, and blend studies. *Journal of Polymer Science, Part B: Polymer Physics* **1987,** 25, (7), 1519-36.

93. Nolte, R.; Ledjeff, K.; Bauer, M.; Muelhaupt, R., Partially sulfonated poly(arylene ether sulfone) - a versatile proton conducting membrane material for modern energy conversion technologies. *Journal of Membrane Science* **1993,** 83, (2), 211-20.

94. Kerres, J.; Zhang, W.; Cui, W., New sulfonated engineering polymers via the metalation route. II. Sulfinated/sulfonated poly(ether sulfone) PSU Udel and its crosslinking. *Journal of Polymer Science, Part A: Polymer Chemistry* **1998,** 36, (9), 1441-1448.

95. Kerres, J.; Cui, W.; Junginger, M., Development and characterization of crosslinked ionomer membranes based upon sulfinated and sulfonated PSU - Crosslinked PSU blend membranes by alkylation of sulfinate groups with dihalogenoalkanes. *Journal of Membrane Science* **1998,** 139, (2), 227-241.

96. Kerres, J.; Cui, W.; Disson, R.; Neubrand, W., Development and characterization of crosslinked ionomer membranes based upon sulfinated and sulfonated PSU - Crosslinked PSU blend membranes by disproportionation of sulfinic acid groups. *Journal of Membrane Science* **1998,** 139, (2), 211-225.

97. Bauer, B.; Jones, D. J.; Roziere, J.; Tchicaya, L.; Alberti, G.; Casciola, M.; Massinelli, L.; Peraio, A.; Besse, S.; Ramunni, E., Electrochemical characterisation of sulfonated polyetherketone membranes. *Journal of New Materials for Electrochemical Systems* **2000,** 3, (2), 93-98.

98. Bailly, C.; Williams, D. J.; Karasz, F. E.; Macknight, W. J., The Sodium-Salts of Sulfonated Poly(Aryl-Ether-Ether-Ketone) (Peek) - Preparation and Characterization. *Polymer* **1987,** 28, (6), 1009-1016.

99. Robeson, L. M.; Matzner, M., US Patent. *to Union carbide,Inc* **1983,** 4,380,598.

100. Ueda, M.; Toyota, H.; Ouchi, T.; Sugiyama, J.; Yonetake, K.; Masuko, T.; Teramoto, T., Synthesis and characterization of aromatic poly(ether sulfone)s containing pendent sodium sulfonate groups. *Journal of Polymer Science, Part A: Polymer Chemistry* **1993,** 31, (4), 853-8.

101. Sankir, M.; Bhanu, V. A.; Harrison, W. L.; Ghassemi, H.; Wiles, K. B.; Glass, T. E.; Brink, A. E.; Brink, M. H.; McGrath, J. E., Synthesis and characterization of 3,3 '-disulfonated-4,4 '-dichlorodiphenyl sulfone (SDCDPS) monomer for proton exchange membranes (PEM) in fuel cell applications. *Journal of Applied Polymer Science* **2006,** 100, (6), 4595-4602.

102. Wang, F.; Hickner, M.; Ji, Q.; Harrison, W.; Mecham, J.; Zawodzinski, T. A.; McGrath, J. E., Synthesis of highly sulfonated poly(arylene ether sulfone) random

(statistical) copolymers via direct polymerization. *Macromolecular Symposia* **2001,** 175, 387-395.

103. Wang, F.; Hickner, M.; Kim, Y. S.; Zawodzinski, T. A.; McGrath, J. E., Direct polymerization of sulfonated poly(arylene ether sulfone) random (statistical) copolymers: candidates for new proton exchange membranes. *Journal of Membrane Science* **2002,** 197, (1-2), 231-242.

104. Wang, F.; Li, J.; Chen, T.; Xu, J., Synthesis of poly(ether ether ketone) with high content of sodium sulfonate groups and its membrane characteristics. *Polymer* **1998,** 40, (3), 795-799.

105. Nolte, R.; Ledjeff, K.; Bauer, M.; Muelhaupt, R., Modified polysulfones as membrane electrolytes. *BHR Group Conference Series Publication* **1993,** 3, (Effective Membrane Processes--New Perspectives), 381-5.

106. Hasiotis, C.; Deimede, V.; Kontoyannis, C., New polymer electrolytes based on blends of sulfonated polysulfones with polybenzimidazole. *Electrochimica Acta* **2001,** 46, (15), 2401-2406.

107. Zhang, W.; Tang, C. M.; Kerres, J., Development and characterization of sulfonated-unmodiftied and sulfonated-aminated PSU Udel (R) blend membranes. *Separation and Purification Technology* **2001,** 22-3, (1-3), 209-221.

108. Cui, W.; Kerres, J.; Eigenberger, G., Development and characterization of ion-exchange polymer blend membranes. *Separation and Purification Technology* **1998,** 14, (1-3), 145-154.

109. Kerres, J.; Ullrich, A.; Meier, F.; Haring, T., Synthesis and characterization of novel acid-base polymer blends for application in membrane fuel cells. *Solid State Ionics* **1999,** 125, (1-4), 243-249.

110. Kerres, J.; Ullrich, A.; Haring, T.; Baldauf, M.; Gebhardt, U.; Preidel, W., Preparation, characterization and fuel cell application of new acid-base blend membranes. *Journal of New Materials for Electrochemical Systems* **2000,** 3, (3), 229-239.

111. Roizard, D.; Clement, R.; Lochon, P.; Kerres, J.; Eigenberger, G., Synthesis, characterization and transport properties of a new siloxane-phosphazene copolymer. Extraction of n-butanol from water by pervaporation. *Journal of Membrane Science* **1996,** 113, (1), 151-60.

112. Kerres, J.; Zhang, W.; Cui, W., New sulfonated engineering polymers via the metalation route. II. Sulfinated/sulfonated poly (ether sulfone) PSU Udel and its crosslinking. *Journal of Polymer Science Part a-Polymer Chemistry* **1998,** 36, (9), 1441-1448.

113. Kerres, J.; Zhang, W.; Tang, C.-M. Covalently- and ionically-crosslinked polymers for use in membranes. 2000-10024576
10024576, 20000519., 2001.

114. Feichtinger, J.; Kerres, J.; Schulz, A.; Walker, M.; Schumacher, U., Plasma modifications of membranes for PEM fuel cells. *Journal of New Materials for Electrochemical Systems* **2002,** 5, (3), 155-162.

115. Kerres, J.; Hein, M.; Zhang, W.; Graf, S.; Nicoloso, N., Development of new blend membranes for polymer electrolyte fuel cell applications. *Journal of New Materials for Electrochemical Systems* **2003,** 6, (4), 223-229.

116. Jorissen, L.; Gogel, V.; Kerres, J.; Garche, J., New membranes for direct methanol fuel cells. *Journal of Power Sources* **2002,** 105, (2), 267-273.

117. Helmer-Metzmann, F.; Osan, F.; Schneller, A.; Ritter, H.; Ledjeff, K.; Nolte, R.; Thorwirth, R. Preparation of sulfonated aromatic polyether ketones as polyelectrolyte membranes. 93-109139
574791, 19930607., 1993.

118. Mao, S. S.; Hamrock, S. J.; Ylitalo, D. A. Crosslinked sulfonated PEEK polyelectrolyte membranes. 99-US1782
9961141, 19990128., 1999.

119. Yen, S.-p. S.; Narayanan, S. R.; Halpert, G.; Graham, E.; Yavrouian, A. Processed sulfonic acid polymer for proton-conducting electrolytic membranes for fuel cells. 96-US188239719480, 19961122., 1997.

120. Mikhailenko, S. U. D.; Wang, K. P.; Kaliaguine, S.; Xing, P. X.; Robertson, G. P.; Guiver, M. D., Proton conducting membranes based on cross-linked sulfonated poly(ether ether ketone) (SPEEK). *Journal of Membrane Science* **2004,** 233, (1-2), 93-99.

121. Nollet, J. A., *Lecons de physique experimentale,Hippolyte-Louis Guerin and Louis-Francios Delatour,Paris* **1748**.

122. Glater, J., The early history of reverse osmosis membrane development. *Desalination* **1998,** 117, (1-3), 297-309.

123. Lonsdale, H. K.; Podall, H. E., ed.,, *Reverse Osmosis Membrane Research* Plenum Press,NewYork-London: 1972.

124. Merten, U.; Editor, *Desalination by Reverse Osmosis*. 1966; p 289 pp.

125. Breton, E. J.; Reid, C. E. *Office of Saline Water R&D Progress Report No. 16*; 1957.

126. Reid, C. E.; Breton, E. J., Water and ion flow across cellulosic membranes. *J. Applied Polymer Sci.* **1959,** 1, 133-43.

127. Reid, C. E.; Kuppers, J. R., Physical characteristics of osmotic membranes of organic polymers. *Journal of Applied Polymer Science* **1959,** 2, 264-72.

128. Loeb, S.; Sourirajan, S., *Advances in Chemistry Series* **1962,** 38, 117.

129. Loeb, S.; Sourirajan, S. *UCLA Dept. of Engineering Report*; July,1960; pp 60-60.

130. Sourirajan, S.; Govindan, T. S., Membrane separation of some onorganic salts in aqueous solution. *Proc. Int. Symp. Water Desalin., 1st* **1967,** 1, 251-69, discussion 269-74.

131. Manjikian, S., Semipermeable desalination membranes from organic coating solutions. *Calif., Univ., Water Resources Center, Contrib.* **1965,** No. 101, 41 pp.

132. Manjikian, S.; Loeb, S.; McCutchan, J. W., Improvement in fabrication techniques for reverse osmosis desalination membranes. *Proceedings of the International Symposium on Water Desalination* **1967,** 2, 159-79.

133. Riley, R. L.; Merten, U.; Gardner, J. O., Replication electron microscopy of cellulose acetate osmotic membranes. *Desalination* **1966,** 1, (1), 30-4.

134. Lonsdale, H. K.; Merten, U.; Riley, R. L., Transport properties of cellulose acetate osmotic membranes. *Journal of Applied Polymer Science* **1965,** 9, (4), 1341-62.

135. Lonsdale, H. K.; Cross, B. P.; Graber, F. M.; Milstead, C. E., Permeability of cellulose acetate membranes to selected solutes. *Journal of Macromolecular Science, Physics* **1971,** 5, (1), 167-87.

136. Richter, J. W.; Hoehn, H. H. Permselective polymer membranes. 69-1941022 1941022, 19690812., 1970.

137. Sourirajan, S.; Editor, *Reverse Osmosis and Synthetic Membranes. Theory-Technology-Engineering*. 1977; p 598 pp.

138. Credali, L.; Chiolle, A.; Parrini, P., New polymer materials for reverse osmosis membranes. *Desalination* **1974,** 14, (2), 137-50.

139. Cadotte, J. E.; Cobian, K. E.; Forester, R. H.; Petersen, R. J. *Continued evaluation of in situ-formed condensation polymers for reverse osmosis membranes*; North Star Res. Div.,Midwest Res. Inst.,Minneapolis,MN,USA.: 1976; p 89 pp.

140. Rozelle, L. T.; Cadotte, J. E.; Cobian, K. E.; Kopp, C. V., Jr., Nonpolysaccharide membranes for reverse osmosis: NS-100 membranes. *Reverse Osmosis Synth. Membr.* **1977**, 249-61.

141. Rozelle, L. T.; Kopp, C. V., Jr.; Cadotte, J. E.; Cobian, K. E., NS-100 membranes for reverse osmosis applications. *Journal of Engineering for Industry* **1975,** 97, (1), 220-3.

142. Belfort, G.; Editor, *Synthetic Membrane Processes: Fundamentals and Water Applications*. 1984; p 552 pp.

143. Glater, J.; Zachariah, M. R., A mechanistic study of halogen interaction with polyamide reverse-osmosis membranes. *ACS Symposium Series* **1985,** 281, (Reverse Osmosis Ultrafiltr.), 345-58.

144. Kawaguchi, T.; Tamura, H., Chlorine-resistant membrane for reverse osmosis. I. Correlation between chemical structures and chlorine resistance of polyamides. *Journal of Applied Polymer Science* **1984,** 29, (11), 3359-67.

145. Glater, J.; Hong, S.-k.; Elimelech, M., The search for a chlorine-resistant reverse osmosis membrane. *Desalination* **1994,** 95, (3), 325-45.

146. Avlonitis, S.; Hanbury, W. T.; Hodgkiess, T., Chlorine degradation of aromatic polyamides. *Desalination* **1992,** 85, (3), 321-34.

147. Singh, R., Polyamide polymer solution behavior under chlorination conditions. *Journal of Membrane Science* **1994,** 88, (2-3), 285-7.

148. Soice, N. P.; Greenberg, A. R.; Krantz, W. B.; Norman, A. D., Studies of oxidative degradation in polyamide RO membrane barrier layers using pendant drop mechanical analysis. *Journal of Membrane Science* **2004,** 243, (1-2), 345-355.

149. Soice, N. P.; Maladono, A. C.; Takigawa, D. Y.; Norman, A. D.; Krantz, W. B.; Greenberg, A. R., Oxidative degradation of polyamide reverse osmosis membranes: Studies of molecular model compounds and selected membranes. *Journal of Applied Polymer Science* **2003,** 90, (5), 1173-1184.

150. Kwon, Y.-N.; Leckie, J. O., Hypochlorite degradation of crosslinked polyamide membranes. *Journal of Membrane Science* **2006,** 282, (1+2), 456-464.

151. LaConti, A. B.; Chludzinski, P. J.; Fickett, A. P., Morphology and reverse osmosis properties of sulfonated poly(2,6-dimethyl phenylene oxide) membranes. *Reverse Osmosis Membrane Res.* **1972**, 263-84.

152. Plummer, C. W.; Kimura, G.; La Conti, A. B. *Development of sulfonated polyphenylene oxide membranes for reverse osmosis*; Gen. Elec. Co.,Lynn,MA,USA.: 1970; p 73 pp.

153. Petersen, R. J., Composite reverse osmosis and nanofiltration membranes. *Journal of Membrane Science* **1993,** 83, (1), 81-150.

154. Dempsey, R. M.; LaConti, A. B. *Reclamation of acid rinse water*; Direct Energy Convers. Programs,Gen. Electr. Co.,Lynn,MA,USA.: 1974; p 47 pp.

155. Amore, J. M.; Enos, J. F.; LaConti, A. B. *Reverse osmosis membranes for purification of wash water at sterilization temperature (165 degrees F)*; Direct Energy Convers. Programs,Gen. Electr. Co.,Lynn,MA,USA.: 1973; p 83 pp.

156. LaConti, A. B., Advances in development of sulfonated PPO and modified PPO membrane systems for some unique reverse osmosis applications. *Reverse Osmosis Synth. Membr.* **1977**, 211-29.

157. Bourganel, J. Anisotropic, semipermeable membranes comprising poly(arylene ether sulfones). 72-22252842225284, 19720524., 1972.

158. Harrison, W. L.; Hickner, M. A.; Kim, Y. S.; McGrath, J. E., Poly(arylene ether sulfone) copolymers and related systems from disulfonated monomer building blocks: Synthesis, characterization, and performance - A topical review. *Fuel Cells* **2005,** 5, (2), 201-212.

159. Kim, Y. S.; Hickner, M. A.; Dong, L. M.; Pivovar, B. S.; McGrath, J. E., Sulfonated poly(arylene ether sulfone) copolymer proton exchange membranes: composition and morphology effects on the methanol permeability. *Journal of Membrane Science* **2004,** 243, (1-2), 317-326.

160. Kinzer, K. E.; Lloyd, D. R.; Gay, M. S.; Wightman, J. P.; Johnson, B. C.; Mcgrath, J. E., Phase Inversion Sulfonated Polysulfone Membranes. *Journal of Membrane Science* **1985,** 22, (1), 1-29.

161. Roy, A.; Hickner, M. A.; Yu, X.; Li, Y.; Glass, T. E.; McGrath, J. E., Influence of chemical composition and sequence length on the transport properties of proton exchange membranes. *Journal of Polymer Science, Part B: Polymer Physics* **2006,** 44, (16), 2226-2239.

162. Sankir, M.; Bhanu, V. A.; Harrison, W. L.; Ghassemi, H.; Wiles, K. B.; Glass, T. E.; Brink, A. E.; Brink, M. H.; McGrath, J. E., Synthesis and characterization of 3,3'-disulfonated-4,4'-dichlorodiphenyl sulfone (SDCDPS) monomer for proton exchange membranes (PEM) in fuel cell applications. *Journal of Applied Polymer Science* **2006,** 100, (6), 4595-4602.

163. Summer, M. J.; Harrison, W. L.; Weyers, R. M.; Kim, Y. S.; McGrath, J. E.; Riffle, J. S.; Brink, A.; Brink, M. H., Novel proton conducting sulfonated poly(arylene ether) copolymers containing aromatic nitriles. *Journal of Membrane Science* **2004,** 239, (2), 199-211.

164. Wang, H.; Badami, A. S.; Roy, A.; McGrath, J. E., Multiblock copolymers of poly(2,5-benzophenone) and disulfonated poly(arylene ether sulfone) for proton-exchange membranes. I. Synthesis and characterization. *Journal of Polymer Science, Part A: Polymer Chemistry* **2006,** 45, (2), 284-294.

165. Park, H. B.; Freeman, B. D.; Zhang, Z.-B.; Fan, G.-Y.; Sankir, M.; McGrath, J. E., Water and salt transport behavior through hydrophilic-hydrophobic copolymer membranes and their relations to reverse osmosis membrane performance. *PMSE Preprints* **2006,** 95, 889-891.

166. Zhang, Z.-B.; Fan, G.-Y.; Sankir, M.; Park, H. B.; Freeman, B. D.; McGrath, J. E., Synthesis of di-sulfonated poly(arylene ether sulfone) random copolymers as novel candidates for chlorine-resistant reverse osmosis membranes. *PMSE Preprints* **2006,** 95, 887-888.

167. Park, H. B.; Freeman, B. D.; Zhang, Z.; Sankir, M.; McGrath, J. E., Chlorine-Tolerant Disulfonated Poly(arylene ether sulfone) Desalination Membrane Materials. *Angewandte Chemie International Edition* **2008 Submitted**.

2. CHAPTER-2-Synthesis and Crosslinking of Partially Disulfonated Poly(Arylene Ether Sulfone)s with Glycidyl Methacrylate as the Crosslinker as Candidates for PEMs*

Mou Paul, Abhishek Roy, Judy S. Riffle
& James E. McGrath

Macromolecules and Interfaces Institute
Department of Chemistry
Virginia Polytechnic Institute and State University, Blacksburg, VA 24061

Abstract

A series of controlled molecular weight, phenoxide-endcapped, 50% disulfonated poly(arylene ether sulfone)s (BPS) copolymers was synthesized. The terminal phenoxide groups were reacted with glycidyl methacrylate via nucleophilic aromatic substitution to produce copolymers endcapped with crosslinkable glycidyl methacrylate moieties. Various blend compositions in varying weight percents of a low molecular weight and a higher molecular weight GMA-endcapped copolymer were made and thermally cured in presence of benzoyl peroxide initiator at 90-95 °C. The cured copolymers were characterized in terms of water uptake, proton conductivity and self-diffusion coefficient of water. Cured copolymers showed reduced water uptake, but no significant change in proton conductivity, improving the overall selectivity of the crosslinked materials for application as PEMs.

---

* Adapted and Reprinted with permission. Paul, Mou; Roy, Abhishek; Riffle, Judy S.; McGrath, James E. Crosslinked sulfonated poly(arylene ether sulfone) membranes as candidate for PEMS. ECS Transactions (2008), 6 (26, Membranes for Electrochemical Applications), 9-16.

2.1. Introduction

Fuel cells are considered as electrochemical devices that convert chemical energy to electrical energy.[1] They have diverse fields of application ranging from stationary power to portable power systems.[2] One of the most important types of fuel cells is the proton exchange membrane type fuel cell (PEMFC). Hydrogen and methanol are the two main types of fuel used for this application. The fuel gets oxidized at the cathode generating protons, which are transported across the proton exchange membrane to anode where they are reduced by oxygen to form water. Hence the central part of a PEMFC is the proton exchange membrane (PEM). A PEM should meet some primary requirements such as high proton conductivity and low water uptake. Besides these, the membrane should also demonstrate both thermal and oxidative stability, low permeability to fuels, dimensional stability under hydrated conditions, and fatigue resistance for long term applications. The current state of the art PEMs are perfluorosulfonic acid membranes such as Nafion® manufactured by DuPont. Nafion has a proton conductivity of 0.1 S/cm under fully hydrated conditions.[2] Although Nafion® shows excellent chemical and electrochemical stability as well as high proton conductivity with relatively low water uptake on a mass basis, it also suffers from some disadvantages including high cost, high methanol permeability (in direct methanol fuel cells), and limited operating temperature (80 °C)[2, 3] due to its depressed hydrated glass transition temperature.

For the past few years our research group is involved in the synthesis of biphenol based partially disulfonated poly(arylene ether sulfone) random copolymers as potential PEMs. This series of copolymers is called BPSH-XX,[4, 5] where BP stands for biphenol, S is for sulfonated, H denotes the acid form and XX represents the degree of disulfonation. Our earlier studies have indicated that for BPSH copolymers, particularly at higher degree of disulfonation, the proton conductivity reaches a very high value close to 0.2 S/cm. The major drawback of going to a higher degree of disulfonation is that the polymer will have extensive water uptake at higher water activities. This results in poor dimensional stability and significant depression in glass transition temperature and hence

limits the application of higher IEC BPSH copolymers as PEMs. Thus the challenge lies in how to decrease the water uptake for BPSH type random copolymers with higher degree of disulfonation without compromising the proton conductivity significantly. One of the approaches is to crosslink BPSH copolymers having higher degree of disulfonation. Introduction of crosslinked networks within the polymer may also improve the mechanical properties under low humidity cycling conditions. In this paper, we describe the synthesis and crosslinking of BPSH random copolymers with high degrees of disulfonation (i.e. 50% disulfonation) for PEM application. A series of controlled molecular weight copolymers with phenolic endgroups was synthesized[6] and further reacted with an excess of glycidyl methacrylate to produce a copolymer with thermally crosslinkable methacrylate endgroups. The crosslink density was varied by controlling the molecular weights. A series of blend membranes between a BPS-50 of 15 kg mol^{-1} and a BPS-50 of 5 kg mol^{-1} in various weight proportions were prepared. Crosslinking through the endgroups only resulted in flexible, ductile membranes. The effect of crosslinking on PEM properties such as proton conductivity, water uptake and water transport was investigated.

2.1. Experimental

2.2.1. Materials

Monomer grade 4,4'–dichlorodiphenylsulfone (DCDPS) and 4,4'-biphenol (BP) were obtained from Solvay Advanced Polymers and Eastman Chemical Company, respectively, and dried under vacuum at 60 °C for one day prior to use. The sulfonated comonomer, 3,3'-disulfonate-4,4'-dichlorodiphenylsulfone (SDCDPS) was prepared following the procedure published previously[7] and dried under vacuum at 160 °C for two days before use. Potassium carbonate was purchased from Aldrich and dried under vacuum at 110 °C for one day before use. Glycidyl methacrylate (GMA) and benzoyl peroxide (BPO) were obtained from Aldrich and used as received. The reaction solvent N,N-dimethylacetamide (DMAc) was purchased from Aldrich and vacuum-distilled from calcium hydride and stored over molecular sieves under nitrogen. Toluene (anhydrous,

99.8%), isopropanol (*ReagentPlus*™, 99%) were obtained from Aldrich and used as received. Sulfuric acid (*ACS Reagent*, 95-98%) was obtained from VWR Internationals and used as received.

2.2.2. Synthesis of a controlled molecular weight phenoxide-endcapped BPS-50 copolymer

A controlled molecular weight, phenoxide-endcapped 50 % disulfonated biphenol based poly(arylene ether sulfone) (BPS-50) was synthesized via nucleophilic aromatic substitution. The molecular weight of the copolymer was controlled by offsetting the stoichiometry of the monomers. A typical polymerization of a 5 $kg.mole^{-1}$ BPS-50 copolymer is reported here. BP (5.00 g, 26.85 mmol), DCDPS (3.49 g, 12.16 mmol), SDCDPS (5.97 g, 12.16 mmol) were added to a three necked round bottom reaction flask equipped with a mechanical stirrer, a nitrogen inlet, a Dean-Stark trap and a condenser. Next, potassium carbonate (4.27 g, 30.88 mmol) and 72 mL DMAc (20 % solids) were introduced in the flask. Toluene (36 mL, DMAc/toluene was 2/1 v/v) was used as the azeotropic reagent. The reaction mixture was refluxed at 150 °C for 4 h and the azeotrope was removed to dehydrate the system. Then the reaction mixture was gradually heated to 170 °C by the controlled removal of toluene and allowed to react for an additional 65-70 h. The viscous product was cooled to room temperature. The product mixture was filtered to remove salts. The copolymer was isolated by precipitation in isopropanol, filtered, and dried for 24 h at 70 °C under ambient pressure, and then for 24 h at 110 °C under vacuum.

The nomenclature of the samples is defined as follows- BPSH-50(yk) where 50 is the degree of disulfonation and y is the molecular weight of the copolymer and k denotes kg mol^{-1} and H is the acid from of the copolymer.

2.2.3. Synthesis of a GMA endcapped BPS-50 copolymer

The terminal phenoxide groups of a BPS-50 copolymer were reacted with glycidyl methacrylate via aromatic nucleophilic substitution to produce methacrylate endcapped BPS-50 copolymers. A typical endcapping reaction is provided below. BPS-

50(5k) (1 g, 0.2 mmol) was dissolved in 10 mL DMAc in a 100 mL round bottom flask. Anhydrous solid potassium carbonate (0.06 g, 0.4 mmol) was added to the reaction flask. Next, GMA (0.11 mL, 0.8 mmol) was introduced in the flask and the reaction was continued for 24 h at 120 °C temperature under strong air purge. The product solution was filtered to remove salt. The copolymer was isolated by precipitation in isopropanol, and further purified by soxhlet extraction in isopropanol for 24 h to remove any unreacted GMA. Then the copolymer was dried under vacuum at 100 °C for 24 h.

The nomenclature of the copolymers is designated as GMA-BPS-50(yk) copolymers.

2.2.4. Casting and curing of GMA-BPS-50-(15k/5k) blend copolymers

Three blend copolymers of GMA-BPS-50(15k) and GMA-BPS-50(5k) copolymers in varying weight ratios of 80:20, 70:30 and 60:40 were prepared. Then 5 wt % solutions of those blend copolymers with 5 mol % (based on copolymer molecular weights) benzoyl peroxide were prepared in DMAc and stirred until transparent homogeneous solutions were obtained. A copolymer solution was then filtered with a 0.45 μm PTFE filter and cast on a glass plate. The glass plate was inserted in a vacuum oven and heated at 90-95 °C for 2.5 h under vacuum. The plate was removed from the oven upon cooling to room temperature and the membrane was released from the glass plate by immersing in water. Later, the residual DMAc was evaporated off by heating the film at 110 °C for 24 h under vacuum. The membranes were acidified by immersing in 1.5 M H_2SO_4 at room temperature for 24 h and then in deionized water for another 24 h.

Characterization Methods

2.2.5. Nuclear Magnetic Resonance (NMR) Spectroscopy

^{1}H NMR experiments were conducted on a Varian Unity 400 MHz NMR spectrometer. All spectra were obtained from 10% solutions (w/v) in DMSO-d_6 at room temperature. Proton NMR was used to determine the molecular weights and copolymer compositions.

2.2.6. Water Uptake

The membranes were immersed in deionized water for at least 48 h. Then they were removed from the water, blotted dry and quickly weighed. The membranes were vacuum dried at 110 °C overnight and the weights were recorded. The ratio of weight gain to the original membrane weight was reported as the water uptake (mass %)

$$Water Uptake = \frac{W_{wet} - W_{dry}}{W_{dry}} \times 100\% \qquad \textbf{Equation 2-1}$$

where W_{wet} and W_{dry} are the masses of wet and dried samples, respectively.

2.2.7. Self-Diffusion coefficient of Water

Water self diffusion coefficients were measured following a standard procedure using a Varian Inova 400 MHz (for protons) nuclear magnetic resonance spectrometer with a 60 G/cm gradient diffusion probe. A total of 16 points were collected across the range of gradient strength and the signal to noise ratio was enhanced by co-adding 4 scans.[8]

2.2.8. Proton Conductivity

Protonic conductivity at 30 °C under full hydration (in liquid water) was determined using a Solartron 1252 + 1287 Impedance/Gain-Phase Analyzer over the frequency range of 10 Hz - 1 MHz.

2.3. Results and Discussion

2.3.1. Synthesis of phenoxide-terminated BPS-50 copolymers

A series of controlled molecular weight BPS-50 copolymers with phenoxide endgroups was synthesized by nucleophilic aromatic substitution. The comonomers were SDCDPS, DCDPS and biphenol (Fig. 2.1). The molecular weights of the copolymers

were controlled by offsetting the stoichiometry between biphenol and the dihalides. Biphenol was added in excess to endcap the copolymers with phenoxide groups. Three copolymers with number average molecular weights (M_n) of five, fifteen and twenty kg mol^{-1} were targeted. The degree of disulfonation was controlled by varying the molar ratio of SDCDPS to DCDPS. For all of the copolymers, the degree of disulfonation was 50 %.

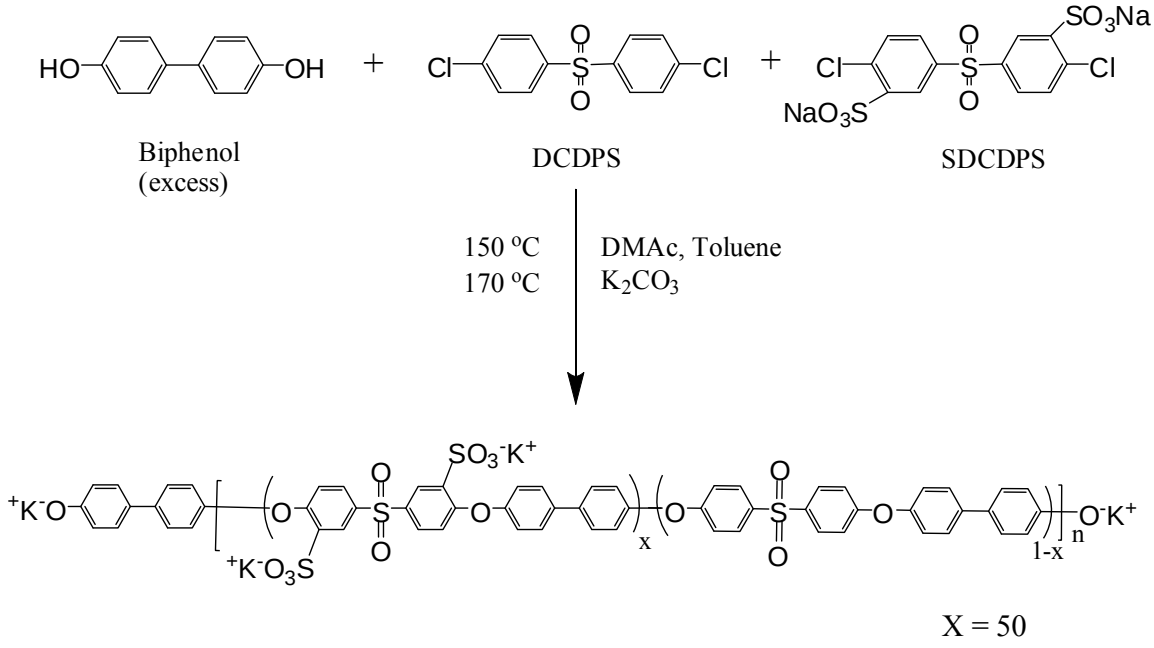

Figure 2.1 Synthesis of a controlled molecular weight phenoxide-endcapped BPS-50 copolymer

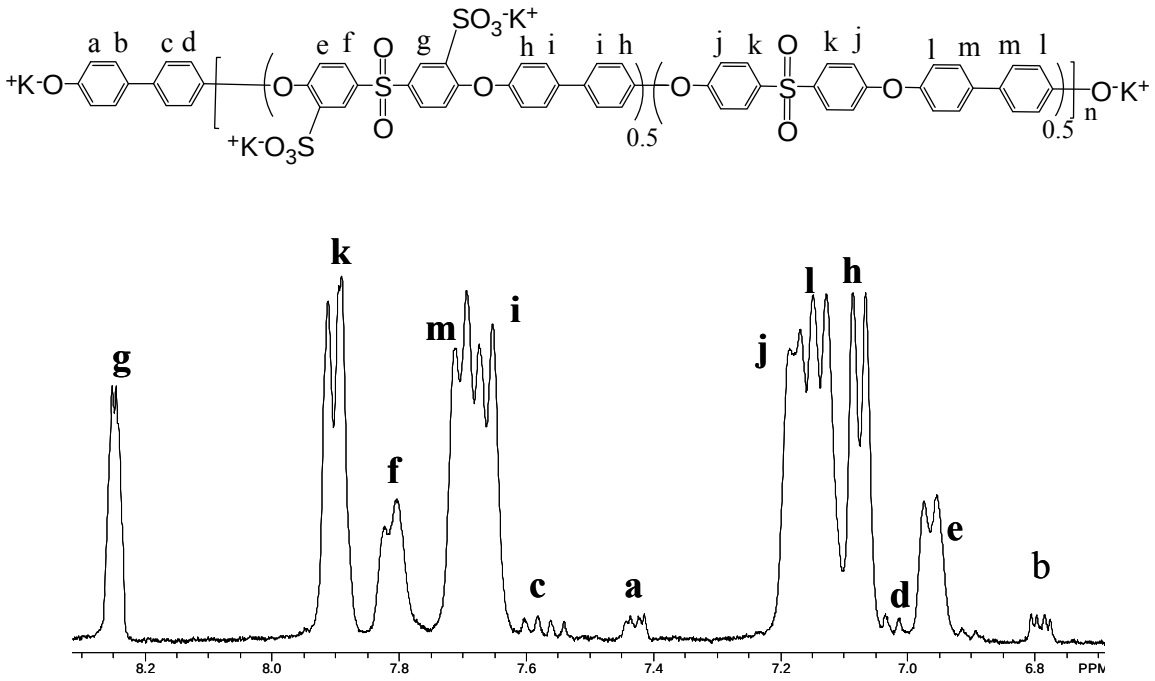

Figure 2.2 ^{1}H NMR of a phenoxide-endcapped BPS-50 copolymer

Fig. 2.2 shows the proton NMR spectrum of a copolymer with a targeted molecular weight of fifteen kg mol^{-1}. The aromatic protons of the biphenol unit in the endgroup at *(b), (d), (a), and (c)* were allocated to peaks at 6.8 ppm, 7.0 ppm, 7.40 ppm and 7.55 ppm respectively. The ratio of the integrals of the aromatic protons at 6.8 ppm (*b*) to those of the aromatic protons of the biphenol moiety in the copolymer repeat units at 7.7 ppm (*m and i*) were utilized to calculate M_n of the copolymers. As shown in Table 2.1, the experimental M_n values derived from both NMR and GPC are in good agreement with targeted values. As expected, intrinsic viscosities ([η]) of the copolymers increased with increasing molecular weight (Table 2.1). The degree of disulfonation was confirmed from the ratio of the integrals of protons at 6.95 ppm (*e*), 7.8 ppm (*f*) and 8.25 ppm (*g*) in the sulfonated unit to the protons at 7.9 ppm (*k*) in the unsulfonated unit. The degrees of disulfonation were used to calculate the ion exchange capacities (IEC- meq of sulfonic acid groups per gram of dry polymer) of the copolymers. Table 2.1 shows that the experimental IEC values of the copolymers obtained from both proton NMR and titration are in good agreement with the targeted values.

Table 2.1 Summary of BPS 50 copolymers

Copolymer	M_n (kg mol^{-1})$^{-}$			IV[a] (dL g^{-1})	IEC (meq g^{-1})		
	Target	^{1}H NMR	GPC		Target	^{1}H NMR	Titration[b]
BPS 50-5k	5	5.8	5.2	0.22	2.08	2.04	-
BPS 50-15k	15	16.5	19.9	0.36	2.08	2.01	1.83
BPS 50-20k	20	20.8	21.8	0.43	2.08	2.03	1.90

[a]From GPC, in NMP with 0.05M LiBr at 60 °C

[b]Titrated by NaOH

2.3.2. Synthesis of GMA-BPS-50 copolymers

GMA-BPS-50 copolymers were synthesized via nucleophilic aromatic substitution reaction between phenoxide endcapped BPS-50 copolymers and GMA under basic conditions in DMAc. A strong air purge was maintained in the reaction vessel to prevent the polymerization of glycidyl methacrylate by itself. The reaction path is shown in Figure 2.3. Figure 2.4 represents the proton NMR spectra of a BPS-50(5k) oligomer before and after endcapping with GMA. The aromatic protons of the biphenol unit in the endgroup at 6.8 ppm (*b*) and 7.40 ppm (*a*) of the phenoxide-terminated BPS-50(5k) oligomer disappeared after the phenoxide groups were reacted with GMA and vinyl proton peaks from GMA unit at 6 ppm and 5.65 ppm appeared.

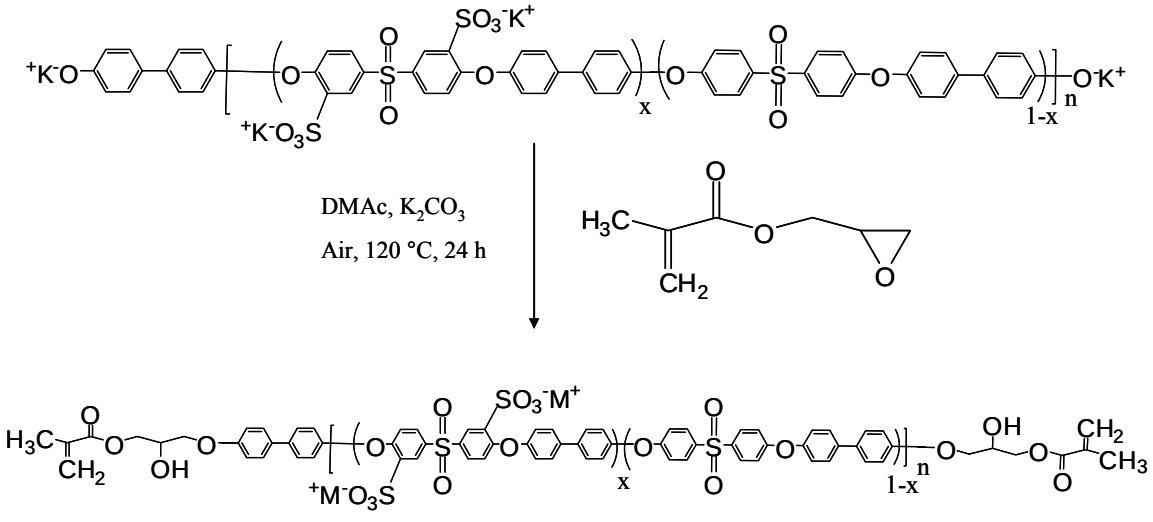

Figure 2.3 Synthesis of a GMA-endcapped BPS-50 copolymer

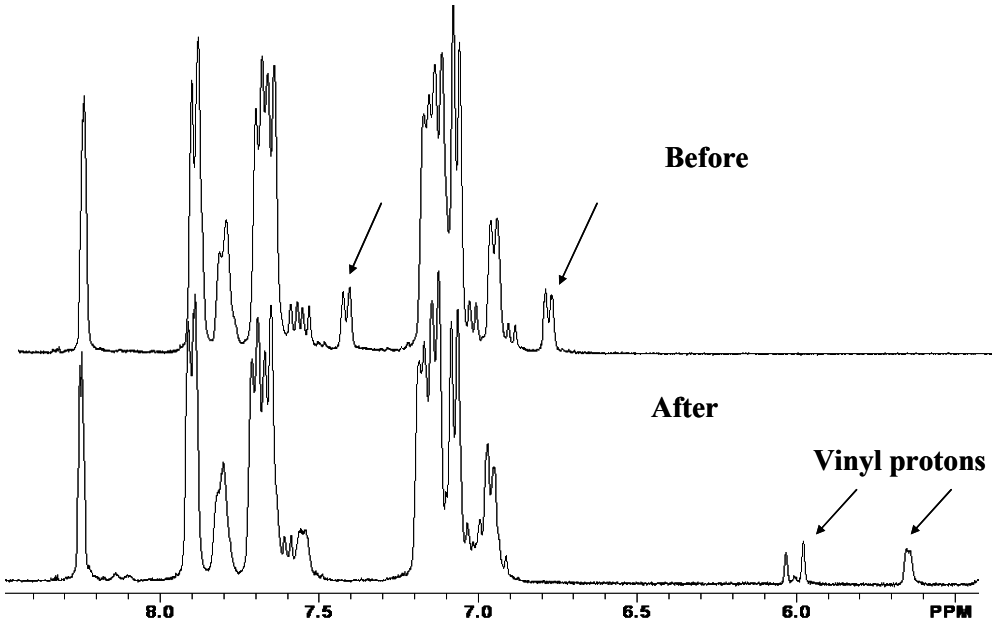

Figure 2.4 ^{1}H NMR of a BPS-50(5k) copolymer before and after endcapping with GMA

From the proton NMR study it was confirmed that all the phenoxide endgroups took part in the endcapping reaction and the oligomer was completely endcapped by GMA. The M_n values after endcapping with GMA was obtained from the ratio of the integrals of the vinyl protons of GMA unit at 5.65/6.0 ppm to those of the aromatic protons of the biphenol moiety in the copolymer repeat units at 7.7 ppm. The experimental M_n values derived from both proton NMR and GPC before and after endcapping with GMA are in good agreement with targeted values (Table 2.2).

Table 2.2 Summary of BPS 50 copolymers before and after endcapping with GMA

BPS 50 Copolymers (Kg/mole)	Before Endcapping			After Endcapping		
	M_n ^{1}H NMR kg/mole	M_n GPC kg/mole	IV[b] dL/g	M_n[a] ^{1}H NMR kg/mole	M_n GPC kg/mole	IV[b] dL/g
5	4.40	8.3	0.20	4.9	8.7	0.21
15	16.5	19.9	0.36	20	15.8	0.39
20	20.8	21.8	0.43	21.7	18.3	0.49

[a] based on vinyl proton of GMA unit

[b]From GPC, in NMP with 0.05M LiBr at 60 °C

A 100 % molar excess of GMA was taken to ensure complete endcapping. The endcapped copolymers were soxhleted in isopropanol for 24 h to remove any unreacted residual GMA. In addition to the proton NMR study, the intrinsic viscosities of the copolymers before and after endcapping were compared (Table 2.2) to investigate that whether any inter-oligomer coupling had taken place or not. There was a nominal, but not any significant increase in the intrinsic viscosities of the oligomers after endcapping with GMA, which suggests that no inter-oligomer coupling occured during the endcapping reaction.

2.3.3. Characterization of blend membranes

For a copolymer endcapped with crosslinkable moieties, the number of crosslinkable sites is inversely related to the number average molecular weight. Hence a high crosslinking density can be achieved with BPS-50(5k) oligomer. However, the molecular weight of BPS-50(5k) is below the minimum film forming molecular weight, whereas BPS-50(15k) and (20k) can form film easily. Hence a non film forming material (5k) was blended with a film forming material (15k) to achieve both film forming property and high crosslinking density. The various blend ratios are displayed in Table 2.3.

Initial characterizations, such as measurements of water uptake, proton conductivity and self-diffusion coefficients of water are given in Table 2.3. The values for the crosslinked materials were compared with an uncrosslinked BPS-50 copolymer. All of the cured membranes showed lower water uptake, hydration number and self-diffusion coefficients of water than the uncrosslinked material, the lesser values associated with the blend membranes having higher amounts of BPS-50(5k). A significant reduction in water uptake was observed for the 60:40 blend membrane compared to the uncrosslinked one. However, no significant reduction in proton conductivity was observed. The hydration number is defined as the number of water molecules per sulfonic acid group. At a constant ionic content, reduction of water uptake reduces hydration number or increases the effective concentration of the proton. As a result the proton transport remains unaffected although the water uptake is reduced by crosslinking.

Table 2.3 Characterization of blend membranes

Blend composition (15k/5k)(wt%)	Water uptake (mass %)	Hydration number (λ)	Proton conductivity (mS/cm)[a]	Self-diffusion coefficient of water (10^{-6} cm^2/s)[b]
uncrosslinked	65	18	130	6.8
80 : 20	55	15	126	6.6
70 : 30	49	13	134	7.2
60 : 40	42	11	126	5.8
Nafion 112	25	15	100	4.4

[a] measured at 30°C in liq. water; [b] at 25°C, hydrated

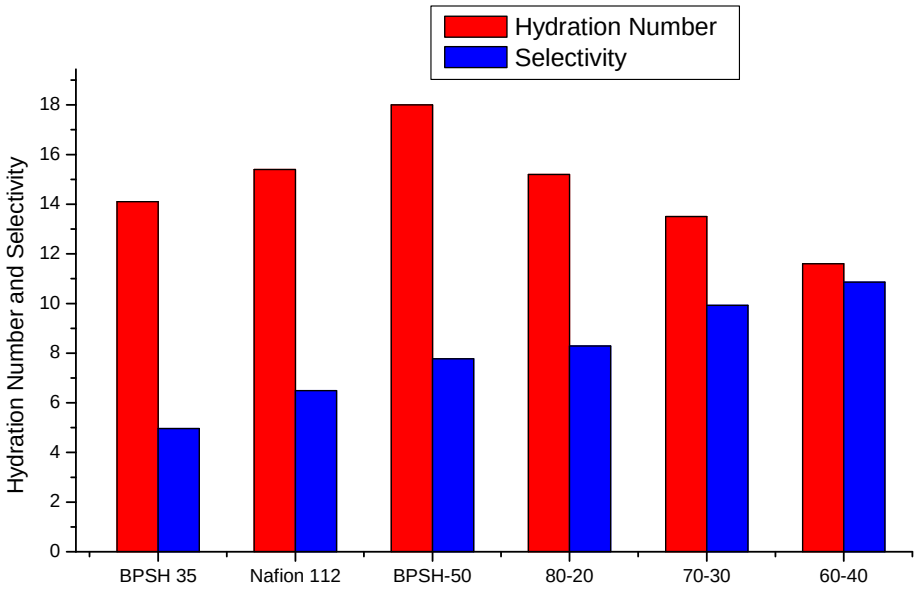

Figure 2.5 Selectivity and hydration number for the copolymers studied

One of the critical issues for the PEMs is the balance between proton conductivity and water uptake. Selectivity can be defined as the ratio of proton conductivity to the hydration number. High selectivity at low hydration number is desired. As indicated in Figure 2.5, the selectivity increases for the crosslinked polymers when compared to Nafion and BPSH-35. Also at the same time, a reduction in hydration number is also observed. Hence by crosslinking, one can achieve high selectivity at low hydration number. However, methacrylate linkage may not show good stability in fuel cell operating condition. Recently we have shown that BPSH can also be crosslinked with a thermally stable, tetrafunctional epoxy crosslinker. Detailed discussion will be reported separately.

2.4. Conclusions

A series of controlled molecular weight phenoxide-endcapped BPS-50 copolymers was synthesized and endcapped by GMA. A series of blend membranes between a GMA-BPS-50 of 15 kg mol^{-1} and a GMA-BPS-50 of 5 kg mol^{-1} in various weight proportions were prepared. The blend membranes were thermally cured by initiator benzoyl peroxide. The cured membranes showed substantial reduction in water uptake without having any significant reduction in proton and water transport. This results in increasing selectivity of proton transport over water transport with increasing crosslinking density.

Acknowledgements

The authors would like to acknowledge NSF-PFI and Nissan Motors for funding.

2.5. References

1. Winter, M.; Brodd, R. J., What are batteries, fuel cells, and supercapacitors? (vol 104, pg 4245, 2003). *Chemical Reviews* **2005,** 105, (3), 1021-1021.

2. Mauritz, K. A.; Moore, R. B., State of understanding of Nafion. *Chemical Reviews* **2004,** 104, (10), 4535-4585.

3. Yeo, R. S., Ion Clustering and Proton Transport in Nafion Membranes and Its Applications as Solid Polymer Electrolyte. *Journal of the Electrochemical Society* **1983,** 130, (3), 533-538.

4. Kim, Y. S.; Wang, F.; Hickner, M.; McCartney, S.; Hong, Y. T.; Harrison, W.; Zawodzinski, T. A.; McGrath, J. E., Effect of acidification treatment and morphological stability of sulfonated poly(arylene ether sulfone) copolymer proton-exchange membranes for fuel-cell use above 100 degrees C. *Journal of Polymer Science Part B-Polymer Physics* **2003,** 41, (22), 2816-2828.

5. Wang, F.; Hickner, M.; Kim, Y. S.; Zawodzinski, T. A.; McGrath, J. E., Direct polymerization of sulfonated poly(arylene ether sulfone) random (statistical) copolymers: candidates for new proton exchange membranes. *Journal of Membrane Science* **2002,** 197, (1-2), 231-242.

6. Paul, M.; Roy, A.; Park, H. B.; Freeman, B. D.; Riffle, J. S.; McGrath, J. E., Synthesis and crosslinking of poly(arylene ether sulfone) blend membranes. *Polymer Preprints (American Chemical Society, Division of Polymer Chemistry)* **2007,** 48, (1), 334-335.

7. Sankir, M.; Bhanu, V. A.; Harrison, W. L.; Ghassemi, H.; Wiles, K. B.; Glass, T. E.; Brink, A. E.; Brink, M. H.; McGrath, J. E., Synthesis and characterization of 3,3 '-disulfonated-4,4 '-dichlorodiphenyl sulfone (SDCDPS) monomer for proton exchange membranes (PEM) in fuel cell applications. *Journal of Applied Polymer Science* **2006,** 100, (6), 4595-4602.

8. Roy, A.; Yu, X.; Badami, A.; McGrath, J. E., Multiblock hydrophilic-hydrophobic proton exchange membranes for fuel cells. *PMSE Preprints* **2006,** 94, 169-170.

3. CHAPTER-3-Synthesis and Crosslinking of Partially Disulfonated Poly(Arylene Ether Sulfone) Random Copolymers as Candidates for Chlorine Resistant Reverse Osmosis Membranes

Mou Paul,[a] Ho Bum Park,[b] Benny D. Freeman,[b] Abhishek Roy,[a] James E. McGrath[a] and J. S. Riffle[a,]*

[a]*Macromolecules and Interfaces Institute, Virginia Polytechnic Institute and State University, Blacksburg, VA 24061*

[b]*Department of Chemical Engineering, Center for Energy and Environmental Resources, University of Texas at Austin, Austin, TX 78758*

Abstract

Biphenol-based, partially disulfonated poly(arylene ether sulfone)s synthesized by direct copolymerization show promise as potential reverse osmosis membranes. They have excellent chlorine resistance over a wide range of pH and good anti-protein and anti-oily water fouling behavior. Crosslinking of these copolymers that have high degrees of disulfonation may improve salt rejection of the membranes for reverse osmosis performance. A series of controlled molecular weight, phenoxide-endcapped, 50% disulfonated poly(arylene ether sulfone)s was synthesized. The copolymers were reacted with a multifunctional epoxy resin and crosslinked thermally. The effects on network properties of various factors such as crosslinking time, copolymer molecular weight and epoxy concentration were investigated. The crosslinked membranes were characterized in terms of gel fraction, water uptake, swelling and self-diffusion

[*] Adapted and reprinted with permission From John Wiley & Sons, Inc
Polymer 2008, 49 (9), 2243-52

coefficients of water. The salt rejection of the cured membranes was significantly higher than for the uncrosslinked copolymer precursors.

Keywords: membrane, disulfonated poly(arylene ether sulfone), reverse osmosis

3.1. Introduction

In recent years, there has been an increasing worldwide need for fresh drinking water.[1] About 41% of the total population in the world lives in water-stressed areas. Membrane technology for desalination, such as reverse osmosis (RO), is an attractive and energy efficient way to develop new sources of fresh water.[2] Over the last four decades, tremendous research has been conducted to develop RO membranes. However, there have been severe gaps in achieving ideal performance. One of the major issues is the chlorine instability of polyamide (PA) RO membranes, which are the most widely used desalination membranes. RO membranes are often exposed to low levels of chorine to prevent biofouling.[3] Unfortunately, the conventional aromatic PA thin film composite membrane is susceptible to oxidative degradation by chlorine, and this leads to irreversible performance loss over time.[4-6] This problem necessitates the use of expensive dechlorination and rechlorination treatment steps when using PA membranes.

Sulfonated poly(arylene ether sulfone)s are promising chlorine resistant RO materials. Unlike commercial aromatic PA membranes, sulfonated poly(arylene ether sulfone)s do not possess the vulnerable amide bond that is susceptible to chlorine attack.[7, 8] The use of sulfonated aromatic polymers as RO membranes began with sulfonated poly(phenylene oxide) in the 1970s.[9] The sulfonate ions on the polymer repel like charges (the anions from the salt in solution) and as a result, the membrane is relatively impermeable to salts. These membranes showed excellent resistance against compaction, hydrolysis and degradation and exhibited good flux and rejection characteristics.[10] Sulfonated poly(arylene ether sulfone) membranes have also been considered for RO applications.[11, 12] Albany International Corporation reported sulfonated polysulfone hollow fiber membranes with constant flux and salt rejection even after exposure to 100 ppm chlorine in feed water.[13] However, all of these membranes were post-sulfonated

(after the non-sulfonated poly(arylene ether sulfone) was prepared) using chlorosulfonic acid or concentrated sulfuric acid, and undesirable side reactions as well as poor quantitative reproducibility were encountered.[14]

Recently, we have described direct copolymerization synthesis of sulfonated biphenol-based poly(arylene ether sulfone)s (BPS) using disulfonated activated aromatic halide monomers.[15-23] These aromatic, film-forming copolymers have well-controlled ion concentrations with excellent oxidative, hydrolytic and mechanical stability. Membranes fabricated from these copolymers have excellent chlorine resistance over a pH range of 4-10. For example, BPS with 40% disulfonation and a commercial PA RO membrane were exposed to feed water containing 500 ppm chlorine at a pH of 9.5. The salt rejection of the PA membrane decreased by 20% after only 20 hours of exposure and it continued to decrease rapidly. In contrast, the BPS membrane showed no significant change in salt rejection, and this clearly demonstrates its excellent chlorine tolerance relative to conventional desalination membranes.[24-26] These polymers also exhibit low fouling in oily or protein contaminated water, and high water flux with moderate salt rejection.

In general for these copolymers, water permeability increases and salt rejection decreases with increasing degree of disulfonation.[22] At high ion concentrations, the membranes swell strongly in water, leading to a loss in mechanical stability and ion rejection. Crosslinking such membranes is one approach for reducing the swelling of these membranes and improving their mechanical stability without significantly impairing water flux. Strategies for crosslinking sulfonated polysulfones include van der Waals interactions, hydrogen bonding, ionic or covalent crosslinking, and forming composite blends.[27] Covalent crosslinking has the most pronounced effect on the polymer structure because it permanently fixes the morphology of the polymer. In the literature, there have been only a few reports of covalently crosslinked ionomer membranes. Nolte *et al*. covalently crosslinked a partially N-imidazolized sulfonated poly(ether sulfone) Victrex® ionomer with 4,4'-diaminodiphenylsulfone.[28] Kerres *et al.* developed a novel covalent crosslinking process in which polysulfones containing

sulfinate groups within the chains were crosslinked via S-alkylation of the sulfinate groups with dihalogenoalkanes. The membranes showed decreased swelling in water but were brittle when dry. The brittleness was partially attributed to inflexibility as a result of crosslinking sites along the backbones of the copolymers.[27, 29, 30]

In this paper, we describe the synthesis and crosslinking of BPS random copolymers with high degrees of disulfonation (e.g., 50% disulfonation) for reverse osmosis applications. A series of controlled molecular weight copolymers with phenolic endgroups was synthesized and further reacted with an approximately tetrafunctional epoxy reagent to produce crosslinked networks. The properties of the crosslinked membranes were evaluated in terms of three variables: curing time, number average molecular weight of the copolymers, and equivalents of epoxy with respect to terminal phenoxide groups in the copolymer (Table 3). The effects of crosslinking on RO properties such as water permeability, salt rejection and salt permeability have been investigated. The fundamental hypothesis is that controlled crosslinking will reduce water swelling and enhance salt rejection of highly charged membrane materials. It is postulated that this approach can lead to highly water permeable desalination membranes that also exhibit high salt rejection. This paper demonstrates that controlled crosslinking can produce the combined properties of reduced water swelling and enhanced salt rejection of highly charged membranes. This approach leads to highly water permeable desalination membranes that also exhibit high salt rejection.

3.2. **Experimental**

3.2.1. Materials

Monomer grade 4,4′–dichlorodiphenylsulfone (DCDPS) and 4,4′-biphenol (BP) were obtained from Solvay Advanced Polymers and Eastman Chemical Company, respectively, and dried under vacuum at 60 °C for one day prior to use. The sulfonated comonomer, 3,3′-disulfonate-4,4′-dichlorodiphenylsulfone (SDCDPS), was prepared following a previously published procedure[20, 22], and dried under vacuum at 160 °C for two days before use. Potassium carbonate (Aldrich) was dried under vacuum at 110 °C

for one day before use. Tetraglycidyl bis(p-aminophenyl)methane (Araldite MY721 epoxy resin) and triphenylphosphine (TPP) were obtained from Aldrich and used as received. The reaction solvent *N*,*N*-dimethylacetamide (DMAc, Aldrich) was vacuum-distilled from calcium hydride, and stored over molecular sieves under nitrogen. Toluene (anhydrous, 99.8%), isopropanol (*ReagentPlus*™, 99%), *N*-methyl-2-pyrrolidinone (NMP, *ReagentPlus*™, 99%) and trimethylchlorosilane (silanizing agent) were obtained from Aldrich and used as received.

3.2.2. Synthesis of a controlled molecular weight phenoxide-endcapped BPS50 copolymer

A controlled molecular weight, phenoxide-endcapped 50% disulfonated biphenol-based poly(arylene ether sulfone) (BPS50) was synthesized via nucleophilic aromatic substitution. The molecular weight of the copolymer was controlled by offsetting the stoichiometry of the monomers. A typical polymerization of a 5 kg mol^{-1} BPS50 (BPS50-5k) copolymer is provided. BP (3.102 g, 16.66 mmol), DCDPS (1.849 g, 6.44 mmol), and SDCDPS (4.824 g, 9.82 mmol) were added to a three-necked, round bottom reaction flask equipped with a mechanical stirrer, nitrogen inlet, Dean-Stark trap and a condenser. Potassium carbonate (2.649 g, 19.17 mmol) and 49 mL DMAc (to achieve 20% solids) were introduced into the flask. Toluene (24 mL, DMAc/toluene was 2/1 v/v) was added as the azeotropic reagent. The reaction mixture was refluxed at 150 °C for 4 h, then the azeotrope was removed to dehydrate the system. The reaction mixture was gradually heated to 170 °C by the controlled removal of toluene, then reacted for an additional 65-70 h. The viscous product was cooled to room temperature. The product mixture was filtered to remove salts. The copolymer was isolated by precipitation in isopropyl alcohol, filtered, and dried for 24 h at 70 °C under ambient pressure, and then for 24 h at 110 °C under vacuum.

3.2.3. Silanization of glass casting plates

A 20% (v/v) solution of trimethylchlorosilane in toluene was prepared. Clean glass plates were immersed in the solution for 2-3 minutes, removed, then reacted in a

convection oven for 1 h at 250 °C. The plates were cooled to room temperature and washed with acetone before use.[31]

3.2.4. Film casting and epoxy curing

A 10 wt% solution of a phenoxide endcapped BPS50 copolymer with various weight concentrations of MY721 epoxy resin and 2.5 wt% of TPP catalyst (based on epoxy resin weight) was prepared in NMP and stirred until a transparent homogeneous solution was obtained. The solution was cast on a silanized glass plate. The plate was inserted in a vacuum oven and heated at 100 °C for 2 h under vacuum, then at 150 °C for 15, 45 or 90 minutes without vacuum. After cooling to room temperature, the plate was removed from the oven and the membrane was peeled from the glass plate. Three different series of crosslinked membranes were prepared. In the first series, the copolymer weight and epoxy concentration were fixed at 5 kg mol^{-1} and 2 equivalents of epoxy groups per phenoxide end group on the copolymer. The crosslinking time was varied from 15, 45 and 90 minutes. Secondly, the epoxy concentration and curing time were held constant at 2 equivalents of epoxy per equivalent of phenoxide and 90 minutes while the copolymer molecular weight was varied from 3 and 5 kg mol^{-1}. In addition, a blend of BPS50-20k and BPS50-5k copolymers in a 30:70 wt% ratio to produce an average molecular weight of 10 kg mol^{-1} was investigated. Thirdly, a series of crosslinked membranes were prepared with a constant curing time of 90 minutes and copolymer molecular weight of 5 kg $mole^{-1}$, but with varied epoxy equivalents of 1, 2, 3 and 4 per phenoxide.

The nomenclature of the samples is defined as follows- Xk-YE-ZM, where X is the M_n of the BPS50 copolymer(s) in kg mol^{-1}, Y equals the equivalents of epoxy per phenoxide group on the ends of the copolymers, and Z is the curing time in minutes.

Characterization

3.2.5. Nuclear magnetic resonance (NMR) spectroscopy

^{1}H NMR experiments were conducted on a Varian Unity 400 MHz NMR spectrometer. All spectra of the copolymers and epoxy resin were obtained from 10% solutions (w/v) in DMSO-d_6 and $CDCl_3$ respectively at room temperature. Proton NMR was used to determine the molecular weights of the copolymers and their compositions, and the functionality of the epoxy resin.

3.2.6. Fourier transform infrared (FT-IR) spectroscopy

FT-IR spectroscopy was used to study the crosslinking reactions of the copolymers. Measurements were recorded using a Tensor 27, Bruker FT-IR spectrometer with the sample solution placed between two sodium chloride discs and with cured membranes.

3.2.7. Gel permeation chromatography (GPC)

GPC experiments were performed on a liquid chromatograph equipped with a Waters 1515 isocratic HPLC pump, Waters Autosampler, Waters 2414 refractive index detector and Viscotek 270 RALLS/viscometric dual detector. The mobile phase was NMP solvent containing 0.05 M LiBr. The column temperature was maintained at 60 °C because of the viscous nature of NMP. Both the solvent and sample solution were filtered before introduction to the GPC system. Molecular weights were determined by universal calibration calibrated with polystyrene standards.

3.2.8. Intrinsic viscosity (IV)

Intrinsic viscosities were determined in NMP with 0.05 M LiBr at 25 ºC using an Ubbelohde viscometer.

3.2.9. Gel fractions

Gel fractions of the networks were measured by placing 0.1-0.15 g of sample in DMAc and soxhlet extracting for 48 h. After removal of the solvent by drying at 120 °C for 24 h under vacuum, the remaining mass was weighed as gel. Gel fractions were calculated by dividing the weights of the gels by the initial weights of the networks.

3.2.10. Water uptake

The membranes were immersed in deionized water for at least 48 h, then they were removed from the water, blotted dry and quickly weighed. The membranes were vacuum dried at 110 °C overnight and the weights were recorded. The ratio of weight gain to the original membrane weight was reported as the water uptake (mass %)

$$\textit{Water uptake (\%)} = \frac{W_{wet} - W_{dry}}{W_{dry}} \times 100 \qquad \textbf{Equation 3-1}$$

where W_{wet} and W_{dry} were the masses of wet and dried samples, respectively.

3.2.11. Volume swelling ratio

The membranes were equilibrated in deionized water for at least 48 h, then they were removed from the water and blotted dry. The dimensions were measured in three directions (length, width and thickness) to calculate the wet volume. The samples were dried in a convection oven for 2 h at 80 °C. The ratio of volume gain to the original membrane volume was reported as the volume swelling ratio.

3.2.12. Differential scanning calorimetry (DSC)

Thermal transitions of the membranes were studied via DSC using a TA Instruments DSC Q-1000 at a heating rate of 10 °C min^{-1} under nitrogen. The onset temperature of the curing exotherm was used to assess the curing temperature. For experiments to determine the states of water and solvent-depressed T_gs, the samples were

placed in thermally sealed, high volume DSC pans (TA Instruments) capable of withstanding pressure up to about 600 psi. Samples were cooled to -70 °C and then heated at a rate of 5 °C min^{-1} under a nitrogen atmosphere.

3.2.13. Thermogravimetric analysis (TGA)

Thermo-oxidative behavior of the cured membranes and residual solvent concentrations were measured on a TA Instruments TGA Q500. The typical heating rate was 10 °C min^{-1} in nitrogen.

3.2.14. Self-diffusion coefficient of water

Water self diffusion coefficients were measured using a Varian Inova 400 MHz (for protons) NMR spectrometer with a 60 G cm^{-1} gradient diffusion probe.[19] A total of 16 points were collected across the range of gradient strength and the signal-to-noise ratio was enhanced by co-adding 4 scans.

3.2.15. Water permeability and salt rejection

In all experiments related to water and salt transport properties, the water was produced by a Millipore MilliQ system (Billerica, MA). Pure water permeability was measured using a high-pressure (up to 1000 psi) dead-end filtration system (Sterlitech TM HP4750 stirred cell, Sterlitech Corp., WA). The membrane size was 49 mm in diameter, and the active membrane area was 14.6 cm^2. The membrane thickness was 50-100 μm. Water permeability (P_w) was calculated from the volumetric water flux, V, per unit time, t, through a membrane of area A and thickness l divided by the pressure difference, Δp:

$$P_W = \frac{V \cdot l}{A \cdot t \cdot \Delta p} \qquad \textbf{Equation 3-2}$$

In this study, NaCl was used for ion rejection studies. Salt rejection experiments were conducted in a dead-end system using feed solutions containing 2000 mg L^{-1} of NaCl (2000 ppm). The salt rejection (R) was calculated as

$$R(\%) = \left(1 - \frac{C_p}{C_f}\right) \times 100 \qquad \textbf{Equation 3-3}$$

where C_p is the salt concentration in the permeant and C_f is the salt concentration in the feed water. Both C_p and C_f were measured with a digital conductivity meter (Oakton® CON 110, Cole Parmer, Vernon-Hills, NJ). The salt rejection data are reported at a feed pressure of 1000 psig (approximately 70 bar); the permeant pressure was atmospheric.

3.2.16. Salt permeability

Salt permeability through the polymer membranes was determined in diffusion cell studies conducted at atmospheric pressure [32]. Samples were rinsed five times with deionized water to completely remove any sorbed salt before beginning these measurements. A membrane coupon was sandwiched between two halves of a diffusion cell (effective membrane diameter was 1.5 cm). One side of the cell (i.e., the donor) was filled with 0.1 M NaCl solution. The other side of the cell (i.e., the receiver) was initially filled with pure, deionized water. Salt permeability through the membranes was determined at 25 °C by measuring the electrolytic conductivity of the receiver solution as a function of time. The salt permeability coefficient, P, was calculated using equation 4, which was derived by applying a transient mass balance to the diffusion cell:

$$Ln\left[1 - 2\frac{\sigma_R(t)}{\sigma_D(0)}\right]\left[-\frac{Vl}{2A}\right] = Pt \qquad \textbf{Equation 3-4}$$

where $\sigma_R(t)$ is the salt concentration at time t in the receiver cell, and $\sigma_D(0)$ is the salt concentration in the donor cell at the beginning of the experiment (i.e., at t=0). V is the

volume of the donor and receiver chambers (cm^3), and in these experiments the donor and receiver volumes were both 35 cm^3, *l* is the membrane thickness (cm), *A* is the membrane area (cm^2), and *P* is the salt permeability ($cm^2\ sec^{-1}$).

3.3. Results and discussion

3.3.1. Synthesis of phenoxide terminated BPS50 copolymers

A series of controlled molecular weight BPS50 copolymers with phenoxide endgroups was synthesized from SDCDPS, DCDPS and biphenol by nucleophilic aromatic substitution (Fig. 3.1). The molecular weights of the copolymers were controlled by offsetting the stoichiometry between biphenol and the dihalides. Biphenol was utilized in excess to endcap the copolymers with phenoxide groups, so that the phenoxide groups could be further reacted in the crosslinking steps. Three copolymers with number average molecular weights (M_n) of three, five and twenty kg mol^{-1} were targeted. The degree of disulfonation was controlled by varying the molar ratio of SDCDPS to DCDPS. For all of the copolymers, the degree of disulfonation was 50%.

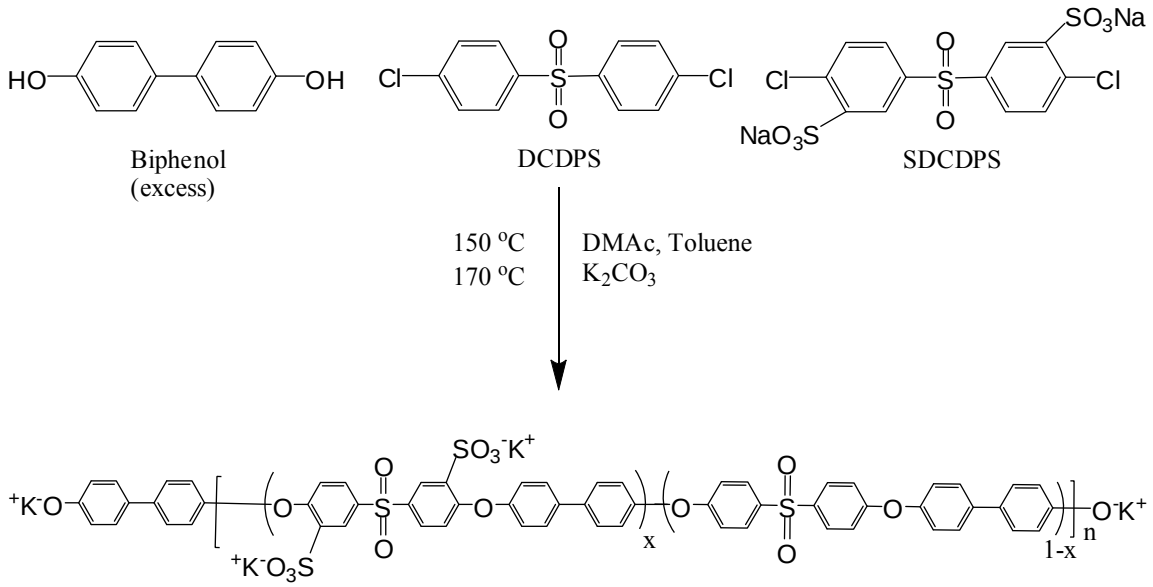

Figure 3.1 Synthesis of a phenoxide endcapped BPS50 copolymer, where, x = 50

Figure 3.2 shows the proton NMR spectrum of a copolymer with a targeted molecular weight of five kg mol^{-1}. The ratio of the integrals of the aromatic protons of the biphenol unit in the endgroup at 6.8 ppm (*b*) to those in the polymer repeat units at 7.7 ppm (*m* and *i*) were utilized to calculate M_n of the copolymers. As shown in Table 3.1, the experimental M_n values derived from both NMR and GPC are in good agreement with the targeted values.

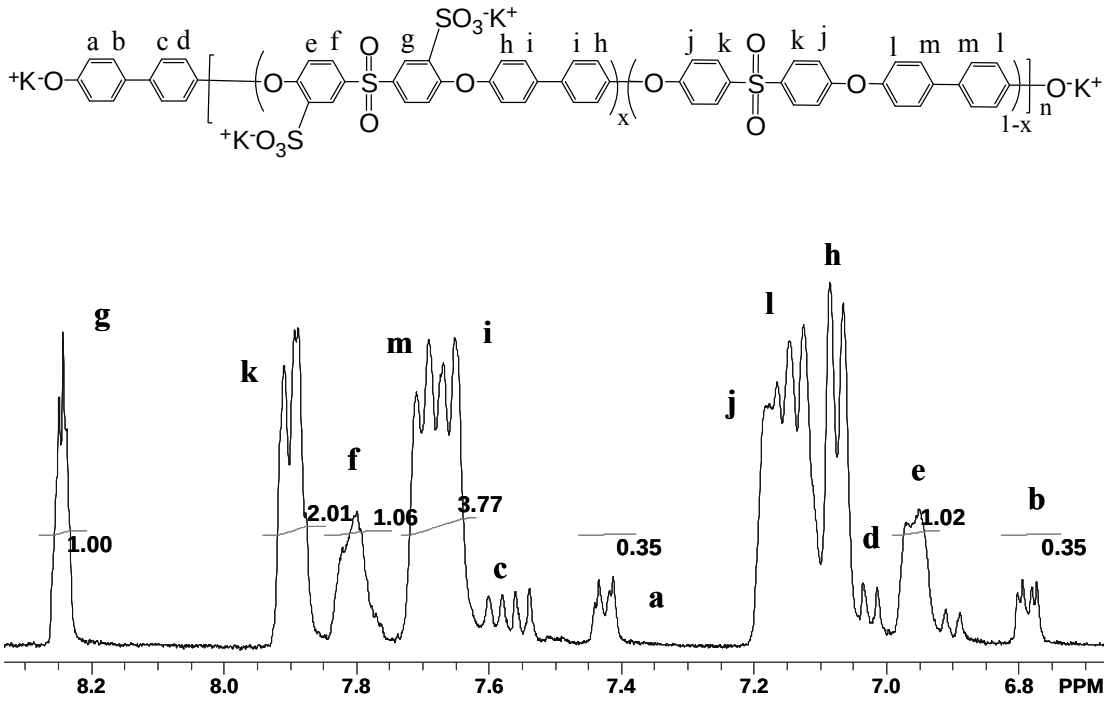

Figure 3.2 ^{1}H NMR of a phenoxide endcapped BPS50 copolymer

As expected, intrinsic viscosities of the copolymers increased with increasing molecular weight (Table 3.1). The degree of disulfonation was confirmed from the ratio of the integrals of protons at 6.95 ppm (*e*), 7.8 ppm (*f*) and 8.25 ppm (*g*) in the sulfonated unit to the protons at 7.9 ppm (*k*) in the unsulfonated unit. The degrees of disulfonation were used to calculate the ion exchange capacities (IEC- meq of sulfonic acid groups per gram of dry polymer) of the copolymers. Table 3.1 shows that the experimental IEC values of the copolymers are in good agreement with the targeted values.

Table 3.1 Summary of BPS50 copolymers

Copolymer	M_n (kg mol^{-1})			IV[a] (dL g^{-1})	IEC (meq g^{-1})		
	Target	^{1}H NMR	GPC		Target	^{1}H NMR	Titration[b]
BPS50-3k	3	3.5	3.6	0.16	2.08	2.08	-
BPS50-5k	5	5.8	5.2	0.22	2.08	2.04	-
BPS50-20k	20	20.8	21.8	0.43	2.08	2.03	1.90

[a] Intrinsic Viscosity (IV) in NMP with 0.05 M LiBr

[b]Back-titration of sulfonic acid groups

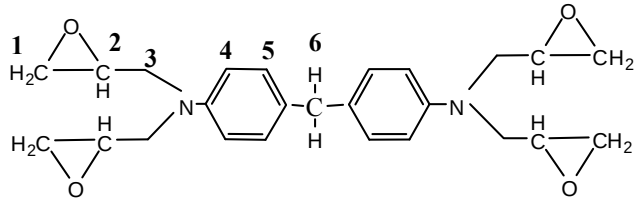

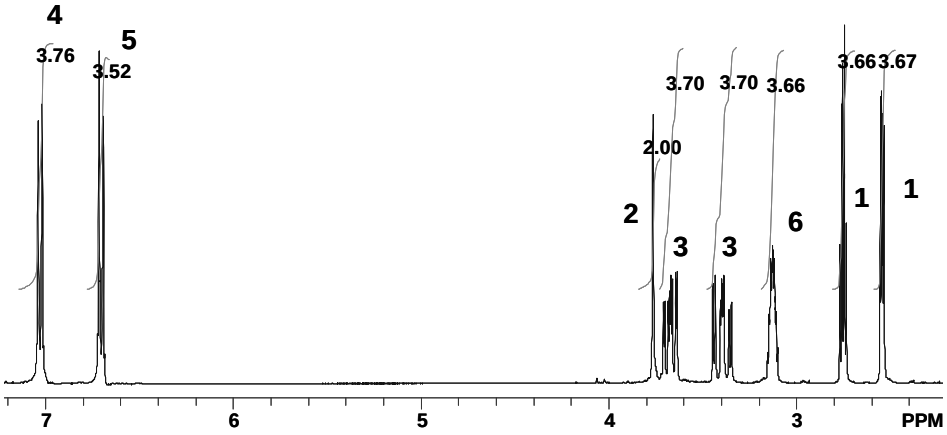

Figure 3.3 ^{1}H NMR of Tetraglycidyl bis-(p-aminophenyl)methane (Araldite MY721)

Tetraglycidyl bis(p-aminophenyl)methane (Araldite MY721) was used as the epoxy crosslinking reagent. The average functionality of the epoxy was 3.66 as determined from the ratio of the integrals of epoxy ring protons (2) at 3.1 ppm to those of the methylene protons (6) at 3.75 ppm (Fig. 3.3).

3.3.2. Investigation of the curing reaction parameters

BPS50 is an ion-containing aromatic copolymer with a high glass transition temperature of ~250 °C. Crosslinking reactions of such a high T_g copolymer are challenging because of the need to avoid vitrification. One method for achieving high conversions is to conduct the crosslinking reaction in the presence of a high boiling solvent such as NMP so that the solvent can depress the T_g of the network as it forms. A DSC thermogram (Fig. 3.4(i)) of a BPS50 oligomer containing about 42% solvent (Table 3.2) shows a solvent-plasticized T_g of ~145 °C. Figure 3.4(ii) shows a curing exotherm at ~150 °C from an epoxy-BPS50 crosslinking reaction. It is evident that the crosslinking reaction occurred above the solvent-depressed glass transition temperature. This DSC study highlights the necessity of the presence of some solvent during such crosslinking reactions. Thermogravimetric analysis (Fig. 3.5) was used to determine the amount of solvent that remained as a function of curing time. Table 3.2 shows that even after 45 minutes of cure, about 23 wt% solvent remained in the system. It is noteworthy that this concentration of solvent should also be sufficient for further crosslinking to take place (i.e., for membranes cured for 90 minutes), since it should be sufficient to depress the T_gs of networks with higher gel fractions to avoid vitrification.

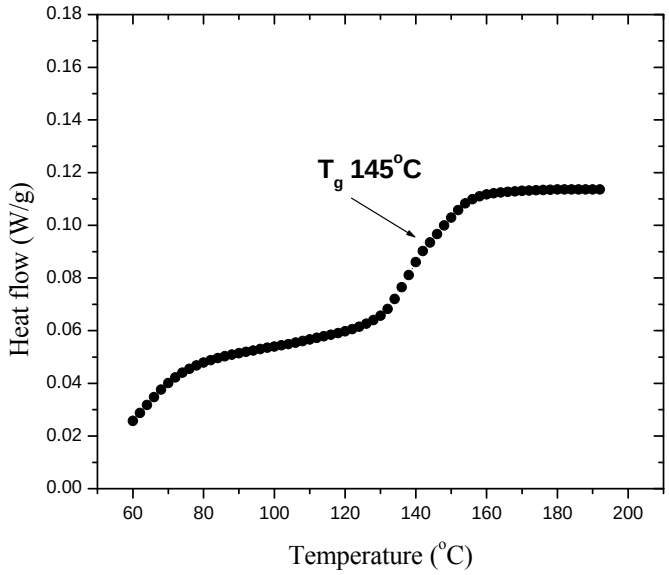

Figure 3.4 (i) DSC thermogram shows solvent depressed Tg of a BPS50 oligomer

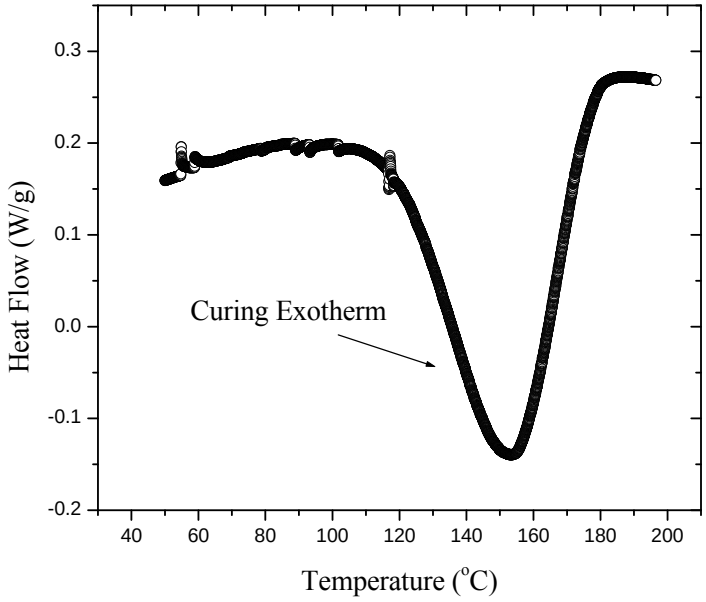

Figure 3.4 (ii) A curing exotherm at 150 °C is observed in the DSC thermogram of an epoxy crosslinked BPS50

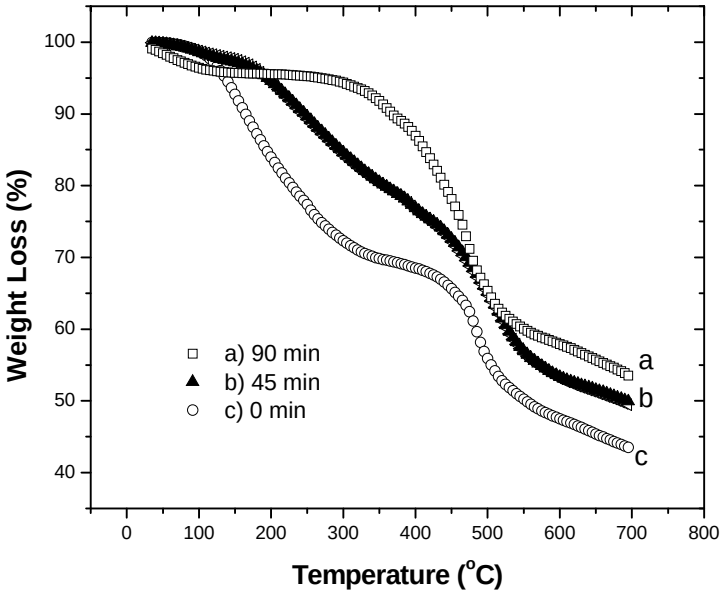

Figure 3.5 TGA study shows presence of solvent required for ongoing crosslinking reaction with increasing curing time

Table 3.2 Retention of solvent as a function of crosslinking time from TGA

Sample	Solvent %
5k-2E-0M	42
5k-2E-45M	23
5k-2E-90M	11

The crosslinking reaction was also studied by FTIR. Araldite MY721 has an epoxide ring deformation [33] at 907 cm^{-1} which does not coincide with any peaks of the BPS50 copolymer (Fig 3.6(i)). Figure 3.6(ii) displays the superimposed spectra of pure epoxy, the uncrosslinked polymer-epoxy mixture (5k-2E-0M) and a crosslinked network (5k-2E-90M). Both the uncrosslinked system and the pure epoxy showed similar epoxide ring deformations at 907 cm^{-1}. However, as expected, a reduction in the peak intensity was observed upon crosslinking.

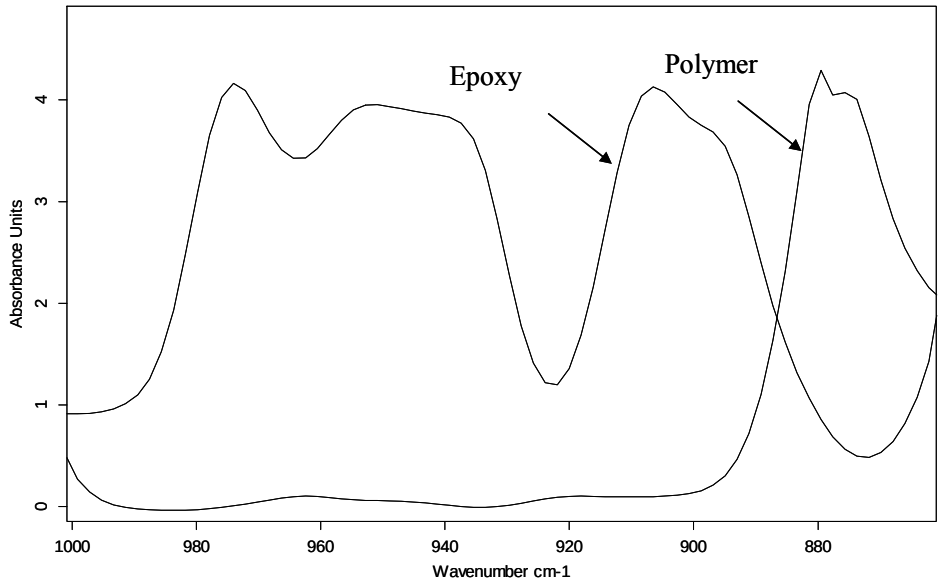

Figure 3.6 (i) FTIR spectrum shows no coincidence of BPS50 copolymer peaks with epoxide ring deformation at 907 cm^{-1}

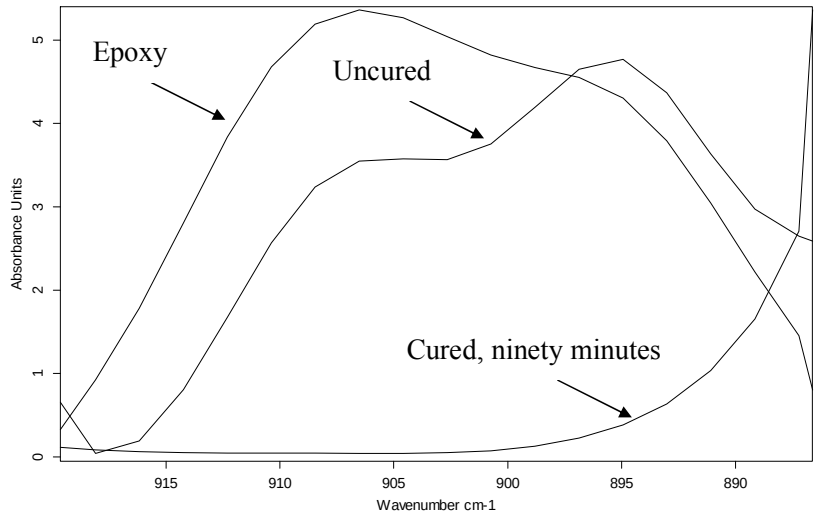

Figure 3.6 (ii) FTIR spectrum shows reduction in epoxide ring deformation at 907 cm^{-1} of a membrane crosslinked for ninety minutes

Membrane properties

3.3.3. Gel fractions

Gel fractions of the crosslinked networks can be considered as an indirect measure for assessing the extent of crosslinking. As expected, the gel fractions of the cured membranes increased with increasing crosslinking time and decreasing copolymer molecular weight (Table 3.3). The terminal crosslinking sites increase with decreasing copolymer molecular weight. The networks formed from two equivalents of epoxy per phenoxide endgroup showed the highest gel fractions, whereas those with more or less than two equivalents of epoxy had lower gel fractions. It is not yet clear why this occurs.

Table 3.3 Properties of cured films as functions of curing time, copolymer molecular weights and epoxy equivalents

System	Curing Time (min)	M_n of BPS50 kg mole^{-1}	Equivalents of Epoxy[a]	Gel Fraction[b] (%) (±10%)	Water Uptake (mass %) (±10%)	Swelling Ratio (volume %) (±10%)
Control	**0**	**5**	**0**	**0**	**51**	**70**
5k-2E-15M	**15**	**5**	**2.1**	**10**	**41**	**67**
5k-2E-45M	**45**	**5**	**2.1**	**20**	**37**	**50**
5k-2E-90M	**90**	**5**	**2.1**	**80**	**30**	**39**
3k-2E-90M	**90**	**3**	**2.1**	**85**	**34**	**40**
10k-2E-90M	**90**	**10**	**2.1**	**17**	**45**	**75**
5k-1E-90M	**90**	**5**	**1**	**10**	**45**	**62**
5k-3E-90M	**90**	**5**	**3**	**50**	**45**	**66**
5k-4E-90M	**90**	**5**	**4**	**9**	**42**	**48**

[a]Calculated with respect to phenoxide endgroups in the polymer

[b]Soxhlet extraction in DMAc for 48 h

3.3.4. Water uptake and volume swelling ratio

Ion-containing polymers typically have high water uptake associated with volume swelling. This reduces the effective charge density of the membrane, and can also result in poor dimensional stability. One of the main objectives of this paper was to investigate the effect of crosslinking on water uptake and swelling of the networks. Table 3.3 shows a general trend of reduction in water uptake and volume swelling ratio with increasing gel fractions. The lowest water uptake and swelling were observed for the network cured with two equivalents of epoxy per phenoxide. A drastic change in water uptake and swelling occurred when the molecular weight of the copolymer was decreased from 10 kg mole^{-1} to five or three kg mole^{-1}. An exponential decrease in water uptake with increasing gel fraction was found with increased curing time (Fig. 3.7). The highest reduction in water uptake upon curing, ~70%, was observed for the network that was cured for 90 minutes.

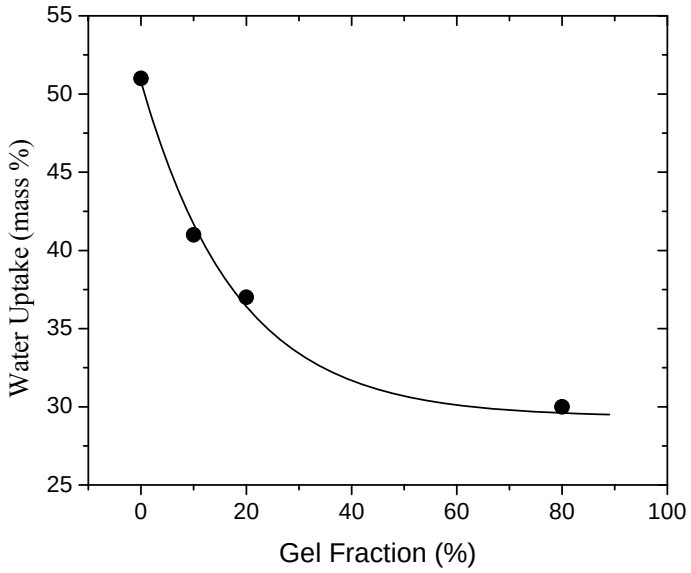

Figure 3.7 Water uptake decreases exponentially as a function of gel fractions for the system with increasing curing time

3.3.5. Self-diffusion coefficients of water

The self-diffusion coefficient of water is an intrinsic transport property of the membrane, and is related to the structure and the chemical composition of the copolymers or networks. In general, the self-diffusion coefficient of water scales with the volume fraction of the solvent or with the free volume of the system. Crosslinking of a polymer is associated with a reduction in the free volume and formation of restricted morphological structure. Self-diffusion coefficients of water were measured for the uncrosslinked and crosslinked samples. Figure 3.8 illustrates the self-diffusion coefficient of water as a function of gel fractions of the networks. A significant reduction is observed at higher gel fractions relative to those for the uncrosslinked or lightly crosslinked materials. This may suggest the formation of restricted morphology and reduced water transport with increasing crosslink density.

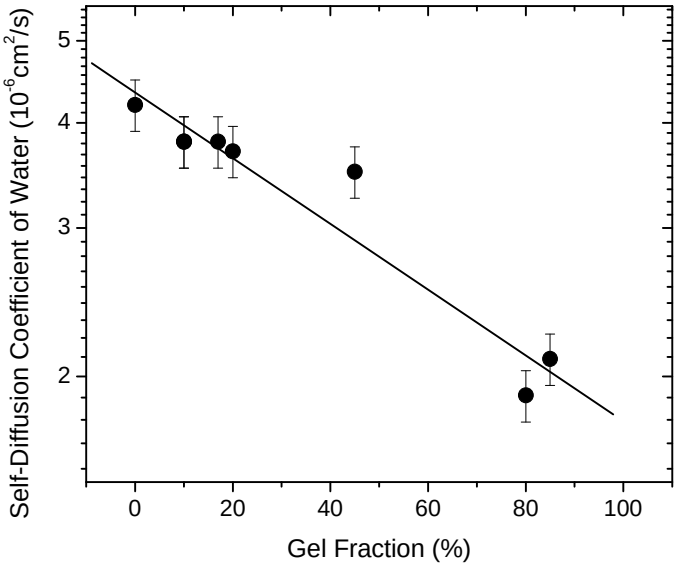

Figure 3.8 Self-diffusion coefficient of water as a function of gel fractions of the cured systems

3.3.6. States of water

There are at least three states of water that have been associated with water residing in hydrophilic phases of polymers.[34-37] The presence of these three states can be defined by thermal properties. *Non-freezing bound water* is strongly associated with the polymer and depresses its T_g, but the water shows no melting endotherm by DSC. *Freezable bound water* is weakly bound to the polymer (or weakly bound to the non-freezing water), and displays broad melting behavior around 0 °C. *Free water* exhibits a sharp melting point at 0 °C. Earlier investigations on states of water in ion containing polymers have shown a strong dependence of transport properties on the types of water. Figure 3.9 displays the melting endotherms of the freezable water as a function of the curing time. A sharp melting peak around 0 °C along with a broad melting endotherm is observed for the system cured for 15 minutes. However the disappearance of the free water peak and a significant decrease in the area under the melting endotherm were observed for the samples cured for 45 and 90 minutes. The ratio of free to bound water decreases with increasing crosslinking time. Since different sites have variable interactions with water, the peaks sometimes appear asymmetric. This may be important in understanding the importance of crosslinking on fundamental transport properties. The influence of the crosslinking reaction on the hydrated T_g was also studied. The hydrated T_g increased with increasing curing time (Fig. 3.10).

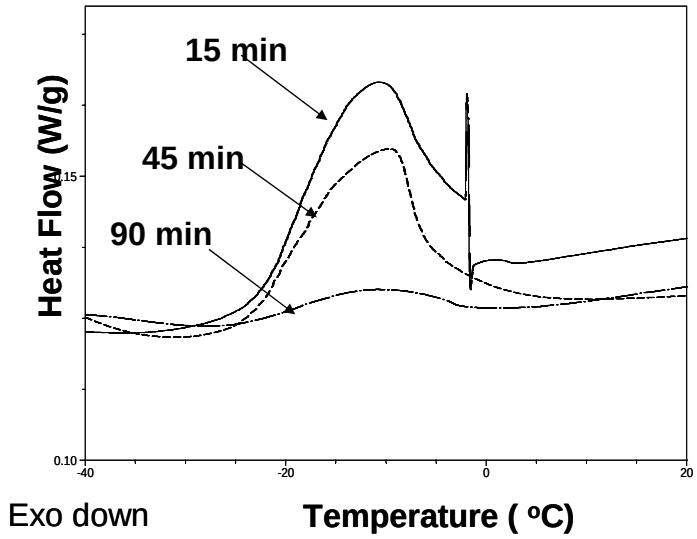

Figure 3.9 DSC thermogram showing water melting endotherm peaks as a function of crosslinking time

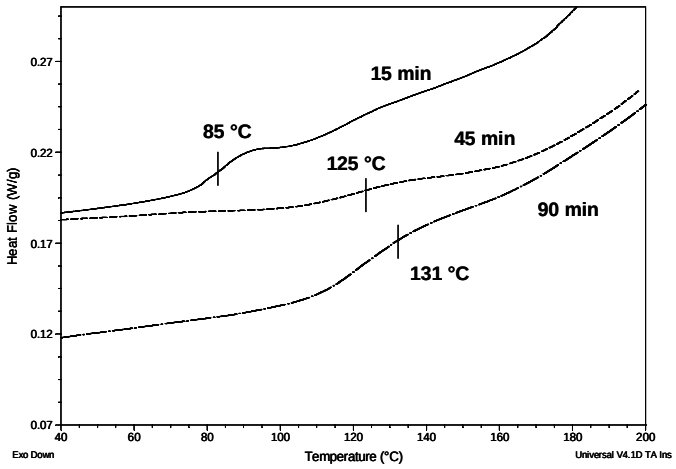

Figure 3.10 DSC thermogram shows increasing hydrated Tg with curing time

3.3.7. Water permeability and salt rejection

For reverse osmosis, membrane materials should have intrinsically high water permeability and low salt permeability. Usually, increasing the sulfonation level in sulfonated polymers increases water permeability by improving hydrophilicity, which leads to higher water uptake. However, excessive water uptake (i.e., swelling) usually increases salt passage, and also decreases mechanical properties. In addition, highly sulfonated polymers can even be soluble in water.

In negatively charged polymer membranes such as in the disulfonated polymers considered in this study, the ionic groups can electrostatically repel negative ions in solution. Therefore, the salt rejection with charged membranes can depend on charge effects as well as on various factors such as feed concentration and permeant flux. Rejection is higher at lower feed concentration due to Donnan exclusion.[38-41] Salt rejection should improve with increasing membrane charge density. For this reason, high degrees of disulfonation might improve rejection if water swelling can be controlled. Crosslinking (to reduce water swelling) of highly charged membranes (to enhance rejection) could lead to materials that are both highly water permeable and exhibit high salt rejection.

Table 3.4 records water permeability and sodium chloride rejection of crosslinked sulfonated polymer membranes as a function of curing time. In this table, results for the sodium sulfonate form of the polymers are reported. Increased curing time is associated with more highly crosslinked structures. For comparison, the properties of BPS50, an uncrosslinked polymer having the same sulfonic acid group concentration as that found in the crosslinked samples, are also presented. As expected, water permeability decreases somewhat as the curing time was increased from 15 to 90 minutes, indicating that crosslinking modifies the pathway for water transport. On the other hand, the NaCl rejection increases strongly with curing time, ranging from 73.4% rejection for the uncrosslinked control to 97.2% for the crosslinked membrane cured for 90 minutes.

Undoubtedly, changes in the material structure brought about by the thermal treatments have subtle effects that systematically reduce the water swelling of the materials. Substantial further studies will be needed to fully understand this phenomenon.

Table 3.4 Water permeability and salt transport of crosslinked BPS copolymer films

System	Curing Time (min)	Water Permeability ($L \cdot \mu m/m^2 \cdot h \cdot bar$)	NaCl Rejection[a] (%)	NaCl Permeability[b] ($\times 10^{-8}$, $cm^2\ s^{-1}$)
BPS-5k-2E-15M	15	3.2	87.8	6.5
BPS-5k-2E-45M	45	1.5	96.1	3.8
BPS-5k-2E-90M	90	1.4	97.2	1.1
Uncrosslinked BPS50	0	3.5	73.4	-
SW30HR-380[c]	-	0.61[d]	99.7	-

[a]Feed = 2000 ppm NaCl; Applied pressure = 1000 psig; Temperature = 25 °C

[b]Measured using direct salt permeability measurement (donor solution = 0.1 M NaCl)

[c]Commercial PA membrane (http://www.dow.com/liquidseps/);[42] Test conditions: Feed = 32000 mg/L NaCl; Applied pressure = 800 psig; Temperature = 25 °C

[d] Unit is permeance ($L/m^2.h.bar$)

The NaCl permeabilities ($cm^2\ sec^{-1}$) of the crosslinked copolymer membranes are also sensitive to the structural changes brought about by the crosslinking reactions. The permeability decreases regularly with increasing curing time (Table 3.4), indicating that crosslinking effectively restrains transport of hydrated salt molecules through the sulfonated polymer films. These results suggest that covalent crosslinking of sulfonated polymers is a promising method to achieve high salt rejection, while maintaining high water permeability.

The crosslinked membranes were compared with a commercial PA membrane, FILMTEC SW30HR-380 [37] in terms of water permeability and salt rejection (Table 3.4). It is hard to obtain a true comparison between the salt rejections of the crosslinked and the commercial PA membrane due to the higher thickness of the crosslinked membranes and also to the difference in testing conditions. Salt rejection of the crosslinked membranes was measured using a dead-end filtration at a higher operating pressure (1000 psig). In fact, salt rejection data derived from a dead-end filtration are usually lower than those from a cross-flow filtration because concentration polarization often occurs in the dead-end filtration, particularly under such a high operating condition (1000 psig). Salt rejection is expected to improve with thinner crosslinked membranes and further optimization of the crosslinking variables.

We have recently demonstrated that thin film composite membranes of thermoplastic random BPS copolymers having comparable selective layers (0.7 – 1.2 μm) as that of commercial polyamides were prepared successfully [42]. The future and ongoing plan is to implement the same strategy for preparing thin film composite membranes for crosslinked BPS systems. Additionally, the influence of crosslinking on chlorine stability of the membranes will also be determined experimentally.

3.4. Conclusions

A series of controlled molecular weight, 50% disulfonated poly(arylene ether sulfone)s was synthesized with phenoxide endgroups. These endgroups were reacted with a multifunctional epoxy resin to produce robust, crosslinked, hydrophilic membranes. By only crosslinking the materials at their endgroups, flexible, ductile films were achieved. In general, gel fraction increased with increasing curing time and decreasing copolymer molecular weight. It was determined that the membrane crosslinked for 90 minutes with two equivalents of epoxy per phenoxide endgroup had the highest gel fraction. All of the cured membranes had lower water uptake and

swelling relative to their uncrosslinked counterparts, and less water uptake and volume swelling were correlated with increasing gel fractions.

The self-diffusion coefficients of water also decreased with increasing gel fraction, indicating restricted water transport with increased crosslinking. Salt rejection of the BPS50 copolymer improved dramatically after crosslinking. The membranes that had been cured for the longer times showed 97.2% salt rejection compared to only 73.4% rejection without crosslinking, while the water permeability of the crosslinked membrane only decreased modestly. Reductions in salt permeability with increasing crosslink density also suggested that crosslinking inhibits salt transport through the membrane. The effects of crosslinking on fundamental water and salt transport properties of these highly disulfonated copolymers are encouraging, and suggests their potential as candidates for RO membranes.

Acknowledgements - The authors would like to thank the Office of Naval Research (N00014-05-01-0772 and N00014-06-1-1109) and the National Science Foundation (IIP-0650277) for their support.

3.5. References

1. Oki, T.; Kanae, S., Global Hydrological Cycles and World Water Resources. *Science (Washington, DC, United States)* **2006,** 313, (5790), 1068-1072.

2. Service, R. F., Desalination Freshens Up. *Science (Washington, DC, United States)* **2006,** 313, (5790), 1088-1090.

3. Graefe, A. F.; Wong, D., Development of a chlorine-resistant composite membrane for reverse osmosis. *NTIS Report No. PB81-115420* **1980**.

4. Avlonitis, S.; Hanbury, W. T.; Hodgkiess, T., Chlorine degradation of aromatic polyamides. *Desalination* **1992,** 85, (3), 321-34.

5. Knoell, T., Municipal wastewater. Chlorine's impact on the performance and properties of polyamide membranes. *Ultrapure Water* **2006,** 23, (3), 24-31.

6. Petersen, R. J., Composite reverse osmosis and nanofiltration membranes. *Journal of Membrane Science* **1993,** 83, (1), 81-150.

7. Allegrezza, A. E., Jr.; Parekh, B. S.; Parise, P. L.; Swiniarski, E. J.; White, J. L., Chlorine resistant polysulfone reverse osmosis modules. *Desalination* **1987,** 64, 285-304.

8. Noshay, A.; Robeson, L. M., Sulfonated polysulfone. *Journal of Applied Polymer Science* **1976,** 20, (7), 1885-903.

9. Plummer, C. W.; Kimura, G.; La Conti, A. B., Development of sulfonated polyphenylene oxide membranes for reverse osmosis. *NTIS Report No. PB-201034* **1970**.

10. LaConti, A. B.; Chludzinski, P. J.; Fickett, A. P., Morphology and reverse osmosis properties of sulfonated poly(2,6-dimethyl phenylene oxide) membranes. *Reverse Osmosis Membrane Res.* **1972**, 263-84.

11. Bourganel, J. Anisotropic, semipermeable membranes comprising poly(aryl ether sulfones). DE 72-2225284, 19720524., 1972.

12. Quentin, J. P. Polysulfones. DE 70-2021383, 19700430., 1970.

13. Schiffer, D. K.; Davis, R. B.; Coplan, M. J.; Kramer, C. E., Development of hollow fiber reverse osmosis membranes. *NTIS Report No. PB81-167215* **1980**.

14. Friedrich, C.; Driancourt, A.; Noel, C.; Monnerie, L., Asymmetric reverse osmosis and ultrafiltration membranes prepared from sulfonated polysulfone. *Desalination* **1981,** 36, (1), 39-62.

15. Harrison, W. L.; Hickner, M. A.; Kim, Y. S.; McGrath, J. E., Poly(arylene ether sulfone) copolymers and related systems from disulfonated monomer building blocks: Synthesis, characterization, and performance - A topical review. *Fuel Cells* **2005,** 5, (2), 201-212.

16. Hickner, M. A.; Ghassemi, H.; Kim, Y. S.; Einsla, B. R.; McGrath, J. E., Alternative polymer systems for proton exchange membranes (PEMs). *Chemical Reviews* **2004,** 104, (10), 4587-4611.

17. Kim, Y. S.; Hickner, M. A.; Dong, L. M.; Pivovar, B. S.; McGrath, J. E., Sulfonated poly(arylene ether sulfone) copolymer proton exchange membranes: composition and morphology effects on the methanol permeability. *Journal of Membrane Science* **2004,** 243, (1-2), 317-326.

18. Kinzer, K. E.; Lloyd, D. R.; Gay, M. S.; Wightman, J. P.; Johnson, B. C.; Mcgrath, J. E., Phase Inversion Sulfonated Polysulfone Membranes. *Journal of Membrane Science* **1985,** 22, (1), 1-29.

19. Roy, A.; Hickner, M. A.; Yu, X.; Li, Y.; Glass, T. E.; McGrath, J. E., Influence of chemical composition and sequence length on the transport properties of proton exchange membranes. *Journal of Polymer Science, Part B: Polymer Physics* **2006,** 44, (16), 2226-2239.

20. Sankir, M.; Bhanu, V. A.; Harrison, W. L.; Ghassemi, H.; Wiles, K. B.; Glass, T. E.; Brink, A. E.; Brink, M. H.; McGrath, J. E., Synthesis and characterization of 3,3'-disulfonated-4,4'-dichlorodiphenyl sulfone (SDCDPS) monomer for proton exchange membranes (PEM) in fuel cell applications. *Journal of Applied Polymer Science* **2006,** 100, (6), 4595-4602.

21. Summer, M. J.; Harrison, W. L.; Weyers, R. M.; Kim, Y. S.; McGrath, J. E.; Riffle, J. S.; Brink, A.; Brink, M. H., Novel proton conducting sulfonated poly(arylene ether) copolymers containing aromatic nitriles. *Journal of Membrane Science* **2004,** 239, (2), 199-211.

22. Wang, F.; Hickner, M.; Kim, Y. S.; Zawodzinski, T. A.; McGrath, J. E., Direct polymerization of sulfonated poly(arylene ether sulfone) random (statistical) copolymers: candidates for new proton exchange membranes. *Journal of Membrane Science* **2002,** 197, (1-2), 231-242.

23. Wang, H.; Badami, A. S.; Roy, A.; McGrath, J. E., Multiblock copolymers of poly(2,5-benzophenone) and disulfonated poly(arylene ether sulfone) for proton-exchange membranes. I. Synthesis and characterization. *Journal of Polymer Science, Part A: Polymer Chemistry* **2006,** 45, (2), 284-294.

24. Park, H. B.; Freeman, B. D.; Zhang, Z.; Sankir, M.; McGrath, J. E., Chlorine-Tolerant Disulfonated Poly(arylene ether sulfone) Desalination Membrane Materials. *Angewandte Chemie International Edition* **2008***, In Press.*

25. Park, H. B.; Freeman, B. D.; Zhang, Z.-B.; Fan, G.-Y.; Sankir, M.; McGrath, J. E., Water and salt transport behavior through hydrophilic-hydrophobic copolymer membranes and their relations to reverse osmosis membrane performance. *PMSE Preprints* **2006,** 95, 889-891.

26. Zhang, Z.-B.; Fan, G.-Y.; Sankir, M.; Park, H. B.; Freeman, B. D.; McGrath, J. E., Synthesis of di-sulfonated poly(arylene ether sulfone) random copolymers as novel candidates for chlorine-resistant reverse osmosis membranes. *PMSE Preprints* **2006,** 95, 887-888.

27. Kerres, J. A., Blended and cross-linked ionomer membranes for application in membrane fuel cells. *Fuel Cells (Weinheim, Germany)* **2005,** 5, (2), 230-247.

28. Nolte, R.; Ledjeff, K.; Bauer, M.; Muelhaupt, R., Partially sulfonated poly(arylene ether sulfone) - a versatile proton conducting membrane material for modern energy conversion technologies. *Journal of Membrane Science* **1993,** 83, (2), 211-20.

29. Kerres, J.; Cui, W.; Junginger, M., Development and characterization of crosslinked ionomer membranes based upon sulfinated and sulfonated PSU - Crosslinked PSU blend membranes by alkylation of sulfinate groups with dihalogenoalkanes. *Journal of Membrane Science* **1998,** 139, (2), 227-241.

30. Kerres, J.; Zhang, W.; Cui, W., New sulfonated engineering polymers via the metalation route. II. Sulfinated/sulfonated poly (ether sulfone) PSU Udel and its crosslinking. *Journal of Polymer Science Part a-Polymer Chemistry* **1998,** 36, (9), 1441-1448.

31. Mecham, S. J. Gas permeability of polyimide/polysiloxane block copolymers. M.S. Thesis, Virginia Polytechnic Institute and State University, Blacksburg, VA, 1994.

32. Yasuda, H.; Lamaze, C. E.; Ikenberry, L. D., Permeability of solutes through hydrated polymer membranes. I. Diffusion of sodium chloride. *Makromolekulare Chemie* **1968,** 118, 19-35.

33. Rocks, J.; Rintoul, L.; Vohwinkel, F.; George, G., The kinetics and mechanism of cure of an amino-glycidyl epoxy resin by a co-anhydride as studied by FT-Raman spectroscopy. *Polymer* **2004,** 45, (20), 6799-6811.

34. Hodge, R. M.; Bastow, T. J.; Edward, G. H.; Simon, G. P.; Hill, A. J., Free volume and the mechanism of plasticization in water-swollen poly(vinyl alcohol). *Macromolecules* **1996,** 29, (25), 8137-8143.

35. Hodge, R. M.; Edward, G. H.; Simon, G. P., Water absorption and states of water in semicrystalline poly(vinyl alcohol) films. *Polymer* **1996,** 37, (8), 1371-1376.

36. Kim, Y. S.; Dong, L. M.; Hickner, M. A.; Glass, T. E.; Webb, V.; McGrath, J. E., State of water in disulfonated poly(arylene ether sulfone) copolymers and a perfluorosulfonic acid copolymer (nafion) and its effect on physical and electrochemical properties. *Macromolecules* **2003,** 36, (17), 6281-6285.

37. Quinn, F. X.; Kampff, E.; Smyth, G.; Mcbrierty, V. J., Water in Hydrogels .1. A Study of Water in Poly(N-Vinyl-2-Pyrrolidone Methyl-Methacrylate) Copolymer. *Macromolecules* **1988,** 21, (11), 3191-3198.

38. Donnan, F. G., Theory of membrane equilibria and membrane potentials in the presence of non-dialysing electrolytes. A contribution to physical-chemical physiology. *Journal of Membrane Science* **1995,** 100, (1), 45-55.

39. Donnan, F. G.; Allmand, A. J., Ionic equilibria across semi-permeable membranes. *Journal of the Chemical Society, Transactions* **1914,** 105, 1941-63.

40. Tsuru, T.; Nakao, S.; Kimura, S., Effective charge density and pore structure of charged ultrafiltration membranes. *Journal of Chemical Engineering of Japan* **1990,** 23, (5), 604-10.

41. Tsuru, T.; Urairi, M.; Nakao, S.; Kimura, S., Reverse osmosis of single and mixed electrolytes with charged membranes: experiment and analysis. *Journal of Chemical Engineering of Japan* **1991,** 24, (4), 518-24.

42. http://www.dow.com/liquidseps/.

4. CHAPTER 4 - Effect of Crosslinking of Disulfonated Poly (Arylene Ether Sulfone) Random Copolymers on Proton Exchange Membrane Behavior

Mou Paul, Abhishek Roy, J.E. McGrath and J.S. Riffle

Macromolecules and Interfaces Institute (MII)
Virginia Polytechnic Institute and State University
Blacksburg, VA 24061

Abstract

Random disulfonated poly(arylene ether sulfone) copolymers (BPSH) were synthesized, endcapped with a multifunctional epoxy and subsequently thermally crosslinked. The networks were characterized in terms of gel fractions, water absorption, proton conductivities, self-diffusion coefficients of water, and methanol permeabilities. Crosslinking resulted in significant reduction in water swelling of BPSH copolymers. Both water and methanol transport were also restricted in the crosslinked membrane networks. A considerable reduction could be achieved with little significant change in the proton conductivities as a function of increasing gel fractions. Selectivities, (defined as the ratio of proton conductivity to swelling/methanol permeability) of the networks suggests application that both H_2/air and direct methanol fuel cells (DMFC) can be improved by crosslinking.

4.1. Introduction

Proton exchange membrane fuel cells (PEMFC)s have shown promise as an alternative source of energy.[1, 2] PEMFCs for H_2/Air systems have the potential to replace internal combustion engines for applications in the automotive industry. PEMFCs with methanol as the fuel (direct methanol fuel cells (DMFC)s) have potential for low power and portable applications.[3] The critical component in a PEMFC is the proton exchange membrane (PEM). The current requirements for both are high proton conductivity, low water uptake, low fuel permeability, and mechanical durability under the fuel cell environment.[4] The current state of the art material is Nafion®, which possesses several advantages such as high proton conductivity, excellent chemical stability and low water uptake.[5] However, high cost, high fuel permeability and reduced stability at high operating temperatures are some of its disadvantages. Significant research has been conducted to develop alternative membranes.[4, 6] McGrath et al. have reported the synthesis and characterization of partially disulfonated poly(arylene ether sulfone) random copolymers (given the acronym BPSH-XX).[7, 8] Here BP stands for biphenol, S for sulfone, H for the acidified form of the membrane, and XX is the degree of disulfonation.[7] The structure-property relationships of these copolymers have been studied extensively to optimize the degree of disulfonation that yields the best balance between proton conductivity and water uptake.[9-15]

The BPSH random copolymers display increased proton conductivity with degree of disulfonation, but water uptake/swelling also increases. High water uptake and swelling in these membranes lead to several undesirable properties. For example, high membrane swelling with water reduces the effective proton concentration and mechanical stability. Proton conductivity is a function of both proton diffusivity and proton concentration.[13] In addition, a high swelling-deswelling ratio can generate swelling stresses in the membrane during humidity cycling operations in the fuel cell.[16]

Membranes with low swelling stresses are desired for maximizing mechanical durability. These issues demonstrate the importance of reducing the water swelling of PEMs.

Water swelling of random copolymers can be reduced by moving toward low IEC materials, but this normally is achieved at the expense of proton conductivities.[17, 18] This paper describes how thermally stable crosslinked networks can reduce water uptake and swelling of the copolymers. Unlike literature reports the crosslinking chemistry does not involve the ionic groups, so that the reduction in water swelling will maximize the effective proton concentration allowing proton conductivity to be maintained. In addition, introduction of crosslinks will reduce the fuel permeability.

Recently it was reported that sodium sulfonate salt form crosslinked random BPS copolymers which had 50 % of the units disulfonated with a multifunctional epoxy resin, show promise as reverse osmosis desalination membranes.[17] The network properties were influenced by crosslinking time, copolymer molecular weight and epoxy concentration. The cured membranes in their salt form showed significantly higher salt rejection than their linear precursors.

This paper extends our earlier study to investigate acid form random disulfonated BPSH copolymers for applications as PEMs. The crosslinking procedure was similar to that reported in our previous study.[17] The effects of crosslinking on transport properties of PEMs such as proton conductivities, self-diffusion coefficients of water, and methanol permeability were evaluated and were compared with those of analogous linear membranes.

4.2. Experimental

4.2.1. Materials

Monomer grade 4,4′–dichlorodiphenylsulfone (DCDPS) and 4,4′-biphenol (BP) were obtained from Solvay Advanced Polymers and Eastman Chemical Company, respectively, and dried under vacuum at 60 °C for one day prior to use. The sulfonated

comonomer, 3,3′-disulfonate-4,4′-dichlorodiphenylsulfone (SDCDPS), was prepared following a previously published procedure, [7, 19] and dried under vacuum at 160 °C for two days before use. Potassium carbonate (Aldrich) was dried under vacuum at 110 °C for one day before use. Tetraglycidyl bis(p-aminophenyl)methane (Araldite MY721 epoxy resin) and triphenylphosphine (TPP) were obtained from Aldrich and used as received. The reaction solvent *N*,*N*-dimethylacetamide (DMAc, Aldrich) was vacuum-distilled from calcium hydride, and stored over molecular sieves under nitrogen. Toluene (anhydrous, 99.8%), isopropanol (*ReagentPlus*™, 99%), *N*-methyl-2-pyrrolidinone (NMP) (*ReagentPlus*™, 99%) and trimethylchlorosilane (silanizing agent) were obtained from Aldrich and used as received. Sulfuric acid (*ACS Reagent*, 95-98%) was obtained from VWR Internationals and used as received. Nafion®117 was purchased from Electrochem Inc. and used as received. NRE211 was kindly donated by Nissan Motor Company.

4.2.2. Synthesis of controlled molecular weight phenoxide endcapped BPSH-XX oligomers

Controlled molecular weight, phenoxide-endcapped partially disulfonated biphenol-based poly(arylene ether sulfone)s (BPSH-XX where XX denotes the degree of disulfonation of the copolymer) were synthesized via nucleophilic aromatic substitution step copolymerization. The molecular weights of the oligomers were controlled by offsetting the stoichiometry of the monomers. A typical polymerization of a 5 kg mol^{-1} BPSH-35 oligomer is provided. BP (4.0 g, 21.48 mmol), DCDPS (3.652 g, 12.72 mmol), and SDCDPS (3.460 g, 7.04 mmol) were added to a three-necked, round bottom reaction flask equipped with a mechanical stirrer, nitrogen inlet, Dean-Stark trap and a condenser. Potassium carbonate (3.414 g, 24.70 mmol) and 56 mL DMAc (to achieve 20% solids) were introduced into the flask. Toluene (28 mL, DMAc/toluene was 2/1 v/v) was added as the azeotropic reagent. The reaction mixture was refluxed at 150 °C for 4 h, then the azeotrope was removed to dehydrate the system. The reaction mixture was gradually heated to 170 °C by the controlled removal of toluene, then reacted for an additional 65-70 h. The viscous product was cooled to room temperature. The product mixture was

filtered to remove salts. The oligomer was isolated by precipitation in isopropanol, filtered, and dried for 24 h at 70 °C under ambient pressure, and then for 24 h at 110 °C under vacuum.

High molecular weight BPSH-XX copolymers for using as controls for this crosslinking study, were synthesized following the 1:1 stoichiometric procedure published previously.[7]

4.2.3. Silanization of glass casting plates

A 20% (v/v) solution of trimethylchlorosilane in toluene was prepared. Clean glass plates were immersed in the solution for 2-3 minutes, removed, then reacted in a convection oven for 1 h at 250 °C. The plates were cooled to room temperature and washed with acetone before use [20]

4.2.4. Film casting, epoxy curing and membrane acidification

A 10 wt % solution of an endcapped BPS-XX oligomer with approximately 8 wt % of MY721 epoxy resin (based on oligomer weight) and 2.5 wt % of TPP catalyst (based on epoxy resin weight) was prepared in NMP and stirred until a transparent homogeneous solution was obtained. The solution was cast on a silanized glass plate. The plate was inserted in a vacuum oven and heated at 100 °C for 2 h under vacuum, then at 150 °C for 15, 45 or 90 minutes without vacuum. After cooling to room temperature, the plate was removed from the oven and the membrane was peeled from the glass plate. The oligomer molecular weight and epoxy concentration were fixed at 5 kg mol^{-1} and 2 equivalents of epoxy groups per phenoxide end group on the copolymer (~ 8 wt % of oligomer weight) respectively, based on the most promising formulation of crosslinking obtained from our earlier studies.[17] Four series of crosslinked membranes were prepared with varying degree of disulfonation of the oligomers from 35, 45, 50 and 60 %. For each series of membranes, the crosslinking time was varied from 15, 45 and 90 minutes (except for the 60 % disulfonated one which was crosslinked for 90 minutes only)(Table

4.2). The nomenclature of the crosslinked samples is defined as follows- BPSH-x-XX(ZM) where x means crosslinked and Z is the curing time in minutes.

Membranes from linear higher molecular weight BPSH-XX copolymers were also cast following the same procedure. Both linear and crosslinked membranes were acidified by boiling in 0.2 M sulfuric acid for 2 h, and then neutralized in deionized water for 2 h.

Characterization

4.2.5. Nuclear magnetic resonance (NMR) spectroscopy

^{1}H NMR experiments were conducted on a Varian Unity 400 MHz NMR spectrometer. All spectra of the copolymers were obtained from 10% solutions (w/v) in DMSO-d_6 at room temperature. Proton NMR was used to determine the molecular weights of the copolymers utilizing end group analysis and their compositions.

4.2.6. Intrinsic viscosity

Intrinsic viscosities were determined from GPC experiments performed on a liquid chromatograph equipped with a Viscotek 270 RALLS/ viscometric dual detector. The mobile phase was 0.05 M LiBr containing NMP solvent.[21] The column temperature was maintained at 60 °C because of the viscous nature of NMP. Both the mobile phase solvent and sample solution were filtered before introduction to the GPC system.

4.2.7. Gel fractions

Gel fractions of the networks were measured by placing 0.1-0.15 g of sample in DMAc and soxhlet extracting for 48 h. After removal of the solvent by drying at 120 °C for 24 h under vacuum, the remaining mass was weighed as gel. Gel fractions were calculated by dividing the weights of the gels by the initial weights of the networks.

4.2.8. Measurement of proton conductivity

Proton conductivity at 30 ^{o}C at full hydration (in liquid water) was determined in a window cell geometry[22] using a Solartron 1252 + 1287 Impedance/Gain-Phase Analyzer over the frequency range of 10 Hz to 1 MHz following the procedure reported in the literature.[23] For determining proton conductivity in liquid water, the membranes were equilibrated at 30 °C in DI water for 24 h prior to testing.

4.2.9. Determination of water uptake and volume fraction of water

The water uptake of all membranes was determined gravimetrically. First, the membranes were soaked in water at 30 °C for 2 days after acidification. The wet membranes were removed from the liquid water, blotted dry to remove surface droplets, and quickly weighed. The membranes were then dried at 120 °C under vacuum for at least 24 h and weighed again. The water uptake of the membranes was calculated according to Equation (4-1), where $mass_{dry}$ and $mass_{wet}$ refer to the mass of the dry membrane and the wet membrane, respectively.

$$\text{water uptake}\% = \frac{\text{mass}_{wet} - \text{mass}_{dry}}{\text{mass}_{dry}} \times 100 \qquad \textbf{Equation 4-1}$$

The hydration number (λ) is the number of water molecules absorbed per sulfonic acid and can be calculated from the mass water uptake and the ion content of the dry copolymer as shown in Equation (4-2), where MW_{H2O} is the molar mass of water (18.01 g/mol) and IEC is the ion exchange capacity of the dry copolymer in milliequivalents per gram.

$$\lambda = \frac{(\text{mass}_{wet} - \text{mass}_{dry})/\text{MW}_{H_2O}}{\text{IEC} \times \text{mass}_{dry}} \text{.....} \qquad \textbf{Equation 4-2}$$

The volume fraction of water (i.e., the hydrophilic phase) was determined from an established formula[20] (Equation 4-3),

$$\phi = \left(\frac{M_{H_2O} / \rho_{H_2O}}{\left[M_{H_2O} / \rho_{H_2O} + EW / \lambda \rho_{ionomer} \right]} \right) \qquad \textbf{Equation 4-3}$$

where Φ is the volume fraction of water, ρ is the density and EW is the equivalent weight of the ionomer.

4.2.10. Determination of swelling ratio, density and effective proton concentration (C_{H^+})

The swelling ratio of all of the membranes was determined from the dimensional changes from wet to dry states, both in-plane and through-plane. Initially, samples were equilibrated in water and wet dimensions were measured. The dried dimensions were obtained by drying the wet membrane at 80 °C in a convection oven for 2 h. Density was also calculated from the volume and weight of the dried membranes. An average of 4 samples was used for each measurement. The effective proton concentration was determined from the water uptake, density and IEC using the following expression:

$$C_{H^+} = \frac{IEC \times Density}{\left(1 + 0.01 \times wateruptake \times Density\right)} \qquad \textbf{Equation 4-4}$$

4.2.11. Methanol permeability and DMFC performance

The methanol permeability of the membranes was determined by measuring the crossover current in a direct methanol fuel cell (DMFC) under open circuit conditions, in a manner identical to that reported by Ren et al.[24] DMFC performance or the VIR curves were obtained using a Fuel Cell Technologies test stand as described earlier.[25] The methanol feed concentration was 0.5 M, the air flow rate at the cathode was 500 sccm at 90 °C, and the cell temperature was 80 °C. Membrane electrode assemblies (MEA)s were prepared as earlier described.[25]

4.2.12. Pulsed-field gradient spin echo nuclear magnetic resonance (PGSE NMR)

The self-diffusion coefficient of water was measured using a Varian Inova 400 MHz (for protons) nuclear magnetic resonance spectrometer with a 60 G/cm gradient diffusion probe. A total of 16 points was collected across a range of gradient strengths and the signal–to-noise ratio was enhanced by co-adding 4 scans.

The measurement was calculated by observing the echo signal intensity (A) as a function of gradient strength (g). The diffusion coefficient (D) was determined by fitting the data to Equation (4-5): [26]

$$A(g) = A(o)\exp[-\gamma^2 D g^2 \delta^2 (\Delta - \delta/3)] \qquad \textbf{Equation 4-5}$$

where, A is the NMR signal intensity (A) as a function of gradient strength, γ is the gyromagnetic ratio (26752 $radG^{-1}s^{-1}$ for protons), δ is length of the gradient pulse, Δ is the time between gradient pulses. The experimental procedures used were similar to those reported earlier.[13] The membranes were fully hydrated and the temperature of the experiment was 25 ^{o}C.

4.2.13. Differential scanning calorimetry (DSC)

The DSC experiments were performed in a TA DSC instrument using liquid nitrogen as cooling medium for subambient operation. The samples were placed in thermally sealed pans capable of withstanding pressure of 100 atm. Samples were cooled to -70 °C and then heated at a rate of 5 °C per min under a N_2 atmosphere.

4.2. Results and Discussion

4.3.1. Synthesis of controlled molecular weight phenoxide-endcapped BPSH-XX oligomers

A series of controlled molecular weight BPSH-XX oligomers with phenoxide endgroups was synthesized from SDCDPS, DCDPS and biphenol by nucleophilic aromatic substitution (Fig. 4.1). The molecular weights of the oligomers (fixed at 5 kg mol^{-1}) were controlled by offsetting the stoichiometry between biphenol and the dihalides. Biphenol was utilized in excess to endcap the oligomers with phenoxide groups, so that the phenoxide groups could be further reacted in the end capping and subsequently crosslinking steps. The degree of disulfonation was controlled by varying the molar ratio of SDCDPS to DCDPS. Four oligomers with degrees of disulfonation of 35, 45, 50 and 60 % were prepared.

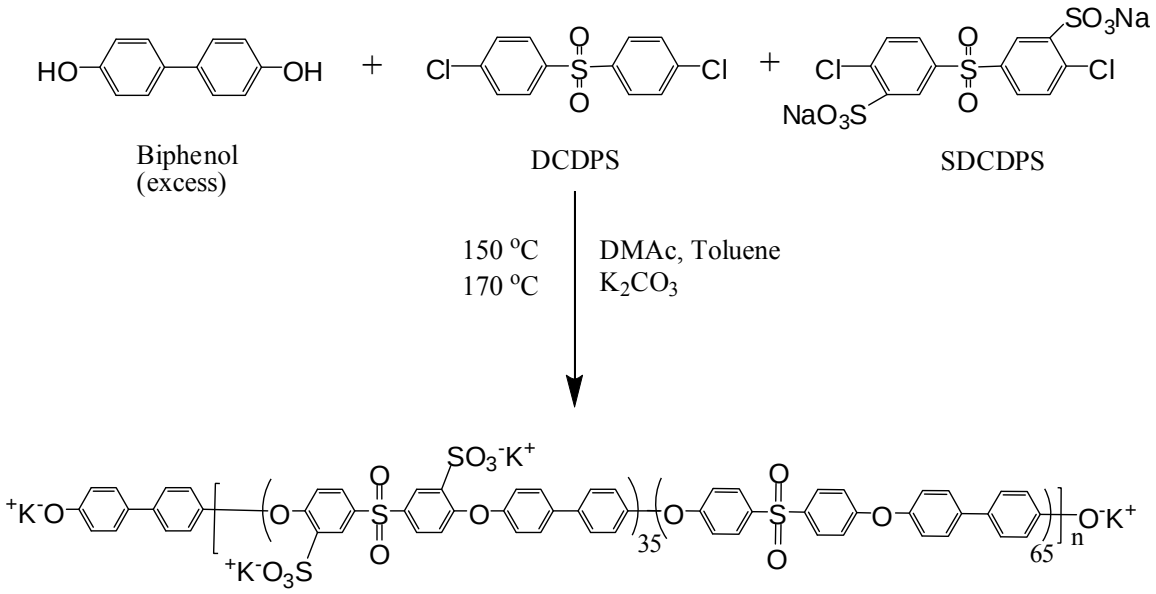

Figure 4.1 Synthesis of a controlled molecular weight phenoxide-endcapped BPS-35 random oligomer

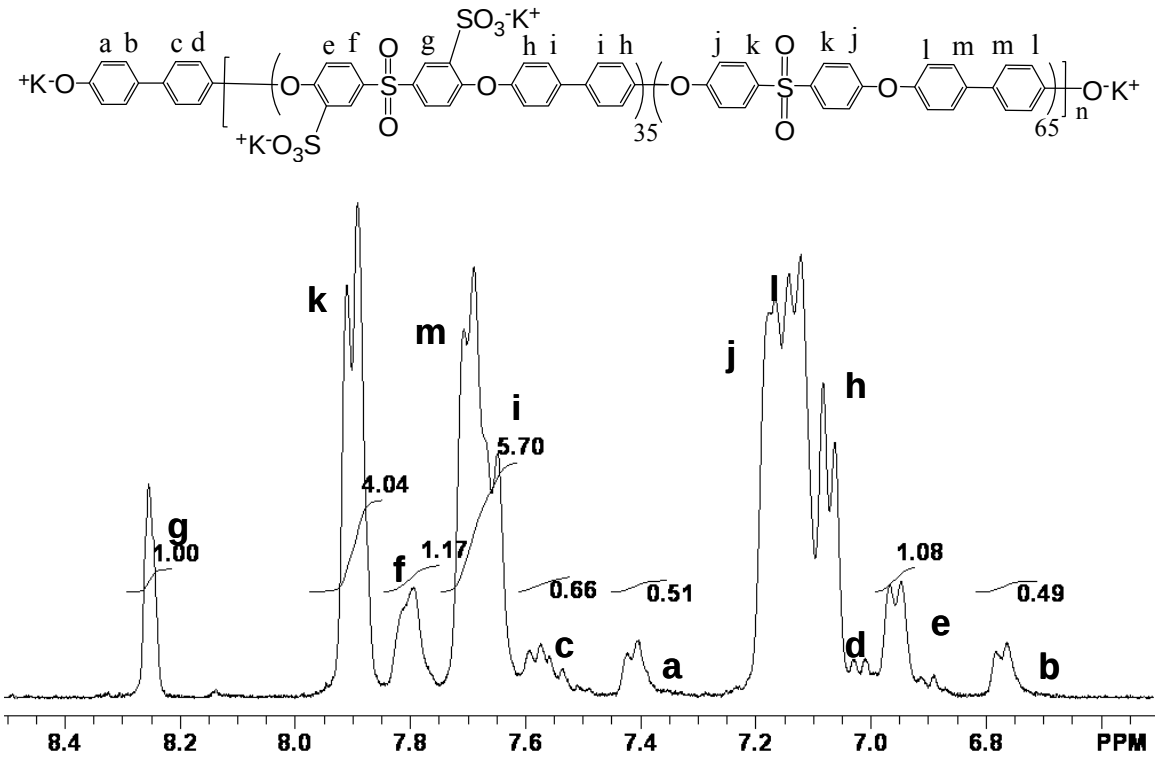

Figure 4.2 ^{1}H NMR of a phenoxide-endcapped BPS-35 random oligomer with number average molecular weight of~ 5 kg mol^{-1}

Fig. 4.2 shows the proton NMR spectrum of a phenoxide-endcapped BPS-35 oligomer with a targeted molecular weight of 5 kg mol^{-1}. The aromatic protons of the biphenol unit in the endgroup at *b, d, a and c* were assigned to peaks at 6.75 ppm, 7.0 ppm, 7.40 ppm and 7.55 ppm respectively. The ratio of the integrals of the aromatic protons at 6.75 ppm (*b*) to those of the aromatic protons of the biphenol endgroups in the oligomer repeat units at 7.65 ppm (*m and i*) were utilized to calculate M_n of the oligomers. As shown in Table 4.1, the experimental M_n values derived from proton NMR are in good agreement with the targeted values. As expected, intrinsic viscosities ([η]) of the oligomers showed similar values and this was expected since these oligomers were approximately the same molecular weight (Table 4.1). The degree of disulfonation was confirmed from the ratio of the integrals of protons at 6.95 ppm (e), 7.8 ppm (f) and 8.25 ppm (g) in the sulfonated unit to the protons at 7.9 ppm (k) in the non-sulfonated unit.

The degrees of disulfonation were used to calculate the ion exchange capacities (IEC-meq of sulfonic acid groups per gram of dry polymer) of the oligomers. Table 4.1 shows that the experimental IEC values of all four oligomers are in good agreement with the targeted values.

High molecular weight BPSH-XX copolymers were synthesized using 1:1 stoichiometry of the monomers[7] for use as controls for this crosslinking study. Attainment of high molecular weights in these controls was confirmed from their high intrinsic viscosities (Table 4.1). The experimental IEC values of these copolymers were also in good agreement with the targeted values, as shown in Table 4.1.

Table 4.1 Summary of controlled molecular weight and high molecular weight BPS-XX random copolymers

Copolymer	M_n (g mol^{-1})		IV[a] (dL g^{-1})	IEC (meq g^{-1})	
	Target	^{1}H NMR		Target	^{1}H NMR
BPS-35	5000	5875	0.24	1.53	1.52
BPS-45	5000	5740	0.23	1.90	1.90
BPS-50	5000	5721	0.21	2.08	2.04
BPS-60	5000	5276	0.21	2.42	2.40
BPS-30*	-	-	1.01	1.32	1.32
BPS-35*	-	-	0.87	1.53	1.51
BPS-40*	-	-	0.99	1.71	1.71
BPS-50*	-	-	0.53	2.08	2.01

[a] Intrinsic viscosity (IV) in NMP with 0.05 M LiBr at 60 °C, from GPC

* High molecular weight control copolymers

4.3.2. Crosslinking and gel fractions

BPSH-XX random copolymers were synthesized with phenoxide endgroups and those endgroups were further reacted with a multifunctional (f~3.66)[17] epoxy resin to produce, after curing, crosslinked membranes. Our earlier studies on crosslinking of BPS copolymers by epoxy investigated the effect of copolymer molecular weight, epoxy concentration and curing time on network properties.[17] Crosslinking of a copolymer with molecular weight ~ 5 kg mol^{-1} and ~ 2 equivalents of epoxy per phenoxide group of the copolymer yielded good membrane properties. Hence in this current study we have utilized the same formulation for crosslinking the BPSH-XX copolymers. Earlier research has also shown that with increasing crosslinking time the gel fraction of the BPS-50 membranes, which is a measure of the extent of crosslinking, increases. In this paper all the BPSH-XX copolymers (except BPSH-60) were cured for 15, 45 and 90 minutes. It was observed that irrespective of the IECs, the gel fractions increased with crosslinking time, which is consistent with our past findings (Table 4.2). The effects of gel fractions on water uptake, swelling and proton conductivity will be discussed.

Table 4.2 Properties of crosslinked and uncrosslinked membranes

Sample	Curing time (min)	IEC[a] (meq g^{-1})	Gel fraction[b] (%)	Density[c] (g cc^{-1})	C_H^+ (meq cc^{-1})	Water uptake (mass %)
BPSH-50	-	2.01	-	1.42	0.69	232
BPSH-40	-	1.71	-	1.38	1.30	60
BPSH-35	-	1.51	-	1.34	1.37	37
BPSH-30	-	1.32	-	1.31	1.34	22
BPSH-x-60	90	2.25	57	1.42	0.78	217
BPSH-x-50	15	1.93	10	1.39	0.53	295
	45	1.93	20	1.42	0.74	192
	90	1.93	80	1.41	1.25	84
BPSH-x-45	15	1.76	4	1.32	1.03	95
	45	1.76	11	1.31	1.06	90
	90	1.76	56	1.35	1.29	62
BPSH-x-35	15	1.45	65	1.25	1.27	34
	45	1.45	80	1.27	1.35	29
	90	1.45	85	1.31	1.40	27

[a] Measured from proton NMR

[b] Soxhlet extraction in DMAc for 48 h

[c] Experimental section

4.3.3. Water uptake and swelling

One desirable property of hydrophilic sulfonated copolymers is water absorption. Water in concert with the sulfonic acid groups in PEMs plays an important role in the proton conduction mechanism. Water acts as a vehicle for proton transport, and the proton conductivity is a strong function of the water content in the PEMs.[27, 28] Although

water absorption is crucial for proton transport, water management in PEMs is also an important issue in achieving the best performance and durability. Low swelling of the membrane is highly desirable for decreasing the swelling-deswelling ratio in membrane electrode assemblies (MEA)s and also for maximizing the effective proton concentration in the membrane.

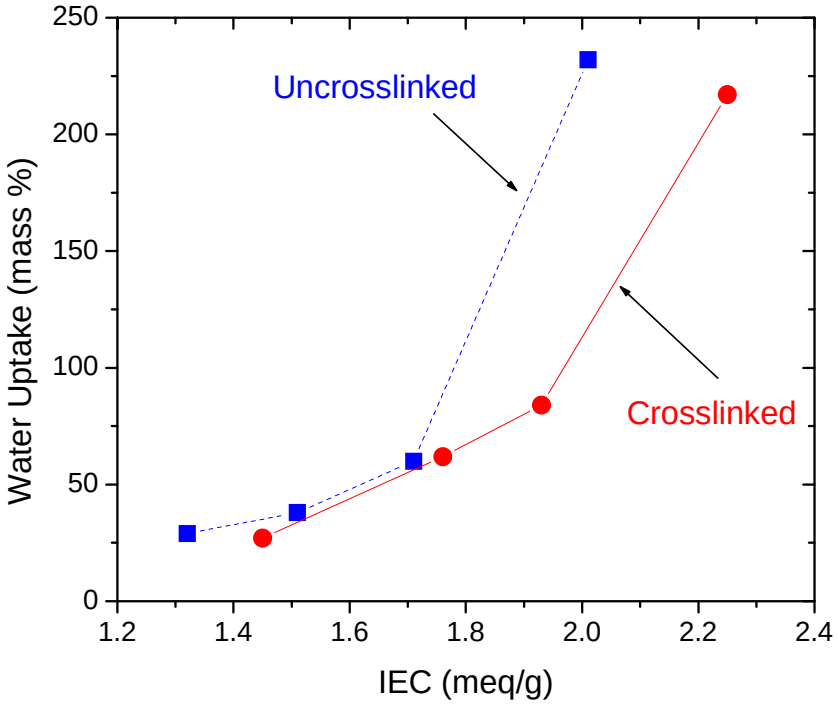

Figure 4.3 Influence of IEC on water uptake for the crosslinked and uncrosslinked BPSH-XX copolymers

Figure 4.3 represents the plots of water uptake as a function of IEC for the crosslinked and the linear control BPSH-XX copolymers. The IECs of the networks were adjusted include the epoxy (~8 wt %) content. Hence, at similar degrees of disulfonation, the crosslinked materials have a lower IEC compared to the starting copolymers.

Water uptake of both the crosslinked and precursor membranes increased with increasing IEC or ionic content in the copolymers. A sudden increase in water uptake was observed for both series of copolymers after reaching a particular IEC, which is unique to each series. Earlier investigations using AFM studies in our group have related

this sharp increase in water uptake to a percolation threshold.[9] A morphological transition from a closed to open—continuous hydrophilic domain morphology is believed to control this property. Below the percolation threshold, proton conductivity scales linearly with water uptake and dimensional stability of the copolymer is acceptable for some fuel cell applications. However, above the percolation threshold, the increase in water uptake with IEC is much higher compared to the increase in proton conductivity with IEC. At the same time, the dimensional stability of the membrane also deteriorates significantly above this threshold. These factors restrict the use of high IEC materials for fuel cell applications. Thus, an objective of this investigation was to investigate the possibility of shifting this morphological transition to a higher IEC, so that the higher concentration of ionic groups would be advantageous for proton transport. By crosslinking, this morphological transition was shifted to a higher IEC of ~1.93 meq g^{-1} compared to the linear system (1.71 meq g^{-1}). While crosslinking reduced the water uptake of the materials that had the higher IECs (2.25 and 1.93 meq g^{-1}), the effect was less prominent for the low IEC (1.76 and 1.45 meq g^{-1}) materials.

Crosslinking of hydrophilic polymers is known to reduce the swelling of membranes in water.[17] In the materials studied herein, the water swelling was reduced dramatically reduced with crosslinking as depicted in Figure 4.4. Crosslinking influenced water swelling at both high IEC and low IEC for BPSH-XX copolymers, but the effect was more pronounced at higher IECs.

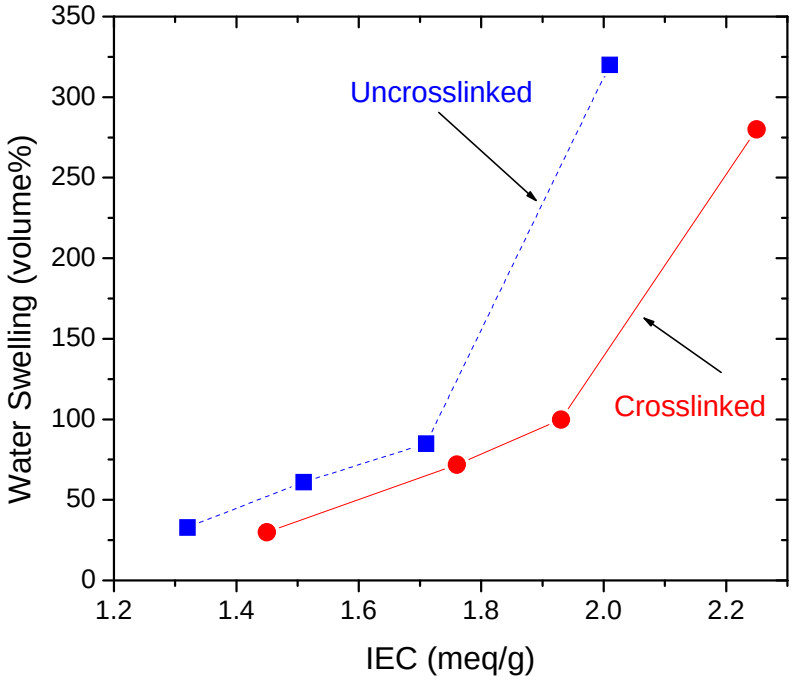

Figure 4.4 Influence of IEC on water swelling for the crosslinked and uncrosslinked BPSH-XX copolymers

We also investigated effects of crosslinking on three dimensional swelling behavior; both in-plane and through-plane swelling. The linear BPSH-XX copolymers showed isotropic swelling which increased with increasing degree of disulfonation (Fig. 4.5). For the networks however, reduction in swelling was modestly anisotropic as shown in Figure 4.6. Through-plane swelling decreased significantly relative to the in-plane swelling. Similarly to the non-crosslinked systems, swelling in all three directions increased with increasing IEC.

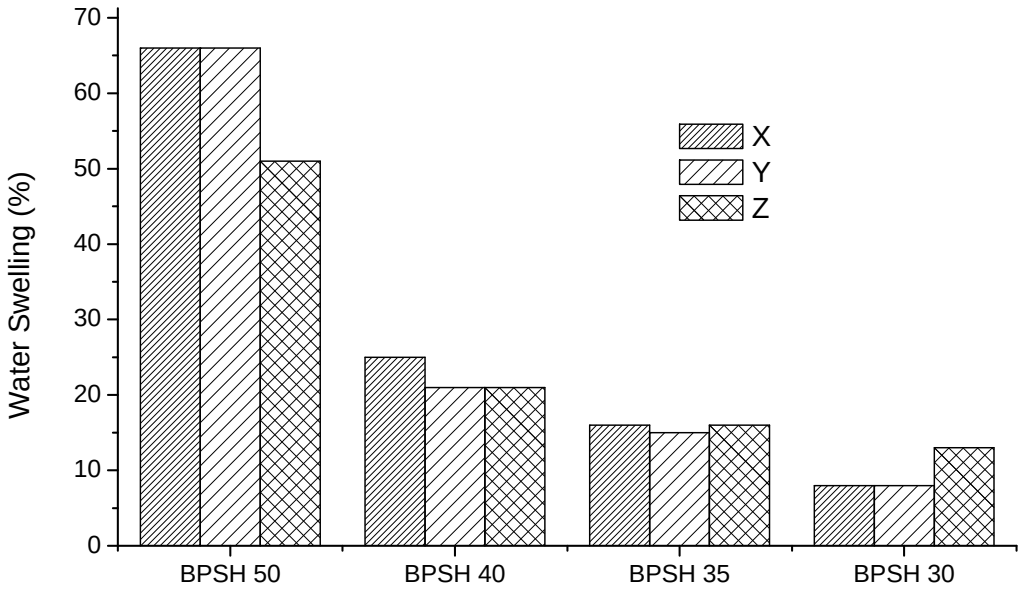

Figure 4.5 Three dimensional water swelling for the linear BPSH-XX random copolymers, the nature of the swelling is isotropic

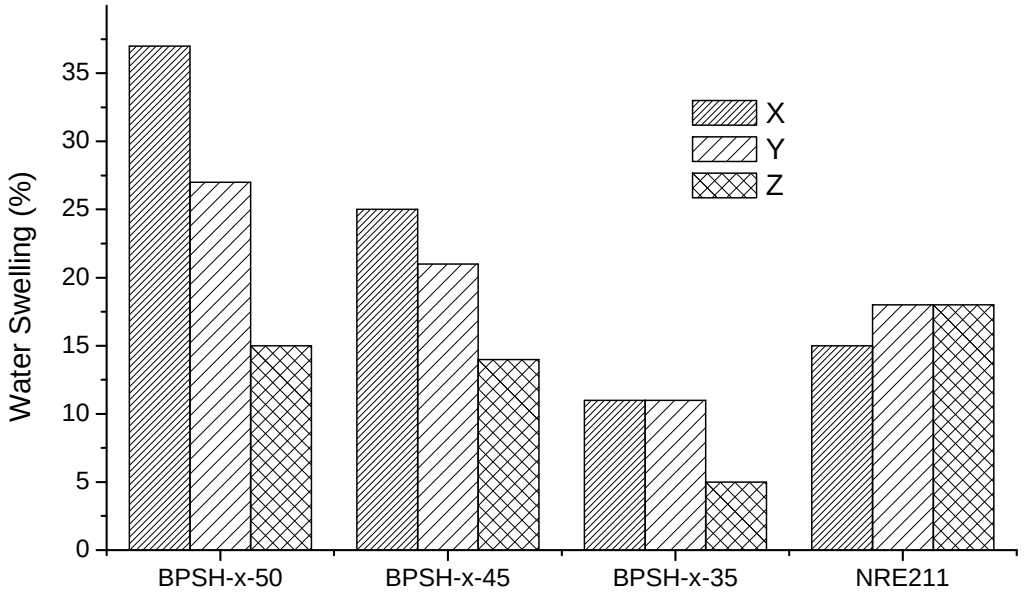

Figure 4.6 Three dimensional water swelling for the crosslinked BPSH-XX random copolymers, an anisotropicity in the swelling was observed

Influence of gel fractions

One of our objectives was to investigate relationships between the extent of crosslinking and water uptake and swelling properties of the membranes. Figures 4.7 and 4.8 demonstrate the influence of gel fraction on water uptake and swelling for the crosslinked BPSH-XX copolymers with varying degrees of disulfonation. Irrespective of the degree of disulfonation, water uptake and swelling decreased with increasing gel fractions, with the most significant reduction (from 295 % to 84 % in water uptake and from 387 % to 95 % in water swelling) observed for the BPSH-x-50 copolymer. An exponential decrease in water uptake and swelling was found with increased curing time (corresponding to increased gel fractions) for this particular copolymer. This trend is very similar to our earlier findings for the salt form of the BPSH-x-50 copolymer. The investigation of the influence of gel fraction on the three dimensional water swelling indicated a preferential reduction of water swelling along the through-plane compared to the in-plane as shown for the BPSH-x-50 material in Figure 4.9.

Since the epoxy covalent crosslinking chemistry did not involve the sulfonic acid groups, the IEC remained unaffected with increasing crosslinking. Hence this study shows that it is possible to tailor both water uptake and water swelling of a PEM by varying the crosslink density without changing the ionic concentrations.

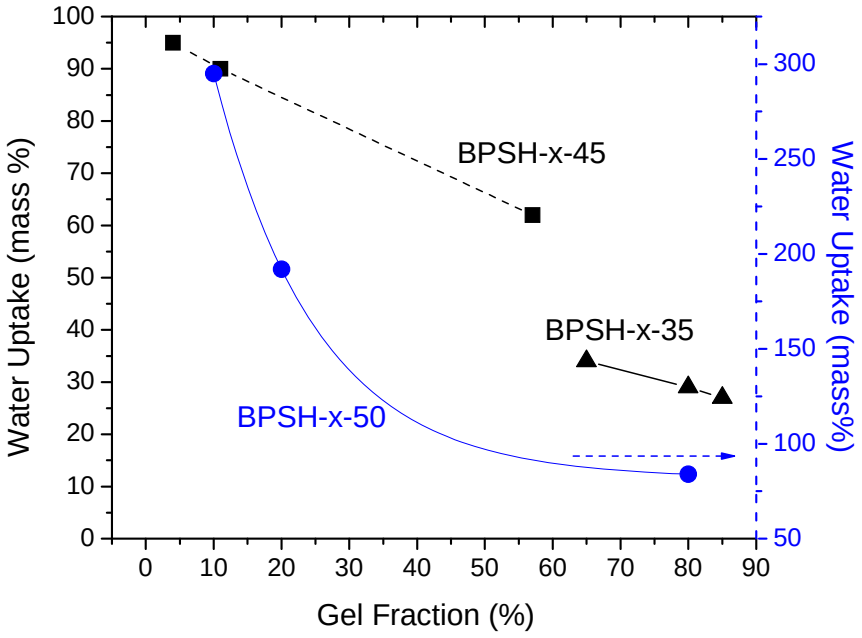

Figure 4.7 Influence of gel fraction on water uptake for the crosslinked BPSH copolymers with varying degree of disulfonation

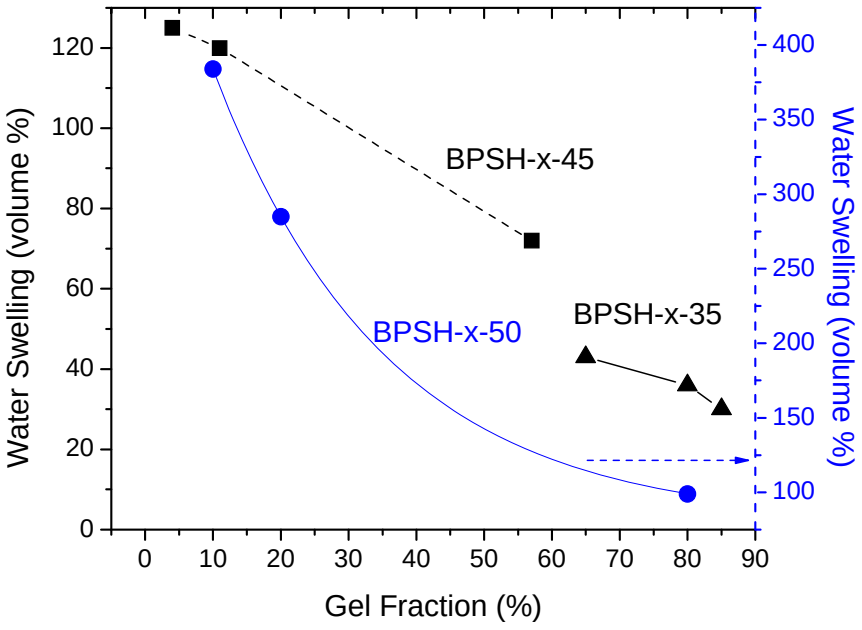

Figure 4.8 Influence of gel fraction on water swelling for the crosslinked BPSH copolymers with varying degree of disulfonation

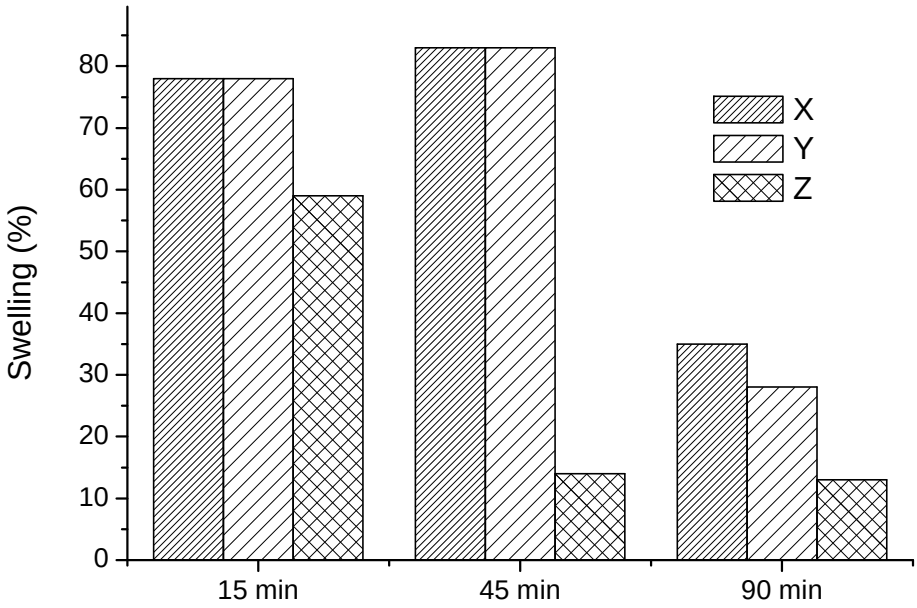

Figure 4.9 Influence of curing time on three dimensional water swelling of BPSH-x-50 copolymers

4.3.4. Self-diffusion coefficient of water

The self-diffusion coefficient of water is an intrinsic transport property of PEMs which strongly influences the proton transport. It has been reported that the self-diffusion coefficient of water equals the proton diffusion coefficient, particularly under partially hydrated conditions, thus underscoring the importance of water transport on proton transport.[29] The self-diffusion coefficient of water within a polymer scales exponentially with the free volume of the polymer (equation 4-6).[30]

$$D \propto \exp - \left(\frac{V^*}{V_t} \right) \qquad \textbf{Equation 4-6}$$

$$V_t \propto \phi$$

In this case, the free volume (V_t) in the copolymer can be correlated to the volume fraction of water (ϕ). Comparing self-diffusion coefficients of water for the non-crosslinked and crosslinked copolymers at a given water volume fraction normalizes the influence of water uptake on water transport. Figure 4.10 represents the semi-log plot of self-diffusion coefficients of water as a function of the reciprocals of water volume fractions for the crosslinked and non-crosslinked copolymers. The self-diffusion coefficient of water was determined using PGSE NMR techniques at 25 ^{o}C under fully hydrated conditions.[13] A linear fit of the experimental data demonstrated the relationship (Eq^{n}. 4-6) between self-diffusion coefficients of water and water volume fractions. Over a wide range of reciprocals of water volume fractions (1.75 to ~4), the networks showed reduced water self-diffusion coefficients compared to the non-crosslinked copolymers. The extent of reduction of the self-diffusion coefficient for the networks compared to the precursors was more pronounced in the lower water volume fraction regime. This suggests the formation of a restricted morphology with introduction of crosslinks, which may be advantageous in reducing fuel permeability. With increase in water volume fraction, the self-diffusion coefficients of water of the networks moved closer to the non-crosslinked copolymers and they became equal at a much higher water volume fraction (the reciprocal is 1.25). In this high water volume fraction regime, the presence of higher concentrations of water (perhaps free water) restores the water-assisted percolated morphology, and hence, improves water transport in the networks.

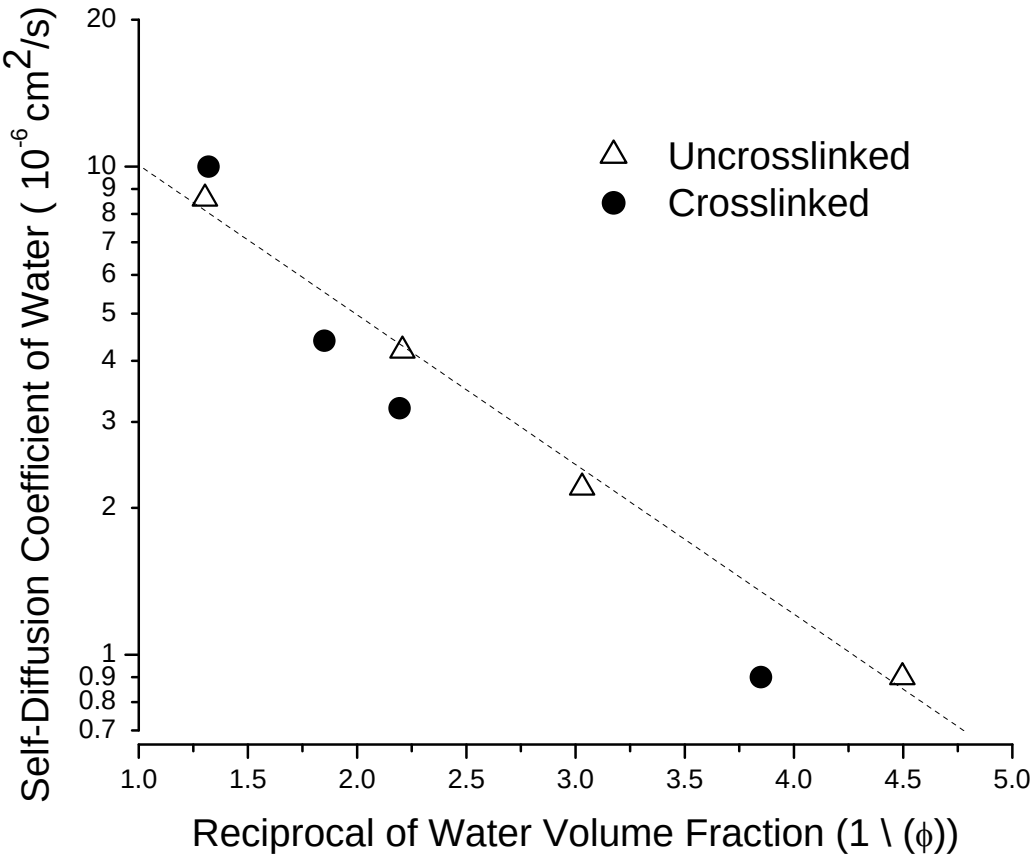

Figure 4.10 Influence of crosslinking on self-diffusion coefficients of water, measured for the crosslinked and uncrosslinked BPSH copolymers as a function of water volume fraction

4.3.5. Proton conductivity

The foremost important property of a PEM is its proton conductivity. Proton conduction is a function of two terms, proton diffusivity and proton concentration.[31] The first depends on the morphology of the system and the latter depends on the overall ionic concentration. As mentioned earlier, a sudden increase in water uptake after reaching a certain IEC, increases membrane swelling significantly. This can decrease the effective

proton concentration and hence the proton conductivity. For example, proton conductivity of non-crosslinked BPSH-XX copolymers increases with increasing IEC up to an IEC of 1.71 as shown in Figure 4.11. After that, a decrease in the proton conductivity is observed, as in the BPSH-50 copolymer with an IEC of 2.01. This is supported by the decreased effective proton concentration (C_H^+) of BPSH-50 compared to BPSH-40, as reported in Table 4.2.

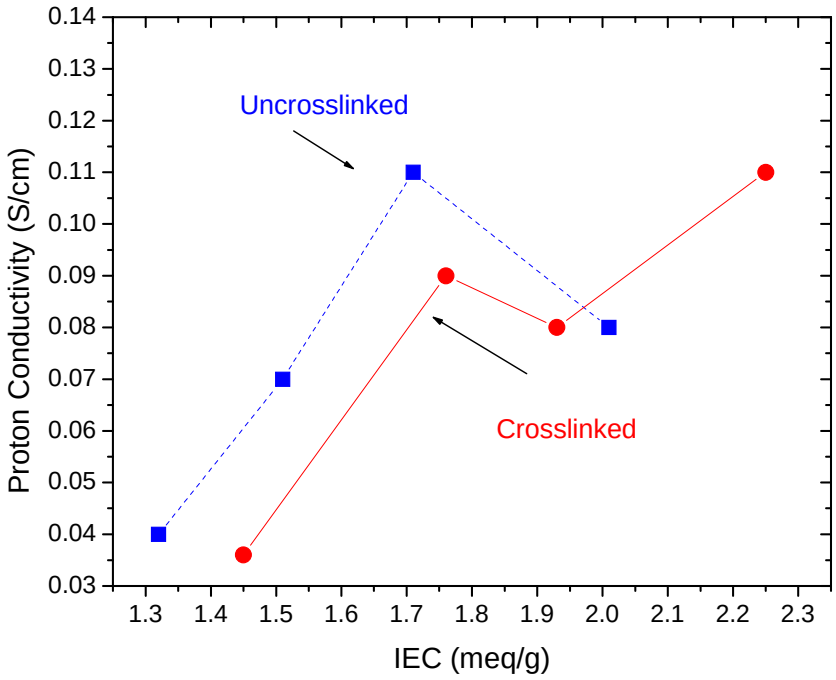

Figure 4.11 Influence of IEC on proton conductivity for the crosslinked and uncrosslinked BPSH-XX copolymers, measured in liquid water at 30 °C

At a given IEC, the proton conductivities networks that were cured for 90 minutes were lower than for the analogous linear copolymers. This is particularly significant in the lower IEC regime. At higher IECs, the proton conductivities of the networks were equal to or higher than those of the non-crosslinked copolymers. Crosslinking reduces the water swelling of the membranes, thus increasing the C_H^+ in the membrane. It is noted that both water uptake and IEC of BPSH-x-50(90M) are lower than for the BPSH-

50 copolymer. However, a higher C_H^+ (1.25 meq/cc) for BPSH-x-50(90M) compared to (0.69 meq/cc) for BPSH-50 resulted in similar proton conductivities. Hence, the water swelling for a high IEC material was reduced while still maintaining the proton conductivity by means of crosslinking.

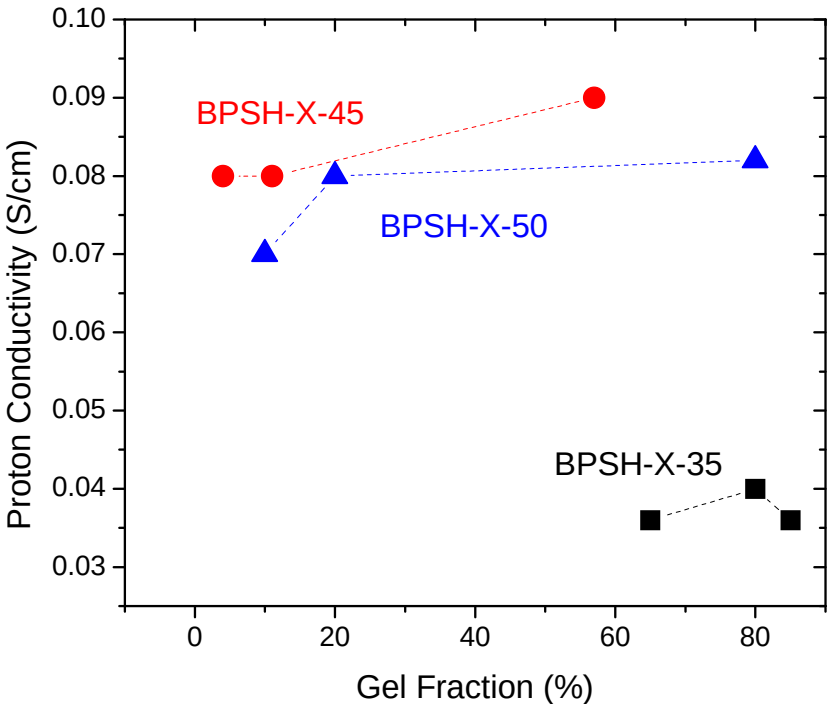

Figure 4.12 Influence of gel fraction on proton conductivity for crosslinked BPSH copolymers with varying degree of disulfonation

The effect of C_H^+ is even more prominent when we consider the influence of the extent of crosslinking on proton conductivity as illustrated in Figure 4.12. Irrespective of the degree of the disulfonation, proton conductivity was not affected by an increase in crossslinking. Although water uptake decreases with gel fractions, the proton conductivity remained unaltered as C_H^+ increases with gel fraction (Table 4.2). Thus we have shown that by increasing the extent of crosslinking within a copolymer, it is possible to reduce water uptake without significantly sacrificing proton conductivity.

4.3.6. Selectivity

The biggest challenge for a PEM is to achieve both high proton conductivity and low water swelling. The normally tradeoff between these properties can be mathematically represented by equation 4-7:

$$Selectivity(\psi) = \frac{\sigma}{waterswelling} \qquad \textbf{Equation 4-7}$$

Here σ is the proton conductivity, measured at 30 ^{o}C in liquid water. High selectivity at low water swelling (volume %) is desired. This property was evaluated for the networks, particularly for BPSH-x-35 copolymers with varying gel fractions and compared with the commercially available NRE211 and non-crosslinked BPSH-35 copolymers (Fig. 4.13). At a similar level of water swelling, NRE 211 had a higher selectivity than the non-crosslinked BPSH-35 random copolymer. However, for the BPSH-x-35 copolymers, a significant improvement in selectivity with increasing gel fractions was observed relative to the non-crosslinked BPSH-35. A decrease in water swelling and at the same time no significant decrease in the proton conductivity with increasing crosslinking, increases the overall selectivity of these BPSH-x-35 membranes. In fact the BPSH-x-35(90M) copolymer with 85 % gel fraction showed equal selectivity to that of the state-of-the art NRE211 material, but at a much lower (desired) amount of water swelling.

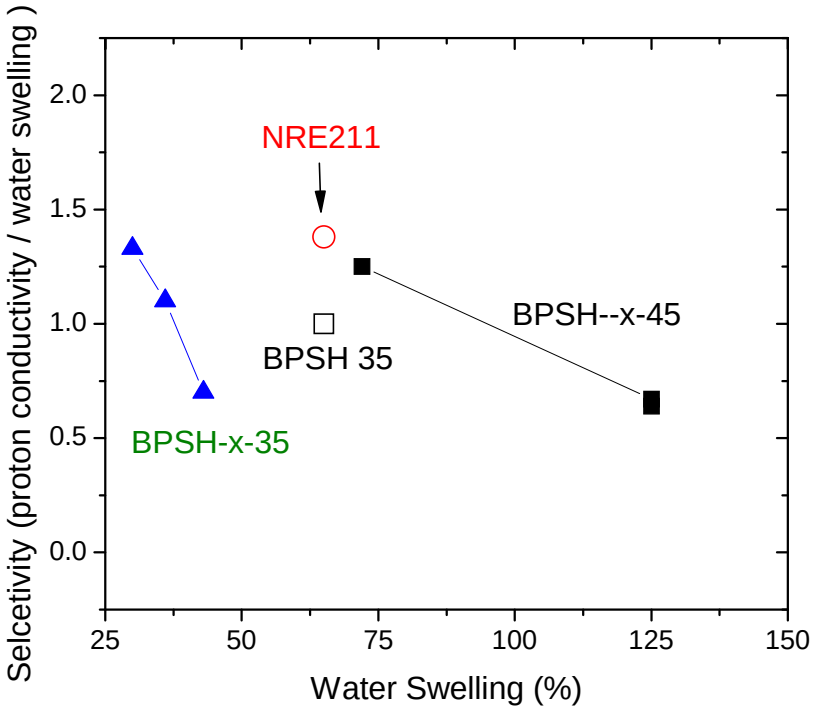

Figure 4.13 Selectivity for PEMs as a function of water swelling

4.3.7. Methanol permeability

The major problem associated with DMFCs is the high methanol permeability of the membrane. Unoxidized methanol permeates across the membrane from anode to cathode and then undergoes oxidation on the Pt catalyst at the cathode (cross over). The methanol oxidation reduces the overall open-circuit voltage and hence reduces the power density of the cell.[24] PEMs with very low methanol permeability are highly desired for DMFC applications. The BPSH-XX random copolymers have very low methanol permeabilities compared to the state-of-the art Nafion® 117 membrane.[9] Significant reduction in methanol permeability can be achieved by lowering the IEC of the copolymers. However, lowering the IEC also results in reduction in proton conductivity. Hence there is a trade-off of selectivity between the proton conductivity and methanol permeability in PEMs. Here we define the selectivity as the ratio between proton

conductivity and methanol permeability. BPSH copolymers have a selectivity of as high as 2.0 times that the Nafion®.[9] One objective was to form networks with the BPSH-XX copolymers to restrict methanol diffusion and improve selectivity.

Methanol permeability and proton conductivity of the BPSH-XX copolymers were measured at 30 ^{o}C. Table 4.3 lists the IEC, proton conductivity, methanol permeability and selectivity for the crosslinked and non-crosslinked[9] BPSH-XX copolymers. Nafion® 117 was used as a control for comparison. Compared to the linear copolymers, the networks had reduced methanol permeabilities. Notably, the BPSH-x-35(90M) copolymer with an IEC of 1.44 meq g^{-1} significantly reduced methanol permeability as compared to the BPSH-30 copolymer which had even a lower IEC (1.32 meq g^{-1}). This finding was complementary to the results from the self-diffusion coefficient of water, where the BPSH-x-35(90M) had a significantly lower self-diffusion coefficient of water compared to BPSH-30 at a similar water volume fraction level. These two different experimental results confirm the same concept, i.e. that a restricted morphology forms with crosslinking, particularly in the lower IEC materials.

This reduced methanol permeability of the BPSH-x-35(90M) copolymer significantly improved its selectivity as reported in Table 4.3. A relative selectivity of as high as 4.2 times over Nafion® 117 was also observed for this particular copolymer. Hence by crosslinking a PEM, the selectivity between proton conductivity and methanol permeability can be considerably improved. We propose to extend this investigation to other systems to better understand DMFC performance in crosslinked systems.

Table 4.3 Methanol permeability and selectivity for the crosslinked and uncrosslinked BPSH-XX copolymers

Sample	IEC meq g^{-1}	Proton conductivity[a] (mS cm^{-1})	Methanol permeability[b] (10^{-7} cm^2 s^{-1})		Relative Selectivity[c]
			30 °C	80 °C	
Nafion117	0.90	90	16.8	47	1
BPSH-x-45(90M)	1.76	90	7.4	18	2.4
BPSH-x-35(90M)	1.45	40	1.8	6	4.2
BPSH 40	1.73	110	8.1	-	2.6
BPSH 30	1.32	40	3.6	-	2.2

[a] Measured in liquid water, 30 °C

[b] Measured at 30 °C

[c] Relative to Nafion117, at 30 °C

4.3.8. States of water

There are at least three states of water that have been associated with water residing in hydrophilic phases of polymers.[11, 32-34] The presence of these three states can be defined by thermal properties. *Non-freezing bound water* is strongly associated with the polymer and depresses its T_g, but the water shows no melting endotherm by DSC. *Freezable bound water* is weakly bound to the polymer (or weakly bound to the non-freezing water), and displays broad melting behavior around 0 °C. *Free water* exhibits a sharp melting point at 0 °C. Earlier investigations on states of water in ion-containing polymers have shown a strong dependence of transport properties on the types of water. Figure 4.14 displays the melting endotherms of the freezable water as a function of the curing time. The area under the endotherms, which is qualitatively related to the amount of the freezing water, decreases with increasing curing time. As the gel fraction increases form 20 to 80%, a significant reduction in the area under the endotherms was observed. The ratio of free to bound water decreases with increasing crosslink density.

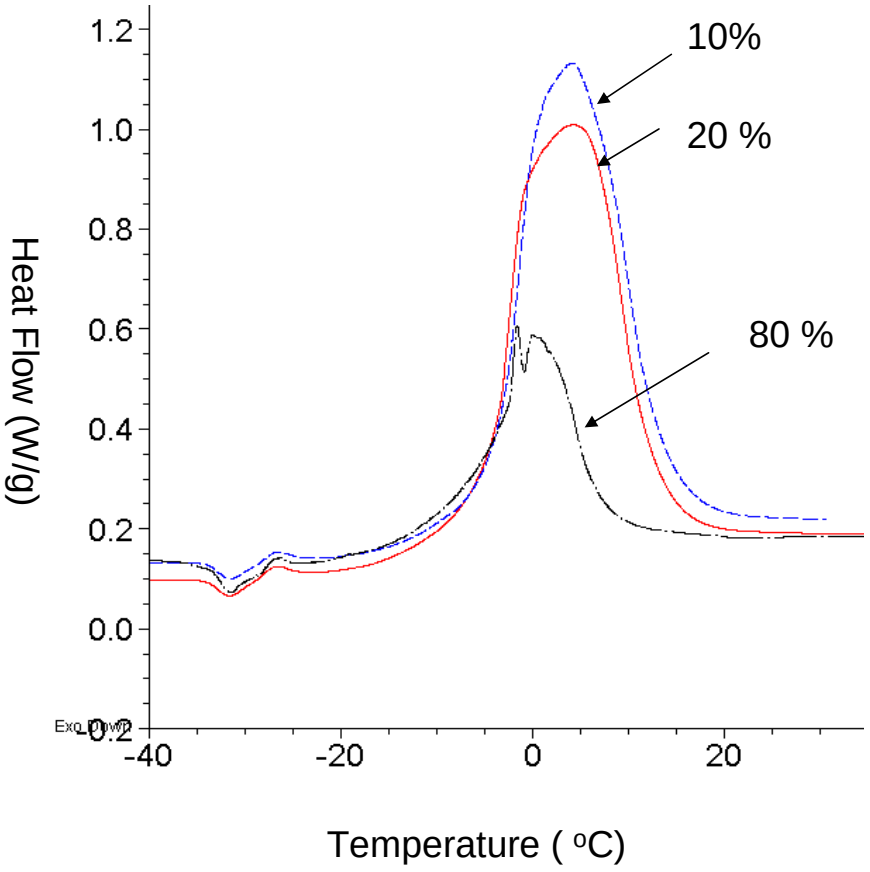

Figure 4.14 Influence of crosslinking on the melting endotherm of freezing water in the BPSH-x-50 copolymer. The numbers in percentage represent gel fraction

Thus by crosslinking one can change the distribution of the states of water in a PEM without changing the ionic content of the material, and this alters selectivity between the different PEM properties.

4.4. Conclusions

The investigation has addressed the synthesis and properties of BPSH-XX random copolymer networks with varying degrees of disulfonation. Using the epoxy crosslinking

chemistry reported earlier, a series of crosslinked BPSH copolymers varying both in degree of disulfonation and gel fractions were synthesized.

Significant reductions in water uptake with crosslinking were observed, with higher reductions found for the higher IEC materials. It was possible to shift the percolation threshold for water absorption to a higher IEC in the networks compared to the non-crosslinked materials. This extends the potential for higher IEC materials for PEMs. Earlier reports have indicated that the distribution of states of water in BPSH-XX copolymers is a function of IEC.[11] The presence of free water in the copolymer develops only after reaching a particular IEC and that IEC is closely associated with the percolation threshold region. We have confirmed herein that crosslinking reduces the fraction of free water in the membrane significantly in the case of BPSH 50 copolymers. Hence the higher IEC BPSH-XX copolymers with high free water content showed a dramatic decrease in the total water content with crosslinking, presumably due to the free water being significantly reduced. As the lower IEC BPSH-XX copolymers were not associated with free water,[11] crosslinking resulted in only a nominal decrease in water uptake.

In conjunction with water absorption, a significant reduction in water swelling was also associated with crosslinking and this effect was valid over a wide range of IECs. Both water uptake and swelling decreased with increasing gel fractions. A preferential reduction in water swelling along through-plane direction was observed compared to the in-plane swelling with increasing gel fractions.

The influence of crosslinking on transport properties of BPSH-XX copolymers was investigated. Self-diffusion coefficients of water measured by PGSE NMR scaled with the water volume fraction for both non-crosslinked and crosslinked copolymers. However, at a given volume fraction of water, particularly in the lower regime, crosslinking significantly reduced water transport in the networks with low IECs. This was aligned with the methanol permeability results, where the low IEC materials showed significantly lower methanol permeability relative to the non-crosslinked materials. Both these

experiments suggest the formation of a restricted morphology in the networks that is associated with reduced water and methanol permeability. However with increasing IECs wherein the networks had high volume fractions of water, both methanol permeability and self-diffusion coefficients of water approached values similar to those of non-crosslinked materials. The low methanol permeability for the BPSH-x-35(90M) resulted in a fourfold improvement in DMFC selectivity over Nafion® 117.

Proton conductivities evaluated as a function of gel fraction and IEC identified the importance of the effective proton concentration on overall proton conductivity. Water absorption in an ion-containing hydrophilic polymer is associated with an overall increase in the volume of the hydrated polymer. As the ionic concentration within the polymer is fixed, the effective proton concentration decreases with increasing water swelling. For the networks investigated herein, increased swelling at high IEC resulted in significant decreases in the effective proton concentrations and hence decreases in proton conductivity. However, with crosslinking it was possible to reduce the swelling and hence improve the proton conductivities of high IEC materials. This was consistent with the findings on the influence of gel fractions on proton conductivity. Although water uptake decreased with increasing gel fractions, no significant changes in proton conductivities of the networks were observed. The increase in the effective proton concentration with increasing gel fractions sustained the proton conductivity even with a reduced water uptake. Hence by crosslinking it was possible to tailor the water uptake without significantly compromising the proton conductivity. This study confirmed that a crosslinked BPSH-35 copolymer had similar selectivity to that of the state-of-the art NRE211 copolymer and importantly, at a much lower swelling ratio than NRE211. The effects of crosslinking on the transport properties of these BPSH-XX copolymers are highly promising, and suggest their potential as candidates for PEMs in both H_2/air and direct methanol fuel cells.

Acknowledgements

Authors would like to acknowledge NSF-PFI and Nissan Motors for funding. We would also like to thank Dr. Zhong-Biao Zhang for kindly providing the high molecular weight BPSH-XX copolymers.

4.5. References

1. Zalbowitz, M.; S, T., Green Power. *Fuel Cells* **1999**.

2. Carrette, L.; Friedrich, K. A.; Stimming, U., Fuel cells: Principles, types, fuels, and applications. *Chemphyschem* **2000,** 1, (4), 162-193.

3. Acres, G. J. K., Recent advances in fuel cell technology and its applications. *Journal of Power Sources* **2001,** 100, (1-2), 60-66.

4. Hickner, M. A.; Ghassemi, H.; Kim, Y. S.; Einsla, B. R.; McGrath, J. E., Alternative polymer systems for proton exchange membranes (PEMs). *Chemical Reviews* **2004,** 104, (10), 4587-4611.

5. Mauritz, K. A.; Moore, R. B., State of understanding of Nafion. *Chemical Reviews (Washington, DC, United States)* **2004,** 104, (10), 4535-4585.

6. Roziere, J.; Jones, D. J., Non-fluorinated polymer materials for proton exchange membrane fuel cells. *Annual Review of Materials Research* **2003,** 33, 503-555.

7. Wang, F.; Hickner, M.; Kim, Y. S.; Zawodzinski, T. A.; McGrath, J. E., Direct polymerization of sulfonated poly(arylene ether sulfone) random (statistical) copolymers: candidates for new proton exchange membranes. *Journal of Membrane Science* **2002,** 197, (1-2), 231-242.

8. Wang, F.; Hickner, M.; Ji, Q.; Harrison, W.; Mecham, J.; Zawodzinski, T. A.; McGrath, J. E., Synthesis of highly sulfonated poly(arylene ether sulfone) random (statistical) copolymers via direct polymerization. *Macromolecular Symposia* **2001,** 175, 387-395.

9. Kim, Y. S.; Hickner, M. A.; Dong, L. M.; Pivovar, B. S.; McGrath, J. E., Sulfonated poly(arylene ether sulfone) copolymer proton exchange membranes:

composition and morphology effects on the methanol permeability. *Journal of Membrane Science* **2004,** 243, (1-2), 317-326.

10. Kim, Y. S.; Wang, F.; Hickner, M.; McCartney, S.; Hong, Y. T.; Harrison, W.; Zawodzinski, T. A.; McGrath, J. E., Effect of acidification treatment and morphological stability of sulfonated poly(arylene ether sulfone) copolymer proton-exchange membranes for fuel-cell use above 100 degrees C. *Journal of Polymer Science Part B-Polymer Physics* **2003,** 41, (22), 2816-2828.

11. Kim, Y. S.; Dong, L. M.; Hickner, M. A.; Glass, T. E.; Webb, V.; McGrath, J. E., State of water in disulfonated poly(arylene ether sulfone) copolymers and a perfluorosulfonic acid copolymer (nafion) and its effect on physical and electrochemical properties. *Macromolecules* **2003,** 36, (17), 6281-6285.

12. Kim, Y. S.; Dong, L. M.; Hickner, M. A.; Pivovar, B. S.; McGrath, J. E., Processing induced morphological development in hydrated sulfonated poly(arylene ether sulfone) copolymer membranes. *Polymer* **2003,** 44, (19), 5729-5736.

13. Roy, A.; Hickner, M. A.; Yu, X.; Li, Y.; Glass, T. E.; McGrath, J. E., Influence of chemical composition and sequence length on the transport properties of proton exchange membranes. *Journal of Polymer Science, Part B: Polymer Physics* **2006,** 44, (16), 2226-2239.

14. Hickner, M. A.; Wang, F.; Kim, Y. S.; Privovar, B.; Zawodzinski, T. A.; McGrath, J. E., Chemistry-morphology-property relationships of novel proton exchange membranes for direct methanol fuel cells. *Abstracts of Papers of the American Chemical Society* **2001,** 222, U467-U467.

15. Harrison, W. L.; Wang, F.; Mecham, J. B.; Glass, T. E.; Hickner, M. A.; McGrath, J. E., Influence of bisphenol structure on the direct synthesis of sulfonated poly(arylene ether)s. *Abstracts of Papers of the American Chemical Society* **2001,** 221, U415-U415.

16. Borup, R.; Meyers, J.; Pivovar, B.; Kim, Y. S.; Mukundan, R.; Garland, N.; Myers, D.; Wilson, M.; Garzon, F.; Wood, D.; Zelenay, P.; More, K.; Stroh, K.; Zawodzinski, T.; Boncella, J.; McGrath, J. E.; Inaba, M.; Miyatake, K.; Hori, M.; Ota, K.; Ogumi, Z.; Miyata, S.; Nishikata, A.; Siroma, Z.; Uchimoto, Y.; Yasuda, K.; Kimijima, K.-i.; Iwashita, N., Scientific Aspects of Polymer Electrolyte Fuel Cell

Durability and Degradation. *Chemical Reviews (Washington, DC, United States)* **2007,** 107, (10), 3904-3951.

17. Paul, M.; Park, H. B.; Freeman, B. D.; Roy, A.; McGrath, J. E.; Riffle, J. S., Synthesis and crosslinking of partially disulfonated poly(arylene ether sulfone) random copolymers as candidates for chlorine resistant reverse osmosis membranes. *Polymer* **2008,** 49, (9), 2243-2252.

18. Paul, M.; Roy, A.; Park, H. B.; Freeman, B. D.; Riffle, J. S.; McGrath, J. E., Synthesis and crosslinking of poly(arylene ether sulfone) blend membranes. *Polymer Preprints (American Chemical Society, Division of Polymer Chemistry)* **2007,** 48, (1), 334-335.

19. Sankir, M.; Bhanu, V. A.; Harrison, W. L.; Ghassemi, H.; Wiles, K. B.; Glass, T. E.; Brink, A. E.; Brink, M. H.; McGrath, J. E., Synthesis and characterization of 3,3'-disulfonated-4,4'-dichlorodiphenyl sulfone (SDCDPS) monomer for proton exchange membranes (PEM) in fuel cell applications. *Journal of Applied Polymer Science* **2006,** 100, (6), 4595-4602.

20. Mecham, S. J. Gas permeability of polyimide/polysiloxane block copolymers. M.S. Thesis, Virginia Polytechnic Institute and State University, Blacksburg, VA, 1994.

21. Yang, J.; Li, Y.; Roy, A.; McGrath, J. E., *Polymer* **2008,** In Press.

22. Zawodzinski, T. A.; Neeman, M.; Sillerud, L. O.; Gottesfeld, S., *J. Phys. Chem.* **1991,** 95, 6040.

23. Springer, T. E.; Zawodzinski, T. A.; Wilson, M. S.; Gottesfeld, S., *J. Electrochem. Soc.* **1996,** 143, 587.

24. Ren, X. M.; Springer, T. E.; Zawodzinski, T. A.; Gottesfeld, S., Methanol transport through nafion membranes - Electro-osmotic drag effects on potential step measurements. *Journal of the Electrochemical Society* **2000,** 147, (2), 466-474.

25. Kim, Y. S.; Sumner, M. J.; Harrison, W. L.; Riffle, J. S.; McGrath, J. E.; Pivovar, B. S., Direct methanol fuel cell performance of disulfonated poly-arylene ether benzonitrile) copolymers. *Journal of the Electrochemical Society* **2004,** 151, (12), A2150-a2156.

26. Stejskal, E. O.; Tanner, J. E., *J.chem.Phys* **1965**, (42), 288.

27. Kreuer, K.-D.; Paddison, S. J.; Spohr, E.; Schuster, M., Transport in Proton Conductors for Fuel-Cell Applications: Simulations, Elementary Reactions, and Phenomenology. *Chemical Reviews (Washington, DC, United States)* **2004,** 104, (10), 4637-4678.

28. Kreuer, K. D., On the complexity of proton conduction phenomena. *Solid State Ionics* **2000,** 136-137, 149-160.

29. Zawodzinski, T. A.; Neeman, M.; Sillerud, L. O.; Gottesfeld, S., Determination of Water Diffusion-Coefficients in Perfluorosulfonate Ionomeric Membranes. *Journal of Physical Chemistry* **1991,** 95, (15), 6040-6044.

30. Yasuda, H.; Lamaze, C. E.; Ikenberry, L. D., Permeability of Solutes Through Hydrated Polymer Membranes. *Die Makromoleculare Chemie* **1968,** 118, (NR-2858), 19-35.

31. Elabd, Y. A.; Napadensky, E.; Sloan, J. M.; Crawford, D. M.; Walker, C. W., Triblock copolymer ionomer membranes Part I. Methanol and proton transport. *Journal of Membrane Science* **2003,** 217, (1-2), 227-242.

32. Hodge, R. M.; Bastow, T. J.; Edward, G. H.; Simon, G. P.; Hill, A. J., Free volume and the mechanism of plasticization in water-swollen poly(vinyl alcohol). *Macromolecules* **1996,** 29, (25), 8137-8143.

33. Hodge, R. M.; Edward, G. H.; Simon, G. P., Water absorption and states of water in semicrystalline poly(vinyl alcohol) films. *Polymer* **1996,** 37, (8), 1371-1376.

34. Quinn, F. X.; Kampff, E.; Smyth, G.; Mcbrierty, V. J., Water in Hydrogels .1. A Study of Water in Poly(N-Vinyl-2-Pyrrolidone Methyl-Methacrylate) Copolymer. *Macromolecules* **1988,** 21, (11), 3191-3198.

5. CHAPTER-5-Synthesis and Crosslinking of Hydrophilic and Hydrophobic Ion Containing Poly(Arylene Ether Sulfone)s based Multiblock copolymer for Proton Exchange Membrane Application

Mou Paul, Abhishek Roy, Ozma Lane, Hae-Seung Lee, James E. McGrath & Judy S. Riffle

Macromolecules and Interfaces Institute
Department of Chemistry
Virginia Polytechnic Institute and State University, Blacksburg, VA 24061

Abstract

Hydrocarbon based ion-containing hydrophilic-hydrophobic multiblock copolymers have shown promise as potential prootn exchange membranes (PEM)s by demonstrating high proton conductivity, particularly under partially hydrated conditions. Both the proton conductivity and water uptake of these multiblock copolymers increased with increasing block lengths. The selectivity of these PEMs will be improved if their water uptake and swelling can be reduced while maintaining their proton conductivity. Light crosslinking of these multiblocks is one of the way to reduce their water uptake and swelling without significantly impairing their proton conductivity. Two series of multiblocks with phenoxide endgroups were synthesized and crosslinked with a multifunctional epoxy resin thermally. The effects of crosslinking on various PEM properties such as water uptake, swelling and proton conductivity were evaluated. Crosslinking showed an improvement in the PEM selectivity of these multiblock copolymers. The multiblock copolymers were endcapped with either a phenoxide-terminated hydrophilic unit or a phenoxide-terminated hydrophobic unit. This preferential endcapping by the oligomers in these multiblocks enabled us to investigate

the effect of sequence distribution on various PEM properties in addition to the crosslinking study.

5.1. Introduction

Fuel cells are attractive sources of energy in today's world due to their environmental friendly nature. Since the electrical energy can be generated through electrochemical reactions only, this process is highly efficient, cleaner (without any pollutant emission) and quieter compared to conventional energy generation technologies.[1-3] Among the various types of fuel cells, proton exchange membrane based fuel cells (PEMFC)s are noteworthy for their potential application in automobiles, portable and stationary power sources. The key component in a PEMFC is the proton exchange membrane (PEM) which serves as the transport pathway of protons from anode to cathode. Several ionomers as candidates for PEMs have been developed over last five decades.[4] The current state-of-the-art membrane is a perfluorosulfonic acid based membrane named Nafion®. Despite of having several advantages like high proton conductivity and excellent chemical stability, Nafion® suffers from some critical shortcomings such as high fuel permeability, limited operating temperature and high cost.[5] These disadvantages of Nafion® have motivated researchers to develop alternative proton exchange membranes.[6] McGrath *et al.* have developed partially disulfonated biphenol-based poly(arylene ether sulfone) (BPSH) random copolymers as potential PEMs.[7, 8] These wholly aromatic, hydrocarbon based membranes have shown excellent proton conductivity at fully hydrated condition, low permeability to fuels and high mechanical stability at elevated temperatures. However one of the current requirements of PEMs is to demonstrate satisfactory proton conductivity even at partially hydrated conditions. This is a challenge with the random copolymers where the sulfonic acid groups are distributed randomly within the copolymer. It results in insufficient connectivity among the acid groups at low hydration level, reducing proton conductivity under partially hydrated conditions. Recent studies by the McGrath group have demonstrated that nanophase separated ion containing hydrophilic-hydrophobic

multiblock copolymers with improved connectivity between the sulfonic acid groups can sustain proton conductivity even under partially hydrated condition.[9-14] At a similar ion exchange capacity, proton conductivity of these multiblock copolymers under partially hydrated conditions increased with increasing block lengths. However, the higher block length multiblock copolymers were associated with both high water uptake and swelling. Increased swelling in a membrane may reduce the effective proton concentration and hence the proton conductivity. Controlling the water uptake for the higher block length materials can maximize the effective proton concentration, expanding the scope of further improvement in PEM selectivity. In addition to this, a reduced swelling-deswelling characteristic of the membrane improves its mechanical durability under low relative humidity cycling operations.

Earlier reports have indicated that multiblock copolymers synthesized with higher molar fraction and higher block length of hydrophobic unit showed reduced water uptake.[13] This is similar to "physical crosslinking" where the higher volume fraction of the hydrophobic block constrains the hydrophilic block leading to reduced water uptake. But there is a certain limit up to which this ratio between the volume fractions of these individual blocks can be altered. Beyond that limit the higher volume fraction of the hydrophobic unit will change the continuous hydrophilic domain morphology of the multiblock copolymer into a discontinuous one which can have unfavorable effect on proton conductivity. Hence, in order to maintain both ideal block copolymer morphology and reduced water uptake, an alternative approach is to chemically crosslink equal block length materials. Recently, we have reported that both water uptake and swelling of random BPSH copolymers reduced significantly by covalent crosslinking.[15] At the same time the proton conductivity of the crosslinked membranes was retained or even improved (in case of highly disulfonated copolymers). Therefore, an increased PEM selectivity was achieved compared to that of uncrosslinked membranes.

In this paper we have extended the chemistry of crosslinking of random copolymers to hydrocarbon based ion-containing BPSH-BPS multiblock copolymers. Lee et al. have reported the synthesis of these hydrophilic-hydrophobic multiblock

copolymer via low temperature coupling reactions.[9] The objective of this paper is to lightly crosslink these multiblock copolymers so that their water uptake and swelling can be reduced while maintaining their proton conductivity. Multiblock copolymers with phenoxide endgroups were synthesized by coupling reactions between telechilic oligomers bearing suitable endgroups (phenoxide or decafluorobiphenyl) and further reacted with an epoxy reagent to produce crosslinked membranes. The effect of crosslinking on PEM properties such as water uptake, swelling and proton conductivity was investigated.

In order to accomplish a phenoxide-terminated multiblock copolymer, the phenoxide-endcapped oligomer was taken in twenty percent molar excess than the deceflurobiphenyl-endcapped oligomer in contrast to the conventional equal molar ratio (1:1)[9] approach. This was achieved by taking in excess either a phenoxide-endcapped hydrophilic oligomer or a phenoxide-endcapped hydrophobic oligomer which generated two series of multiblock copolymers endcapped with either hydrophilic or hydrophobic oligomer respectively. It can be hypothesized that this stoichiometric imbalance approach may lead to preferential sequence distributions of the oligomers in these multiblocks in contrast to the statistical sequence distribution resulting from equal molar ratio approach. Hence, in addition to the crosslinking study, this paper also proposes to study the influence of sequence distributions on various PEM properties such as water uptake, water swelling and proton conductivity.

The nomenclature of the samples is provided below. Hydrophilic and hydrophobic oligomers are termed as BPSH100 and BPS0 respectively. A hydrophilic-hydrophobic multiblock copolymer is named as BPSH100-BPS0(A:B) where A and B equal the molecular weights of BPSH100 and BPS0 in kg $mole^{-1}$ respectively. Phenoxide-terminated, hydrophilic, and hydrophobic oligomer endcapped multiblock copolymers are named as *hydrophilic*-BPSH100-BPS0(A:B) and *hydrophobic*-BPSH100-BPS0(A:B) respectively.

5.2. Experimental

5.2.1. Materials

Monomer grade 4,4′–dichlorodiphenylsulfone (DCDPS) and 4,4′-biphenol (BP) were obtained from Solvay Advanced Polymers and Eastman Chemical Company, respectively, and dried under vacuum at 60 °C for one day prior to use. The sulfonated comonomer, 3,3′-disulfonate-4,4′-dichlorodiphenylsulfone (SDCDPS), was prepared following a previously published procedure [7, 16], and dried under vacuum at 160 °C for two days before use. Decafluorobiphenyl (DFBP) was obtained from Lancaster and used as received. Potassium carbonate (Aldrich) was dried under vacuum at 110 °C for one day before use. Tetraglycidyl bis(p-aminophenyl)methane (Araldite MY721 epoxy resin) and triphenylphosphine (TPP) were obtained from Aldrich and used as received. The reaction solvent *N*,*N*-dimethylacetamide (DMAc, Aldrich) was vacuum-distilled from calcium hydride, and stored over molecular sieves under nitrogen. Toluene (anhydrous, 99.8%), isopropyl alcohol (*ReagentPlus*™, 99%), methanol, acetone, *N*-methyl-2-pyrrolidinone (NMP) (*ReagentPlus*™, 99%) and trimethylchlorosilane (silanizing agent) were obtained from Aldrich and used as received. Sulfuric acid (*ACS Reagent*, 95-98%) was obtained from VWR Internationals and used as received.

5.2.2. Synthesis of a controlled molecular weight, phenoxide-endcapped, fully disulfonated, hydrophilic BPSH100 oligomer

A controlled molecular weight, phenoxide-endcapped 100% disulfonated biphenol-based poly(arylene ether sulfone) (BPSH100) oligomer was synthesized via nucleophilic aromatic substitution. The molecular weight of the copolymer was controlled by offsetting the stoichiometry of the monomers. A typical polymerization of a 5 kg mol^{-1} BPSH100 copolymer is provided. BP (3.236 g, 17.38 mmol) and SDCDPS (7.661 g, 15.59 mmol) were added to a three-necked, round bottom reaction flask equipped with a mechanical stirrer, nitrogen inlet, Dean-Stark trap and a condenser. Potassium carbonate (2.882 g, 20.85 mmol) and 55 mL DMAc (to achieve 20% solids) were introduced into the flask. Toluene (27 mL, DMAc/toluene was 2/1 v/v) was added as the azeotropic reagent. The reaction mixture was refluxed at 150 °C for 4 h, then the

azeotrope was removed to dehydrate the system. The reaction mixture was gradually heated to 170 °C by the controlled removal of toluene, then reacted for an additional 48 h. The viscous product was cooled to room temperature. The product mixture was filtered to remove salts. The copolymer was isolated by precipitation in acetone, filtered, and dried for 24 h at 110 °C under vacuum. The nomenclature of the samples is defined as follows-BPSH100(A) where A denotes the molecular weight of the oligomer in kg $mole^{-1}$

5.2.3. Synthesis of a controlled molecular weight, phenoxide-endcapped, unsulfonated, hydrophobic BPS0 oligomer

A controlled molecular weight, phenoxide-endcapped unsulfonated biphenol-based poly(arylene ether sulfone) (BPS0) oligomer was synthesized via nucleophilic aromatic substitution. The molecular weight of the copolymer was controlled by offsetting the stoichiometry of the monomers. A typical polymerization of a 5 kg mol^{-1} BPS0 copolymer is provided. BP (2.74 g, 14.71 mmol) and DCDPS (3.901 g, 13.58 mmol) were added to a three-necked, round bottom reaction flask equipped with a mechanical stirrer, nitrogen inlet, Dean-Stark trap and a condenser. Potassium carbonate (2.338 g, 16.92 mmol) and 33 mL DMAc (to achieve 20% solids) were introduced into the flask. Toluene (16 mL, DMAc/toluene was 2/1 v/v) was added as the azeotropic reagent. The reaction mixture was refluxed at 150 °C for 4 h, then the azeotrope was removed to dehydrate the system. The reaction mixture was gradually heated to 170 °C by the controlled removal of toluene, then reacted for an additional 24 h. The viscous product was cooled to room temperature. The product mixture was filtered to remove salts. The copolymer was isolated by precipitation in isopropyl alchohol, filtered, and dried for 24 h at 110 °C under vacuum. The nomenclature of the samples is defined as follows- BPS0(B) where B denotes the molecular weight of the oligomer in kg $mole^{-1}$.

5.2.4. End-functionalization of phenoxide-endcapped hydrophobic BPS0 and hydrophilic BPSH100 oligomers by DFBP

The terminal phenoxide groups of BPS0 or BPSH100 oligomers were reacted with DFBP via nucleophilic aromatic substitution reaction to produce DFBP-endcapped

BPS0 or BPSH100 oligomers. A typical endcapping reaction of a BPS0(10) or BPSH100(10) copolymer is provided. Phenoxide-endcapped BPS0 (3 g, 0.3 mmol) or BPSH100 (3 g, 0.3 mmol) was added to a three-necked, round bottom reaction flask equipped with a mechanical stirrer, nitrogen inlet, Dean-Stark trap and a condenser. Potassium carbonate (0.083 g, 0.6 mmol) and 30 mL DMAc (to achieve 10% solids) were introduced into the flask. The mixture was stirred at about 80 °C until all the reactants were completely dissolved. Cyclohexane (6 mL, DMAc/cyclohexane was 5/1 v/v) was added as the azeotropic reagent. The reaction mixture was refluxed at 90 °C for 4 h, then the azeotrope was removed to dehydrate the system. The reaction mixture was gradually heated to 105 °C by the controlled removal of cyclohexane. Then DFBP (0.601 g, 1.8 mmol) was added into the reaction flask and reacted for an additional 24 h. The product was cooled to room temperature. The product mixture was filtered to remove salts. The copolymer was isolated by precipitation in methanol (BPS0) or isopropyl alchohol (BPSH100), filtered, and dried for 24 h at 110 °C under vacuum. The nomenclature of the samples is defined as follows- DFBP-BPS0(B) or DFBP-BPSH100(A) where B & A denote the molecular weights of the respective oligomers in kg mole^{-1}.

5.2.5. Synthesis of a phenoxide-terminated, hydrophilic oligomer endcapped multiblock (hydrophilic-BPSH100-BPS0)

A *hydrophilic*-BPSH100-BPS0 multiblock copolymer was synthesized via coupling reaction between a phenoxide-endcapped BPSH100 and a DFBP-endcapped BPS0. BPSH100 was taken in 20 % molar excess compared to the DFBP-BPS0 in order to ensure the endcapping of the BPSH100-BPS0 multiblock with the phenoxide-terminated hydrophilic oligomer. A typical coupling reaction between a BPSH100(5) oligomer and a DFBP-BPS0(5) oligomer is provided. BPSH100 (2 g, 0.4 mmol) was added to a three-necked, round bottom reaction flask equipped with a mechanical stirrer, nitrogen inlet, Dean-Stark trap and a condenser. Potassium carbonate (0.111 g, 0.8 mmol) and 20 mL DMAc (to achieve 10% solids) were introduced into the flask. The mixture was stirred at about 80 °C until all the reactants were completely dissolved. DFBP-BPS0(5) (1.667 g, 0.33 mmol) and 16 mL DMAc were added into the flask. The

stirring was continued at 80 °C until all the reactants were completely dissolved. Cyclohexane (7 mL, DMAc/cyclohexane was 5/1 v/v) was added as the azeotropic reagent. The reaction mixture was refluxed at 90 °C for 4 h, then the azeotrope was removed to dehydrate the system. The reaction mixture was gradually heated to 105 °C by the controlled removal of cyclohexane, then reacted for an additional 24 h. The viscous product was cooled to room temperature. The product mixture was filtered. The copolymer was precipitated in isopropyl alchohol and isolated by filtration. The copolymer was soxhlet extracted in methanol for 24 h to remove any unreacted BPSH100 oligomer, and dried for 24 h at 110 °C under vacuum.

5.2.6. Synthesis of a phenoxide-terminated, hydrophobic oligomer endcapped multiblock (hydrophobic-BPSH100-BPS0)

A *hydrophobic*-BPS100-BPS0 multiblock copolymer was synthesized via coupling reaction between a phenoxide-endcapped BPS0 and DFBP-endcapped BPSH100 oligomer. BPS0 was taken in 20 % molar excess compared to DFBP-BPSH100 in order to ensure the endcapping of the BPSH100-BPS0 multiblock with the phenoxide terminated hydrophobic oligomer. A typical coupling reaction between a BPS0(10) oligomer and a DFBP-BPSH100(10) oligomer is provided. DFBP-BPSH100 (2 g, 0.2 mmol) and 20 mL DMAC were added to a three-necked, round bottom reaction flask equipped with a mechanical stirrer, nitrogen inlet, Dean-Stark trap and a condenser. The mixture was stirred at about 80 °C until the reactant was completely dissolved. BPS0(10) (2.4 g, 0.24 mmol), potassium carbonate (0.066 g, 0.48 mmol) and 24 mL DMAc were introduced into the flask. The stirring was continued at 80 °C until all the reactants were completely dissolved. Cyclohexane (9 mL, DMAc/cyclohexane was 5/1 v/v) was added as the azeotropic reagent. The reaction mixture was refluxed at 90 °C for 4 h, then the azeotrope was removed to dehydrate the system. The reaction mixture was gradually heated to 105 °C by the controlled removal of cyclohexane, then reacted for an additional 24 h. The viscous product was cooled to room temperature. The product mixture was filtered. The copolymer was precipitated in isopropyl alchohol and isolated

by filtration. The copolymer was soxhlet extracted in chloroform for 24 h to remove any unreacted BPS0 oligomer, and dried for 24 h at 110 °C under vacuum.

5.2.7. Silanization of glass casting plates

A 20% (v/v) solution of trimethylchlorosilane in toluene was prepared. Clean glass plates were immersed in the solution for 2-3 minutes, removed, then reacted in a convection oven for 1 h at 250 °C. The plates were cooled to room temperature and washed with acetone before use [17].

5.2.8. Film casting, epoxy curing, and acidification

A 10 wt % solution of a *hydrophilic*-BPSH100-BPS0 or *hydrophobic*-BPSH100-BPS0 multiblock copolymer with around 8 wt % of MY721 epoxy resin (based on copolymer weight) and 2.5 wt % of TPP catalyst (based on epoxy resin weight) was prepared in NMP and stirred until a transparent homogeneous solution was obtained. The solution was cast on a silanized glass plate. The plate was inserted in an oven and heated at 100 °C for 120 minutes, then at 150 °C for 90 minutes. After cooling to room temperature, the plate was removed from the oven and the membrane was peeled from the glass plate. The uncrosslinked membranes from the multiblock copolymers were also prepared following the same procedure, except the addition of epoxy resin and TPP catalyst. The nomenclature of the crosslinked membranes is as follows- *hydrophilic*-x-BPSH100-BPS0(A:B) and *hydrophobic*-x-BPSH100-BPS0(A:B).

The uncrosslinked and crosslinked membranes were acidified by boiling in 0.5 M sulfuric acid for 2h, then boiling in deionized water for 2 h.

Characterization

5.2.9. Nuclear magnetic resonance (NMR) spectroscopy

^{1}H NMR experiments were conducted on a Varian Unity 400 MHz NMR spectrometer. All spectra of the oligomers and multiblock copolymers were obtained

from 10 % solutions (w/v) in DMSO-d_6 at room temperature. Proton NMR was used to determine the molecular weights of the copolymers and their compositions, and the completion of endcapping reactions.

5.2.10. Intrinsic viscosity

Intrinsic viscosities were determined from GPC experiments performed on a liquid chromatograph equipped with a Viscotek 270 RALLS/ viscometric dual detector. The mobile phase was 0.05 M LiBr containing NMP solvent. The column temperature was maintained at 60 °C because of the viscous nature of NMP. Both the mobile phase solvent and sample solution were filtered before introduction to the GPC system.

5.2.11. Ion exchange capacity (IEC)

Ion exchange capacities of the uncrosslinked and crosslinked multiblock copolymers in acid form were determined by titration with 0.01 M NaOH solution.

5.2.12. Gel fractions

Gel fractions of the networks were measured by placing 0.1-0.15 g of sample in DMAc and soxhlet extracting for 48 h. After removal of the solvent by drying at 120 °C for 24 h under vacuum, the remaining mass was weighed as gel. Gel fractions were calculated by dividing the weights of the gels by the initial weights of the networks.

5.2.13. Water uptake

The membranes were immersed in deionized water for at least 48 h, then they were removed from the water, blotted dry and quickly weighed. The membranes were vacuum dried at 110 °C overnight and the weights were recorded. The ratio of weight gain to the original membrane weight was reported as the water uptake (mass %),

$$\text{Water uptake (\%)} = \frac{W_{wet} - W_{dry}}{W_{dry}} \times 100 \quad \textbf{Equation 5-1}$$

where W_{wet} and W_{dry} were the masses of wet and dried samples, respectively.

5.2.14. Volume swelling ratio

The membranes were equilibrated in deionized water for at least 48 h, then they were removed from the water and blotted dry. The dimensions were measured in three directions (length, width and thickness) to calculate the wet volume. The samples were dried in a convection oven for 2 h at 80 °C. The ratio of volume gain to the original membrane volume was reported as the volume swelling ratio.

5.2.15. Proton conductivity

Proton conductivity at 30 ^{o}C at full hydration (in liquid water) was determined in a window cell geometry[18] using a Solartron 1252 + 1287 Impedance/Gain-Phase Analyzer over the frequency range of 10 Hz to 1 MHz following the procedure reported in the literature.[19] For determining proton conductivity in liquid water, the membranes were equilibrated at 30 °C in DI water for 24 h prior to testing.

5.2.16. AFM Image Analysis

The morphological characterization was carried out using a Veeco Multimode Atomic Force Microscope, using a 80N/m silicon tip, a free air amplitude of 6.00 V and a setpoint ratio of 0.78-0.83. Prior to characterization, the films were equilibrated at 30 C and 40% relative humidity for 12 hours.

5.3. Results and discussion

5.3.1. Synthesis of controlled molecular weight, phenoxide-endcapped, BPSH100 and BPS0 oligomers

Two series of controlled molecular weight, BPSH100 and BPS0 oligomers with phenoxide endgroups were synthesized from biphenol and SDCDPS or DCDPS respectively by nucleophilic aromatic substitution (Fig. 5.1 and Fig. 5.2). The molecular weights of the BPS100 and BPS0 oligomers were controlled by offsetting the stoichiometry between biphenol and SDCDPS or DCDPS respectively. Biphenol was utilized in excess to endcap the oligomers with phenoxide groups. For both of the series, a set of two oligomers with number average molecular weights (M_n) of five and ten kg mol^{-1} was targeted.

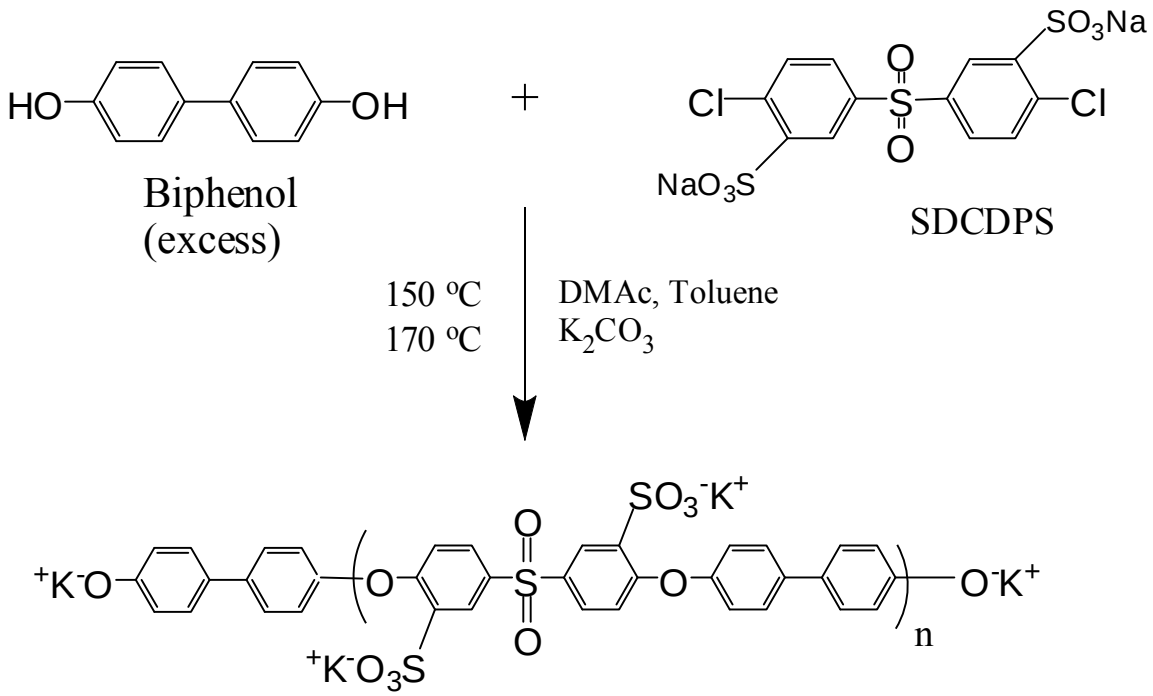

Figure 5.1 Synthesis of a controlled molecular weight, phenoxide-endcapped, fully disulfonated hydrophilic (BPSH100) oligomer

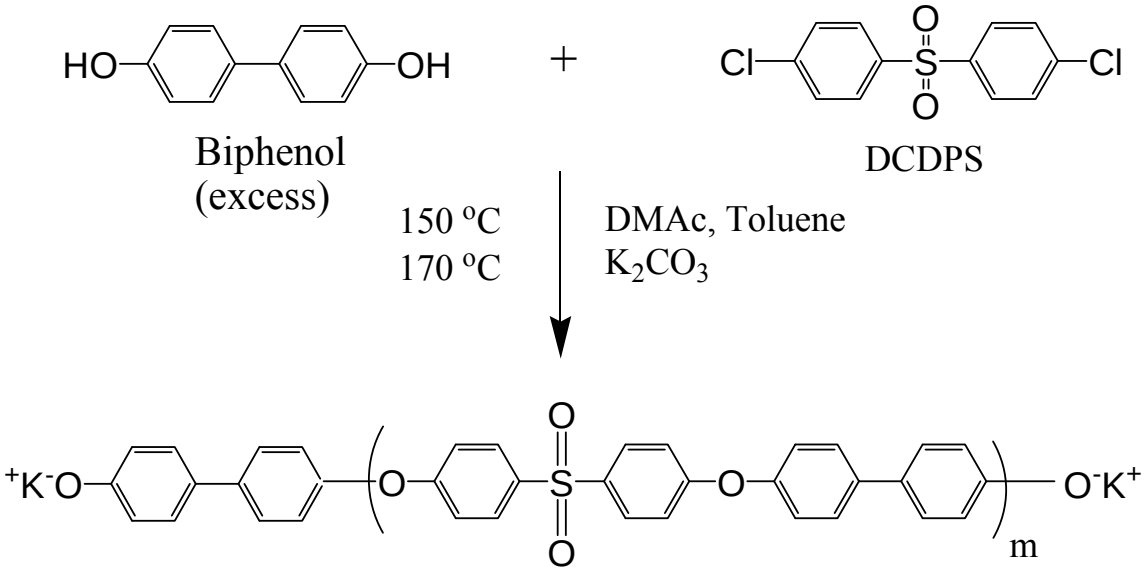

Figure 5.2 Synthesis of a controlled molecular weight, phenoxide-endcapped, unsulfonated hydrophobic (BPS0) oligomer

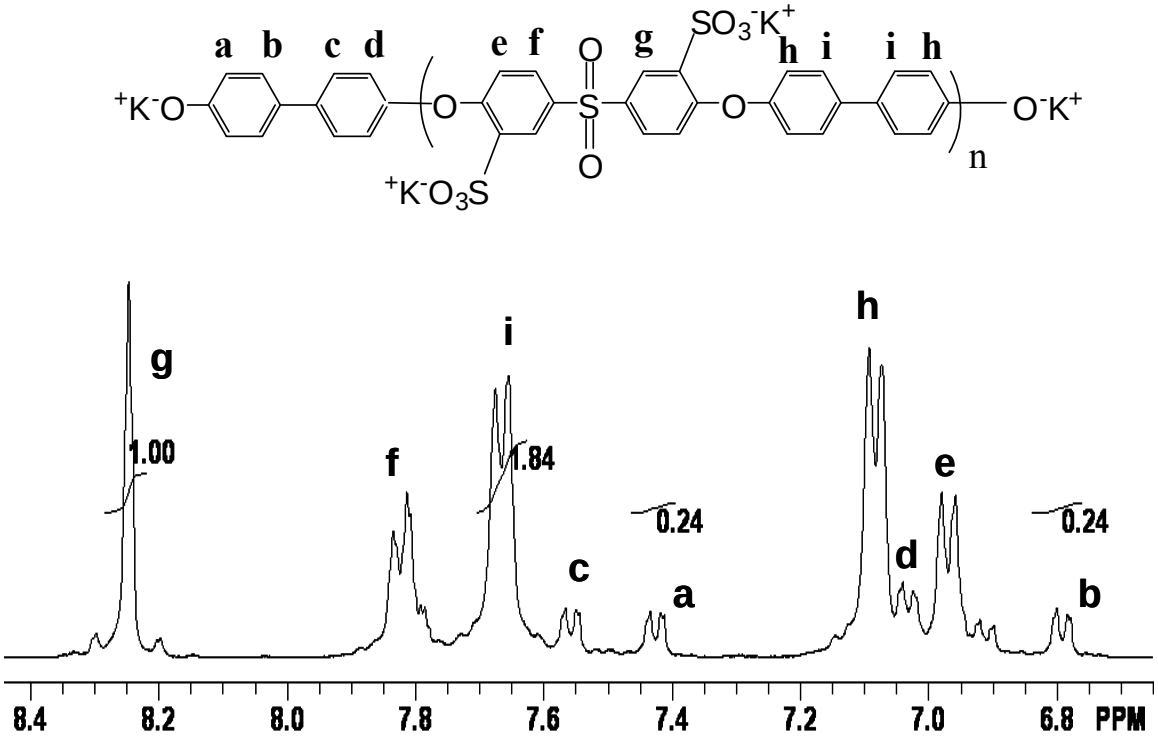

Figure 5.3 ^{1}H NMR of a phenoxide endcapped BPSH100(5) oligomer

Figure 5.3 shows the proton NMR spectrum of a phenoxide endcapped BPSH100 oligomer with a targeted molecular weight of five kg mol^{-1}. The aromatic protons of the biphenol unit in the endgroup at *(b), (d), (a), and (c)* were allocated to peaks at 6.8 ppm, 7.05 ppm, 7.45 ppm and 7.55 ppm respectively. The ratio of the integrals of the aromatic protons at 6.8 ppm (*b*) to those of the aromatic protons of the biphenol moiety in the polymer repeat units at 7.65 ppm (*i*) were utilized to calculate M_n of the oligomers.

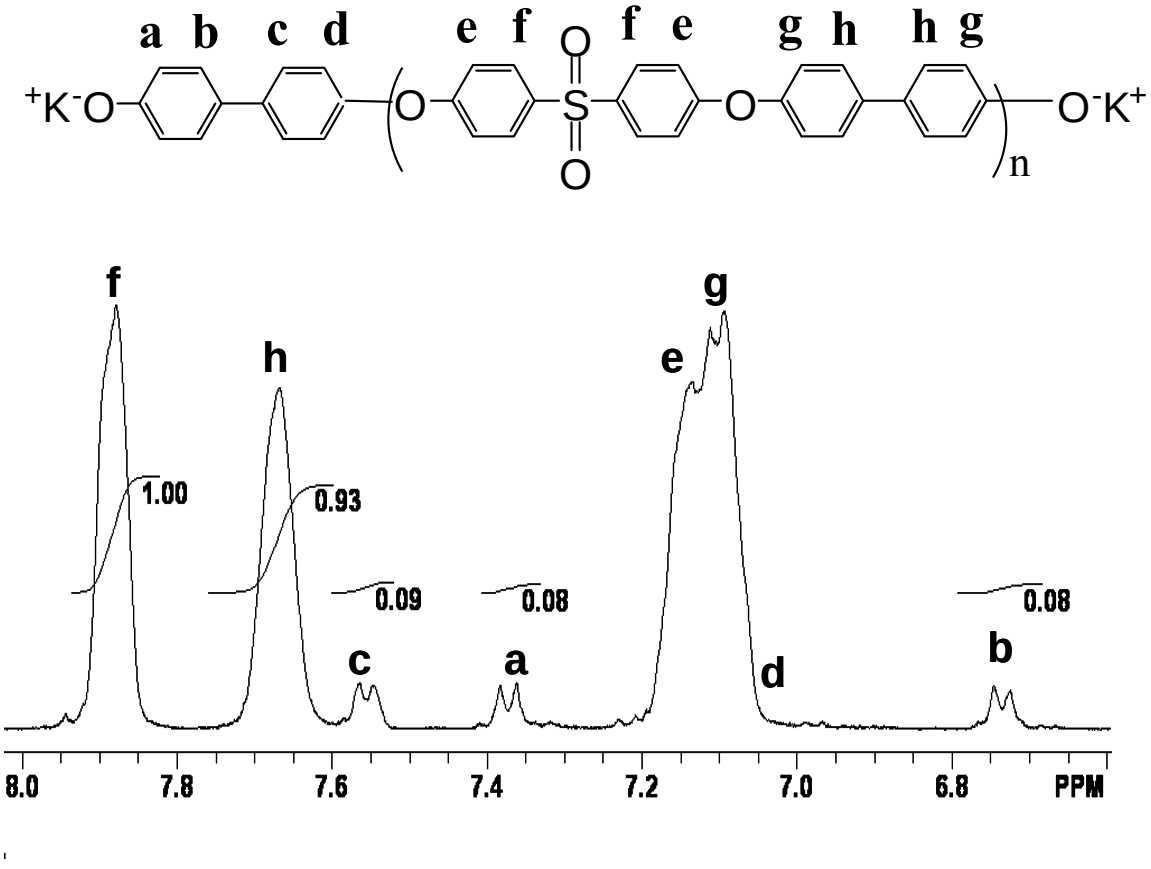

Figure 5.4 ^{1}H NMR of a phenoxide endcapped BPS0(5) oligomer

Figure 5.4 shows the proton NMR spectrum of a phenoxide endcapped BPS0 oligomer with a targeted molecular weight of five kg mol^{-1}. The aromatic protons of the biphenol unit in the endgroup *(b), (a), and (c)* were allocated to the peaks at 6.75 ppm , 7.40 ppm and 7.55 ppm respectively. The ratio of the integrals of the aromatic protons at 6.75 ppm (*b*) to those of the protons of the biphenol moiety in the polymer repeat units at 7.65 ppm (*h*) were utilized to calculate M_n of the oligomers. As shown in Table 5.1, the experimental M_n values derived from NMR are in good agreement with the targeted values. As expected, intrinsic viscosities ([η]) of the oligomers increased with increasing molecular weight (Table 5.1).

Table 5.1 Summary of properties of the oligomers synthesized

Target M_n ($g\ mol^{-1}$)	Hydrophilic Oligomer(BPS100)			Hydrophobic Oligomer(BPS0)		
	M_n[a] ($g\ mol^{-1}$)	IV[b] ($dL\ g^{-1}$)	IV[c] ($dL\ g^{-1}$)	M_n[a] ($g\ mol^{-1}$)	IV[b] ($dL\ g^{-1}$)	IV[c] ($dL\ g^{-1}$)
5000	5139	0.20	-	4913	0.25	0.32
10000	9030	0.33	0.29	9260	0.36	0.42

[a] from ^1H NMR

[b] measured at 60 ^oC, GPC, 0.05 M LiBr in NMP

[c] measured at 60 ^oC, GPC, 0.05 M LiBr in NMP after endcapping with DFBP

5.3.2. End-functionalization of phenoxide-endcapped BPS0 and BPSH100 oligomers by DFBP

The terminal phenoxide groups of BPS0 or BPSH100 oligomers were reacted with DFBP via nucleophilic aromatic substitution reaction to produce DFBP endcapped BPS0 or BPSH100 oligomers (Fig. 5.5). DFBP was utilized in excess to endcap the oligomers with fluoro-terminal groups, so that these groups can be further reacted in the coupling reaction step during the synthesis of multiblocks. A 200 % molar excess of DFBP was taken to ensure complete endcapping without any inter-oligomer coupling reaction. [9]

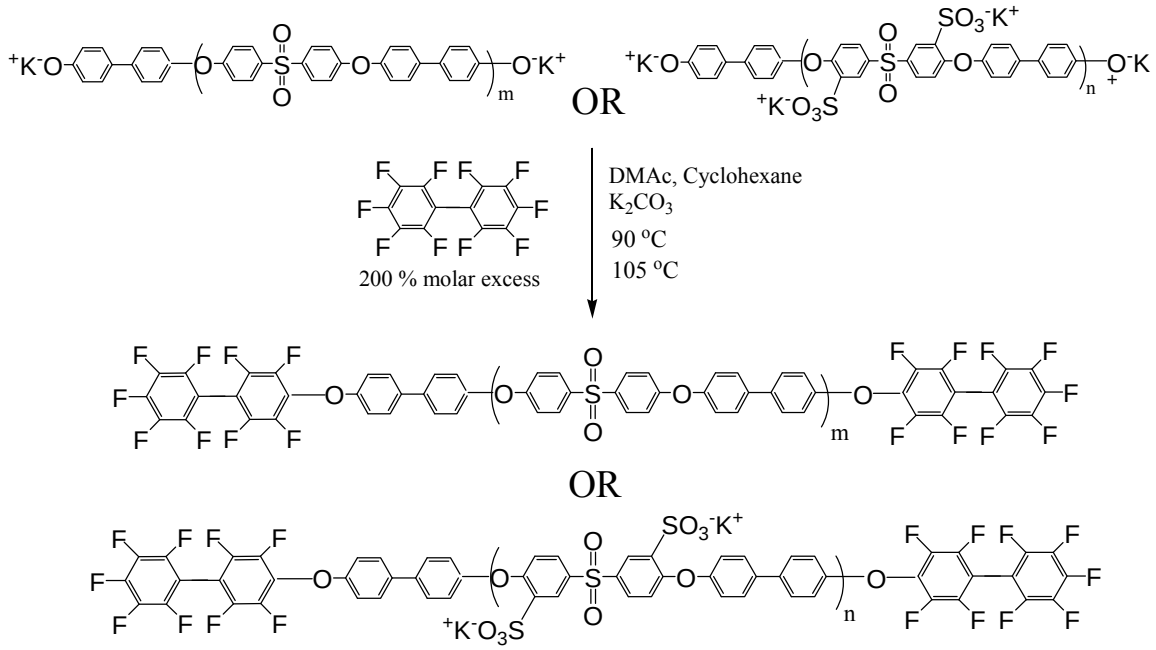

Figure 5.5 End-functionalization of phenoxide-endcapped BPS0 and BPSH100 oligomers by DFBP

Figure 5.6a represents the proton NMR spectrum of a DFBP-BPS0(5) oligomer. The aromatic protons of the biphenol unit in the endgroup at 6.75 ppm (*b*), 7.40 ppm (*a*)

and 7.55 ppm (*c*) of the phenoxide-terminated BPS0 oligomer disappeared after the phenoxide groups were reacted with DFBP and a new peak at about 7.30 ppm appeared which can be assigned to the biphenol aromatic protons linked with DFBP. From the proton NMR study it was confirmed that all the phenoxide endgroups took part in the endcapping reaction and the oligomer was completely endcapped by DFBP.

Figure 5.6b represents the proton NMR spectra of a DFBP-BPSH100(10) oligomer. The aromatic protons of the biphenol unit in the endgroup at 6.8 ppm (*b*), 7.05 ppm (*d*), 7.45 ppm (*a*) and 7.55 ppm (*c*) of the phenoxide-terminated BPS100 oligomer disappeared after the phenoxide groups were reacted with DFBP and a new peak at about 7.30 ppm appeared which can be assigned to the biphenol aromatic protons linked with DFBP. From the proton NMR study it was confirmed that all the phenoxide endgroups took part in the endcapping reaction and the oligomer was completely endcapped by DFBP.

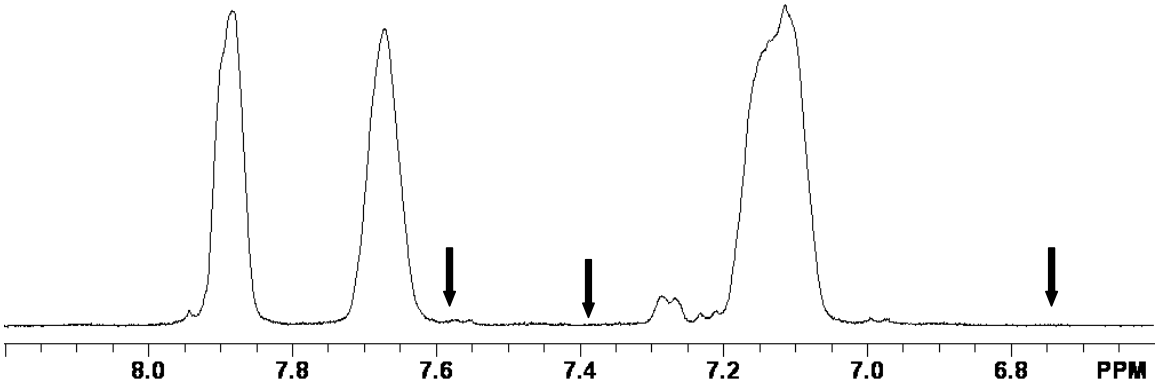

Figure 5.6a) ^{1}H NMR of a DFBP endcapped BPS0(5) oligomer;the arrows indicate the disappearance of aromatic proton peaks of the biphenol unit in the end group

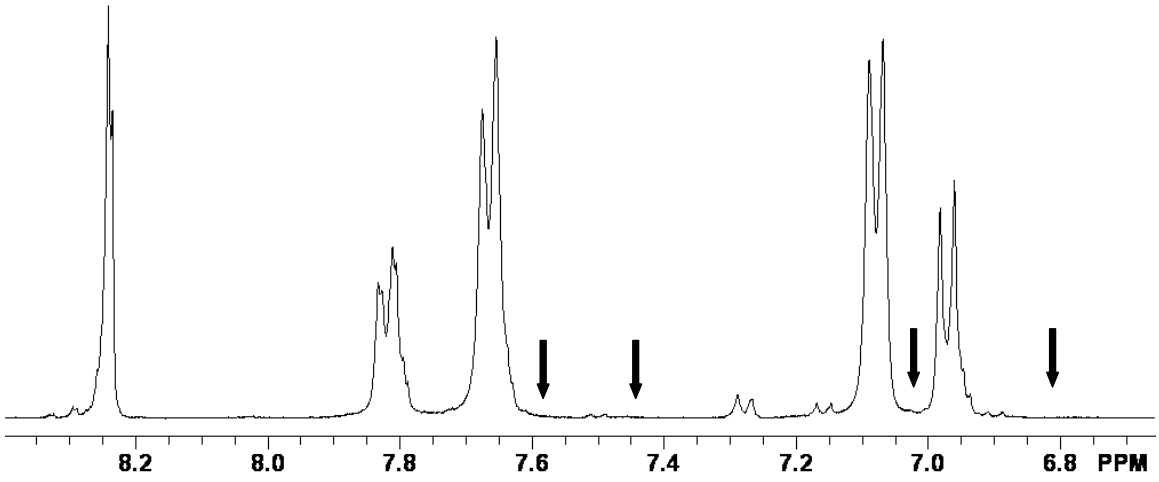

Figure 5.6b) ^{1}H NMR of a DFBP endcapped BPSH100(10) oligomer;arrows indicate the disappearance of aromatic proton peaks of the biphenol unit in the end group

In addition to the proton NMR study, the intrinsic viscosities of the oligomers before and after endcapping were compared to investigate that whether any inter-oligomer coupling by the multifunctional DFBP had taken place or not (Table 5.1). There was not any significant increase in the intrinsic viscosities of the oligomers after endcapping with DFBP. This result is in accordance with earlier study which reported that a molar excess of 200 % is sufficient to endcap the oligomers with DFBP without any inter-oligomer coupling. [9]

5.3.3. Synthesis of a hydrophilic-BPSH100-BPS0 multiblock

A phenoxide-terminated, *hydrophilic*-BPSH100-BPS0 multiblock copolymer was synthesized via coupling reaction between a phenoxide-endcapped BPSH100 and a DFBP-BPS0 oligomer (Fig. 5.7). In contrast to the conventional equimolar approach,[9] BPSH100 was taken in 20 % molar excess compared to DFBP-BPS0 to endcap the multiblock with phenoxide groups so that the phenoxide groups can be further reacted in

the crosslinking steps. As the hydrophilic oligomer was taken in excess, the resulting multiblock was expected to be preferentially endcapped with a hydrophilic moiety in contrast to the statistical endcapping of the multiblocks by either a hydrophilic or a hydrophobic moiety generated by the conventional equimolar approach. Figure 5.8 represents the proton NMR spectrum of a phenoxide-terminated *hydrophilic*-BPSH100-BPS0(5:5) multiblock. The appearance of the aromatic protons of the biphenol unit in the endgroup of BPSH100 oligomer at 6.8 ppm, 7.05 ppm, 7.45 ppm and 7.55 ppm in the multiblock NMR spectra confirms that the multiblock is endcapped with a phenoxide-terminated hydrophilic oligomer. As expected, intrinsic viscosities ([η]) of the multiblocks increased with increasing block lengths (Table 5.2).

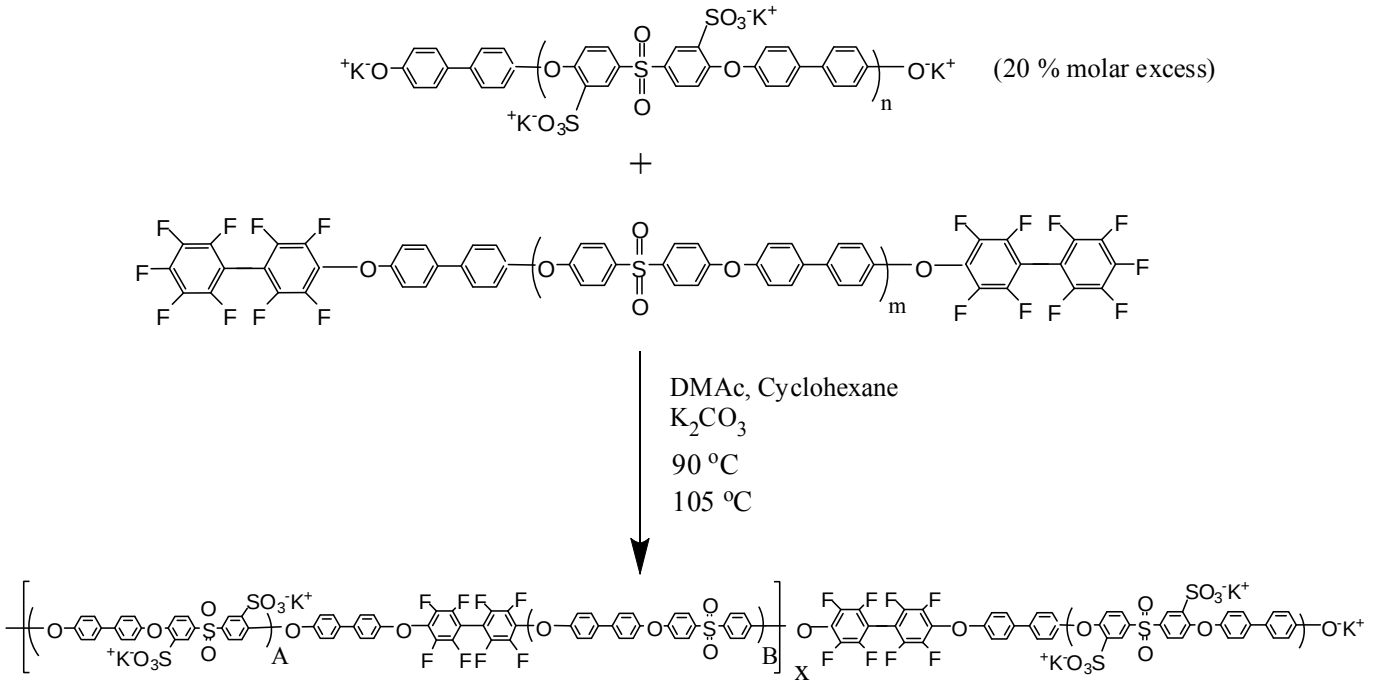

Figure 5.7 Synthesis of a phenoxide-terminated *hydrophilic*-BPSH100-BPS0(A:B) multiblock

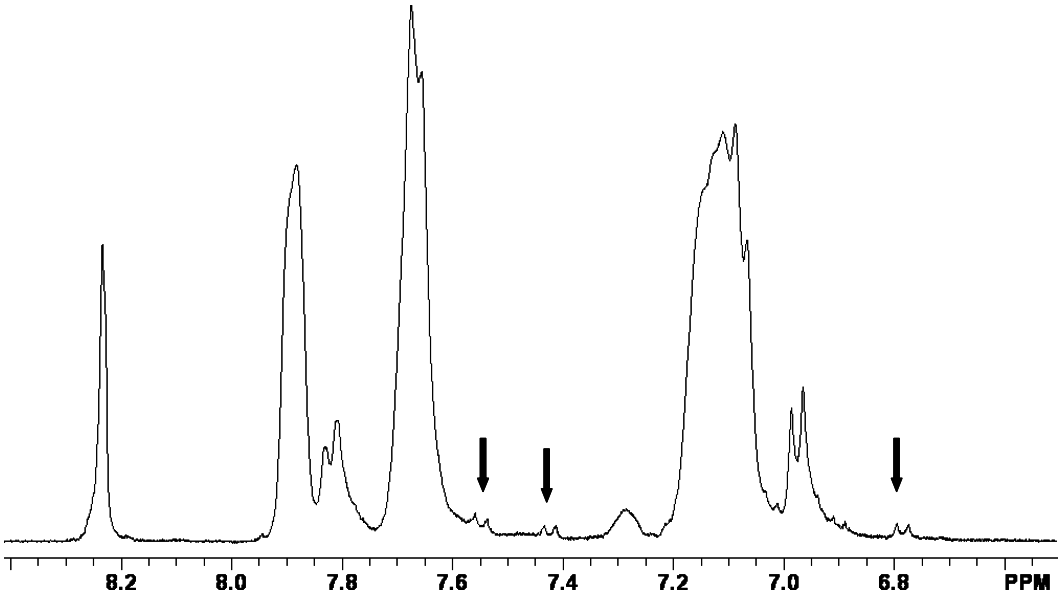

Figure 5.8 ^{1}H NMR of a phenoxide-terminated *hydrophilc*-BPSH100-BPS0(5:5) multiblock;arrows indicate the aromatic proton peaks of the biphenol unit of the end groups of BPSH100 oligomer

Table 5.2 Summary of the properties of crosslinked and uncrosslinked hydrophilic-BPSH100-BPS0(A:B) multiblocks. BPSH100-BPS0(5:5) and BPSH100-BPS0(10:10) were added as control

Sample	Block length (A:B)	IV[a] (dl/g)	IEC[b] (meq/g)	Water uptake (mass %)	Swelling ratio (volume%)	Proton conductivity[c] (S/cm)
Uncrosslinked	5:5	0.59-	1.54	75	125	0.10
Crosslinked	5:5	-	1.48	66	70	0.11
Control(1:1)[d]	5:5	1.01	1.39	33	52	0.088
Uncrosslinked	10:10	1.14	1.46	74	110	0.11
Crosslinked	10:10	-	1.28	50	74	0.11
Control(1:1)[d]	10:10	0.68	1.28	60	100	0.095

[a] measured at 60 ^{o}C, GPC, 0.05 M LiBr in NMP

[b] by titration with NaOH

[c] measured at 30 ^{o}C, liquid water

[d] obtained from Ref:[9]

5.3.4. Synthesis of a hydrophobic-BPSH100-BPS0 multiblock

A phenoxide-terminated, *hydrophobic*-BPSH100-BPS0 multiblock copolymer was synthesized via coupling reaction between a phenoxide-endcapped BPS0 and a DFBP-BPSH100 oligomer (Fig. 5.9). In contrast to the conventional 1:1 stoichiometric approach,[9] BPS0 was taken in 20 % molar excess compared to the DFBP-BPSH100 to endcap the multiblock with phenoxide groups so that the phenoxide groups can be further reacted in the crosslinking steps. As the hydrophobic oligomer was taken in excess, the resulting multiblock was preferentially endcapped with a hydrophobic moiety in contrast to the statistical endcapping of the multiblocks by either a hydrophilic or a hydrophobic moiety generated by the conventional 1:1 stoichiometric approach.

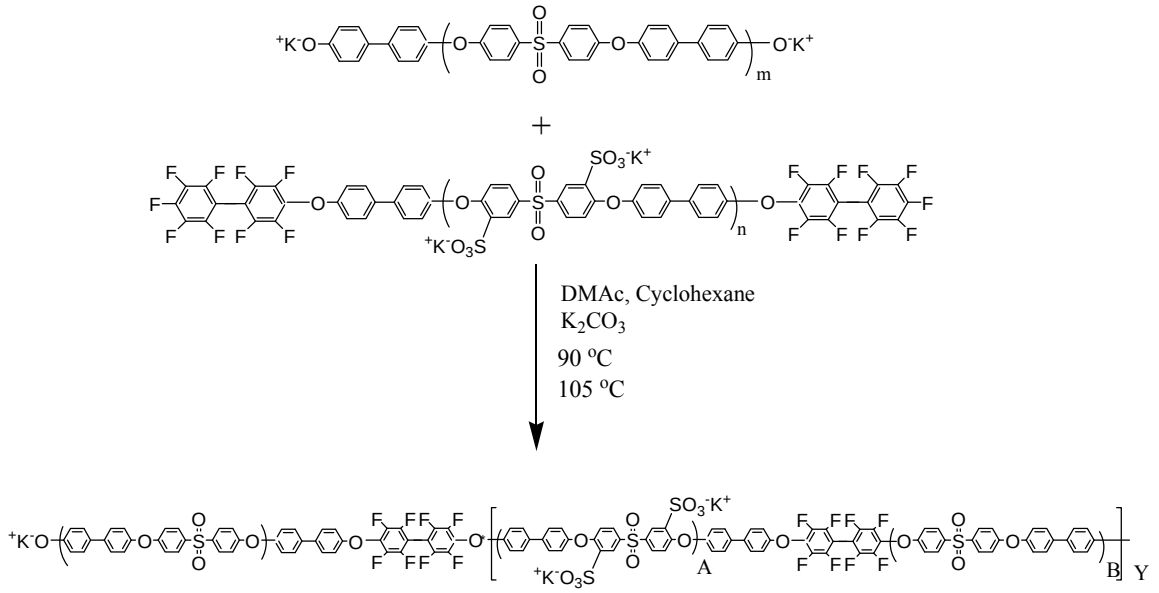

Figure 5.9 Synthesis of a phenoxide-terminated, *hydrophobic*-BPSH100-BPS0(A:B) multiblock

Figure 5.10 represents the proton NMR spectrum of a phenoxide-terminated *hydrophobic*-BPSH100-BPS0(10:10) multiblock copolymer. The appearance of the aromatic protons of the biphenol unit in the endgroup of BPS0 oligomer at 6.75 ppm, 7.40 ppm and 7.55 ppm confirms that the multiblock is endcapped with a phenoxide-

terminated hydrophobic oligomer. As expected, the intensities of the end group proton peaks are low due to their low concentration in the BPS0(10) oligomer with a longer block length.

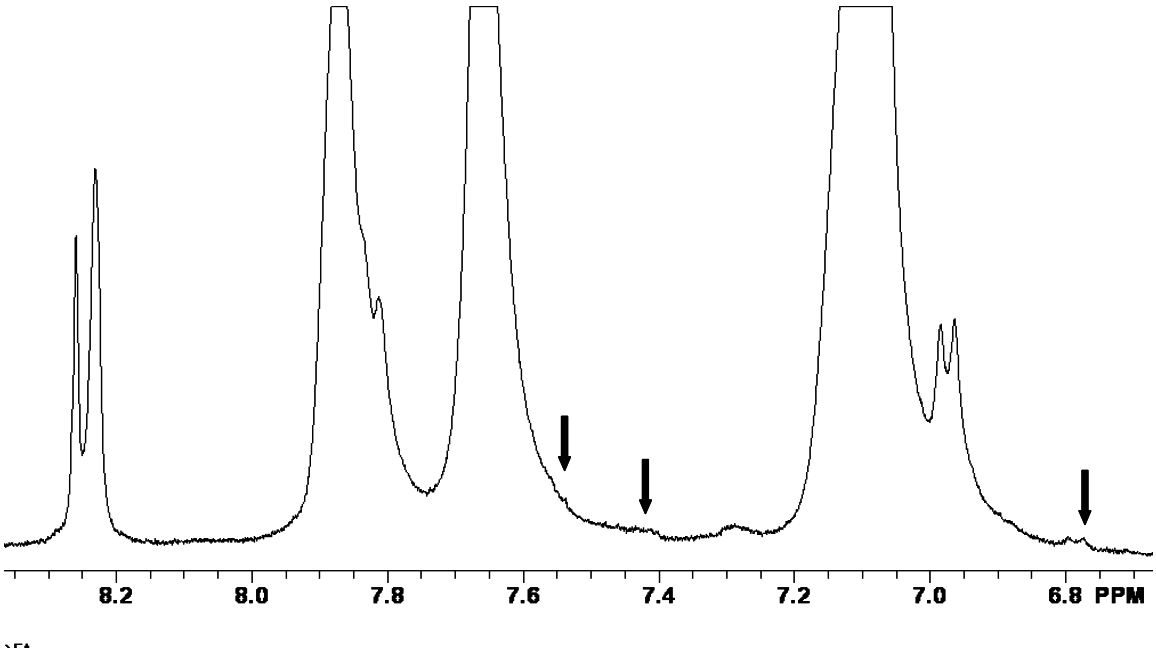

Figure 5.10 ^{1}H NMR of a phenoxide-terminated *hydrophobic*-BPSH100-BPS0(10:10) multiblock;arrows indicate the aromatic proton peaks of the biphenol unit of the end groups of BPS0 oligomer

5.3.4. Crosslinking and gel fractions

The objective of this study was to lightly crosslink multiblock copolymers so that their water uptake and swelling can be reduced modestly without significantly compromising the proton conductivity. However, in the case of multiblocks as it was hard to estimate the exact number of end groups, we fixed the amount of epoxy resin as approximately 8 wt % of the copolymer, which is similar to the amount used in case of random BPSH system.

Gel fraction values are indirective measures of the extent of crosslinking. Higher the value of gel fraction, more crosslinked is the sample. As in the current study the crosslinking was done by reacting the phenoxide endgroups of the multibock copolymers with a multifunctional epoxy resin, the concentration of the endgroups is crucial in controlling the extent of crosslinking. This is evident from the decrease in gel fraction of *hydrophilic*-x-BPSH100-BPS0 multiblock copolymers with increase in block lengths from 5-5 to 10-10 (from ~25 % to 10 %). *Hydrophobic*–x-BPSH100-BPS0(10:10) also showed a low gel fraction(~9 %) similar to its hydrophilic analogue due to the low concentration of phenoxide endgroups available for crosslinking.

Table 5.3 Summary of the properties of crosslinked and uncrosslinked hydrophobic-BPSH100-BPS0(A:B) multiblocks BPSH100-BPS0(10:10) was added as control

Sample	Block length (A:B)	IV[a] (dl/g)	IEC[b] (meq/g)	Water uptake (mass %)	Swelling ratio (volume %)	Proton conductivity[c] (S/cm)
Uncrosslinked	10-10	1.08	1.32	41	57	0.060
Crosslinked	10-10	-	1.10	38	45	0.050
Control(1:1)[d]	10-10	0.68	1.28	60	100	0.095

[a] measured at 60 ^{o}C, GPC, 0.05 M LiBr in NMP

[b] by titration with NaOH

[c] measured at 30 ^{o}C, liquid water

[d] obtained from Ref: [9]

5.3.5. Water uptake, swelling and proton conductivity

5.3.5.1.Hydrophilic-BPSH100-BPS0(A:B) multiblocks

Water uptake on mass basis and water swelling on volume basis were evaluated for both the uncrosslinked and crosslinked *hydrophilic*-BPSH100-BPS0(5:5) and *hydrophilic*-BPSH100-BPS0(10:10) multiblock copolymers (Table 5.2). BPSH100-BPS0 (5:5) and BPSH100-BPS0 (10:10) multiblocks having molar ratio between the individual blocks as 1:1 were added for comparison. The data for these two copolymers were obtained from our earlier publication.[9] The current study allows investigating both the influence of crosslinking and the influence of sequence distribution on the properties of these multiblock copolymers. When compared between the crosslinked and uncrosslinked multiblocks, a significant reduction in swelling ratio was observed irrespective of the molecular weights of the individual blocks. For example, almost a 44 % reduction in the swelling of the crosslinked *hydrophilic-x*-BPSH100-BPS0(5:5) was observed compared to the uncrosslinked one. Although the IECs of these two multiblocks were not exactly identical, they were similar enough to convey the concept. A reduction in water uptake with crosslinking was also observed, but at a lower extent, when compared with the trend as seen for water swelling. This finding is consistent with our earlier findings with the crosslinked random BPSH copolymers.[15, 20]

Proton conductivities of all copolymers were measured in liquid water at 30 ^{o}C. No significant change in proton conductivity was observed when compared between the crosslinked and uncrosslinked copolymers. This is very encouraging as this allows improving the selectivity between water uptake and proton conductivity of these ionic multiblocks. The control BPSH100-BPS0(10:10) has demonstrated satisfactory proton conductivity at all hydration levels.[9] The current crosslinking study allowed to decrease the water swelling and water uptake of that material without changing the proton conductivity at least under fully hydration case. Future studies on determining proton conductivity under partially hydrated conditions are ongoing.

Our earlier research with multiblock copolymers has confirmed that water absorption in these copolymers is a strong function of block length or morphology.[9, 12] Even at a similar IEC, both water uptake and proton conductivity increase significantly after reaching a particular block length. This particular block length has been identified to be associated with a morphological transition from isolated hydrophilic-hydrophobic domain morphology to co-continuous hydrophilic-hydrophobic domain morphology. This is supported by AFM, TEM and self-diffusion coefficient of water studies.[12, 13, 21] Once this morphology is achieved, any further increase in block length without having any changes in IEC raises the water uptake modestly. This increase in water uptake is documented as the block length increased from 5-5 to 10-10 for the control BPSH100-BPS0(A:B) copolymers.

In the current study, the *hydrophilic*-BPSH100-BPS0(5:5) shows significantly higher water uptake than the control BPSH100-BPS0(5:5) copolymer. As the titrated IEC of the *hydrophilic*-BPSH100-BPS0(5:5) is higher than the control by a small extent, it may not be an effect of IEC only. A 20 % molar excess of hydrophilic unit was used for synthesizing the *hydrophilic*-BPSH100-BPS0(5:5) multiblock. This increased hydrophilic volume fraction in the multiblock may have resulted in formation of a co-continuous hydrophilic morphology even at a lower block length of 5-5, which raised the water absorption. Hence no further significant increase in water uptake was observed in going to higher block length *hydrophilic*-BPSH100-BPS0(10:10) copolymer. At this point, this is a speculation and other studies in conjunction are needed to fully understand this proposed theory. However, the AFM image of the *hydrophilic*-BPSH100-BPS0(10:10) multiblock (Fig. 5.11a) shows a co-continuous hydrophilic morphology.

5.3.5.2.Hydrophobic-BPSH100-BPS0(A:B)

Similar studies of water uptake and water volume swelling were done for the crosslinked and uncrosslinked *hydrophobic*-BPSH100-BPS0(10:10) copolymers (Table 5.3). A decrease in both water swelling and water uptake was observed for the crosslinked copolymer when compared to those of uncrosslinked ones. However the

extent of decrease in these two properties was not as high as we observed in the *hydrophilic*-BPSH100-BPS0(10:10) multiblock. This may be due to the fact that the effect of crosslinking is more prominent in the higher IEC materials (in this case, *hydrophilic*-BPSH100-BPS0) and this is consistent with the findings from our earlier study on crosslinked random BPSH copolymers.[15]

However a significant influence of the microstructure or the sequence distribution of the oligomers on water uptake and swelling was observed. The *hydrophobic*-BPSH100-BPS0(10:10) had an excess of 20 mol % of the hydrophobic unit, resulting in a preferential endcapping of the multiblock by the hydrophobic unit in contrast to the control BPSH100-BPS0(10:10), which represented a statistical distribution of the two blocks. The titrated IECs were found similar for these two multiblock copolymers. However, a significant decrease in both water uptake and swelling was observed for the *hydrophobic*-BPSH100-BPS0(10:10) multiblock. This indicates that this preferential endcapping by hydrophobic unit may have changed the co-continuous hydrophilic domain morphology into a discontinuous one which can have unfavorable effect on proton conductivity. This is evident from the AFM image (5.11b) which clearly shows a co-continuous hydrophobic morphology and supported by the significant decrease in the proton conductivity of the *hydrophobic*-BPSH100-BPS0(10:10) multiblock in contrast to the control BPSH100-BPS0(10:10) multiblock.

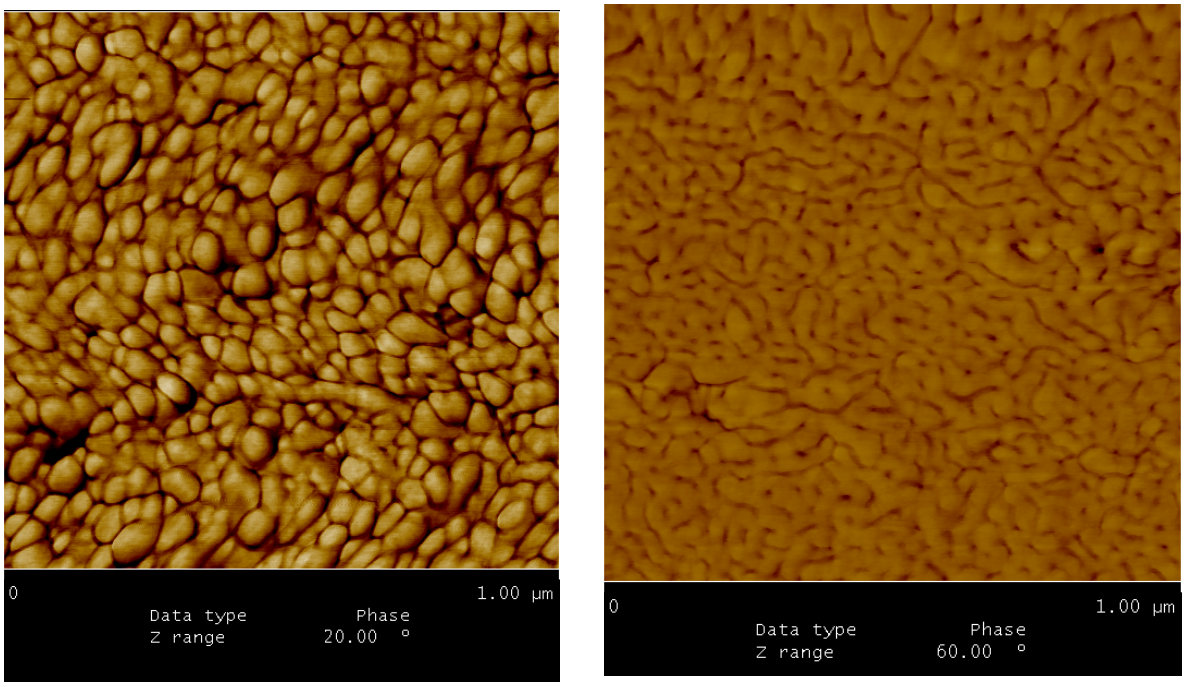

Figure 5.11 a) AFM image of a *Hydrophilic*–BPSH100-BPS0(10:10) multiblock shows co-continuous hydrophilic morphology, b) AFM image of a *Hydrophobic*–BPSH100-BPS0(10:10) multiblock shows co-continuous hydrophobic morphology

5.4. Conclusions

The objective of this study was to lightly crosslink ion-containing hydrocarbon based hydrophilic-hydrophobic multiblock copolymers so that their water uptake and swelling could be reduced modestly without significantly compromising the proton conductivity. In addition to the crosslinking study, the effect of sequence distributions of the hydrophilic and hydrophobic blocks in the multiblock copolymers was also investigated. Two series of multiblock copolymers with either endcapped by a hydrophilic oligomer or by a hydrophobic oligomer were synthesized. Proton NMR spectra of these multiblock copolymers confirmed that they were endcapped by

phenoxide-terminated hydrophilic or hydrophobic blocks. The multiblock copolymers were crosslinked by the reaction of their phenoxide endgroups with a multifunctional epoxy resin. The extent of crosslinking in these multiblocks was found to be a function of the concentration of their phenoxide endgroups. In general, higher value of gel fraction was linked with lower block length materials. All of the crosslinked membranes showed lower water uptake and swelling compared to their uncrosslinked analogues, and the effect of crosslinking on these two properties was more prominent in higher IEC materials. There was no significant change in proton conductivities of the membranes after crosslinking. This is highly encouraging as a similar proton conductivity (to that of uncrosslinked counterparts), but at a lower water uptake and swelling can significantly improve the selectivity of the crosslinked multiblock PEMs.

This study also highlighted the influence of sequence distribution of the individual blocks in a multiblock copolymer. It was observed that the increasing hydrophilic volume fraction in a hydrophilic oligomer endcapped multiblock copolymer resulted in a co-continuous hydrophilic morphology even at a lower block length (5-5) supported by its higher water uptake and swelling relative to the control multiblock copolymer. Similarly the hydrophobic oligomer endcapped multiblock copolymer showed reduced water uptake, swelling and a significantly lower proton conductivity than the control due to its unfavorable morphological transition from a co-continuous hydrophilic to a discontinuous one as a result of higher fraction of hydrophobic unit. In conclusion, the effects of crosslinking on the PEM properties of these multiblocks are very promising, suggesting their potential in increasing the selectivity of the multiblock PEMs.

Acknowledgements- The authors would like to acknowledge funding agencies (Nissan, NSF-PFI) for their support.

5.5. References

1. Zalbowitz, M.; S, T., Green Power. *Fuel Cells* **1999**.
2. Carrette, L.; Friedrich, K. A.; Stimming, U., Fuel cells: Principles, types, fuels, and applications. *Chemphyschem* **2000,** 1, (4), 162-193.
3. Acres, G. J. K., Recent advances in fuel cell technology and its applications. *Journal of Power Sources* **2001,** 100, (1-2), 60-66.
4. Hickner, M. A.; Ghassemi, H.; Kim, Y. S.; Einsla, B. R.; McGrath, J. E., Alternative polymer systems for proton exchange membranes (PEMs). *Chemical Reviews* **2004,** 104, (10), 4587-4611.
5. Mauritz, K. A.; Moore, R. B., State of understanding of Nafion. *Chemical Reviews (Washington, DC, United States)* **2004,** 104, (10), 4535-4585.
6. Roziere, J.; Jones, D. J., Non-fluorinated polymer materials for proton exchange membrane fuel cells. *Annual Review of Materials Research* **2003,** 33, 503-555.
7. Wang, F.; Hickner, M.; Kim, Y. S.; Zawodzinski, T. A.; McGrath, J. E., Direct polymerization of sulfonated poly(arylene ether sulfone) random (statistical) copolymers: candidates for new proton exchange membranes. *Journal of Membrane Science* **2002,** 197, (1-2), 231-242.
8. Li, Y.; Wang, F.; Yang, J.; Liu, D.; Roy, A.; Case, S.; Lesko, J.; McGrath, J. E., Synthesis and characterization of controlled molecular weight disulfonated poly(arylene ether sulfone) copolymers and their applications to proton exchange membranes. *Polymer* **2006,** 47, (11), 4210-4217.
9. Lee, H.-S.; Roy, A.; Lane, O.; Dunn, S.; McGrath, J. E., Hydrophilic-hydrophobic multiblock copolymers based on poly(arylene ether sulfone) via low-temperature coupling reactions for proton exchange membrane fuel cells. *Polymer* **2008,** 49, (3), 715-723.
10. Roy, A.; Hickner, M. A.; Lee, H.-S.; Badami, A.; Yu, X.; Li, Y.; Glass, T.; McGrath, J. E., Transport properties of proton exchange membranes. *ECS Transactions* **2007,** 2, (24, Direct Methanol Fuel Cells), 45-54.

11. Li, Y.; Roy, A.; Badami, A. S.; Hill, M.; Yang, J.; Dunn, S.; McGrath, J. E., Synthesis and characterization of partially fluorinated hydrophobic-hydrophilic multiblock copolymers containing sulfonate groups for proton exchange membrane. *Journal of Power Sources* **2007,** 172, (1), 30-38.

12. Lee, H.-S.; Badami, A. S.; Roy, A.; McGrath, J. E., Segmented sulfonated poly(arylene ether sulfone)-b-polyimide copolymers for proton exchange membrane fuel cells. I. Copolymer synthesis and fundamental properties. *Journal of Polymer Science, Part A: Polymer Chemistry* **2007,** 45, (21), 4879-4890.

13. Yu, X.; Roy, A.; Dunn, S.; Yang, J.; McGrath, J. E., Synthesis and characterization of sulfonated-fluorinated, hydrophilic-hydrophobic multiblock copolymers for proton exchange membranes. *Macromolecular Symposia* **2006,** 245/246, (World Polymer Congress--MACRO 2006), 439-449.

14. Roy, A.; Hickner, M. A.; Yu, X.; Li, Y.; Glass, T. E.; McGrath, J. E., Influence of chemical composition and sequence length on the transport properties of proton exchange membranes. *Journal of Polymer Science, Part B: Polymer Physics* **2006,** 44, (16), 2226-2239.

15. Paul, M.; Roy, A.; McGrath, J. E.; Riffle, J. S., Effect of Crosslinking on PEM Properties of Random Poly(Arylene Ether Sulfone)s with Varying Degree of Disulfonations on PEM Properties. *To be Submitted* **2008**.

16. Sankir, M.; Bhanu, V. A.; Harrison, W. L.; Ghassemi, H.; Wiles, K. B.; Glass, T. E.; Brink, A. E.; Brink, M. H.; McGrath, J. E., Synthesis and characterization of 3,3'-disulfonated-4,4'-dichlorodiphenyl sulfone (SDCDPS) monomer for proton exchange membranes (PEM) in fuel cell applications. *Journal of Applied Polymer Science* **2006,** 100, (6), 4595-4602.

17. Mecham, S. J. Gas permeability of polyimide/polysiloxane block copolymers. M.S. Thesis, Virginia Polytechnic Institute and State University, Blacksburg, VA, 1994.

18. Zawodzinski, T. A.; Neeman, M.; Sillerud, L. O.; Gottesfeld, S., *J. Phys. Chem.* **1991,** 95, 6040.

19. Springer, T. E.; Zawodzinski, T. A.; Wilson, M. S.; Gottesfeld, S., *J. Electrochem. Soc.* **1996,** 143, 587.

20. Paul, Mou; Roy, Abhishek; Riffle, Judy S.; McGrath, James E. Crosslinked sulfonated poly(arylene ether sulfone) membranes as candidate for PEMS. ECS Transactions (**2008**), 6 (26, Membranes for Electrochemical Applications), 9-16.

21. Lee, H.-S.; Roy, A.; Badami, A. S.; McGrath, J. E., Synthesis and characterization of sulfonated poly(arylene ether) polyimide multiblock copolymers for proton exchange membranes. *Macromolecular Research* **2007,** 15, (2), 160-166.

6. CHAPTER-6-Synthesis and Crosslinking of Partially Disulfonated Poly(Arylene Ether Sulfone)s with 4-Nitrophthalonitrile as the Crosslinker for Application as PEMs

Mou Paul and J.S. Riffle

Macromolecular Science and Engineering Program,
Macromolecules and Interfaces Institute (MII),
Virginia Polytechnic Institute and State University,
Blacksburg, VA 24061

Abstract

A series of controlled molecular weight, partially disulfonated poly(arylene ether sulfone)s with phenoxide endgroups was synthesized. The terminal phenoxide groups were reacted with 4-nitrophthalonitrile so that the copolymers were endcapped with crosslinkable phthalonitrile moieties. The phthalonitrile groups crosslinked at elevated temperatures. Since these materials crosslinked only at their reactive ends, the molecular weights of the precursor polymers dictated the crosslink densities. The curing of blends of relatively high and low molecular weight oligomers were also investigated. The cured membranes showed reduced water uptake compared to their uncrosslinked analogues. However, proton conductivities of the cured membranes did not change significantly, and this was promising for applications of these membranes as PEMs.

6.1. Introduction

Fuel cells are efficient, environmental friendly energy sources that convert chemical energy to electrical energy.[1] They have diverse fields of application ranging from stationary to portable power systems.[2] A major class of fuel cells is the proton exchange membrane type fuel cell (PEMFC). A key component of PEMFCs is the proton-conducting or proton exchange membrane (PEM). The principal requisites of a PEM are high proton conductivity, low water uptake, stability at a high operating temperature and dimensional stability under hydrated conditions.

Our research group has been engaged for the past few years in syntheses of biphenol-based partially disulfonated poly(arylene ether sulfone) random copolymers as potential PEMs. The nomenclature for this series of polymers has been established as BPSH-XX,[3] where BP stands for biphenol, S is for sulfonated, and H denotes the proton form of the acid where XX represents the degree of disulfonation. These sulfonic acid containing ionomers tend to phase separate to form nano-scale hydrophilic and hydrophobic domain morphologies. Hence, by increasing the degree of disulfonation, one can increase the extent of nanophase separation, and this may result in improved proton conductivity under partially hydrated conditions. It has been reported that proton conductivity increases with increasing degree of disulfonation in this series of sulfonic acid containing ionomers.[4] However, higher degrees of disulfonation are accompanied by extensive water uptake at higher relative humidities. For this BPSH copolymer series, water uptake increases at a degree of disulfonation of about 45%.[4-6] That degree of disulfonation has been correlated to the onset of continuity of the hydrophilic phase or the percolation threshold and the exact composition where this occurs varies depending on the polymer chemical features. Very high water uptake results in poor dimensional stability and a significant depression in glass transition temperature,[7] making the high IEC copolymers unsuitable for PEM applications. If the water uptake of these high IEC materials can be reduced while maintaining their proton conductivity, they may have potential for PEM applications. To achieve this goal, we have investigated chemically

crosslinking the copolymers via their endgroups. Kerres *et al*. have shown that crosslinking can reduce the swelling ratio of a polymer significantly.[8] We have also studied various crosslinking reagents for BPSH including glycidyl methacrylate (chapter 2) and epoxy (chapter 3 & 4) crosslinkers. BPSH copolymers cured by glycidyl methacrylate (GMA) showed improved selectivity (lower water uptake with high conductivity) as PEMs. However, the stability of the ester linkage in the GMA unit in the acidic fuel cell environment was questionable. Hence we utilized the GMA results as a proof-of-concept that BPSH copolymers could be crosslinked via endcapping them by a suitable crosslinker. More stable epoxy reagents such as the tetrafunctional epoxide derived from reaction of methylene dianiline with epichlorohydrin were also investigated. That epoxy system demonstrated the most promising results, shifting the percolation threshold to a higher IEC value after crosslinking, while maintaining satisfactory proton conductivity.

This chapter will describe crosslinking processes utilizing 4-nitrophthalonitrile curing reagents that have higher thermal stability than the epoxies. Phthalonitrile curing agents are of current research interest as they can form heterocyclic network structures with high thermal and thermo-oxidative stability when cured thermally.[9, 10] Previous research in our group by Sumner et al.[11, 12] and Baranauskas et al.[13] support this fact. Thus we have synthesized phenoxide-endcapped BPS copolymers with controlled molecular weights. The terminal phenoxide groups react with 4-nitrophthalonitrile via nucleophilic aromatic substitution to produce phthalonitrile-endcapped BPS copolymers. These copolymers were then cured thermally at elevated temperatures. The crosslink density was controlled by varying the molecular weights of the precursor disulfonated copolymers. The curing reaction was monitored by DSC and FTIR and the networks were characterized in terms of water uptake and conductivity.

6.2. Experimental

6.2.1. Materials

Monomer grade 4,4′–dichlorodiphenylsulfone (DCDPS) and 4,4′-biphenol (BP) were obtained from Solvay Advanced Polymers and Eastman Chemical Company, respectively, and dried under vacuum at 60 °C for one day prior to use. The sulfonated comonomer, 3,3′-disulfonate-4,4′-dichlorodiphenylsulfone (SDCDPS), was prepared following a previously published procedure,[3, 14] and dried under vacuum at 160 °C for two days before use. Potassium carbonate (Aldrich) was dried under vacuum at 110 °C for one day before use. 4-Nitrophthalonitrile was obtained from Aldrich and used as received. The reaction solvent *N*, *N*-dimethylacetamide (DMAc, Aldrich) was vacuum-distilled from calcium hydride, and stored over molecular sieves under nitrogen. Toluene (anhydrous, 99.8%), isopropanol (*ReagentPlus*™, 99%), *N*-methyl-2-pyrrolidinone (NMP) (*ReagentPlus*™, 99%) were obtained from Aldrich and used as received. Sulfuric acid (*ACS Reagent*, 95-98%) was obtained from VWR International and used as received.

6.2.2. Synthesis of controlled molecular weight phenoxide-endcapped BPS copolymers

Controlled molecular weight, phenoxide-endcapped BPS copolymers were synthesized via nucleophilic aromatic substitution. The molecular weights of the copolymers were controlled by offsetting the stoichiometry of the monomers. A typical polymerization of a 5 kg mol^{-1} 50 % disulfonated BPS oligomer is provided. BP (3.102 g, 16.66 mmol), DCDPS (1.849 g, 6.44 mmol), and SDCDPS (4.824 g, 9.82 mmol) were added to a three-necked, round bottom reaction flask equipped with a mechanical stirrer, nitrogen inlet, Dean-Stark trap and a condenser. Potassium carbonate (2.649 g, 19.17 mmol) and 49 mL DMAc (to achieve 20% solids) were introduced into the flask. Toluene (24 mL, DMAc/toluene was 2/1 v/v) was added as the azeotropic reagent. The reaction mixture was refluxed at 150 °C for 4 h, then the azeotrope was removed to dehydrate the system. The reaction mixture was gradually heated to 170 °C by the controlled removal of toluene, then reacted for an additional 65-70 h. The viscous product was cooled to room temperature. The product mixture was filtered to remove

salts. The copolymer was isolated by precipitation in isopropyl alcohol, filtered, and dried for 24 h at 70 °C under ambient pressure, and then for 24 h at 110 °C under vacuum.

The nomenclature of the samples is defined as follows- BPSH-XX(yk) where XX is the degree of disulfonation, y denotes the molecular weight of the copolymer, k denotes the number average molecular weight in kg mol^{-1} and H is the acid form of the copolymer.

6.2.3. End-functionalization of BPS-XX copolymers with 4-nitrophthalonitrile

The terminal phenoxide groups of BPS-XX copolymers were reacted with 4-nitrophthalonitrile via aromatic nucleophilic substitution to produce phthalonitrile-endcapped BPS-XX copolymers. A typical endcapping reaction is provided below. BPS-50(5k) (4 g, 0.8 mmol) was dissolved in 40 mL DMAc (to achieve 10 % solids) in a 100 mL round bottom flask. Anhydrous solid potassium carbonate (0.22 g, 1.6 mmol) was added to the reaction flask. Next, 4-nitrophthalonitrile (0.55 g, 3.2 mmol) was introduced into the flask and the mixture was reacted for 24 h at 60 °C. The product solution was filtered to remove salts. The copolymer was isolated by precipitation in isopropanol. The copolymer was soxhlet extracted in chloroform for 24 h to remove any unreacted 4-nitrophthalonitrile, then dried at 110 °C for 24 h under vacuum. The nomenclature of the copolymers is designated as Phth-BPSH-XX(yk).

6.2.4. Membrane casting, curing and acidification

A 10 wt % solution of a Phth-BPS-XX copolymer was prepared in NMP and stirred until a transparent homogeneous solution was obtained. The solution was then filtered through a 0.45 μm syringe filter, and cast on a clean glass plate. The membrane was dried under an infrared lamp at gradually increasing temperatures (up to ~60 ^{o}C) for 2 days. The membrane was removed from the glass plate by submersion in water and then dried at 70 ^{o}C for ~12 h at ambient pressure.

Membranes were cured in a convection oven at ≥ 300 ^{o}C. Details of the curing procedure are discussed in the results section. The crosslinked membranes are designated as BPS-z-XX where z means that the materials have been crosslinked.

BPS-60 membranes were acidified utilizing an established procedure (designated Method 1).[4] The membranes were immersed in 1.5 M sulfuric acid for 24 h at room temperature, then for an additional 24 h in deionized water at room temperature. BPS-50 membranes were acidified[4] by immersing them in boiling 0.2 M sulfuric acid for 2 h, then in boiling deionized water for 2 h. This was designated as Method 2.

Characterization

6.2.5. Nuclear Magnetic Resonance (NMR) Spectroscopy

^{1}H NMR experiments were conducted on a Varian Unity 400 NMR spectrometer operating at 400 MHz. All spectra of the copolymers were obtained from 10% solutions (w/v) in DMSO-d_6 at room temperature. Proton NMR was used to determine the molecular weights of the copolymers and their compositions.

6.2.6. Fourier Transport Infrared (FTIR) Spectroscopy

FT-IR spectroscopy was used to verify the presence of phthalonitrile groups in the copolymer as well as to study the curing reactions. Measurements were recorded using either a Tensor 27, Bruker FT-IR spectrometer or a Nicolet Impact 400 FTIR spectrometer using thin polymer films.

6.2.7. Intrinsic viscosity

Intrinsic viscosities were determined from GPC experiments performed on a liquid chromatograph equipped with a Viscotek 270 RALLS/ viscometric dual detector. The mobile phase was NMP containing 0.05 M LiBr. The column temperature was maintained at 60 °C because of the viscous nature of NMP. Both the mobile phase and

sample solution were filtered through a 0.2 μm filter before introduction to the GPC system.

6.2.8. Water Uptake

The membranes were immersed in deionized water for at least 48 h, then they were removed from the water, blot-dried and quickly weighed. The membranes were vacuum dried at 110 °C overnight and the weights were recorded. The ratio of weight gain to the original membrane weight was reported as the water uptake (mass %)

$$WaterUptake = \frac{W_{wet} - W_{dry}}{W_{dry}} \times 100\% \qquad \textbf{Equation 6-1}$$

where W_{wet} and W_{dry} were the masses of wet and dried samples, respectively.

6.2.9. Proton conductivity

Proton conductivity at 30 °C at full hydration (in liquid water) was determined in a window cell geometry using a Solartron 1260 Impedance/Gain-Phase Analyzer over the frequency range of 10 Hz - 1 MHz. The cell geometry was chosen to ensure that the membrane resistance dominated the response of the system. The resistance of the film was taken at the frequency which produced the minimum imaginary response. The conductivity of the membrane was calculated from the measured resistance and the geometry of the cell according to Equation 6-2:

$$\sigma = \frac{l}{Z'A} \qquad \textbf{Equation 6-2}$$

where σ is the proton conductivity, l is the length between the electrodes, A is the cross sectional area available for proton transport, and Z' is the real impedance response.

6.2.10. Differential Scanning Calorimetry (DSC)

Thermal transitions of the membranes were studied via DSC using a TA Instruments DSC Q-1000 at a heating rate of 10 °C min^{-1} under nitrogen. The onset temperature of the curing exotherm was used to assess the curing temperature.

6.3. Results and Discussions

6.3.1. Synthesis of controlled molecular weight phenoxide-endcapped BPS-XX copolymers

Controlled molecular weight BPS-XX copolymers with phenoxide endgroups were synthesized from SDCDPS, DCDPS and biphenol by nucleophilic aromatic substitution (Fig. 6.1). The degree of disulfonation was controlled by varying the molar ratio of SDCDPS to DCDPS. Two series of copolymers with degrees of disulfonation of 50 and 60 % were targeted.

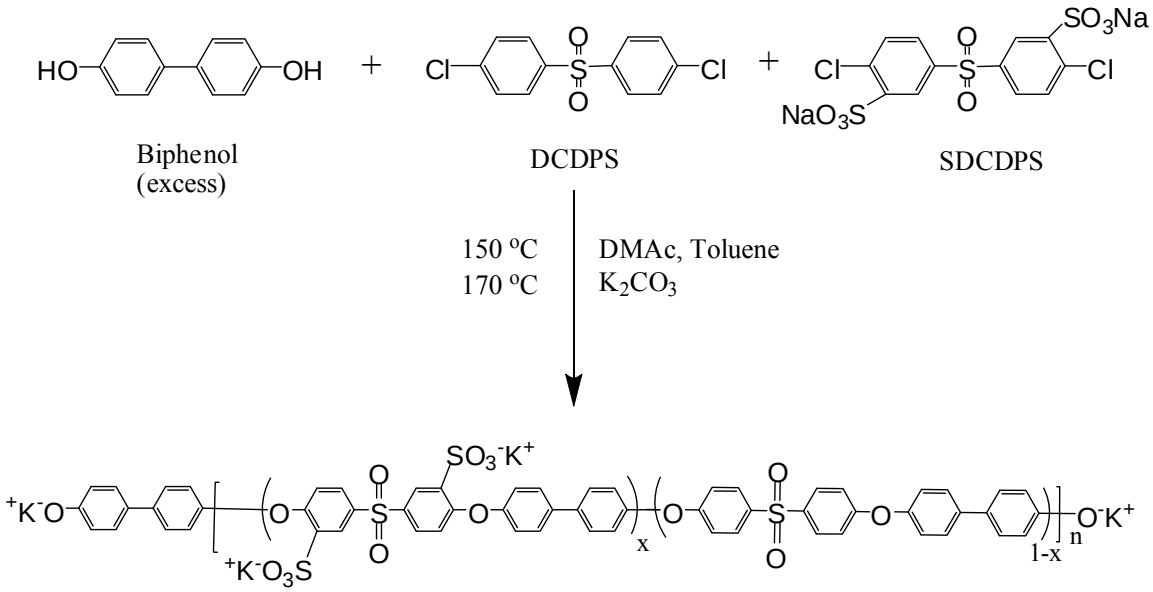

Figure 6.1 Synthesis of a controlled molecular weight phenoxide-endcapped BPS-XX copolymer

The molecular weights of the copolymers were controlled by offsetting the stoichiometry between biphenol and the dihalides. Biphenol was utilized in excess to endcap the copolymers with phenoxide groups, so that the phenoxide groups could be further reacted with 4-nitrophthalonitrile. BPS-50 copolymers with number average molecular weights (M_n) of 5 and 20 kg mol^{-1} and BPS-60 copolymers with M_ns of 5, 10, 15, and 25 kg mol^{-1} were targeted.

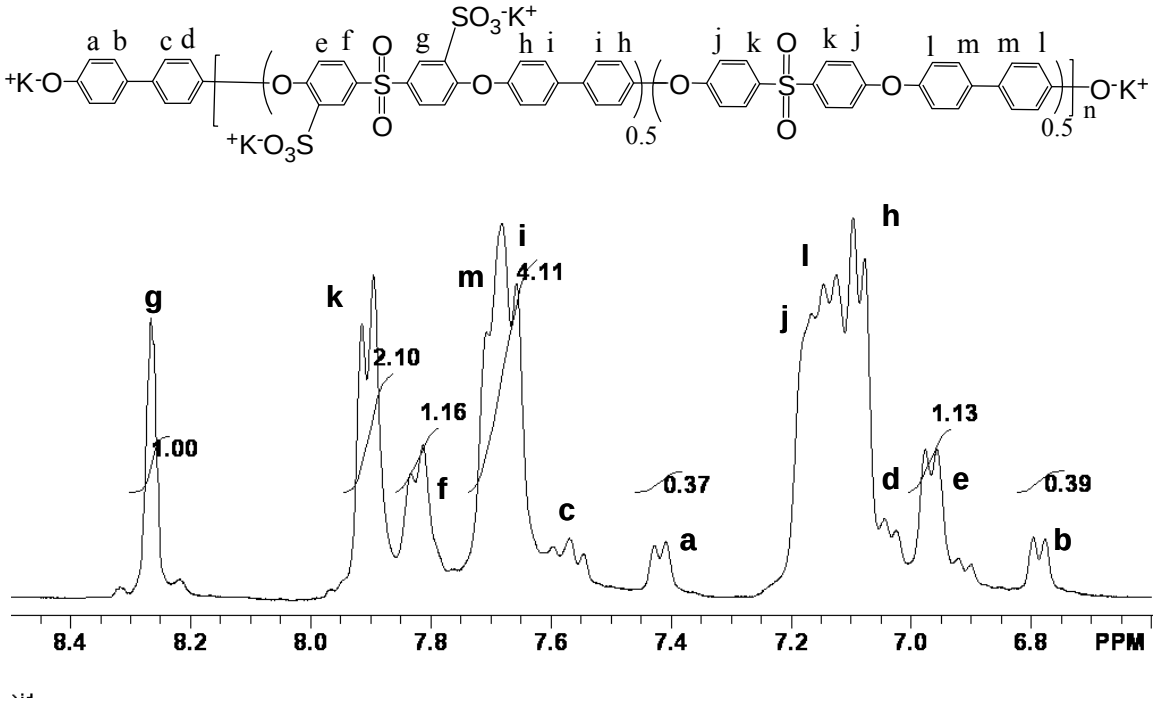

Figure 6.2 ^{1}H NMR of a phenoxide-endcapped BPS-50 random oligomer with molecular weight of~ 5 kg mol^{-1}

Figure 6.2 shows the proton NMR spectrum of a BPS-50 oligomer with a targeted molecular weight of 5 kg mol^{-1}. The aromatic protons of the biphenol unit in the endgroups at *(b), (d), (a), and (c)* were assigned to peaks at 6.8, 7.0, 7.40 and 7.55 ppm respectively. The ratio of the integrals of the aromatic protons at 6.8 ppm (*b*) to those of the aromatic protons of the biphenol moiety in the oligomer repeat units at 7.7 ppm (*m*

and i) were utilized to calculate M_ns of the oligomers. As shown in Table 6.1, the experimental M_n values derived from NMR are in good agreement with the targeted values. As expected, intrinsic viscosities ([η]) of the copolymers increased with increasing molecular weight (Table 6.1). The degree of disulfonation was confirmed from the ratio of the integrals of protons at 6.95 (*e*), 7.8 (*f*) and 8.25 ppm (*g*) in the sulfonated unit to the protons at 7.9 ppm (*k*) in the unsulfonated unit. The degrees of disulfonation were used to calculate the ion exchange capacities (IEC- meq of sulfonic acid groups per gram of dry polymer) of the copolymers. Table 6.1 shows that the experimental IEC values of the copolymers obtained from both proton NMR and titration are in good agreement with the targeted values.

Table 6.1 Summary of BPS-50 and BPS-60 copolymers

Copolymer	M_n (kg mol^{-1})		IV[a] (dL g^{-1})	IEC (meq g^{-1})		
	Target	^{1}H NMR		Target	^{1}H NMR	Titrated[b]
BPS-50	5	5.7	0.21	2.08	2.04	-
BPS-50	20	20.8	0.43	2.08	2.03	1.9
BPS-60	5	5.3	0.21	2.42	2.40	-
BPS-60	10	9.1	0.28	2.42	2.27	-
BPS-60	15	14.9	0.44	2.42	2.39	2.33
BPS-60	25	25.2	0.59	2.42	2.37	2.34

[a] Intrinsic Viscosity (IV) in NMP with 0.05 M LiBr at 60 °C, from GPC

[b]Back-titration of sulfonic acid groups by 0.01 M NaOH

6.3.2. Synthesis of 4-nitrophthalonitrile-endcapped BPS-XX copolymers (Phth-BPS-XX)

Phth-BPS-XX copolymers were synthesized via nucleophilic aromatic substitution reactions between phenoxide-endcapped BPS-XX and 4-nitrophthalonitrile under basic conditions in DMAc (Fig. 6.3). Two moles of 4-nitrophthalonitrile per phenoxide equivalent were utilized in these reactions to aid in quantitatively capping the copolymers. The endcapped copolymers were soxhlet-extracted with chloroform for 24 hours to remove the remaining unreacted 4-nitrophthalonitrile. BPS-50(5k), BPS-50(20k) and BPS-60(15k) were endcapped in this manner with phthalonitrile moieties.

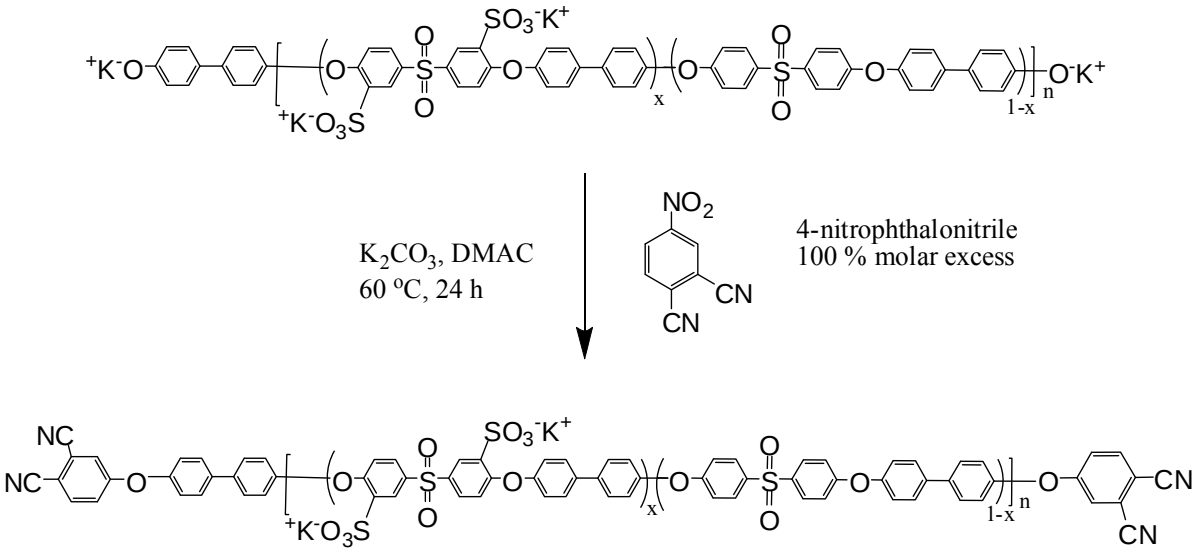

Figure 6.3 Synthesis of a 4-nitrophthalonitrile-endcapped BPS-XX copolymer

Figure 6.4 represents the proton NMR spectrum of a Phth-BPS-50(5k) oligomer. The aromatic protons of the biphenol unit in the endgroup at 6.8 (*b*), 7.0 (*d*), and 7.55 ppm (*c*) of the phenoxide-terminated BPS-50(5k) oligomer disappeared after the phenoxide groups were reacted with 4-nitrophthalonitrile and new peaks at about 7.25

and 8.05 ppm appeared. From the proton NMR study it was confirmed that all the phenoxide endgroups reacted and the oligomer was completely endcapped.

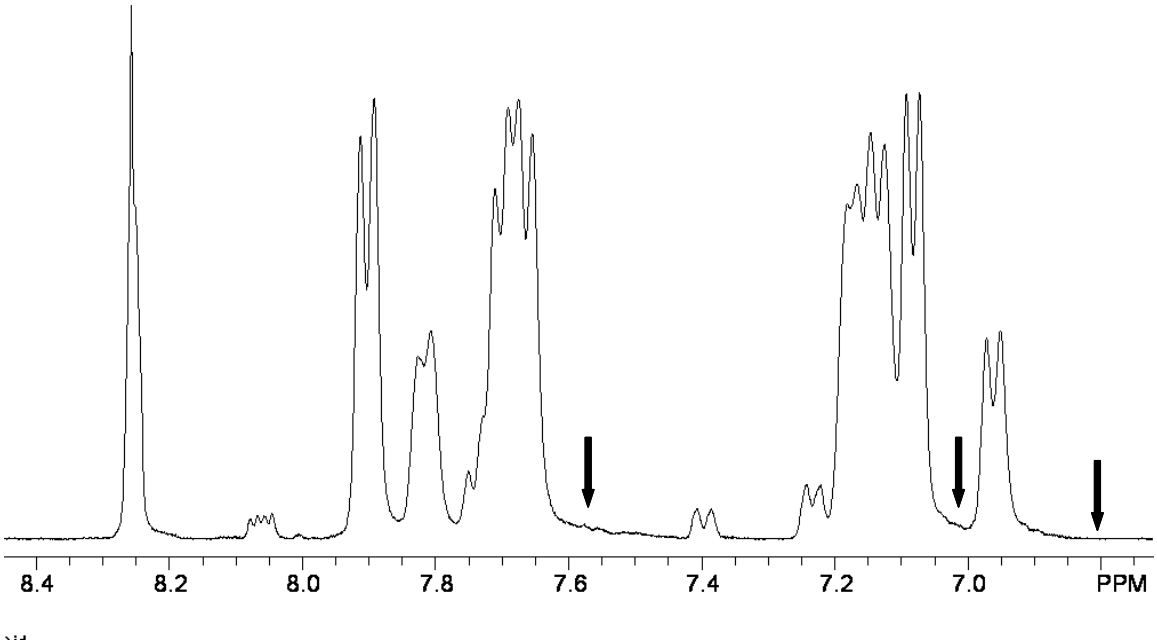

Figure 6.4 ^{1}H NMR of a 4-nitrophthalonitrile-endcapped BPS-50(5k) oligomer;the arrows indicate the disappearance of aromatic proton peaks of the biphenol unit in the end group

6.3.3. Crosslinking and characterization of Phth-BPS-XX copolymers

6.3.3.1. Differential Scanning Calorimetry

Figure 6.5 represents DSC thermograms of cure reactions utilizing a Phth-BPS-60(15k) and a Phth-BPS-50(5k). BPS-XX are wholly aromatic, ion-containing copolymers with high glass transition temperatures (~250 °C). Curing reactions generally take place at a temperature above the glass transition temperature of the copolymer. Both of the copolymers exhibited a curing exotherm at around 300 °C, which indicates that the crosslinking reaction takes place at that temperature. As expected, the area under the exothermic curing peak for the Phth-BPS-50(5k) is much higher than for

the Phth-BPS-60(15k), signifying that more phthalonitrile had reacted with the lower molecular weight material.

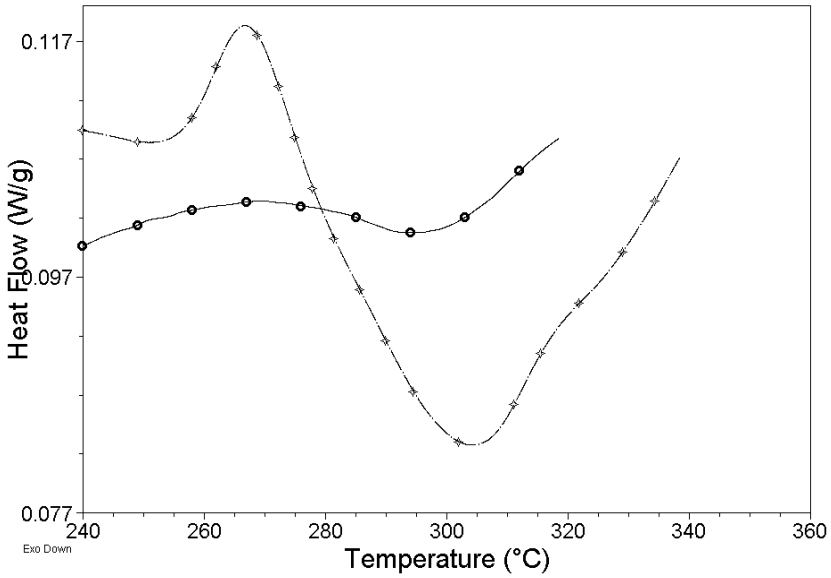

Figure 6.5 DSC curing exotherms of Phth-BPS-50(5k) & Phth-BPS-60(15k) Copolymers

6.3.3.2. Curing reaction parameters and Fourier transform infrared (FTIR) spectroscopy

In our earlier studies on crosslinking of BPS-XX with glycidyl methacrylate (chapter 2) or epoxy (chapters 3 and 4), crosslinking and membrane formation occurred at the same time. This was possible as the curing temperatures in both of those cases (~ 90 °C for the glycidyl methacrylate and 150 °C for the epoxy system) were lower than the boiling points of the casting solvents (DMAc ~175 °C and NMP ~200 °C) respectively. However, in the present case, the curing temperature was much higher (~300 °C) than the boiling points of common casting solvents. Hence membranes were first cast from solutions of copolymers and then they were cured. In order to produce good membranes, a copolymer should have a minimum molecular weight to form a good film. Therefore, we began the initial curing study with a Phth-BPS-60(15k) copolymer.

Figure 6.6a shows the FTIR spectra of a Phth-BPS60(15k) membrane before and after curing at 300 °C for 24 hours. The significant reduction in the nitrile stretch at ~2230 cm^{-1} in the crosslinked membrane confirmed that at least some crosslinking occurred. Unfortunately, the mechanical properties of the crosslinked membrane were unsatisfactory, especially after acidification. In fact, this membrane could not be acidified by Method 2,[4] which involves a hydrothermal treatment. The membrane lost its dimensional stability after acidification by Method 2. However, the crosslinked membrane could be acidified by Method 1 which involves a room temperature acidification method and is less harsh than Method 2. The poor mechanical properties of the crosslinked BPS-60(15k) membrane could be a result of several phenomena. For a copolymer endcapped with crosslinkable moieties, the number of crosslinkable sites is inversely related to the number average molecular weight. This suggests that the BPS-60 copolymer with 15 kg mol^{-1} may not have a sufficient number of crosslinkable groups to achieve a tough membrane. This is consistent with our earlier findings with epoxy systems.[15] Another reason could be that the long curing time at a high curing temperature may have degraded the membrane properties.

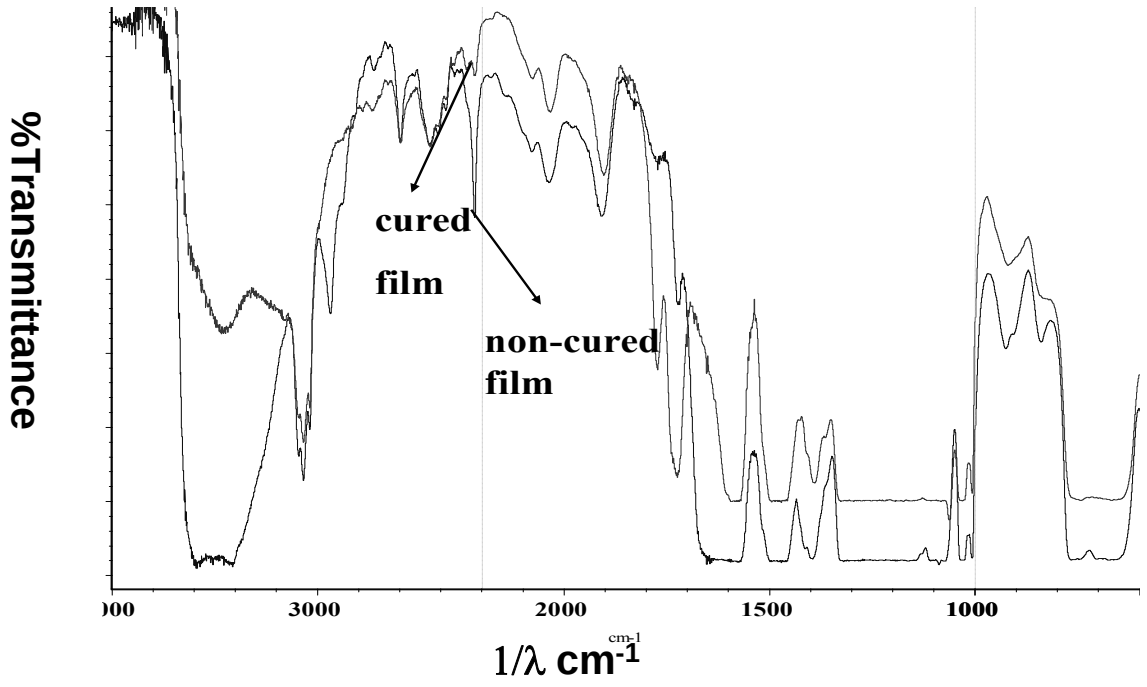

Figure 6.6a FTIR spectra of cured and uncured Phth-BPS-60(15k) membranes

Hence in order to achieve both sufficient crosslink density and film-forming properties, a non-film forming material was blended with a film-forming material. A Phth-BPS-50(5k) copolymer was blended with a Phth-BPS-50(20k) copolymer in a 25:75 wt % ratio. The curing temperature and time were also modified. The blend membrane was cured at 300 °C for only one hour, then post cured at 333 °C for one and a half hours, then at 350 °C for one half hours. Figure 6.6b shows the FTIR spectra of a BPS-50 blend membrane before and after curing. The reduction in the nitrile peak intensity at ~2230 cm^{-1} indicated that crosslinking had occurred. The crosslinked blend membrane showed satisfactory mechanical properties, even after acidification in refluxing sulfuric acid. We intend to implement the blend strategy for the BPS-60 copolymers also.

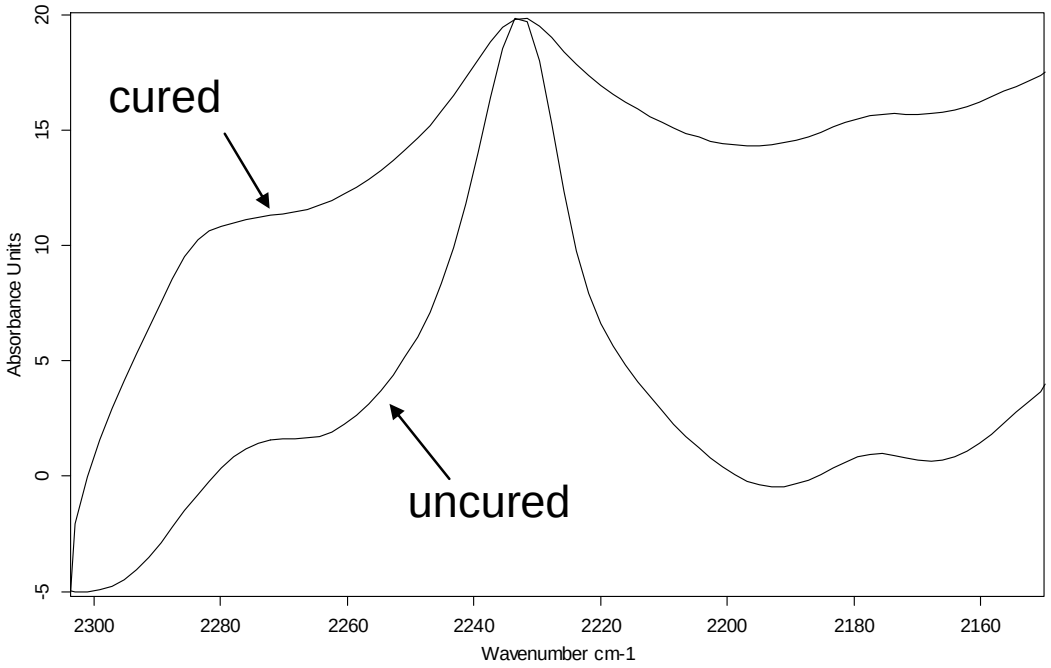

Figure 6.6b FTIR spectra of cured and uncured Phth-BPS-50 blend membranes

6.3.3.3. Water uptake and proton conductivity

Table 6.2 shows the water uptake and proton conductivity values for the cured and uncured BPSH-60 and BPSH-50 membranes. Irrespective of the degree of disulfonation and method of acidification, both of the membranes showed a reduction in water uptake after crosslinking, and the proton conductivities of the membranes did not change significantly. This is also consistent with our earlier studies on epoxy systems.[15] In fact the crosslinked Phth-BPSH-50 membrane showed similar water uptake and proton conductivity as the epoxy-BPSH-50 membrane that had been cured for 90 minutes. Membranes from BPS-50 copolymers were acidified by Method 1 and those from BPS-60 were done by Method 2.

Table 6.2 Properties of uncrosslinked and crosslinked membranes

Sample	Water uptake (mass %)	Proton conductivity[a] ($S\ cm^{-1}$)
BPSH-50	232	0.08
BPSH-z-50	70	0.09
BPSH-60	91	0.13
BPSH-z-60	56	0.11

[a] @30 °C in liquid water, ± 10 %

6.4. Conclusions

A series of controlled molecular weight phenoxide-endcapped BPS-50 and BPS-60 copolymers were synthesized and characterized by proton NMR. The copolymers were chemically modified with 4-nitrophthalonitrile to produce phthalonitrile-endcapped BPS-XX copolymers and then cured at elevated temperatures (> 300°C). The curing reaction was monitored by FTIR. The membrane properties were improved by preparing blend membranes with a low and high molecular weight copolymer to achieve both sufficient crosslink density and film-forming properties. Cured samples showed lower water uptake relative to their uncrosslinked counterparts, and had satisfactory proton conductivities.

Acknowledgements – The author would like to acknowledge Abhishek Roy for his contribution in proton conductivity measurements.

6.5. References

1. Winter, M.; Brodd, R. J., What are batteries, fuel cells, and supercapacitors? (vol 104, pg 4245, 2003). *Chemical Reviews* **2005,** 105, (3), 1021-1021.
2. Mauritz, K. A.; Moore, R. B., State of understanding of Nafion. *Chemical Reviews* **2004,** 104, (10), 4535-4585.
3. Wang, F.; Hickner, M.; Kim, Y. S.; Zawodzinski, T. A.; McGrath, J. E., Direct polymerization of sulfonated poly(arylene ether sulfone) random (statistical) copolymers: candidates for new proton exchange membranes. *Journal of Membrane Science* **2002,** 197, (1-2), 231-242.
4. Kim, Y. S.; Wang, F.; Hickner, M.; McCartney, S.; Hong, Y. T.; Harrison, W.; Zawodzinski, T. A.; McGrath, J. E., Effect of acidification treatment and morphological stability of sulfonated poly(arylene ether sulfone) copolymer proton-exchange membranes for fuel-cell use above 100 degrees C. *Journal of Polymer Science Part B-Polymer Physics* **2003,** 41, (22), 2816-2828.
5. Kim, Y. S.; Dong, L. M.; Hickner, M. A.; Pivovar, B. S.; McGrath, J. E., Processing induced morphological development in hydrated sulfonated poly(arylene ether sulfone) copolymer membranes. *Polymer* **2003,** 44, (19), 5729-5736.
6. Harrison, W. L.; Wang, F.; Mecham, J. B.; Bhanu, V. A.; Hill, M.; Kim, Y. S.; McGrath, J. E., Influence of the bisphenol structure on the direct synthesis of sulfonated poly(arylene ether) copolymers. I. *Journal of Polymer Science Part a-Polymer Chemistry* **2003,** 41, (14), 2264-2276.
7. Kim, Y. S.; Dong, L. M.; Hickner, M. A.; Glass, T. E.; Webb, V.; McGrath, J. E., State of water in disulfonated poly(arylene ether sulfone) copolymers and a perfluorosulfonic acid copolymer (nafion) and its effect on physical and electrochemical properties. *Macromolecules* **2003,** 36, (17), 6281-6285.
8. Kerres, J. A., Development of ionomer membranes for fuel cells. *Journal of Membrane Science* **2001,** 185, (1), 3-27.

9. Sastri, S. B.; Armistead, J. P.; Keller, T. M.; Sorathia, U., Phthalonitrile-glass fabric composites. *Polymer Composites* **1997,** 18, (1), 48-54.
10. Sastri, S. B.; Keller, T. M., Phthalonitrile cure reaction with aromatic diamines. *Journal of Polymer Science Part a-Polymer Chemistry* **1998,** 36, (11), 1885-1890.
11. Sumner, M. J.; Sankarapandian, M.; McGrath, J. E.; Riffle, J. S.; Sorathia, U., Flame retardant novolac-bisphthalonitrile structural thermosets. *Polymer* **2002,** 43, (19), 5069-5076.
12. Sumner, M. J.; Weyers, R. Y.; Rosario, A. C.; Riffle, J. S.; Sorathia, U., Synthesis and characterization of vinyl ester networks containing phthalonitrile moieties. *Polymer* **2004,** 45, (15), 5199-5206.
13. Baranauskas, V. V.; Zalich, M. A.; Saunders, M.; St Pierre, T. G.; Riffle, J. S., Poly(styrene-b-4-vinylphenoxyphthalonitrile) - Cobalt complexes and their conversion to oxidatively stable cobalt nanoparticles. *Chemistry of Materials* **2005,** 17, (21), 5246-5254.
14. Sankir, M.; Bhanu, V. A.; Harrison, W. L.; Ghassemi, H.; Wiles, K. B.; Glass, T. E.; Brink, A. E.; Brink, M. H.; McGrath, J. E., Synthesis and characterization of 3,3'-disulfonated-4,4'-dichlorodiphenyl sulfone (SDCDPS) monomer for proton exchange membranes (PEM) in fuel cell applications. *Journal of Applied Polymer Science* **2006,** 100, (6), 4595-4602.
15. Paul, M.; Park, H. B.; Freeman, B. D.; Roy, A.; McGrath, J. E.; Riffle, J. S., Synthesis and crosslinking of partially disulfonated poly(arylene ether sulfone) random copolymers as candidates for chlorine resistant reverse osmosis membranes Polymer **2008**, 49 (9), 2243-52.

7. CHAPTER-7-Synthesis and Crosslinking of Phenylethynyl-Terminated Partially Disulfonated Poly(Arylene Ether Sulfone) Random Copolymers for Application as Proton Exchange or Reverse Osmosis Membranes

Mou Paul[a], Abhishek Roy[a], Wei Xie[b], Benny D. Freeman[b], James E. McGrath[a] & Judy S. Riffle[a]

[a]Macromolecules and Interfaces Institute
Virginia Polytechnic Institute and State University, Blacksburg, VA 24061
[b]Department of Chemical Engineering, Center for Energy and Environmental Resources, University of Texas at Austin, Austin, TX 78758

Abstract

High temperature curing reactions of disulfonated poly(arylene ether sulfone) random copolymers bearing terminal phenylethynyl groups were utilized to produce crosslinked proton exchange membranes with reduced water swelling. Controlled molecular weight, partially disulfonated poly(arylene ether sulfone) random copolymers with phenoxide endgroups were systematically synthesized. The terminal phenoxide groups were endcapped at 160 °C with 4 fluoro-4'-phenylethynyl benzophenone (FPEB) to afford oligomers endcapped with thermally crosslinkable phenylethynyl moieties. Bimodal curing of blends of relatively high and low molecular weight oligomers was investigated and afforded transparent ductile film membranes. The membranes were cured in salt form at 360 °C at various curing times. Networks had very high gel fractions and showed significant reduction in water uptake and swelling compared to their linear analogues. However, proton conductivities of the cured membranes did not change significantly, and the systems are promising for applications of these membranes

as PEMs. They are also candidates for reverse osmosis water purification membranes with improved salt rejection.

7.1. Introduction

Ion-exchange membranes have major applications in electro-membrane processes like fuel cells, electrodialysis, electrolysis and also in various separation processes like reverse osmosis (RO) or pervaporation.[1] The ion-exchange groups of these membranes are capable of rejecting charged solutes or charged molecules and thus can be utilized for desalination or water purification. In the proton form they also can transport charged ions so they have potential for applications as membranes in fuel cells or electrolysis processes.

Over the last decade, our research group has been actively involved in the syntheses of poly(arylene ether sulfone) random and block copolymer based ionomer membranes. These disulfonated, biphenol-based random copolymers have been given the acronym BPSH-XX,[2] where BP stands for biphenol, S is for sulfonated, H denotes the proton form of the acid and XX represents the degree of disulfonation. The salt form of the copolymers is denoted as BPS-XX. The ion concentration in these copolymers can be easily and reproducibly controlled as they are synthesized via direct copolymerization of activated disulfonated comonomers. BPSH based copolymers have shown promise as alternative proton exchange membranes (PEM) for application in fuel cells.[3] They have several advantages over the state-of-the-art membrane Nafion, for example higher open circuit voltage (OCV) stability, lower fuel and oxidant permeability, higher operating temperatures, etc. Recently, it has been demonstrated that these disulfonated membranes in their salt forms also have high potential for application as chlorine-resistant desalination membranes.[4-7] The membranes exhibited excellent chlorine tolerance over a wide pH range (e.g., 4-10) relative to conventional polyamide-based desalinization membranes.[8] BPSH random and particularly block copolymers are nanophase separated into hydrophilic-hydrophobic domains. This morphology strongly depends on the sequence and ion concentration or degree of disulfonation of the copolymer.[9]

Theoretically, flux (for RO application) of these charged membranes should increase with increasing ion concentration. However, at high disulfonation levels, the membranes swell strongly in water and this leads to reduced salt rejection. Similarly, proton conductivities (for PEM application) of these membranes in their acid forms increase with increasing ion concentration. However, the acidified copolymers have significantly higher water absorption, particularly at degrees of disulfonation higher than 45%.[9-11] This high water uptake results in poor dimensional stability, lower proton concentration and a significant depression in glass transition temperature,[12] which are undesirable for PEM applications. It is evident that the membrane properties of high ion exchange capacity (IEC) copolymers for applications in either RO or PEM fuel cells could be improved by reducing their water swelling.

One of the prospective options to reduce water swelling of hydrophilic copolymers is to crosslink them. Our hypothesis is that crosslinked high IEC BPS copolymers with reduced water swelling will have enhanced salt rejection while maintaining high water permeability (RO), as well as good selectivity between water uptake and proton conductivity (PEM). We have investigated several crosslinking reagents for BPSH copolymers such as glycidyl methacrylate[13] and multifunctional epoxies.[14] Though BPSH copolymers cured with tetrafunctional methacrylate endgroups showed improved selectivity for PEMs (high proton conductivity at lower water uptake), the uncertainty regarding the stability of the ester group in the methacylate unit under either acidic fuel cell or reverse osmosis environments directed us to progress towards a more hydrolytically and thermally stable multifunctional epoxy crosslinked system. BPSH copolymers crosslinked with epoxy showed significant reduction in water swelling while still maintaining satisfactory proton conductivities.[15] Moreover, the epoxy crosslinked BPS copolymers also had significantly enhanced salt rejection with high water permeability when tested in for RO applications.[16]

These results have motivated us to further improve the crosslinking system even more in terms of thermal and hydrolytic stability. To achieve these goals, we have investigated the formation of a phenylethynyl-functional system and its subsequent

crosslinking. Phenylethynyl crosslinked systems are of enormous interest due to their wholly aromatic, highly stable chemical structure combined with a cure rection that does not produce any volatiles. Moreover, due to a high crosslinking temperature (> 350 °C), these functionalized polymers have a broad processing window between the glass transition temperature and curing temperature. This could be quite important in this case since the BPSH materials are wholly aromatic ion-containing copolymers with high glass transition temperatures (T_g > 250 °C). The phenylethynyl moiety has been used previously as a crosslinking site at the termini of several polymer systems[17-21] including poly(arylene ether)s.[22-24] Earlier research from our group utilized 3-phenylethynylphenol as a crosslinkable endcapping reagent for a series of high T_g poly(arylene ether sulfone) resins,[25] and these produced tough, solvent resistant thermoset networks. Poly(arylene ether sulfone)s terminated with a series of phenylethynyl moieties which differed in their electron-withdrawing abilities through substituent effects were also investigated. It was established that the rate of curing, T_g and the elastic moduli above the T_g of the cured networks increased with increasing electron withdrawing ability of the substituent in the endcapper.[26,27]

In the present study, we have extended the polymer matrices to include ion-containing poly(arylene ether sulfone)s. BPS copolymers with 50 % degree of disulfonation having phenylethynyl endgroups adjacent to an electron-withdrawing ketone substituent have been explored. A series of phenoxide-endcapped BPS-50 copolymers was synthesized and reacted with the phenylethynyl component at 160 °C. The ethynyl-terminated membranes were then crosslinked at elevated temperatures above the T_g, in the thermally stable salt form. The effects of crosslinking on various PEM and RO properties were investigated.

7.2. Experimental

7.2.1. Materials

Monomer grade 4,4′–dichlorodiphenylsulfone (DCDPS) and 4,4′-biphenol (BP) were obtained from Solvay Advanced Polymers and Eastman Chemical Company,

respectively, and dried under vacuum at 60 °C for one day prior to use. The sulfonated comonomer, 3,3′-disulfonate-4,4′-dichlorodiphenylsulfone (SDCDPS), was prepared following a previously published procedure,[2,28] and dried under vacuum at 160 °C for two days before use. Potassium carbonate (Aldrich) was dried under vacuum at 110 °C for one day before use. 4-Fluoro-4'-phenylethynyl benzophenone (FPEB) was obtained from Aldrich and used after drying under vacuum at 80 °C overnight. The reaction solvent *N*, *N*-dimethylacetamide (DMAc, Aldrich) was vacuum-distilled from calcium hydride, and stored over molecular sieves under nitrogen. Toluene (anhydrous, 99.8%) and isopropanol (*ReagentPlus*™, 99%), were obtained from Aldrich and used as received. Sulfuric acid (*ACS Reagent*, 95-98%) was obtained from VWR International and used as received.

7.2.2. Synthesis of controlled molecular weight, phenoxide-endcapped BPS-XX copolymers

Controlled molecular weight, phenoxide-endcapped BPS copolymers were synthesized via nucleophilic aromatic substitution step copolymerization. The number average molecular weights of the copolymers were controlled by offsetting the stoichiometry. A typical copolymerization of a 5 kg mol^{-1} 50 % disulfonated BPS oligomer is provided. BP (3.102 g, 16.66 mmol), DCDPS (1.849 g, 6.44 mmol), and SDCDPS (4.824 g, 9.82 mmol) were added to a three-necked, round bottom reaction flask equipped with a mechanical stirrer, nitrogen inlet, Dean-Stark trap and a condenser. Potassium carbonate (2.649 g, 19.17 mmol) and 49 mL DMAc (to achieve 20% solids) were introduced into the flask. Toluene (24 mL, DMAc/toluene was 2/1 v/v) was added as the azeotropic reagent. The reaction mixture was refluxed at 150 °C for 4 h, then the azeotrope was removed to dehydrate the system. The reaction mixture was gradually heated to 170 °C by the controlled removal of toluene, then reacted for an additional 65-70 h. The viscous product was cooled to room temperature, filtered to remove salts and isolated by precipitation in isopropyl alcohol. It was dried for 24 h at 70 °C under ambient pressure, and then for 24 h at 110 °C under vacuum.

The practical nomenclature of the samples is defined as follows- BPSH-XX(yk) where XX is the degree of disulfonation, y denotes the molecular weight of the copolymer, k denotes the number average molecular weight in kg mol^{-1} and H is the acid form of the copolymer.

7.2.3. End-functionalization of BPS-XX copolymers with FPEB

The terminal phenoxide groups of BPS-XX copolymers were reacted with FPEB via nucleophilic substitution to produce phenylethynyl-endcapped BPS-XX copolymers. A typical endcapping reaction is provided below. Phenoxide-endcapped BPS-50 (5000 g mol^{-1}) (4 g, 0.8 mmol) was added to a three-necked, round bottom reaction flask equipped with a mechanical stirrer, nitrogen inlet, Dean-Stark trap and a condenser. Potassium carbonate (0.22 g, 1.6 mmol) and 40 mL DMAc (to achieve 10 wt % solids) were introduced into the flask. The mixture was stirred at about 50 °C until all the reactants were completely dissolved. Cyclohexane (12 mL, DMAc/cyclohexane was ~3/1 v/v) was added as the azeotropic reagent. The reaction mixture was refluxed at 90 °C for 4 h, and then the azeotrope was removed to dehydrate the system. The reaction mixture was gradually heated to 160 °C by the controlled removal of cyclohexane. Then FPEB (1.44 g, 4.8 mmol) was added into the reaction flask and reacted for an additional 24 h. The product was cooled to room temperature and filtered to remove salts. The copolymers were isolated by precipitation in isopropyl alcohol. The copolymers were extracted in a soxhlet with chloroform for 24 h to remove any excess FPEB and dried for 24 h at 110 °C under vacuum. The descriptive nomenclature of the samples is defined as follows- FPEB-BPSH-XX(yk).

7.2.4. Membrane casting, curing and acidification

A FPEB-BPS-50(5k) copolymer was blended with a FPEB-BPS-50(20k) copolymer in a 20:80 wt % ratio to produce a 10 wt % solution in DMAc and stirred until a transparent homogeneous solution was obtained. The solution was then filtered through a 0.45 μm syringe filter and cast on a clean glass plate. The membrane was dried under an infrared lamp at gradually increasing temperatures. The membrane was removed from

the glass plate by submersion in water. The membrane was cured at 360 °C for a designated time (45 or 90 min) under nitrogen atmosphere.

The crosslinked membranes were acidified[9] by immersing them in boiling 0.2 M sulfuric acid for 2 h, then in boiling deionized water for 2 h.

Characterization

7.2.5. Nuclear Magnetic Resonance (NMR) Spectroscopy

^{1}H NMR and ^{19}F experiments were conducted on a Varian Unity 400 NMR spectrometer operating at 400 MHz. All spectra of the copolymers were obtained from 10% solutions (w/v) in DMSO-d_6 at room temperature. Proton NMR was used to determine the molecular weights of the copolymers and their compositions and ^{19}F NMR was used to monitor the completion of the endcapping reaction.

7.2.6. Fourier Transport Infrared (FTIR) Spectroscopy

FT-IR spectroscopy was used to verify the presence of ethynyl groups in the copolymer as well as to study the curing reactions. Measurements were recorded using a Tensor 27, Bruker FT-IR spectrometer using thin polymer films.

7.2.7. Intrinsic viscosity

Intrinsic viscosities were determined from GPC experiments performed on a liquid chromatograph equipped with a Viscotek 270 RALLS/ viscometric dual detector. The mobile phase was NMP containing 0.05 M LiBr. The column temperature was maintained at 60 °C to minimize the viscous nature of NMP. Both the mobile phase and sample solution were filtered through a 0.2 μm filter before introduction to the GPC system.

7.2.8. Thermogravimetric analysis (TGA)

Thermo-oxidative behavior of the FPEB-endcapped BPS membranes was measured on a TA Instruments TGA Q500. The typical heating rate was 10 °C min^{-1} in nitrogen.

7.2.9. Gel fractions

Gel fractions of the networks were measured by placing 0.1-0.15 g of sample in DMAc and soxhlet-extracting for 48 h. After removal of the solvent by drying at 120 °C for 24 h under vacuum, the remaining mass was weighed as gel. Gel fractions were calculated by dividing the weights of the gels by the initial weights of the networks.

7.2.10. Water Uptake

The membranes were immersed in deionized water for at least 48 h, then they were removed from the water, blot-dried and quickly weighed. The membranes were vacuum dried at 110 °C overnight and the weights were recorded. The ratio of weight gain to the original membrane weight was reported as the water uptake (mass %)

$$WaterUptake = \frac{W_{wet} - W_{dry}}{W_{dry}} \times 100\% \qquad \textbf{Equation 7-1}$$

where W_{wet} and W_{dry} were the masses of wet and dried samples, respectively.

7.2.11. Water volume swelling ratio, density and effective proton concentration (C_H^+)

The membranes were equilibrated in deionized water for at least 48 h, then they were removed from the water and blotted dry. The dimensions were measured in three directions (length, width and thickness) to calculate the wet volume. The samples were dried in a convection oven for 2 h at 80 °C. The ratio of volume gain to the original membrane volume was reported as the volume swelling ratio.

For density determination, the samples were equilibrated in water. The dried dimensions were obtained by drying the wet membrane at 80 °C in a convection oven for 2 h. Density was calculated from the volume and weight of the dried membranes. An average of 4 samples was taken for each measurement. The effective proton concentration was determined from the water uptake, density and IEC using the following expression:[29]

$$C_{H^+} = \frac{IEC \times Density}{(1 + 0.01 \times wateruptake \times Density)} \qquad \textbf{Equation 7-2}$$

7.2.12. Proton conductivity

Proton conductivity at 30 °C at full hydration (in liquid water) was determined in a window cell geometry using a Solartron 1260 Impedance/Gain-Phase Analyzer over the frequency range of 10 Hz - 1 MHz. The cell geometry was chosen to ensure that the membrane resistance dominated the response of the system. The resistance of the film was taken at the frequency which produced the minimum imaginary response. The conductivity of the membrane was calculated from the measured resistance and the geometry of the cell according to Equation 7-3:

$$\sigma = \frac{l}{Z'A} \qquad \textbf{Equation 7-3}$$

where σ is the proton conductivity, l is the length between the electrodes, A is the cross sectional area available for proton transport, and Z' is the real impedance response.

7.2.13. Water permeability and salt rejection

In all experiments related to water and salt transport properties, the water was produced by a Millipore MilliQ system (Billerica, MA). Pure water permeability was measured using a high-pressure dead-end filtration system (Sterlitech TM HP4750 stirred cell, Sterlitech Corp., WA). The membrane size was 49 mm in diameter, and the active membrane area was 14.6 cm^2. The membrane thickness was 50-100 μm. Water permeability (P_w) was calculated from the volumetric water flux, V, per unit time, t, through a membrane of area A and thickness l divided by the pressure difference, Δp:

$$P_W = \frac{V \cdot l}{A \cdot t \cdot \Delta p} \qquad \textbf{Equation 7-4}$$

In this study, NaCl was used for ion rejection studies. Salt rejection experiments were conducted in a dead-end system using feed solutions containing 2000 mg L^{-1} of NaCl (2000 ppm). The salt rejection (R) was calculated as

$$R(\%) = \left(1 - \frac{C_p}{C_f}\right) \times 100 \qquad \textbf{Equation 7-5}$$

where C_p is the salt concentration in the permeant and C_f is the salt concentration in the feed water. Both C_p and C_f were measured with an Oakton 100 conductivity meter (Cole Parmer, Vernon-Hills, NJ).

7.3 Results and Discussions

7.3.1. Synthesis of controlled molecular weight phenoxide-endcapped BPS-XX copolymers

Controlled molecular weight BPS-XX copolymers with phenoxide endgroups were synthesized from SDCDPS, DCDPS and biphenol by nucleophilic aromatic substitution (Fig. 7.1). The degree of disulfonation was controlled by varying the molar ratio of SDCDPS to DCDPS. The molecular weights of the copolymers were controlled by offsetting the stoichiometry between 4, 4'-biphenol and the activated dihalides. Biphenol was utilized in excess to endcap the copolymers with phenoxide groups, so that the phenoxide groups could be further reacted with FPEB. BPS-50 copolymers with number average molecular weights (M_n) of five and twenty kg mol^{-1} were targeted. Initial studies showed that ductile transparent film could be prepared.

Figure 7.2 shows the proton NMR spectrum of a BPS-50 oligomer with a targeted molecular weight of 5 kg mol^{-1}. The aromatic protons of the biphenol unit in the endgroups at *(b), (d), (a), and (c)* were assigned to peaks at 6.8, 7.0, 7.40 and 7.55 ppm respectively. The ratio of the integrals of the aromatic protons at 6.8 ppm (*b*) to those of the aromatic protons of the biphenol moiety in the oligomer repeat units at 7.7 ppm (*m and i*) were utilized to calculate M_ns of the oligomers.

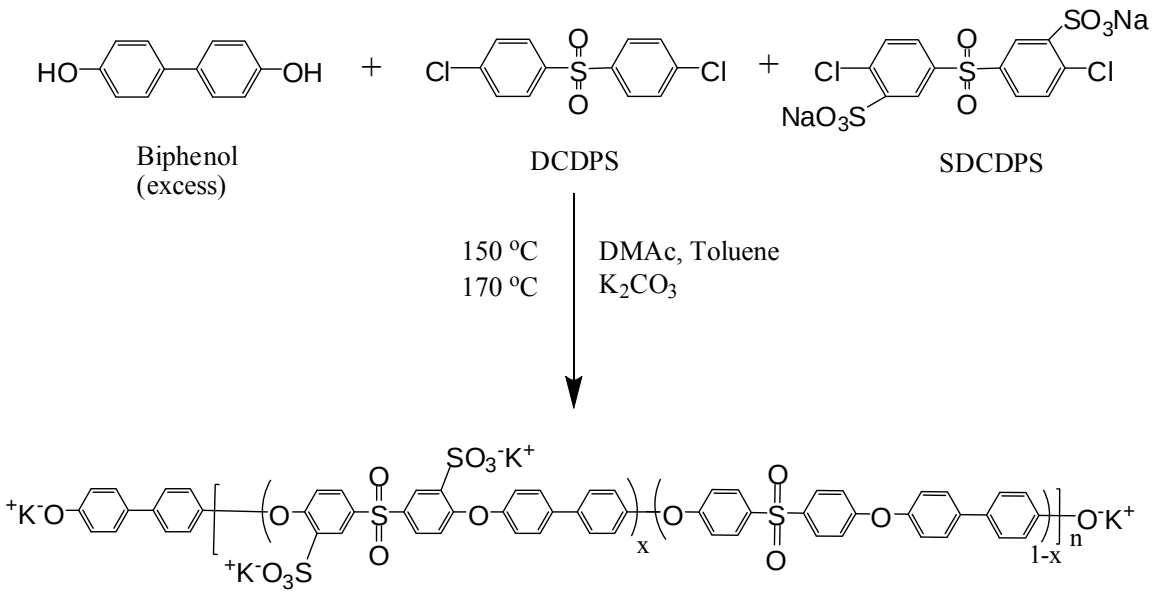

Figure 7.1 Synthesis of a controlled molecular weight phenoxide-endcapped BPS-XX copolymer

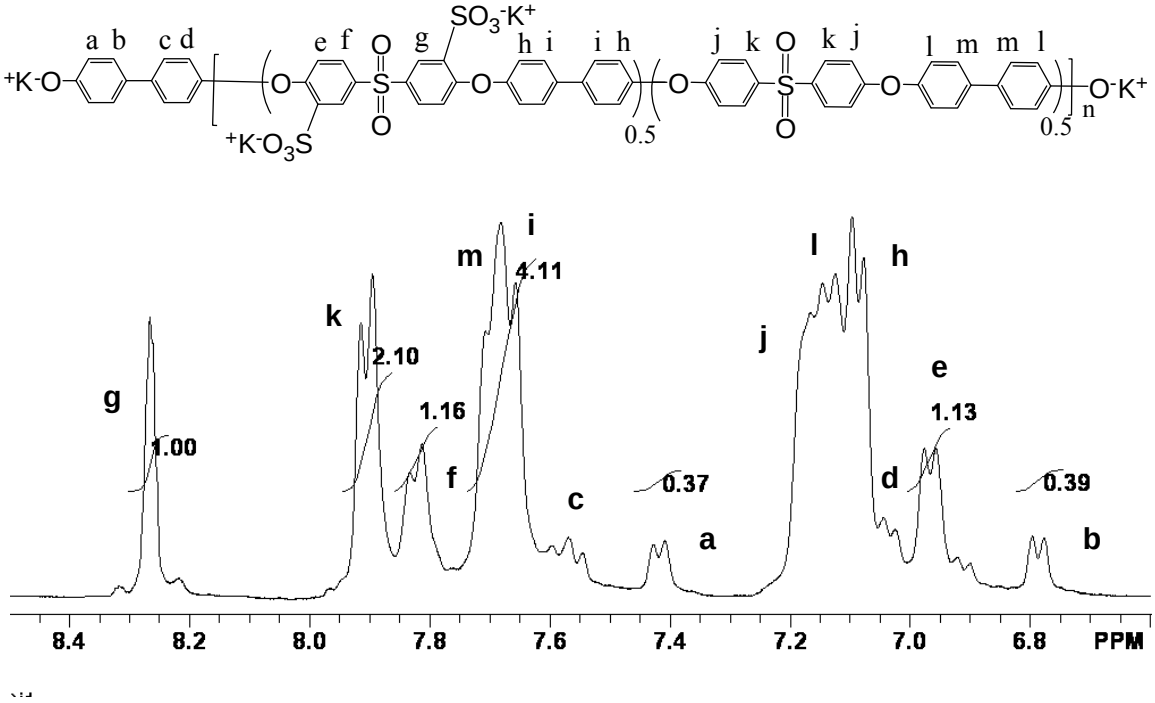

Figure 7.2 ^{1}H NMR of a phenoxide-endcapped BPS-50 random oligomer with molecular weight of~ 5 kg mol^{-1}

As shown in Table 7.1, the experimental M_n values derived from NMR are in good agreement with the targeted values. As expected, intrinsic viscosities ([η]) of the copolymers increased with increasing molecular weight (Table 7.1). The degree of disulfonation was confirmed from the ratio of the integrals of protons at 6.95 (*e*), 7.8 (*f*) and 8.25 ppm (*g*) in the sulfonated unit to the protons at 7.9 ppm (*k*) in the non-sulfonated unit. The degrees of disulfonation were used to calculate the ion exchange capacities (IEC- meq of sulfonic acid groups per gram of dry polymer) of the copolymers. Table 7.1 shows that the experimental IEC values of the copolymers obtained from proton NMR are in good agreement with the targeted values.

Table 7.1 Summary of BPS-50 copolymers before and after endcapping with FPEB

Copolymer	M_n (kg mol^{-1})		IEC (meq g^{-1})		IV[a] (dL g^{-1})	IV[b] (dL g^{-1})
	Target	^{1}H NMR	Target	^{1}H NMR		
BPS-50	5	5.7	2.08	2.04	0.21	0.26
BPS-50	20	20.8	2.08	2.03	0.43	0.45

[a] Intrinsic Viscosity (IV) in NMP with 0.05 M LiBr at 60 °C, from GPC

[b] Intrinsic Viscosity (IV) in NMP with 0.05 M LiBr at 60 °C, from GPC, after endcapping with FPEB

7.3.2. Synthesis of FPEB-endcapped BPS-XX copolymers (FPEB-BPS-XX)

FPEB-BPS-XX copolymers were synthesized via nucleophilic aromatic substitution reactions between phenoxide-endcapped BPS-XX and FPEB under basic conditions in DMAc (Fig. 7.3). Three moles of FPEB per phenoxide equivalent were utilized in these reactions to aid in quantitatively capping the copolymers. The endcapped copolymers were soxhlet-extracted with chloroform for 24 hours to remove the remaining unreacted FPEB. Both BPS-50(5k) and BPS-50(20k) were endcapped in this manner with phenylethynyl moieties.

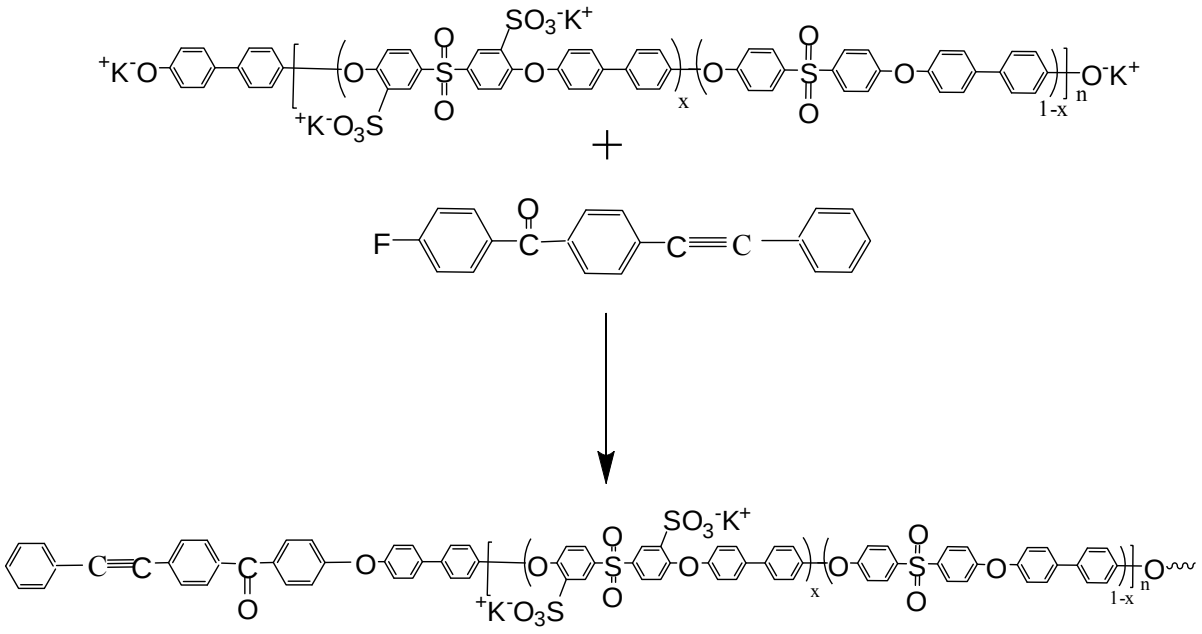

Figure 7.3 Synthesis of a FPEB-endcapped BPS-50 copolymer

Figure 7.4 shows the proton NMR spectrum of the monomer FPEB and Figure 7.5 represents the proton NMR spectrum of a FPEB-BPS-50(5k) oligomer. The aromatic protons of the biphenol unit in the endgroup at 6.8 (*b*) and 7.0 (*d*) of the phenoxide-terminated BPS-50(5k) oligomer disappeared after the phenoxide groups were reacted with FPEB. The peaks at about 7.35, 7.4 and 7.55 ppm originated from FPEB moiety.

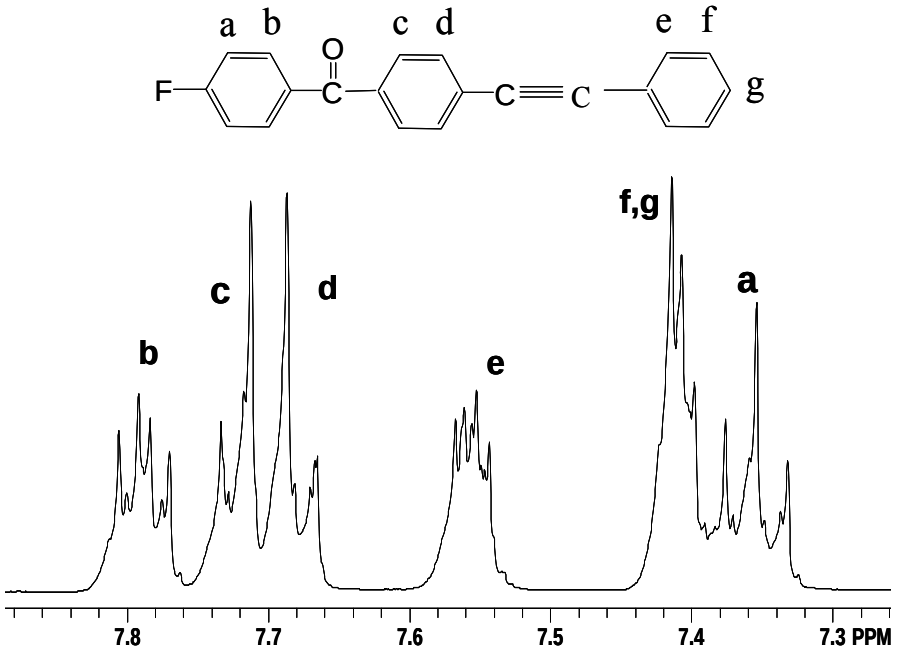

Figure 7.4 ^{1}H NMR of FPEB monomer

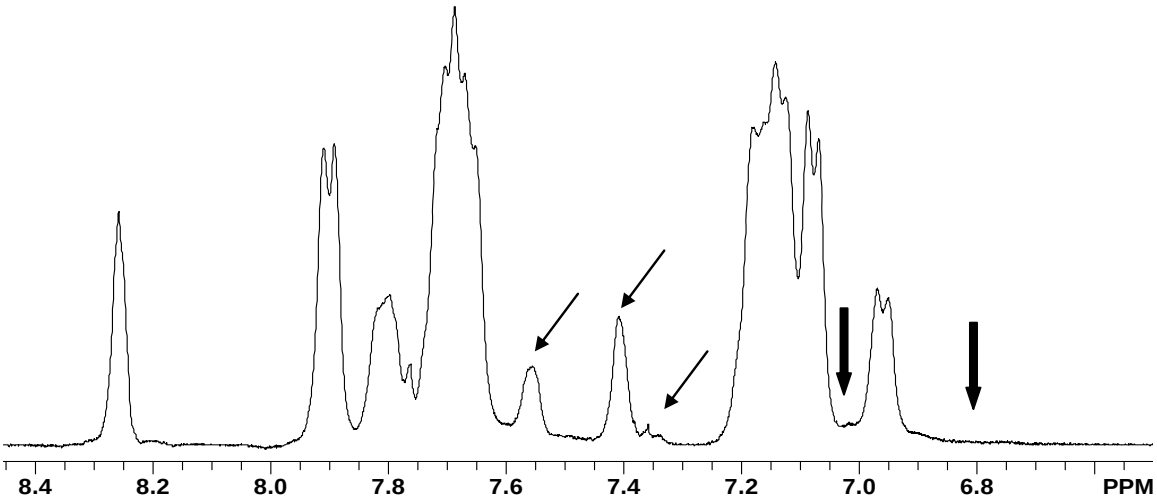

Figure 7.5 ^{1}H NMR of a FPEB-endcapped BPS-50(5k) oligomer;the block arrows indicate the disappearance of aromatic proton peaks of the biphenol unit in the end group and the other arrows indicate new proton peaks originated from FPEB moiety

Figure 7.6 represents the comparison between the ^{19}F NMR spectra of FPEB monomer and a FPEB-BPS-50(5k) oligomer. The disappearance of the fluorine peak at about -106 ppm in the oligomer spectrum indicates complete endcapping of BPS-50 by FPEB and also the absence of any residual FPEB in the oligomer. From the proton and ^{19}F NMR study it was confirmed that all the phenoxide endgroups reacted and the oligomer was completely endcapped with FPEB. The intrinsic viscosities of the oligomers before and after endcapping with FPEB were also compared (Table 7.1). The absence of any significant increase in the intrinsic viscosities after endcapping suggests the lack of significant inter-oligomer coupling during the endcapping reaction.

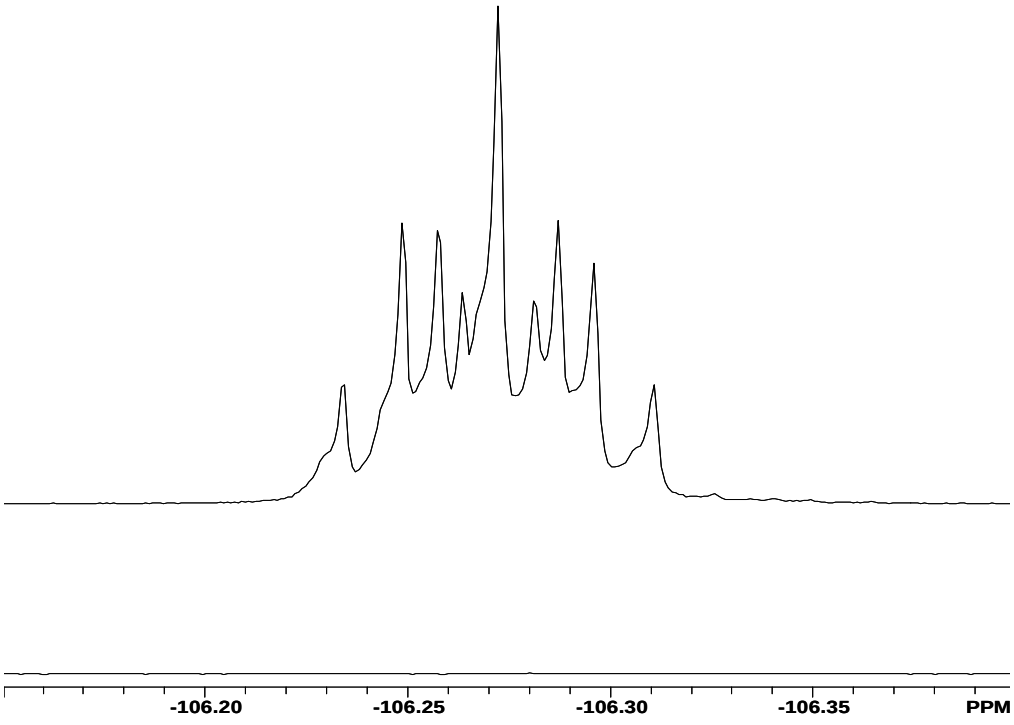

Figure 7.6 Absence of fluorine peak in the ^{19}F NMR spectrum of a FPEB-endcapped BPS-50(5k) oligomer suggests complete endcapping reaction

7.3.3. Casting, crosslinking and characterization of FPEB-BPS-XX copolymers

Phenylethynyl-endcapped copolymers require very high curing temperatures, typically > 350 °C, and this is much higher than the boiling points of common solvents. Hence it was not required that the membrane be formed and cured simultaneously, as was the case with our earlier methacrylate[13] and epoxy-crosslinked systems.[16] In the present case, the membranes were first solution cast from DMAc, dried, and then cured at a higher temperature. In order to produce good membranes, it is required that a copolymer should have a minimum molecular weight to form a good film. However at the same time, for a copolymer endcapped with crosslinkable moieties, the number of crosslinkable sites is inversely related to the number average molecular weight. Hence in order to achieve both sufficient crosslink density and film-forming properties, a non-film forming low molecular weight material was blended with a film-forming material. A FPEB-BPS-50(5k) copolymer was blended with a FPEB-BPS-50(20k) copolymer in a 20:80 wt % ratio. Figure 7.7 represents the FTIR spectra of a BPS-50 copolymer and a FPEB endcapped blended membrane. The appearance of the peak at 2217 cm^{-1} in the blend membrane spectrum confirmed that the membrane contained the crosslinkable ethynyl groups.

Dynamic thermogravimetric analysis of the uncrosslinked blend membrane under nitrogen atmosphere showed a 5 % weight loss temperature at about 449 °C (Fig. 7.8), representing the excellent thermal stability of FPEB-endcapped BPS systems. In a separate TGA experiment, the membrane was isothermally heated at 360 °C for 90 min (Fig. 7.9). There was not any significant weight loss after the isothermal treatment, supporting its ability to be crosslinked at a high temperature without degradation.

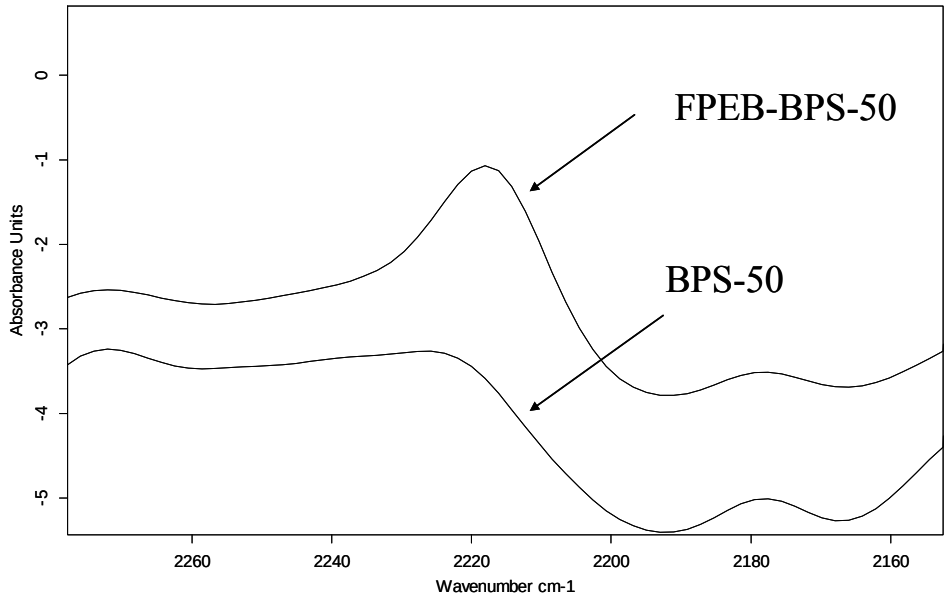

Figure 7.7 Ethynyl stretch at ~2217 cm^{-1} appears after endcapping BPS-50 by FPEB

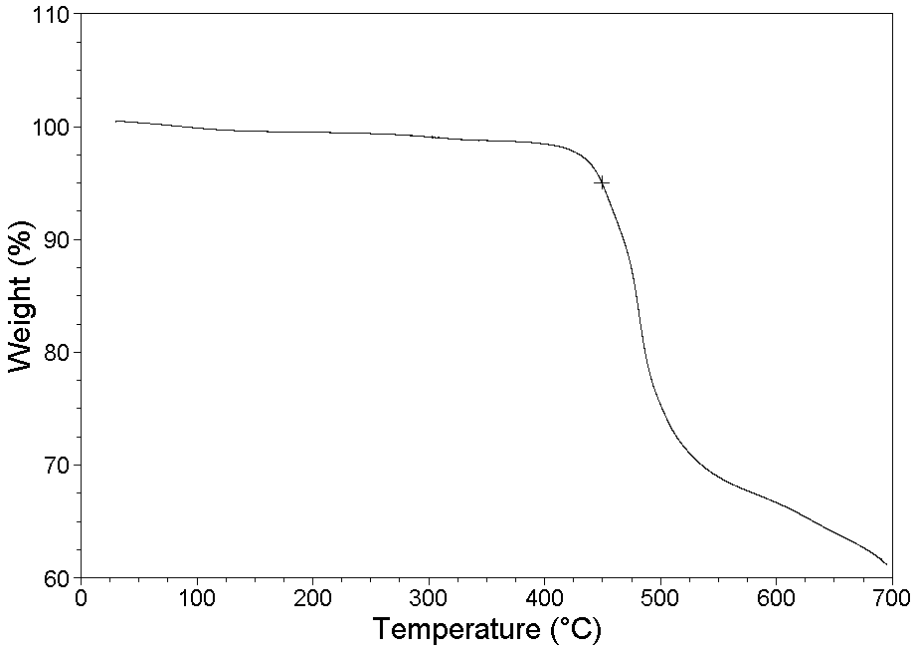

Figure 7.8 TGA graph of FPEB-BPS-50 blend membrane shows 5 % weight loss at ~ 449 °C

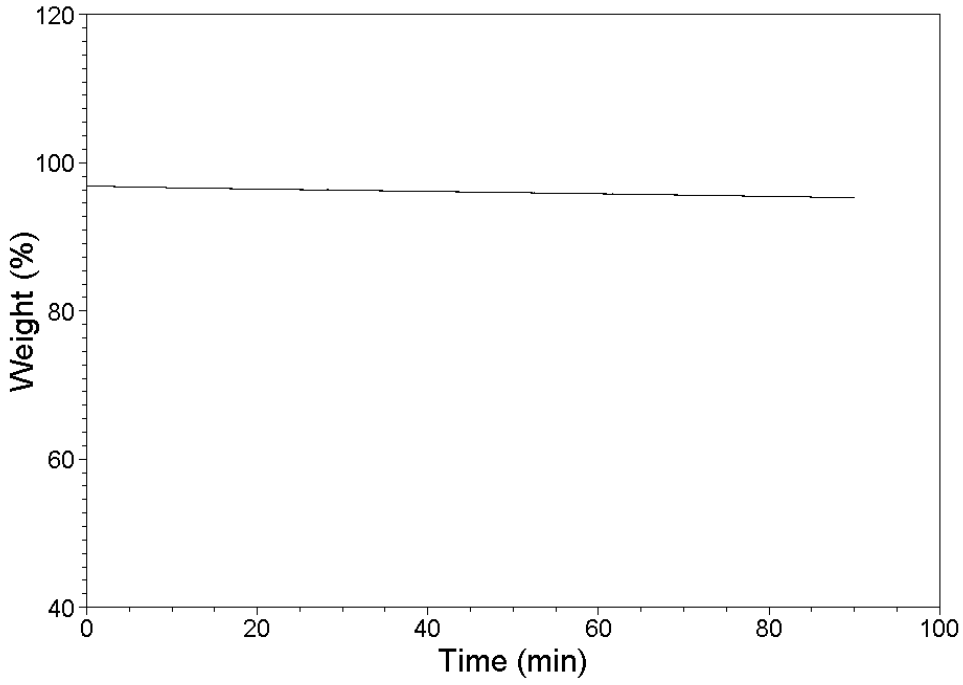

Figure 7.9 Isothermal heating of a FPEB-BPS-50 blend membrane at 360 °C for 90 min shows no significant weight change

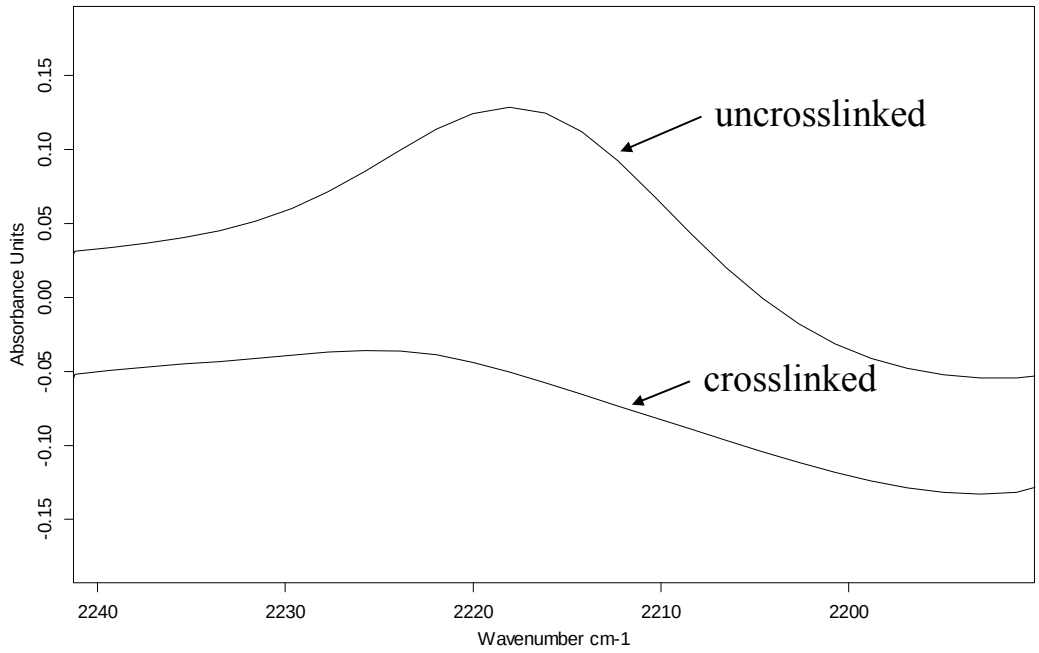

Figure 7.10 Ethynyl stretch at ~2217 cm^{-1} diminishes after crosslinking FPEB-BPS-50 at 360 °C for 45 minutes

The blend membranes were cured at 360 °C under a nitrogen atmosphere, and curing time was varied from 45 to 90 minutes. Figure 7.10 shows the FTIR spectra of a BPS-50 blend membrane before and after curing for 45 minutes. The reduction in the ethynyl peak intensity at ~2217 cm^{-1} indicated that crosslinking had occurred.

Crosslinked membranes were soxhlet-extracted in DMAc for 48 h to measure the gel fraction, i.e. the insoluble fraction of the networks. Gel fraction is an indirect measure of the extent of crosslinking since it increases with the extent of crosslinking. Both of the membranes, which were crosslinked for 45 or 90 minutes, had high gel fractions (around 80%, Table 7.2). There was only a modest increase in the gel fraction when the curing time was increased from 45 to 90 minutes, probably due to the fact that it already attained a high gel fraction after 45 minutes. The crosslinked blend membranes showed satisfactory ductile mechanical properties, even after acidification in refluxing sulfuric acid.

7.3.4. Water uptake, water swelling and proton conductivity

In proton exchange membranes, it is quite well established that a trade-off exists between water uptake and proton conductivity. In general, proton transport is facilitated by water uptake as water acts as a vehicle for proton transport. However, higher water uptake results in reduced dimensional stability leading to loss in fuel cell performance. Moreover, increased water swelling in the membrane causes a reduction in effective proton concentration, which may lead to a loss in proton conductivity, unless the proton diffusivity is high enough to overcome the loss in proton conduction.

Table 7.2 Summary of the properties of crosslinked FPEB-BPS-50 copolymers

Copolymer	Curing time (min)	IEC [a] (meq.g^{-1})	Gel fraction[b] (%)	Water uptake (mass%)	Water swelling (volume%)	C_H^+ (meq cc^{-1})	Proton conductivity[c] (S cm^{-1})
Uncrosslinked BPSH-50	0	2.01	0	232	325	0.69	0.08
Crosslinked FPEB-BPSH-50	45	2.04	80	63	84	1.43	0.07
Crosslinked FPEB-BPSH-50	90	2.04	84	54	75	1.62	0.09

[a]Theoretical IEC

[b]Soxhlet extraction in DMAc for 48 h

[c]Measured at 30 ^{o}C, liquid water

In this study, the proton conductivity, water uptake and water swelling of the non-crosslinked and crosslinked BPSH-50 (crosslinked for 45 and 90 min) samples were compared (Table 7.2). Significant reduction in water uptake and more importantly, in water swelling was observed for the crosslinked materials when compared with the non-crosslinked materials at similar IECs. For the materials that were cured for 45 versus 90 minutes, both water uptake and swelling decreased modestly with increasing curing time. From this study it has been confirmed that it is possible to decrease the water absorption significantly for an ion-containing copolymer, at similar IEC values.

The immediate effect of the reduction in water uptake is an increase in the effective proton concentration for the crosslinked copolymer. The effective ionic concentration was determined using the procedure described in the experimental section. Although increasing the crosslinking time from 45 to 90 min resulted in a reduction in water uptake, the increased proton concentration with crosslinking time was associated

with an increase in overall proton conductivity. Hence by crosslinking, one can alter the balance between water uptake and proton transport which increases the selectivity of PEMs.

7.3.5. Water permeability and salt rejection

Ideally for reverse osmosis, membrane materials should have both high water permeability and high salt rejection. A trade-off exists between these two properties for sulfonated polymers. Water permeability increases with increasing degree of disulfonation, but at the expense of increased salt passage through the membrane. Crosslinking can reduce the water swelling and restrict the salt passage through membranes and thus salt rejection of highly charged membranes can be improved. Table 7.3 reports a preliminary study on water permeability and salt rejections of a 45 minute crosslinked FPEB-BPS-50 membrane and two linear BPS-30 and BPS-40 membranes in their salt forms.

Table 7.3 Water permeability and salt rejection of crosslinked and uncrosslinked membranes

System	Curing Time (min)	Water Permeability[a] (X 10^{-6} cm^2 s^{-1})	NaCl Rejection[b] (%)
Crosslinked FPEB-BPS-50	45	1.19	95.9
Uncrosslinked BPS-40	0	2.50	94.3
Uncrosslinked BPS-30	0	1.10	95.9

[a]Measured by dead-end filtration, 400 psi

[b]Feed = 2000 ppm NaCl; Applied Pressure = 800 psi; Temperature = 25 °C

Salt rejection of uncrosslinked BPS copolymers decreased with increasing degree of dilsulfonation from 30% to 40%. But the crosslinked BPS-50 copolymer was able to maintain similar salt rejection to that of BPS-30 inspite of its higher degree of

disulfonation. As expected, water permeability decreased to some extent with crosslinking. These results are in accordance with our earlier data obtained from epoxy crosslinked BPS system (Chapter 3). Further studies on salt permeabilities are needed to fully understand the effect of crosslinking on membrane structure.

7.4 Conclusions

A series of controlled molecular weight phenoxide-endcapped BPS-50 copolymers was synthesized and characterized by proton NMR. The copolymers were chemically modified with FPEB to produce phenylethynyl-endcapped BPS-50 copolymers and then cured at elevated temperatures (~360 °C) for varying times and this was monitored by FTIR. The membrane properties were improved by preparing blend membranes containing a low and high molecular weight copolymer to achieve both sufficient crosslink density and ductile film-forming properties. Cured samples showed lower water uptake relative to their non-crosslinked counterparts, while maintaining satisfactory proton conductivities. Preliminary studies showed that the crosslinked membrane in its salt form had high salt rejection. In conclusion, the effects of crosslinking on the PEM and RO properties of these phenylethynyl-endcapped BPSH copolymers are very promising, suggesting their potential in increasing the selectivity of PEMs and RO membranes.

7.5. Reference:

1. Eisenberg, A.; Rinaudo, M., Polyelectrolytes and ionomers. *Polymer Bulletin (Berlin, Germany)* **1990,** 24, (6), 671.

2. Wang, F.; Hickner, M.; Kim, Y. S.; Zawodzinski, T. A.; McGrath, J. E., Direct polymerization of sulfonated poly(arylene ether sulfone) random (statistical) copolymers: candidates for new proton exchange membranes. *Journal of Membrane Science* **2002,** 197, (1-2), 231-242.

3. Hickner, M. A.; Ghassemi, H.; Kim, Y. S.; Einsla, B. R.; McGrath, J. E., Alternative polymer systems for proton exchange membranes (PEMs). *Chemical Reviews* **2004,** 104, (10), 4587-4611.

4. Park, H. B.; McGrath, J. E., Desalination properties of sulfonated polysulfones. *Abstracts of Papers, 233rd ACS National Meeting, Chicago, IL, United States, March 25-29, 2007* **2007**, IEC-016.

5. Park, H. B.; Freeman, B. D.; Zhang, Z.-B.; Fan, G.-Y.; Sankir, M.; McGrath, J. E., Water and salt transport behavior through hydrophilic-hydrophobic copolymer membranes and their relations to reverse osmosis membrane performance. *PMSE Preprints* **2006,** 95, 889-891.

6. Park, H. B.; Freeman, B. D.; Zhang, Z.-B.; Fan, G.-Y.; Sankir, M.; McGrath, J. E., Water and salt transport behavior through hydrophilic-hydrophobic copolymer membranes and their relations to reverse osmosis membrane performance. *Abstracts of Papers, 232nd ACS National Meeting, San Francisco, CA, United States, Sept. 10-14, 2006* **2006**, PMSE-495.

7. Zhang, Z.-B.; Fan, G.-Y.; Sankir, M.; Park, H. B.; Freeman, B. D.; McGrath, J. E., Synthesis of di-sulfonated poly(arylene ether sulfone) random copolymers as novel candidates for chlorine-resistant reverse osmosis membranes. *Abstracts of Papers, 232nd ACS National Meeting, San Francisco, CA, United States, Sept. 10-14, 2006* **2006**, PMSE-494.

8. Park, H. B.; Freeman, B. D.; Zhang, Z.; Sankir, M.; McGrath, J. E., Chlorine-Tolerant Disulfonated Poly(arylene ether sulfone) Desalination Membrane Materials. *Angewandte Chemie International Edition* **2008 Submitted**.

9. Kim, Y. S.; Wang, F.; Hickner, M.; McCartney, S.; Hong, Y. T.; Harrison, W.; Zawodzinski, T. A.; McGrath, J. E., Effect of acidification treatment and morphological stability of sulfonated poly(arylene ether sulfone) copolymer proton-exchange membranes for fuel-cell use above 100 degrees C. *Journal of Polymer Science Part B-Polymer Physics* **2003,** 41, (22), 2816-2828.

10. Kim, Y. S.; Dong, L. M.; Hickner, M. A.; Pivovar, B. S.; McGrath, J. E., Processing induced morphological development in hydrated sulfonated poly(arylene ether sulfone) copolymer membranes. *Polymer* **2003,** 44, (19), 5729-5736.

11. Harrison, W. L.; Wang, F.; Mecham, J. B.; Bhanu, V. A.; Hill, M.; Kim, Y. S.; McGrath, J. E., Influence of the bisphenol structure on the direct synthesis of sulfonated poly(arylene ether) copolymers. I. *Journal of Polymer Science Part a-Polymer Chemistry* **2003,** 41, (14), 2264-2276.

12. Kim, Y. S.; Dong, L. M.; Hickner, M. A.; Glass, T. E.; Webb, V.; McGrath, J. E., State of water in disulfonated poly(arylene ether sulfone) copolymers and a perfluorosulfonic acid copolymer (nafion) and its effect on physical and electrochemical properties. *Macromolecules* **2003,** 36, (17), 6281-6285.

13. Paul, Mou; Roy, Abhishek; Riffle, Judy S.; McGrath, James E. Crosslinked sulfonated poly(arylene ether sulfone) membranes as candidate for PEMS. ECS Transactions (2008), 6 (26, Membranes for Electrochemical Applications), 9-16.

14. Park, H. B.; Xie, W.; Freeman, B. D.; Paul, M.; Roy, A.; Sankir, M.; Lee, H.-S.; Riffle, J. S.; McGrath, J. E., Chlorine-tolerant desalination membranes. *Abstracts of Papers, 235th ACS National Meeting, New Orleans, LA, United States, April 6-10, 2008* **2008**, POLY-312.

15. Paul, M., Roy, A.; McGrath, J.E.; Riffle, J.S. , Effect of Crosslinking on PEM Properties of Random Poly(Arylene Ether Sulfone)s with Varying Degree of Disulfonations, **to be submitted**.

16. Paul, M.; Park, H. B.; Freeman, B. D.; Roy, A.; McGrath, J. E.; Riffle, J. S., Synthesis and crosslinking of partially disulfonated poly(arylene ether sulfone) random

copolymers as candidates for chlorine resistant reverse osmosis membranes. *Polymer* **2008,** 49, (9), 2243-2252.

17. Hergenrother, P. M.; Bryant, R. G.; Jensen, B. J.; Smith, J. G., Jr.; Wilkinson, S. P., Chemistry and properties of phenylethynyl terminated imide oligomers and their cured polymers. *International SAMPE Symposium and Exhibition* **1994,** 39, (Moving Forward with 50 Years of Leadership), 961-8.

18. Hergenrother, P. M.; Bryant, R. G.; Jensen, B. J.; Havens, S. J., Phenylethynyl-terminated imide oligomers and polymers therefrom. *Journal of Polymer Science, Part A: Polymer Chemistry* **1994,** 32, (16), 3061-7.

19. Harrington, K. A.; Orwoll, R. A.; Jensen, B. J.; Young, P. R., Characterization of cure chemistry of selected phenylethynyl-terminated polyimides and model compounds. *International SAMPE Symposium and Exhibition* **1996,** 41, (Materials and Process Challenges: Aging Systems, Affordability, Alternative Applications, Book 1), 135-148.

20. Tan, B.; Vasudevan, V.; Lee, Y. J.; Gardner, S.; Davis, R. M.; Bullions, T.; Loos, A. C.; Parvatareddy, H.; Dillard, D. A.; McGrath, J. E.; Cella, J., Design and characterization of thermosetting polyimide structural adhesive and composite matrix systems. *Journal of Polymer Science Part a-Polymer Chemistry* **1997,** 35, (14), 2943-2954.

21. Hinkley, J. A.; Jensen, B. J., Crosslinking in phenylethynyl-terminated polyimides. *High Performance Polymers* **1996,** 8, (4), 599-605.

22. Jensen, B. J.; Hergenrother, P. M., Poly(arylene ether)s with pendant ethynyl groups. *Journal of Macromolecular Science, Pure and Applied Chemistry* **1993,** A30, (6-7), 449-58.

23. Bryant, R. G.; Jensen, B. J.; Hergenrother, P. M., Synthesis and properties of phenylethynyl-terminated arylene ethers. *Polymer Preprints (American Chemical Society, Division of Polymer Chemistry)* **1992,** 33, (1), 910-11.

24. Hergenrother, P. M., Acetylene-containing precursor polymers. *Journal of Macromolecular Science, Reviews in Macromolecular Chemistry* **1980,** C19, (1), 1-34.

25. Jayaraman, S.; Srinivasan, R.; Mcgrath, J. E., Synthesis and Characterization of 3-Phenylethynyl Endcapped Matrix Resins. *Journal of Polymer Science Part a-Polymer Chemistry* **1995,** 33, (10), 1551-1563.

26. Ayambem, A.; Mecham, S. J.; Sun, Y.; Glass, T. E.; McGrath, J. E., Endgroup substituent effects on the rate/extent of network formation and adhesion for phenylethynyl-terminated poly(arylene ether sulfone) oligomers. *Polymer* **2000,** 41, (13), 5109-5124.

27. Mecham, S. J. Synthesis and characterization of phenylethynyl-terminated poly(arylene ether sulfone)s as thermosetting structural adhesives and composite matrixes. PhD Dissertation, Virginia Polytechnic Institute & State University, 1997.

28. Sankir, M.; Bhanu, V. A.; Harrison, W. L.; Ghassemi, H.; Wiles, K. B.; Glass, T. E.; Brink, A. E.; Brink, M. H.; McGrath, J. E., Synthesis and characterization of 3,3'-disulfonated-4,4'-dichlorodiphenyl sulfone (SDCDPS) monomer for proton exchange membranes (PEM) in fuel cell applications. *Journal of Applied Polymer Science* **2006,** 100, (6), 4595-4602.

29. Kim, Y. S.; Einsla, B.; Sankir, M.; Harrison, W.; Pivovar, B. S., Structure-property-performance relationships of sulfonated poly(arylene ether sulfone)s as a polymer electrolyte for fuel cell applications. *Polymer* **2006,** 47, (11), 4026-4035.

8. CHAPTER-8-Future and Suggested Research

8.1. Introduction

BPSH random copolymers have shown excellent proton conductivity at fully hydrated condition, low permeability to fuels and high mechanical stability at elevated temperatures; all the properties required for a high performance proton exchange membrane. However, due to the random distribution of the sulfonic acid groups along the backbone of this copolymer, a high ion exchange capacity is needed to achieve the desirable connectivity in the hydrophilic phase for proton conduction under partially hydrated conditions. But, this high IEC can lead to high water swelling and subsequent deterioration of membrane mechanical properties. One way to overcome this problem is to synthesize graft or block copolymers where the hydrophilic and hydrophobic units will be well phase separated. Graft copolymers of polystyrene-*g*-polysulfonate showed reduced water uptake and higher proton conductivities than their random analogues[1]. In another approach, both the concept of crosslinking and grafting were utilized, by radiation induced grafting of styrene on fluoropolymers, simultaneously crosslinking of polystyrene and subsequent sulfonation[2-4]. For the multiblock system, recent studies by the McGrath group have demonstrated that nanophase separated ion containing hydrophilic-hydrophobic multiblock copolymers with improved connectivity between the sulfonic acid groups can sustain proton conductivity even under partially hydrated condition.[5-10] In chapter 5, we have demonstrated that the water uptake and swelling of hydrocarbon based ion-containing BPSH-BPS multiblock copolymers can be reduced by lightly crosslinking them.

In this current study, we propose to synthesize a graft copolymer system where the fully disulfonated hydrophilic grafts will be attached to a hydrophobic backbone through reactive pendant phenolic sites. The hydrophobic backbone will be terminated with phenoxide-endgroups which can be further reacted with a suitable crosslinker, such as

epoxy. Due to the selective crosslinking of the hydrophobic unit only, a better phase separation between the two units will be facilitated and it may produce a pseudo-Nafion like morphology.

A hydrophobic oligomer containing pendant methoxy groups was synthesized[11] and subsequently the methoxy groups were deprotected to form reactive pendant phenolic sites. On the other hand, a fluorine-terminated hydrophilic oligomer was synthesized. A graft copolymer was formed by a side chain coupling reaction between the two oligomers.

8.2. Experimental

8.2.1. Materials

Monomer grade 4,4′–dichlorodiphenylsulfone (DCDPS) and 4,4′-biphenol (BP) were obtained from Solvay Advanced Polymers and Eastman Chemical Company, respectively, and dried under vacuum at 60 °C for one day prior to use. The sulfonated comonomer, 3,3′-disulfonate-4,4′-dichlorodiphenylsulfone (SDCDPS), was prepared following a previously published procedure [12, 13], and dried under vacuum at 160 °C for two days before use. Decafluorobiphenyl (DFBP) was obtained from Lancaster and used as received. Methoxyhydroquinone (MHQ) was obtained from Aldrich and was dried at room temperature under vacuum for 24 before use. Potassium carbonate (Aldrich) was dried under vacuum at 110 °C for one day before use. Boron tribromide (BBr_3) was obtained from Aldrich and used as received. The reaction solvent *N*,*N*-dimethylacetamide (DMAc, Aldrich) was vacuum-distilled from calcium hydride, and stored over molecular sieves under nitrogen. Toluene (anhydrous, 99.8%), isopropyl alcohol (*ReagentPlus*™, 99%), methanol, acetone were obtained from Aldrich and used as received.

8.2.2. Synthesis and end-functionalization of a controlled molecular weight, fully disulfonated, hydrophilic BPSH100 oligomer by DFBP

A controlled molecular weight, phenoxide-endcapped 100% disulfonated biphenol-based poly(arylene ether sulfone) (BPSH100) oligomer was synthesized via nucleophilic aromatic substitution according to the procedure outlined in chapter 5.

The terminal phenoxide groups of BPSH100 oligomers were reacted with DFBP via nucleophilic aromatic substitution reaction to produce DFBP-endcapped BPSH100 oligomers following the procedure outlined in the same chapter. The nomenclature of the samples is defined as follows-DFBP-BPSH(yk) where y denotes the molecular weights of the respective oligomers in kg $mole^{-1}$.

8.2.3. Synthesis of a controlled molecular weight, phenoxide-endcapped, unsulfonated, hydrophobic BPS80MHQ20 oligomer

A controlled molecular weight, phenoxide-endcapped, unsulfonated, 80% biphenol and 20% methoxyhydroquinone-based poly(arylene ether sulfone) (BPS80MHQ20) oligomer was synthesized via nucleophilic aromatic substitution. The molecular weight of the copolymer was controlled by offsetting the stoichiometry of the monomers. A typical polymerization of a 10 kg mol^{-1} BPS80MHQ20 oligomer is provided. BP (2.697 g, 14.48 mmol), MHQ (0.507 g, 3.62 mmol), and DCDPS (5 g, 17.41 mmol) were added to a three-necked, round bottom reaction flask equipped with a mechanical stirrer, nitrogen inlet, Dean-Stark trap and a condenser. Potassium carbonate (2.878 g, 20.82 mmol) and 41 mL DMAc (to achieve 20% solids) were introduced into the flask. Toluene (20 mL, DMAc/toluene was 2/1 v/v) was added as the azeotropic reagent. The reaction mixture was refluxed at 150 °C for 4 h, then the azeotrope was removed to dehydrate the system. The reaction mixture was gradually heated to 170 °C by the controlled removal of toluene, then reacted for an additional 24 h. The viscous product was cooled to room temperature. The product mixture was filtered to remove salts. The copolymer was isolated by precipitation in isopropyl alchohol, filtered, and dried for 24 h at 110 °C under vacuum. The nomenclature of the samples is defined as

follows- BPS80MHQ20(yk) where y denotes the molecular weight of the respective oligomer in kg $mole^{-1}$.

8.2.4. Deprotection of the pendant methoxy groups in the hydrophobic BPS80MHQ20 oligomer

The pendant methoxy groups of the hydrophobic oligomer were converted to hydroxyl groups by the deprotection reagent BBr_3. A typical deprotection reaction is as follows. BPS80MHQ20 (1 g) is dissolved in 20 mL chloroform in a three-necked, round bottom reaction flask equipped with a mechanical stirrer, nitrogen inlet, Dean-Stark trap and a condenser. Next 0.5 mL BBr_3 in 10 mL chloroform was added dropwise to the reaction flask and the reaction mixture was stirred overnight at room temperature. The copolymer was isolated by filtration, washed several times with methanol and water and then dried for 24 h at 110 °C under vacuum. The nomenclature of the samples is defined as follows- BPS80HHQ20(yk) where y denotes the molecular weight of the respective oligomer in kg $mole^{-1}$.

8.2.5. Synthesis of a (BPSH-BPS80HHQ20) graft copolymer

The copolymer was synthesized via coupling reaction between a phenoxide-endcapped BPS80HHQ20 and a DFBP-endcapped BPSH100 oligomer. A typical coupling reaction between a BPS80HHQ20(10k) oligomer and a DFBP-BPSH(10k) oligomer is provided. DFBP-BPSH (2 g, 0.2 mmol) and 20 mL DMAC were added to a three-necked, round bottom reaction flask equipped with a mechanical stirrer, nitrogen inlet, Dean-Stark trap and a condenser. The mixture was stirred at about 80 °C until the reactant was completely dissolved. Next BPS80HHQ20(10k) (2 g, 0.2 mmol), potassium carbonate (0.055 g, 0.4 mmol) and 24 mL DMAc were introduced into the flask. The stirring was continued at 80 °C until all the reactants were completely dissolved. Cyclohexane (9 mL, DMAc/cyclohexane was 5/1 v/v) was added as the azeotropic reagent. The reaction mixture was refluxed at 90 °C for 4 h, then the azeotrope was removed to dehydrate the system. The reaction mixture was gradually heated to 105 °C

by the controlled removal of cyclohexane, then reacted for an additional 24 h. The viscous product was cooled to room temperature. The product mixture was filtered. The copolymer was precipitated in isopropyl alchohol, isolated by filtration, and dried for 24 h at 110 °C under vacuum. The nomenclature of the copolymer is BPSH-*g*-BPS80HHQ20 (10k : 10k) where the molecular weight of each of the oligomers is 10000 g $mole^{-1}$.

8.2.6. Nuclear magnetic resonance (NMR) spectroscopy

^{1}H NMR experiments were conducted on a Varian Unity 400 MHz NMR spectrometer. All spectra of the copolymers were obtained from 10 % solutions (w/v) in DMSO-d_6 or $CDCl_3$ at room temperature. Proton NMR was used to determine the molecular weights of the copolymers and their compositions, and the completion of endcapping reactions.

8.2.7. Intrinsic viscosity

Intrinsic viscosities were determined from GPC experiments performed on a liquid chromatograph equipped with a Viscotek 270 RALLS/ viscometric dual detector. The mobile phase was 0.05 M LiBr containing NMP solvent. The column temperature was maintained at 60 °C because of the viscous nature of NMP. Both the mobile phase solvent and sample solution were filtered before introduction to the GPC system.

8.3 Results and discussion

8.3.1. Synthesis and end-functionalization of controlled molecular weight, BPSH100 oligomers by DFBP

Controlled molecular weight BPSH100 oligomer with phenoxide endgroups was synthesized from biphenol and SDCDPS by nucleophilic aromatic substitution (Fig. 8.1). The molecular weight of the BPSH100 oligomer was controlled by offsetting the stoichiometry between biphenol and SDCDPS. Biphenol was utilized in excess to endcap the oligomers with phenoxide groups.

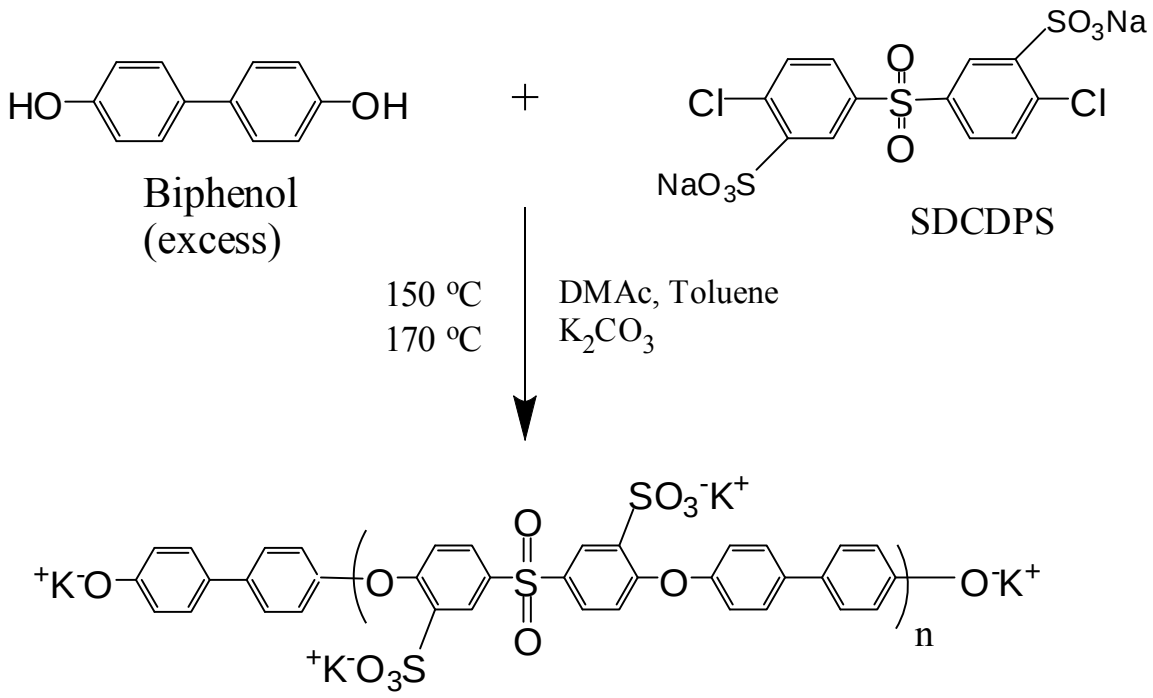

Figure 8.1 Synthesis of a controlled molecular weight, phenoxide-endcapped, fully disulfonated hydrophilic (BPSH100) oligomer

Figure 8.2 shows the proton NMR spectrum of a phenoxide endcapped BPSH100 oligomer with a targeted molecular weight of ten kg mol^{-1}. The aromatic protons of the biphenol unit in the endgroup at *(b), (d), (a), and (c)* were allocated to peaks at 6.8 ppm, 7.05 ppm, 7.45 ppm and 7.55 ppm respectively. The ratio of the integrals of the aromatic protons at 6.8 ppm (*b*) to those of the aromatic protons of the biphenol moiety in the polymer repeat units at 7.65 ppm (*i*) were utilized to calculate M_n of the oligomers. As shown in Table 8.1, the experimental M_n value derived from NMR is in good agreement with the targeted value.

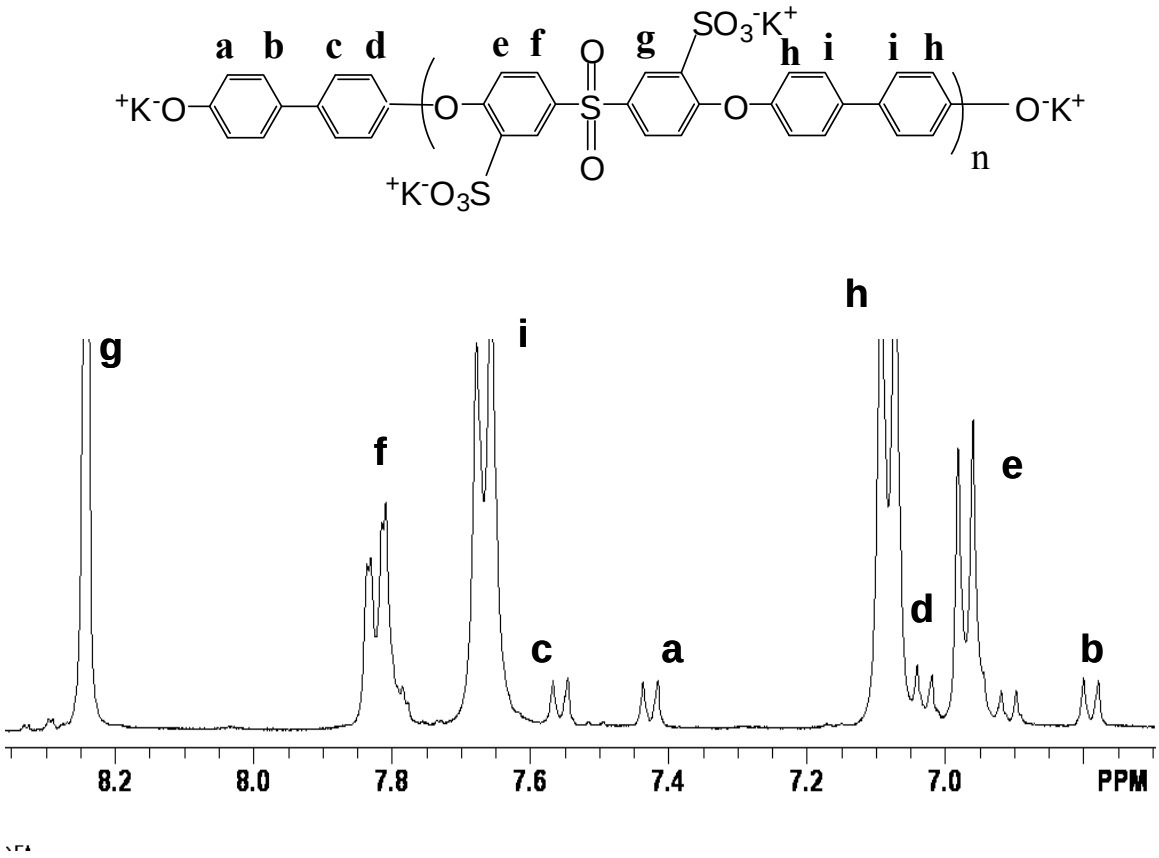

Figure 8.2 ^{1}H NMR of a phenoxide endcapped BPSH(10k) oligomer

The terminal phenoxide groups of BPSH100 oligomers were reacted with DFBP via nucleophilic aromatic substitution reaction to produce DFBP endcapped BPSH100 oligomers (Fig. 8.3). DFBP was utilized in excess to endcap the oligomers with fluoro-terminal groups, so that these groups can be further reacted in the coupling reaction step during the synthesis of multiblocks. Six moles of DFBP per mole of oligomer were taken to ensure complete endcapping without any inter-oligomer coupling reaction. [5]

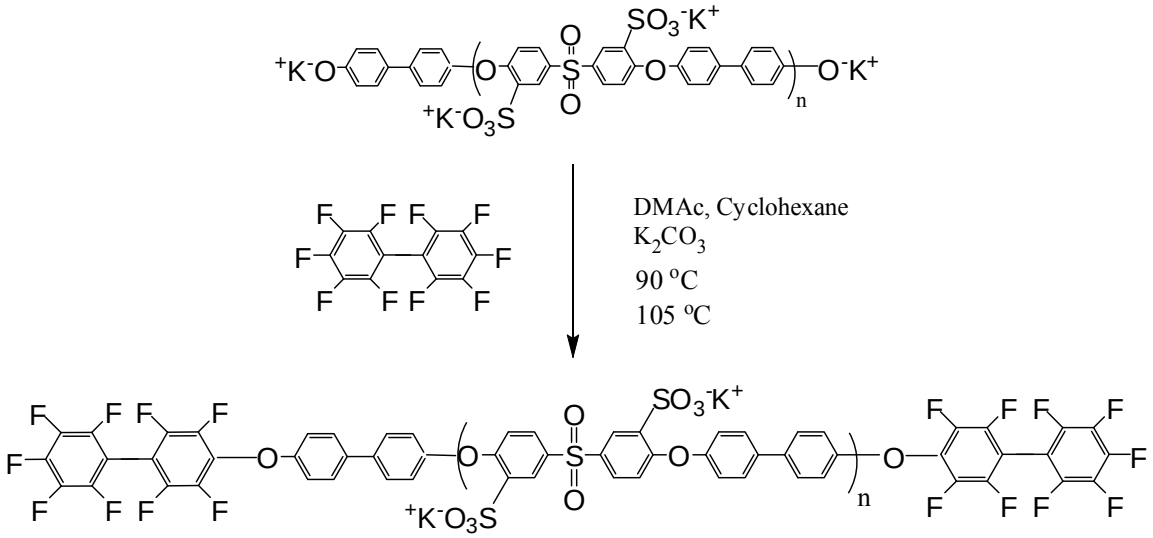

Figure 8.3 End-functionalization of phenoxide-endcapped BPSH100 oligomer by DFBP

Figure 8.4 represents the proton NMR spectrum of a DFBP-BPSH(10k) oligomer. The aromatic protons of the biphenol unit in the endgroup at 6.8 ppm (*b*), 7.05 ppm (*d*), 7.45 ppm (*a*) and 7.55 ppm (*c*) of the phenoxide-terminated BPSH(10k) oligomer disappeared after the phenoxide groups were reacted with DFBP and a new peak at about 7.30 ppm appeared which can be assigned to the biphenol aromatic protons linked with DFBP. From the proton NMR study it was confirmed that all the phenoxide endgroups took part in the endcapping reaction and the oligomer was completely endcapped by DFBP.

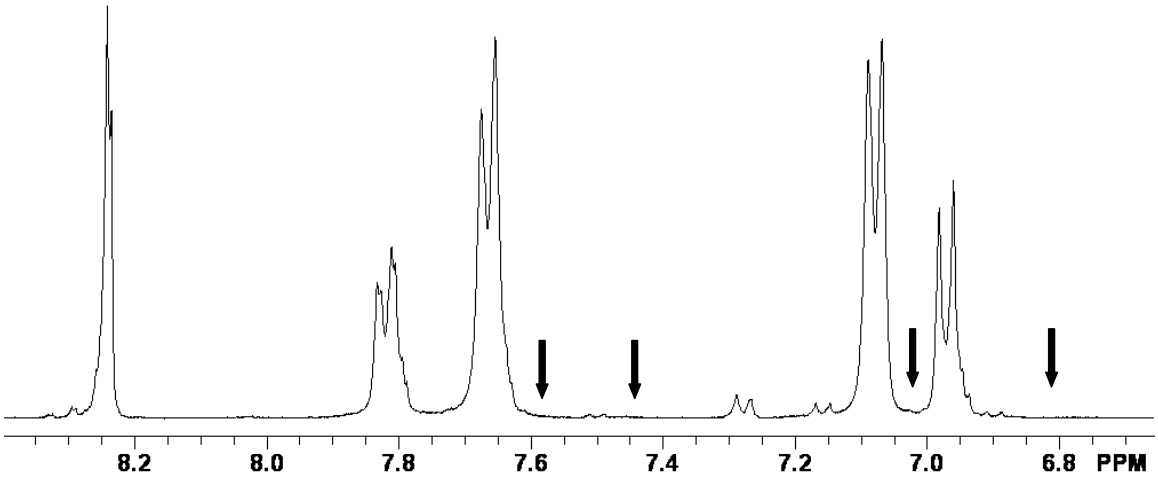

Figure 8.4 ^{1}H NMR of a DFBP- endcapped BPSH(10k) oligomer;arrows indicate the disappearance of aromatic proton peaks of the biphenol unit in the end group

In addition to the proton NMR study, the intrinsic viscosities of the oligomers before and after endcapping were compared to investigate that whether any inter-oligomer coupling by the multifunctional DFBP had taken place or not (Table 8.1). There was not any significant increase in the intrinsic viscosities of the oligomers after endcapping with DFBP. This result is in accordance with earlier study which reported that a molar excess of 200 % is sufficient to endcap the oligomers with DFBP without any inter-oligomer coupling. [5]

Table 8.1 Summary of the properties of the oligomers

Target M_n (g mol^{-1})	Hydrophilic Oligomer (BPSH100)			Hydrophobic Oligomer (BPS80MHQ20)		
	M_n[a] (g mol^{-1})	IV[b] (dL g^{-1})	IV[c] (dL g^{-1})	M_n[a] (g mol^{-1})	IV[b] (dL g^{-1})	IV[d] (dL g^{-1})
10000	9030	0.34	0.27	10400	0.39	0.32

[a] from ^{1}H NMR

[b] measured at 60 ^{o}C, GPC, 0.05 M LiBr in NMP

[c] measured at 60 ^{o}C, GPC, 0.05 M LiBr in NMP after endcapping with DFBP

[d] measured at 60 ^{o}C, GPC, 0.05 M LiBr in NMP after deprotection with BBr_3

8.3.2. Synthesis and deprotection of controlled molecular weight BPS80MHQ20 hydrophobic oligomer

Controlled molecular weight BPS80MHQ20 oligomer with phenoxide endgroups was synthesized from biphenol, methoxyhydroquinone and DCDPS by nucleophilic aromatic substitution (Fig. 8.5). The molecular weight of the hydrophobic oligomer was controlled by offsetting the stoichiometry between BP, MHQ and DCDPS. BP and MHQ were utilized in excess to endcap the oligomers with phenoxide groups.

The NMR spectrum in Figure 8.6 shows a phenoxide-endcapped BPS80MHQ20 oligomer with a targeted molecular weight of ten kg mol^{-1}. The incorporation of methoxy groups can be quantitatively found out from the proton NMR. The ratio of the integrals

of the methoxy protons at 3.7 ppm (*z*) to those of the aromatic protons of the biphenol moiety in the polymer repeat units at 7.5 ppm (*h*) were utilized to calculate the amount of MHQ, which was about 19% in that case.

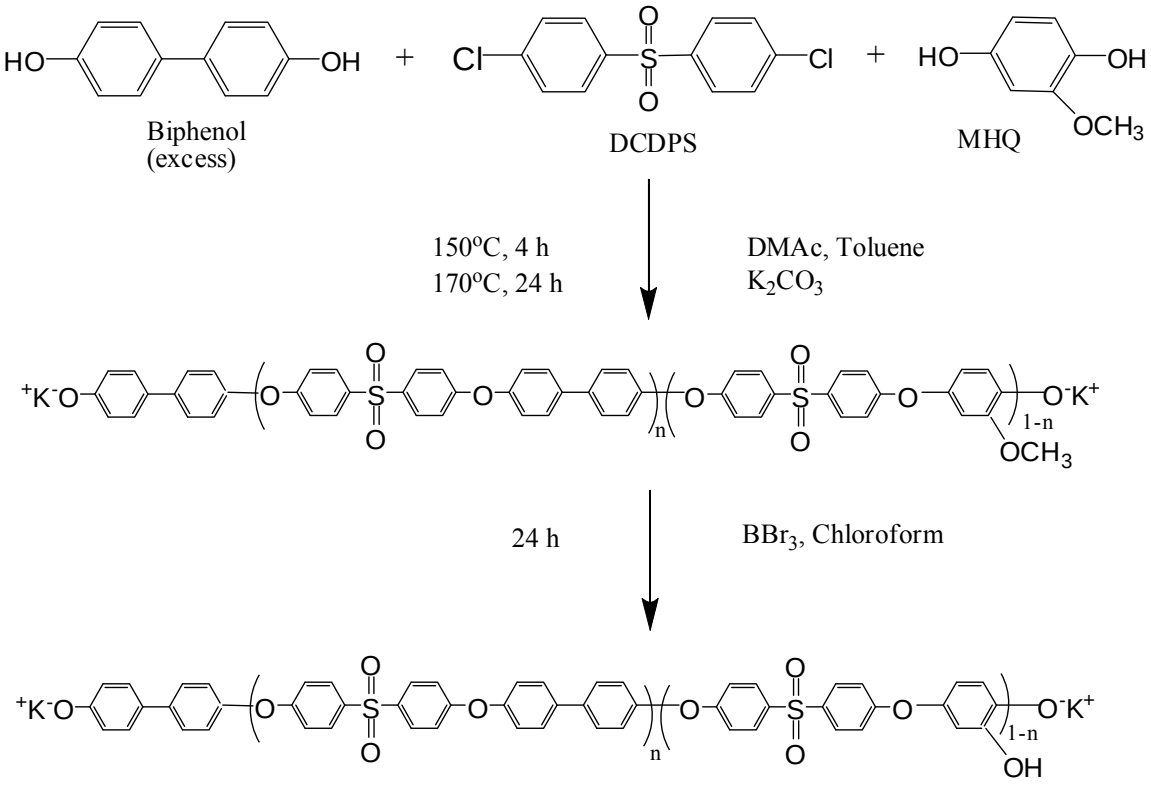

Figure 8.5 Synthesis of a controlled molecular weight, phenoxide endcapped BPS80MHQ20 oligomer and deprotection of methoxy groups to produce BPS80HHQ20 oligomer

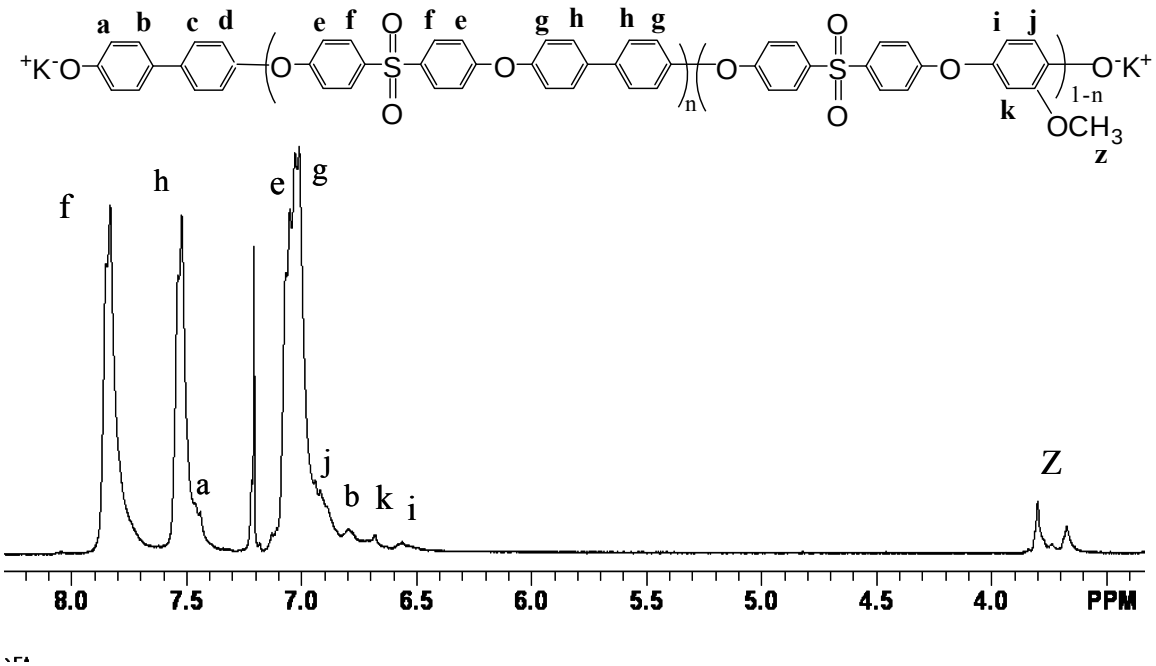

Figure 8.6 ^{1}H NMR of a phenoxide-endcapped BPS80MHQ20(10k) oligomer (solvent – CDCl3)

As the oligomer comprises of 80% BP and 20% MHQ, it can be either endcapped by a BP unit or a MHQ unit, but the probability of being endcapped by the BP unit will be much higher. In the proton NMR spectrum of the oligomer with a targeted molecular weight of ten kg mol^{-1}, the aromatic protons of the biphenol unit in the endgroup *(b)* and *(a)* were allocated to the peaks at 6.8 ppm and 7.40 ppm respectively. The ratio of the integrals of the aromatic protons at 6.8 ppm (*b*) to those of the protons of the biphenol moiety in the polymer repeat units at 7.5 ppm (*h*) were utilized to calculate M_n of the oligomers. As shown in Table 8.1, the experimental M_n value derived from NMR is in good agreement with the targeted value.

The MHQ containing oligomer was reacted with BBr_3 to convert the methoxy groups into hydroxyl groups. The reaction scheme is shown in Figure 8.5. The bottom NMR spectrum of BPS80HHQ20 oligomer in Figure 8.7 shows the disappearance of

methoxy group at ~ 3.7 ppm and appearance of hydroxyl group at ~ 10.1 ppm which confirms the successful deprotection of the methoxy groups by BBr_3.

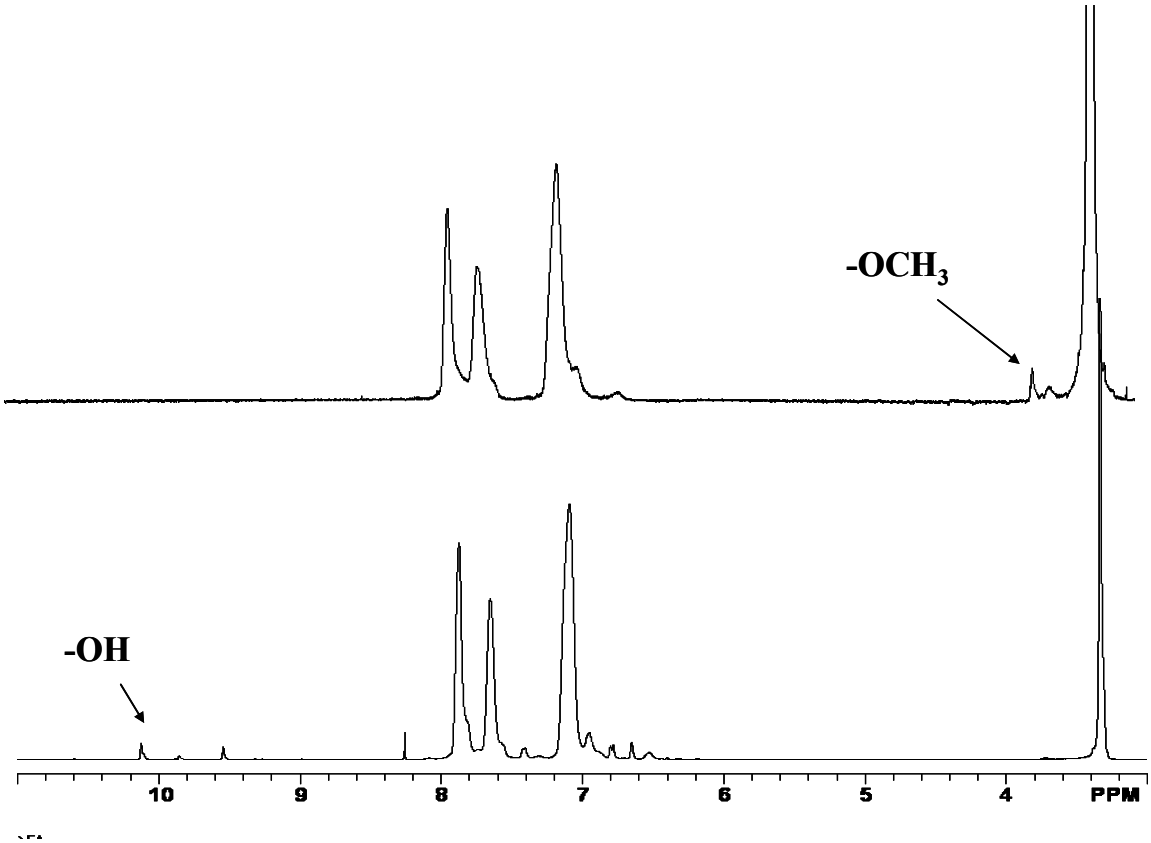

Figure 8.7 1H NMR of BPS80MHQ20 (Top) ; BPS80HHQ20 (Bottom) ;methoxy protons disappear and hydroxyl proton appear after deprotection (solvent-*d*-DMSO)

8.3.3. Synthesis of BPSH-g-BPS80HHQ20 (10k :10k)copolymer

A BPSH-*g*-BPS80HHQ20 copolymer was synthesized via coupling reaction between a DFBP-endcapped BPSH100 hydrophilic oligomer and a phenoxide-endcapped BPS80HHQ20 hydrophobic oligomer (Fig. 8.8).

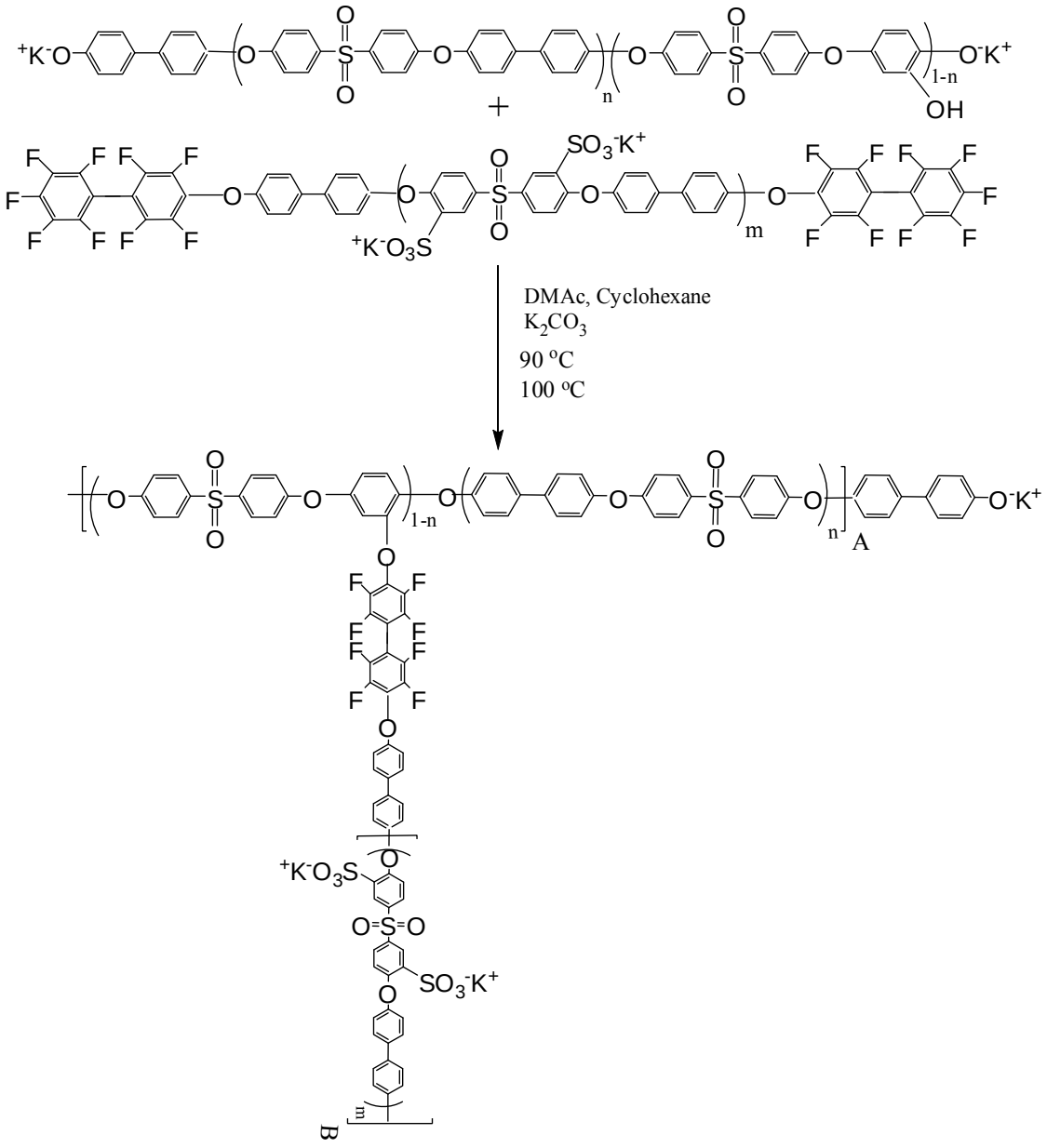

Figure 8.8 Synthesis of a BPSH-*g*-BPS80HHQ20 graft copolymer

Figure 8.9 shows the proton NMR spectrum of the copolymer. The appearance of the aromatic protons of the biphenol unit in the endgroup of BPS80HHQ oligomer at 6.8 ppm and 7.40 ppm and disappearance of aromatic protons in the HHQ unit at 6.5 and 6.7 ppm and the hydroxyl peak at 10.1 ppm suggest that the fluorine groups reacted with the pendant phenolic sites. In that case, a graft copolymer with hydrophilic side chains and a hydrophobic backbone with phenoxide endgroups was generated. These phenoxide endgroups can be further reacted with an epoxy crosslinker to produce crosslinked membranes. The intrinsic viscosity value of the copolymer was 0.36 dL g^{-1}.

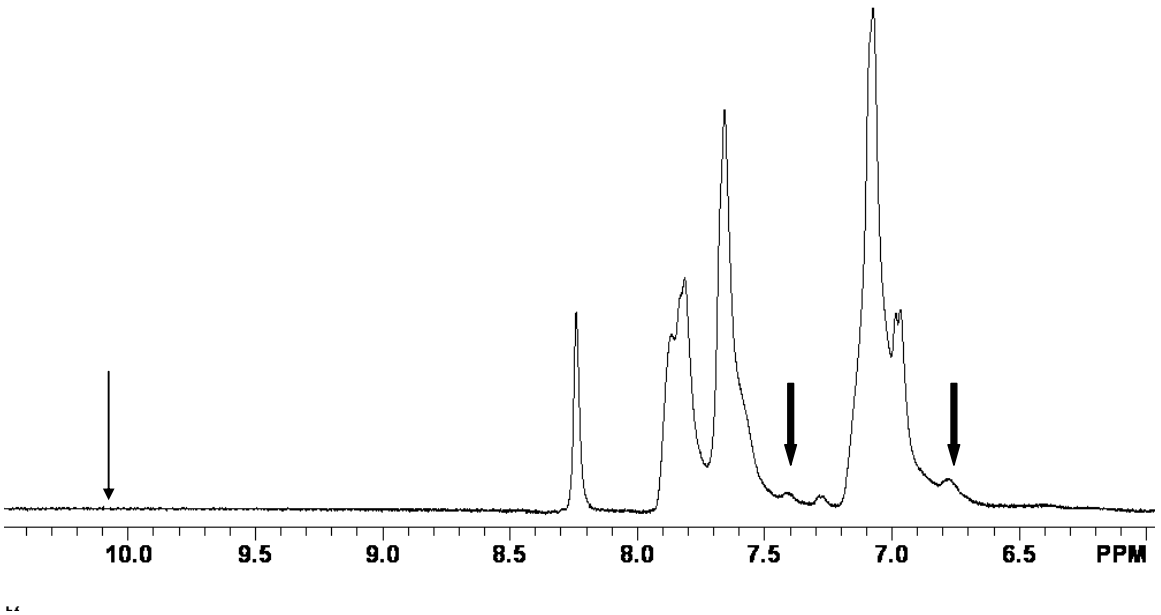

Figure 8.9 ^{1}H NMR of a BPSH-*g*-BPS80MHQ20(10k : 10k)copolymer;block arrows indicate the aromatic protons of the biphenol end unit in the hydrophobic oligomer and the other arrow indicates disappearance of –OH group

8.4 Conclusion

A fluoro terminated hydrophilic oligomer and a hydrophobic oligomer containing recative pendant phenolic groups were synthesized. A graft copolymer synthesis was

attempted through side chain coupling between the fluoro and pendant phenolic groups. A thorough understanding of the reaction mechanism and vast amount of research is needed to fully explore the possibility of this project.

8.5. References:

1. Ding, J.; Chuy, C.; Holdcroft, S., Enhanced Conductivity in Morphologically Controlled Proton Exchange Membranes: Synthesis of Macromonomers by SFRP and Their Incorporation into Graft Polymers. *Macromolecules* **2002,** 35, (4), 1348-1355.

2. Buchi, F. N.; Gupta, B.; Haas, O.; Scherer, G. G., Study of Radiation-Grafted Fep-G-Polystyrene Membranes as Polymer Electrolytes in Fuel-Cells. *Electrochimica Acta* **1995,** 40, (3), 345-353.

3. Gupta, B.; Scherer, G. G., Proton-Exchange Membranes by Radiation-Induced Graft-Copolymerization of Monomers into Teflon-Fep Films. *Chimia* **1994,** 48, (5), 127-137.

4. Gupta, B.; Buchi, F. N.; Scherer, G. G., Cation-Exchange Membranes by Preirradation Grafting of Styrene into Fep Films .1. Influence of Synthesis Conditions. *Journal of Polymer Science Part a-Polymer Chemistry* **1994,** 32, (10), 1931-1938.

5. Lee, H.-S.; Roy, A.; Lane, O.; Dunn, S.; McGrath, J. E., Hydrophilic-hydrophobic multiblock copolymers based on poly(arylene ether sulfone) via low-temperature coupling reactions for proton exchange membrane fuel cells. *Polymer* **2008,** 49, (3), 715-723.

6. Roy, A.; Hickner, M. A.; Lee, H.-S.; Badami, A.; Yu, X.; Li, Y.; Glass, T.; McGrath, J. E., Transport properties of proton exchange membranes. *ECS Transactions* **2007,** 2, (24, Direct Methanol Fuel Cells), 45-54.

7. Li, Y.; Roy, A.; Badami, A. S.; Hill, M.; Yang, J.; Dunn, S.; McGrath, J. E., Synthesis and characterization of partially fluorinated hydrophobic-hydrophilic multiblock copolymers containing sulfonate groups for proton exchange membrane. *Journal of Power Sources* **2007,** 172, (1), 30-38.

8. Lee, H.-S.; Badami, A. S.; Roy, A.; McGrath, J. E., Segmented sulfonated poly(arylene ether sulfone)-b-polyimide copolymers for proton exchange membrane fuel cells. I. Copolymer synthesis and fundamental properties. *Journal of Polymer Science, Part A: Polymer Chemistry* **2007,** 45, (21), 4879-4890.

9. Yu, X.; Roy, A.; Dunn, S.; Yang, J.; McGrath, J. E., Synthesis and characterization of sulfonated-fluorinated, hydrophilic-hydrophobic multiblock copolymers for proton exchange membranes. *Macromolecular Symposia* **2006,** 245/246, (World Polymer Congress--MACRO 2006), 439-449.

10. Roy, A.; Hickner, M. A.; Yu, X.; Li, Y.; Glass, T. E.; McGrath, J. E., Influence of chemical composition and sequence length on the transport properties of proton exchange membranes. *Journal of Polymer Science, Part B: Polymer Physics* **2006,** 44, (16), 2226-2239.

11. Einsla, B. R. High Temperature Polymers for Proton Exchange Membrane Fuel Cells. PhD Dissertation, Virginia Polytechnic Institute & State University, 2005.

12. Sankir, M.; Bhanu, V. A.; Harrison, W. L.; Ghassemi, H.; Wiles, K. B.; Glass, T. E.; Brink, A. E.; Brink, M. H.; McGrath, J. E., Synthesis and characterization of 3,3'-disulfonated-4,4'-dichlorodiphenyl sulfone (SDCDPS) monomer for proton exchange membranes (PEM) in fuel cell applications. *Journal of Applied Polymer Science* **2006,** 100, (6), 4595-4602.

13. Wang, F.; Hickner, M.; Kim, Y. S.; Zawodzinski, T. A.; McGrath, J. E., Direct polymerization of sulfonated poly(arylene ether sulfone) random (statistical) copolymers: candidates for new proton exchange membranes. *Journal of Membrane Science* **2002,** 197, (1-2), 231-242.

A.1. Addendum to Chapter-3- Crosslinked BPS Asymmetric Membrane

One of the future directions for application of BPS copolymers in water purification is to synthesize crosslinked asymmetric BPS membranes. The concept of asymmetric membranes was first developed by Loeb and Sourirajan. Asymmetric membranes comprise of a thin barrier layer which rejects the salt, on top of a thicker porous support which provides the necessary mechanical support for the membrane. Loeb and Sourirajan prepared asymmetric membranes from cellulose acetate by phase inversion technique.[1] In this method, cellulose acetate was first dissolved in a solvent i.e. acetone with aqueous magnesium perchlorate as a swelling agent or pore former and then cast onto glass plates. After air-drying for a brief moment, the membranes were immersed in the non-solvent i.e. ice water producing asymmetric membranes[2, 3].

In the current study, we selected NMP as the solvent for BPS copolymers and acetone as the non-solvent.

Initial Approach - A BPS-50 oligomer of ~ 5000 g mol^{-1} was mixed with 2.1 equivalent epoxy and 2.5 wt% of catalyst (based on epoxy weight). A 40 wt% solution in NMP was prepared to facilitate the initial membrane formation from such a low molecular weight oligomer. The solution was cast onto clean glass plates by Doctor's blade and air-dried at about ~35 °C for 30 minutes. Then the glass plate was immersed in the non-solvent i.e. acetone. Unfortunately, the membrane did not form properly. We believe that acetone being a solvent for epoxy, the epoxy and the copolymer were no longer in the same phase, hindering the membrane formation process. Hence our next approach was to make a copolymer which will be already end-functionalized with epoxy.

Second Approach – End-functionalization of BPS-50 with epoxy

The terminal phenoxide groups of a BPS-50 copolymer were reacted with the multifunctional epoxy resin via aromatic nucleophilic substitution to produce epoxy-functionalized BPS-50 copolymers (Fig. A.1.1). A typical endcapping reaction is provided below. BPS-50(5k) (1 g, 0.2 mmol) was dissolved in 10 mL DMAc in a 100 mL round bottom flask. Anhydrous solid potassium carbonate (0.06 g, 0.4 mmol) was added to the reaction flask. Next, epoxy (0.21 g, 0.5 mmol) was introduced in the flask and the reaction was continued for 24 h at 110 °C**.** The product solution was filtered and the copolymer was isolated by precipitation in isopropanol. The copolymer was further purified by soxhlet extraction in chloroform for 24 h to remove any residual epoxy. Then the copolymer was dried under vacuum at 110 °C for 24 h.

Figure A.1.2 represents the proton NMR spectra of a BPS-50(5k) oligomer before and after endcapping with epoxy. The aromatic protons of the biphenol unit in the endgroup at 6.8 ppm (*b*), 7.0 ppm (*d*) and 7.40 ppm (*a*) of the phenoxide-terminated BPS-50 oligomer disappeared after the phenoxide groups were reacted with epoxy.

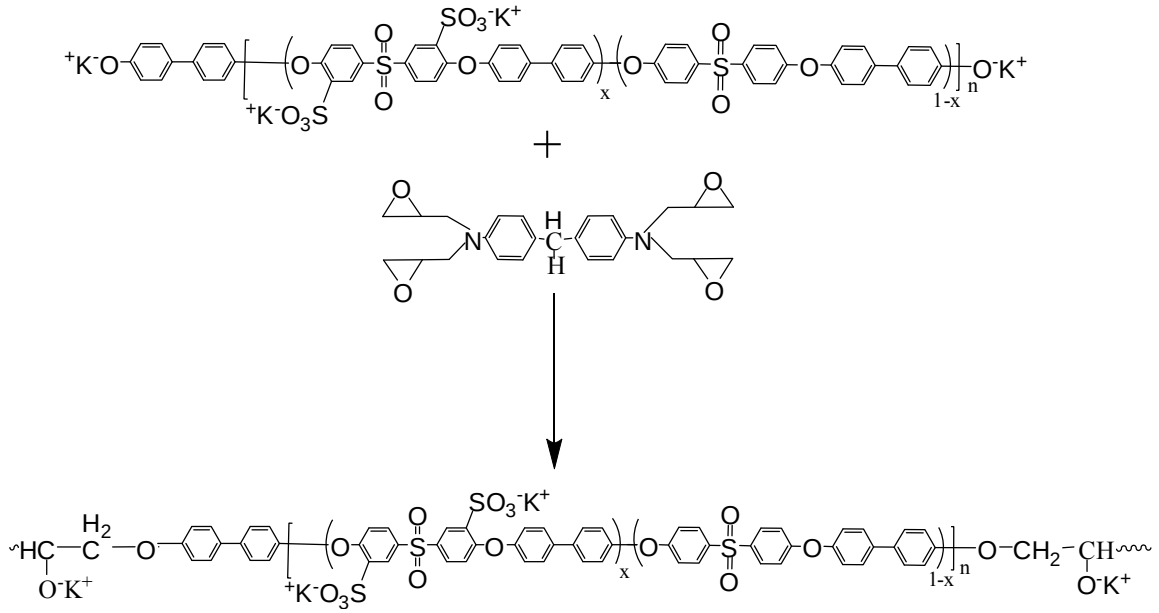

Figure A.1.1 End-functionalization of a BPS-XX copolymer by a multifunctional epoxy

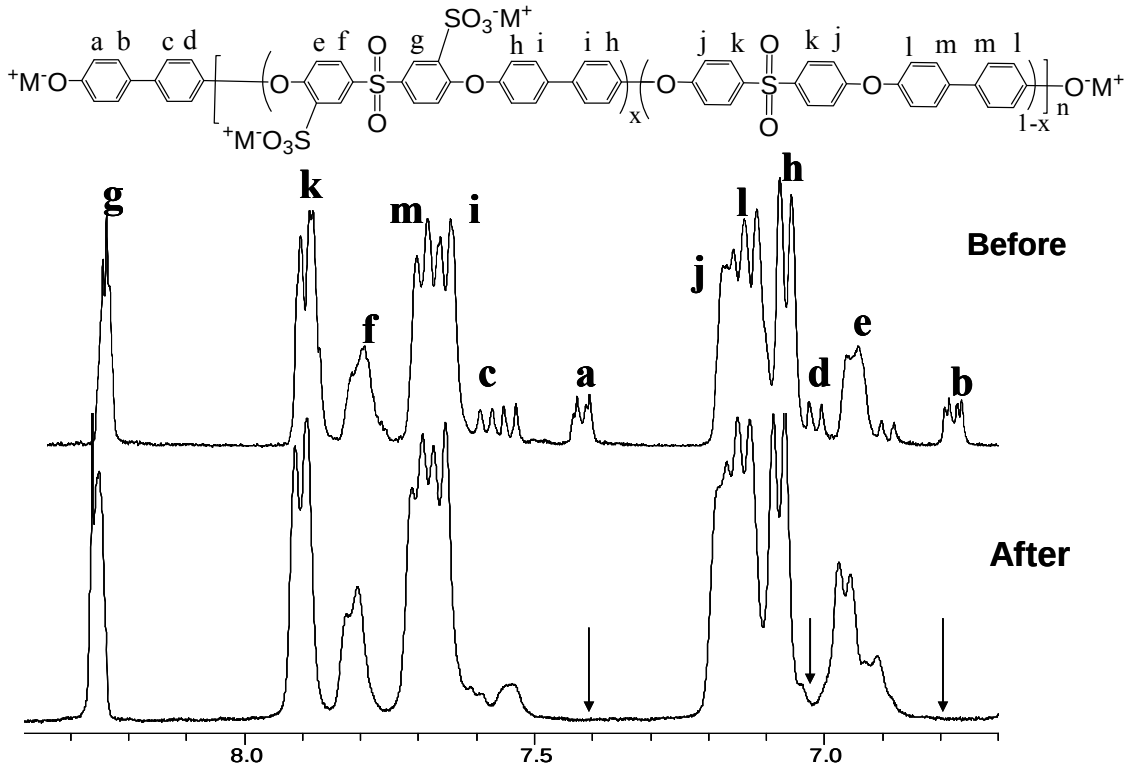

Figure A.1.2 ^{1}H NMR of a BPS-50(5k) oligomer before and after endcapping with epoxy;the arrows indicate the disappearance of aromatic proton peaks of the biphenol unit in the end group

A 40 wt% solution of the epoxy-functionalized BPS-50 copolymer with TPP catalyst (2.5 wt% of epoxy) was made in NMP. Similar to the earlier process, the solution was cast onto clean glass plates by a Doctor's blade, air-dried at about ~35 °C for 30 minutes and immersed in the non-solvent i.e. acetone for 24 h. This time the membrane could be formed easily. After 1 day, the glass plate was heated in a convection oven at ~ 50 °C for 30 minutes and the membrane was peeled out of the glass plate. Then the membrane was cured at 150 °C for 90 min. After crosslinking, the cured membrane was immersed in water. No swelling or reduction in the dimensional stability of the membrane was observed even after 4 months. For comparison, an uncrosslinked analogue was made from a high molecular weight BPS-50 copolymer. The membrane

swelled significantly losing its dimensional and mechanical stability within 30 minutes after immersing it in water.

In conclusion, a BPS-50 oligomer was successfully end-functionalized by epoxy. The end-fuctionalization process ensured the endcapping of the copolymer by epoxy prior to crosslinking. A membrane could be formed from this epoxy-functionalized copolymer by phase inversion technique. The crosslinked membrane showed significantly higher dimensional stability in water, compared to an uncrosslinked analogue. However, significant research in optimization of the crosslinking formulation and knowledge of the morphology of the membrane are needed to further explore the future of this study.

References

1. Glater, J., The early history of reverse osmosis membrane development. *Desalination* **1998,** 117, (1-3), 297-309.

2. Loeb, S.; Sourirajan, S. *UCLA Dept. of Engineering Report*; July,1960; pp 60-60.

3. Sourirajan, S.; Govindan, T. S., Membrane separation of some onorganic salts in aqueous solution. *Proc. Int. Symp. Water Desalin., 1st* **1967,** 1, 251-69, discussion 269-74.